




Chair of Processing of Composites

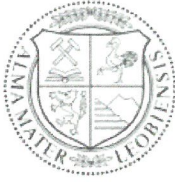
Doctoral Thesis



Inline monitoring and control for Automated  
Tape Laying

Neha Yadav, M.Sc.

July 2023



**MONTANUNIVERSITÄT LEOBEN**

www.unileoben.ac.at

**AFFIDAVIT**

I declare on oath that I wrote this thesis independently, did not use other than the specified sources and aids, and did not otherwise use any unauthorized aids.

I declare that I have read, understood, and complied with the guidelines of the senate of the Montanuniversität Leoben for "Good Scientific Practice".

Furthermore, I declare that the electronic and printed version of the submitted thesis are identical, both, formally and with regard to content.

Date 04.07.2023

*Neha*

---

Signature Author  
Neha Yadav

*This thesis is dedicated to the memory of Univ-Prof. Dr.-Ing. Ralf Schledjewski*

## Acknowledgments

This work would not have been possible without the support and encouragement of a number of people, to whom I would like to express my gratitude.

I would like to thank my main supervisor Univ-Prof. Dr.-Ing. Ralf Schledjewski, for giving me this incredible opportunity of working at LVV (Chair of Processing of Composites, Montanuniversität Leoben). His constant support, guidance and valuable feedback helped me always keep my focus on the main goal and finalize this thesis. I would also like to thank Assoc-Prof. Dr. mont. Ewald Fauster for his expertise and help with the lab equipment and scientific discussions. Thank you for taking over the supervision of the thesis during difficult times and helping with the final steps.

I have immense gratitude towards Dr. mont. Maximilian Tonjec for developing the test-rig and easing the knowledge transfer. A heartfelt thanks to Gustavo Vilaça Lourenço and Dr. mont. Anastasiia Galakhova for all our discussions and their insightful comments. I would like to thank all of the scientific and non-scientific staff at LVV. Special thanks to the student workers for their dedication and efforts, namely, Magdalena, Paul, Daniela, Michaela, Lukas, Zahra and Martin.

I would like to express my gratitude to the whole team at the Chair of Automation, especially Priv.-Doz. Dr. techn. Beata Oswald-Tranta. My deepest appreciation goes to the Department of Mechanics, Materials and Biomedical Engineering at Wrocław University of Science and Technology. In particular, Prof. Dr. Hab. Inż. Jerzy Kaleta and Dr. Inż. Paweł Gašior, for access to their research facilities and generous hospitality. I would also like to thank my wonderful colleague, Karol Wachtarczyk for all our scientific undertakings and delightful conversations.

Words fall short describing the love, support and care I have received from my family. They believed in my dreams more than I could. The gratitude I have for my parents, siblings and husband is beyond measure. They have been a constant source of inspiration and their presence helps me improve and nurture my aspirations.

Main parts of this research work were done within the context of the project InP4 [project no. 864824] provided by the Austrian Ministry for Climate Action, Environment, Energy, Mobility, Innovation and Technology within the frame of the FTI initiative “Produktion der Zukunft”, which is administered by the Austrian Research Promotion Agency (FFG). I kindly acknowledge the possibilities for the research work which were given to me in the course of this project. I would also like to thank the industrial partner, FACC Operations GmbH, for their support throughout the project.

## Abstract

Automated tape laying (ATL) is an advanced composite manufacturing technique which is used extensively for high performance industries such as aerospace and automotive. The aerospace industry, with the growing use of composites and ATL, demands greater complexity, reduced waste and stricter control over product quality and geometric tolerances. ATL as a process, even though highly automated, is susceptible to manufacturing defects which are not only detrimental to the structural performance, but also, due to a lack of robust monitoring and control system, lead to productivity loss. In-process defect monitoring is the most relevant research topic for process development, considering that defect detection and rectification are the main process bottlenecks.

This thesis provides an industry ready, engineering solution-based, holistic defect monitoring and control concept for thermoplastic in-situ consolidated ATL. The frequency of incidence of defects and the effect of defects concerning severity to the structure serve as defect selection criteria. A complete monitoring cycle consisting of defect identification, detection, treatment and control based on analysis of the process behavior is established. The monitoring concept builds upon easy integration, handling and accuracy and effectiveness of defect detection for real manufacturing process. Implementation of such a tool is bound to increase productivity, reliability and material and cost savings.

In the context of the research work elaborated in this dissertation, infrared thermography has been found to be capable of detecting foreign objects and debris as small as 2.5 mm. Local temperature anomaly and thereby, bonding defects can be detected as well. Profilometry has been proven to be capable of detecting gaps and overlaps having a size of 0.2 mm and above. Fiber Bragg Grating (FBG) sensors are utilized for monitoring residual strain at both lamina and laminate level. A novel defect management technique for selective defect rectification, prediction and prevention is demonstrated. For the given monitoring concept, residual strain, substrate temperature and compaction force/width can be controlled to alleviate shape distortion, bond inhomogeneity and gaps and overlaps (shape compliance) respectively.

The concept has been designed with highest regards to modularity and flexibility. The industrial applications for such a concept are immense. The gap and overlap management techniques are especially useful for variable angle tow/variable stiffness panels and near net shape laminates. Shape conformity will help in generating advanced, lightweight and complex structures. Defect management on the fly will improve manufacturing rates, bringing the process speed closer to traditionally metal manufactured components. The design flexibility offered by width control and shape conformity for thermoplastics will help the process in accommodating components having a vast range of size and design complexity. In summary, a monitoring concept is presented that leads to greater design freedom, quality and reliability enhancement, weight and cost savings and productivity rise.

## Kurzfassung

Mit dem Automatisierten Tapelegen (ATL) wird ein Verfahren zur Herstellung von kontinuierlich faserverstärkten, polymeren Verbundwerkstoffen bezeichnet, die für Hochleistungsbauteile, insbesondere in der Luft- und Raumfahrt wie auch in der Automobilindustrie, zum Einsatz kommen. Dabei kommen stetig steigende Anforderungen hinsichtlich Bauteilkomplexität, Abfallvermeidung sowie Produktqualität und geometrischer Toleranzen zum Tragen. ATL ist trotz seines hohen Automatisierungsgrades anfällig für Fertigungsfehler, die nicht nur die mechanischen Eigenschaften des Bauteils beeinträchtigen, sondern auch zu Produktivitätsverlusten führen können. Robuste Verfahren zur Prozessüberwachung und -regelung fehlen hier derzeit. In diesem Zusammenhang stellt die prozessbegleitende Fehlerüberwachung ein wichtiges Forschungsfeld für der Prozessentwicklung dar.

Die vorliegende Arbeit zielt auf ein industrietaugliches, ganzheitliches Fehlerüberwachungs- und Regelungskonzept für ATL ab. Die Arbeit stellt ein vollständiges Überwachungskonzept, bestehend aus Fehleridentifikation, -erkennung und -behebung vor, das auf Basis einer Analyse des Fertigungsverfahrens entwickelt wurde. Das Überwachungskonzept berücksichtigt Ansätze zur einfachen Integration, Handhabung und Effektivität der Fehlererkennung im realen Fertigungsprozess. Die Implementierung eines solchen Konzepts zielt auf positive Wirkungen hinsichtlich Produktivität, Zuverlässigkeit sowie Material- und Kosteneinsparungen ab.

Im Rahmen dieser Dissertation hat sich gezeigt, dass die Infrarot-Thermografie in der Lage ist, Fremdkörper und Ablagerungen ab einer Größe von 2,5 mm zuverlässig zu erkennen. Dieser Ansatz basiert auf der Erkennung von lokalen Temperaturanomalien. Die Profilometrie ist nachweislich in der Lage, Lücken und Überlappungen ab einer Größe von 0,2 mm zu erkennen. Fiber Bragg Grating (FBG) Sensoren werden insbesondere zur Überwachung von Eigenspannungs-induzierten Dehnungen im Bauteil verwendet und auf der Ebene von Einzellagen als auch im gesamten Laminat eingesetzt. In dieser Arbeit wird ein neuartiges Verfahren zum Fehlermanagement aufgezeigt, welches Aspekte der selektiven Fehlerbehebung, -vorhersage und -vermeidung vereint. Damit können Eigenspannungs-induzierte Dehnungen wie auch Substrattemperatur sowie Kompaktierungskraft bzw. Tapebreite gezielt beeinflusst werden. Dies ermöglicht die Verringerung von Formabweichungen, Inhomogenitäten sowie zur Vermeidung von unerwünschten Lücken und Überlappungen von Tapes.

Bei der Entwicklung dieses Konzepts wurde ein besonderes Augenmerk auf Modularität und Flexibilität gelegt, nachdem die industriellen Anforderungen an ein solches Konzept äußerst vielfältig gelagert sind. Das Management von Lücken und Überlappungen ist beispielsweise besonders nützlich für die Herstellung von Laminaten mit variabler Tapeorientierung oder variabler Steifigkeit sowie für endkonturnahe Lamine. Über ein aktives Fehlermanagement können Prozessgeschwindigkeit und Fertigungsraten gesteigert werden. Die Regelung der Tapebreite wiederum ermöglicht Formkonformität in engeren Toleranzen wie auch erhöhte Designflexibilität. Das hier vorgestellte Konzept zur Fehlerüberwachung im ATL-Verfahren ermöglicht somit größere Designfreiheit, erhöhte Zuverlässigkeit im Prozess, gesteigerte Bauteilqualität sowie Einsparungen bei Bauteilmasse und Fertigungskosten.

# Contents

Declaration .....	ii
Acknowledgments .....	iv
Abstract .....	v
Kurzfassung.....	vi
Contents.....	vii
1 Introduction .....	1
1.1 Dissertation Structure .....	3
2 Literature Review .....	5
2.1 State of the Art .....	5
2.2 Motivation and Research Questions .....	24
2.3 Approach and Scope.....	25
3 Experimental .....	27
3.1 Materials.....	27
3.2 Test-bench.....	28
3.3 Technical Specifications .....	29
3.4 Capability Analysis: FBG .....	32
4 Defect Monitoring and Control .....	49
4.1 FOD and Bond Inhomogeneity: Thermography .....	49
4.2 Gaps and Overlaps: Profilometry and Force Control .....	73
4.3 Correlation Models.....	85
5 Discussion .....	88
5.1 Conclusion.....	88
5.2 Outlook.....	91
References .....	93
Publications .....	96

# 1

## Introduction

Automated tape laying (ATL) is an advanced automated composite manufacturing technology, which originated over 30 years ago [1, 2]. The process makes use of unidirectional (UD) tapes that are continuously laid onto a layup tool with varying degree of freedom both in terms of layup direction and curvature of the material. It is a low-level **additive manufacturing** process where parts and products are built in a layer-by-layer fashion. Each layer/lamina consists of multiple tapes laid adjacent to each other and each laminate consists of multiple layers/lamina stacked on top of each other. The technology is a cross-over between conventional and contemporary composite manufacturing and is thereby used as an industrial benchmark for new additive processes utilizing composites [2]. The working principles of ATL are very similar to that of automated fiber placement (AFP), except for the width of the individual tapes and sometimes the complexity of the parts being manufactured. The width of tapes used by ATL is typically 75-300 mm. AFP uses 3.175-12.7 mm wide tows, and each ply comprises of 2-32 tows [1–3].

Apart from the rather high facility costs, precise manufacturing of large parts at a high level of processing speed with effective process control makes the technology suitable for high performance industries, especially **aerospace**. Composites account for over 50 % by weight composition for large commercial aircrafts, such as Airbus A350 and Boeing 787 [4, 5]. For Airbus A350, 92 % of the fuselage and spar are manufactured using ATL and AFP [6]. Landing gear and wings are considered to be one of the most critical parts of the structure of an aircraft. Including these [5], frames, stringers, and highly complex shaped parts such as cowlings, nacelles, ducts and fan blades are being manufactured using this technology [6, 7]. AFP accounts for 55 % added value in the value chain of composites manufacturing [4]. Traditionally the process utilizes thermoset prepregs, however, the use of **thermoplastics** has seen steady growth over the years. Thermoplastics have been used for Airbus A380 and US supersonic aircrafts [8]. The popularity is owed to the short processing times, and possibility of out of autoclave or single step processing making use of **in-situ consolidation** [9–11]. Thermoplastics also offer excellent fatigue strength and fire/smoke/toxicity properties [5]. Another lucrative aspect considering sustainability is the possibility of recycling and reuse [12, 13].

One of the major productivity bottlenecks for the process is **defect detection** and **rectification**. Most industrial solutions still rely on manual visual inspection, making the inspection process tedious, time consuming and unreliable. Inspection and rework for the process usually amounts to 32-63 % of the cycle time [14–18]. The floor-to-floor cycle time can be reduced by 20 % if fully automated inspection systems are employed. This would lead to a productivity increase of 25 % [14]. Defect monitoring and control for minimal defect and in-situ thermoplastic layup has been the focus of recent technological inventions [19, 20]. An automated, inline solution is especially suited for aerospace sector, where tolerances for quality assessment and product



qualification are very stringent. Flexible methods of automation throughout the process chain leading to a fast, controllable process with minimum defects are needed to meet future demands, such as for Industry 4.0 [6] and Manufacturing III (atomic and close-to-scale manufacturing) [21].

**Inline monitoring** is a form of non-destructive testing (NDT) which is employed during the running process to provide qualitative and quantitative information about the condition of the inspected structure. The process step where inline monitoring is employed is shown in *Figure 1*. When used conventionally, i.e. post-manufacturing, NDT techniques detect existing flaws and help with quality assurance. At this stage, depending on the severity of flaw, the structure can either be repaired or needs to be rejected entirely. Inline monitoring helps with in-process detection, localization and quantification of **manufacturing defects**. Early detection of defects in a ply-by-ply manner provides better options for defect treatment and helps curtail scrap rate. A smaller area with ease of access has to be reworked instead of the whole structure. Combined knowledge of defect significance, anticipation, progression and detection with an understanding of effect of defect on structural performance is crucial for **defect management**; where, the overall aim of defect management is rectification, prediction and prevention of defects. Analytical models and defect correlation with process parameters will lead to enhanced **defect and process control**. Implementation of a holistic inline monitoring tool with defect control capabilities facilitates increased productivity and reliability, reduced error margins as well as improved time and cost savings.

*The aim of this dissertation is inline monitoring and control of manufacturing defects for thermoplastic in-situ consolidated automated tape laying.* A combination of monitoring techniques is used to detect commonly occurring manufacturing defects and process variables throughout the process. The defects are selected on the basis of frequency of occurrence and severity of their impact on the structure. Type of defect and information extraction necessary for successful detection serve as the guiding factors for selection of monitoring techniques. The process control concept builds upon the information gained from the defect detection and process variables by interlinking them. In this way, by controlling the process variables, certain selective defects can be controlled. Defect management strategies considering industry specific applications are devised. The modularity and flexibility of the overall concept is also discussed.

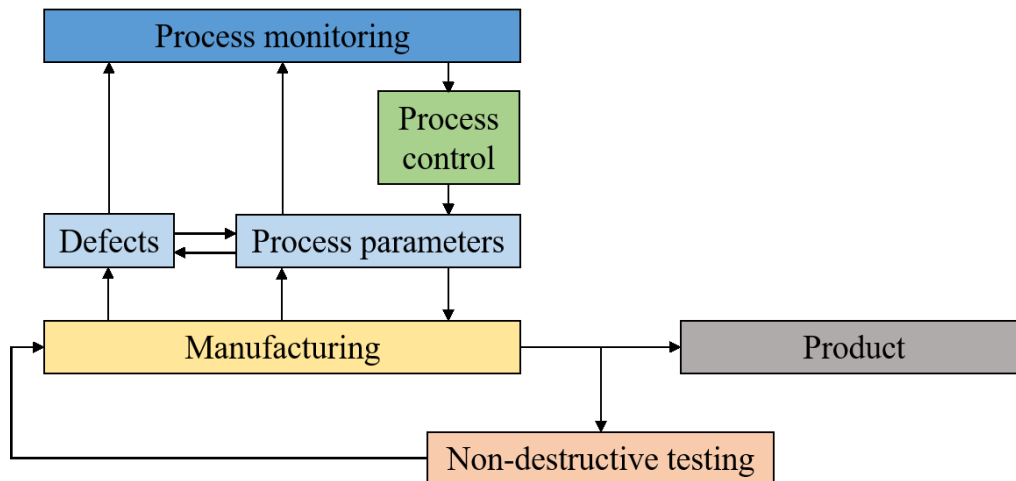


*Figure 1 Process steps for composite manufacturing*

## 1.1 Dissertation Structure

The thesis at hand represents a "cumulative work" involving five peer-reviewed articles, published in scientific journals.

The present chapter, **Chapter 1**, provides a short introduction and an overview of the work done in the context of this dissertation. Main keywords pertaining to the scope of the work are highlighted in bold. A schematic of the dissertation structure is shown in *Figure 2*.

A detailed literature review presenting the state of the art of defect detection techniques for ATL and AFP are discussed in **Chapter 2**. The need for inline monitoring, types of manufacturing defects, effect of defect, monitoring techniques and defect rectification strategies are described therein (**Article A**). This chapter also forms the core of the motivation behind this work. The research questions arising thereof are formulated subsequently and the main objectives of the research work are derived from these questions.

**Chapter 3** summarizes the set-up used throughout the experimental work conducted as a part of this research. Details of used materials, test-bench and hardware and software considerations are listed. An example of the pre-trials as a part of capability and feasibility study is also presented (**Article B**).

The central concept of defect monitoring and control with various defect detection and management studies, including validation and benchmarking (**Article C**, **Article D** and **Article E**) is presented in **Chapter 4**. Correlation models between selective defects (gaps and overlaps) and process variables are discussed subsequently.

Finally, a summary and outlook of the entire work is presented in **Chapter 5**. A conclusive overview of best practices for defect detection and monitoring techniques, limitations of the work and outlook from a process control perspective is described.

*Article A: Review of in-process defect monitoring for automated tape layup*

*Article B: In-line residual strain monitoring for thermoplastic automated tape layup using fiber Bragg grating sensors*

*Article C: Ply-by-ply inline thermography inspection for thermoplastic automated tape layup*

*Article D: In-line and off-line NDT defect monitoring for thermoplastic automated tape layup*

*Article E: Inline tape width control for thermoplastic automated tape layup*

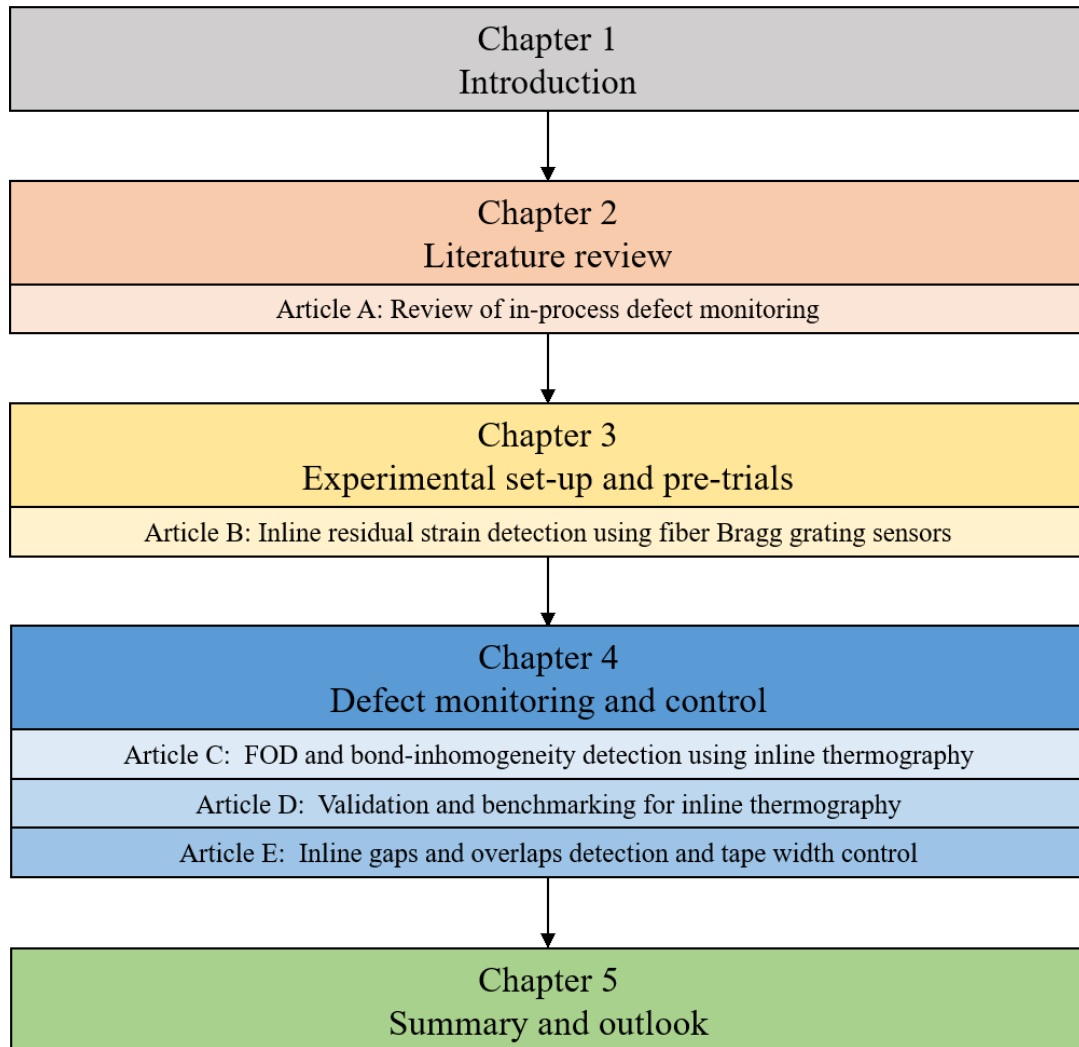


*Figure 2 Dissertation structure*

## Literature Review

### 2.1 State of the Art

*Article A [22]: “Review of in-process defect monitoring for automated tape layup”*

A short overview of the article is provided here. The article is supplemented directly after the overview. This work explores the research question: *Which manufacturing defects are crucial for detection and can they be detected inline?*

A lack of organized knowledge and standards for manufacturing defect types and defect detection techniques has been identified. The review article talks about commonly occurring manufacturing defects, their impact on structural performance, monitoring techniques and defect rectification strategies. Manufacturing defects occurring as a result of process environment/mis-handling are divided into four categories, positioning defects, bonding defects, foreign object debris (FOD) and tow (tape) defects.

Most experimental and analytical studies researching the effect of defects on mechanical properties and structural performance concentrate on gaps and overlaps. In general, gaps are more critical when it comes to damage to the structure than overlaps. Systematized defects occurring in an orderly manner have proven to be more damaging than randomly introduced ones. A combination of defects is more detrimental than individual defects [22]. These insights should be kept in mind during path planning and control. The relevance of such studies is highlighted for structures such as variable stiffness panels (VSP), where occurrence of such defects is unavoidable and a coverage ratio is used to either have gaps, overlaps or a combination of both. Staggering and offsetting helps with migration of defects but is insufficient for gap reduction and elimination.

Most commonly used inline monitoring techniques are thermography, profilometry and machine vision. Best practices and most promising defect detection approaches considering defect types are as follows (*Figure 3*): thermography (infrared camera) for FOD, profilometry (light section sensors) for gaps and overlaps and machine vision for twisted tows and wrinkles. The evolution and commercial adoption of these technologies are highly dependent on cost and ease of integration; as well as accuracy and effectiveness of defect detection. For greatest accuracy and detection of wide variety of defects, a combination of different techniques is suggested.

Defect rectification comprising of removal, rework and repair has received little to no interest in the scientific literature. A few solutions have been discussed, but none of them involve automated standardized industrial solution with a direct integration on the ATL machine.

The answer to the research question is: *Positioning defects, especially gaps are crucial for detection considering their impact on mechanical properties. FOD and bonding defects are frequent and thus, crucial for detection for a holistic monitoring concept and quality assurance. Tape defects such as twisted tows and wrinkles are of little concern for thermoplastic composite materials.*

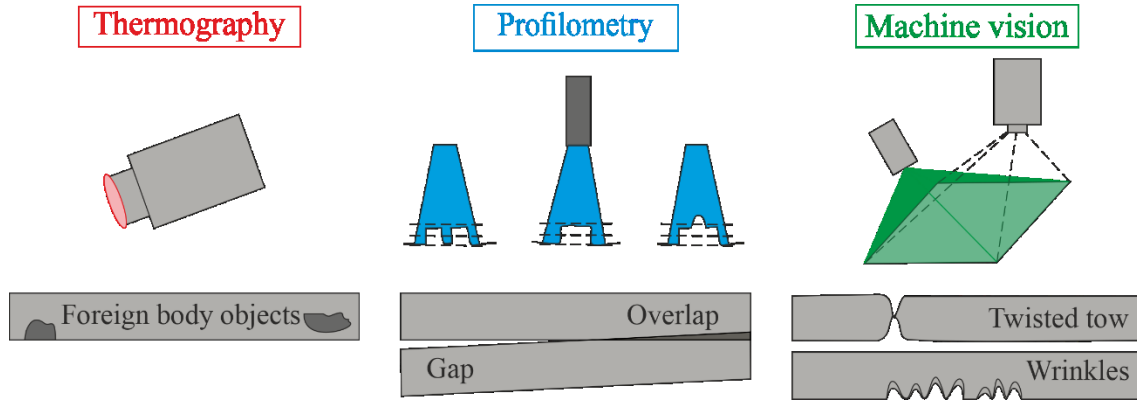


Figure 3 Best suited monitoring techniques by defect types [22]

*Article A [22]: “Review of in-process defect monitoring for automated tape layup”*



## Review

## Review of in-process defect monitoring for automated tape laying

Neha Yadav<sup>\*</sup>, Ralf Schledjewski*Processing of Composites Group, Department Polymer Engineering and Science, Montanuniversität Leoben, Otto-Glöckel-Strasse 2/3, 8700 Leoben, Austria*

## ARTICLE INFO

This article is dedicated to Univ.-Prof. Dr.-Ing. Ralf Schledjewski.

## Keywords:

- A. Polymer-matrix composites (PMCs)
- E. Tape placement
- B. Defects
- D. Process monitoring

## ABSTRACT

Automated tape laying is a well-established composite manufacturing process for high performance industries. While the process has seen vast growth over the 30 years of its conception, in-process monitoring is the most relevant and researched topic for present and future process development. The presented review highlights the importance of developing in-process monitoring tools and provides a detailed overview of such techniques for defect detection. Commonly occurring manufacturing defects, their influence on part and structural performance are assessed and discussed. The evolution of defect detection technologies considering defects types, accuracy, and speed are detailed. A summary of most promising approaches as per defect detection capabilities is presented. Defect rectification techniques are also discussed.

## 1. Introduction

The past years have witnessed an extensive use of composites as structural components in several industries such as aerospace, automotive, marine and wind energy sector. Composites offer high strength to weight ratio, better flexibility and adaptability to complex shapes and dynamic (design and local enforcement based on load path analysis) use of directional properties [1]. One of the processes to manufacture composites is Automated Tape Laying (ATL). A low-level additive manufacturing technique, comprising of layer by layer multi-directional placement of continuous tape. The working principles of the process are similar to Automated Fiber Placement (AFP), except for the width of the material and sometimes, complexity of the parts. These manufacturing techniques are also used as industrial benchmarks for new additive processes for composites [2].

ATL was developed over 30 years ago [2,3] and typically uses 75–300 mm wide tapes. While AFP uses 2–32 individual tows having 3.175–12.7 mm width [2–4]. The technology has seen vast growth in aerospace industry. Large commercial aircrafts, such as Boeing 787 and Airbus A350, contain over 50 % by weight of composites [5,6]. In the value chain of composites, the added value of fiber placement is 55 % [5]. To bring clearer perspective with regards to the scale of ATL and AFP implementation in aerospace composites manufacturing, it is important to note here that 92 % of the fuselage and spar of Airbus A350 are manufactured using the said technology [7]. Both flat structures such as frames, stringers and spars and highly contoured complex structures such as fuselage panels, bulkheads, cowlings, nacelles, wing

skins, fan blades and ducts are being manufactured alike [7,8].

The process has also found use in varied innovative applications and sustainable materials. A few examples being, shape adaptive hydrofoil [9], morphing airfoil with variable stiffness bi-stable laminates [10], bio-inspired 'brick-and-mortar' structure [11] and bio-composite Flax/PP [12].

While thermosets have been traditionally used for the process, use of thermoplastics has seen steady growth over the past ~30 years. The most lucrative aspect of thermoplastics being short processing times, that is the possibility of in-situ consolidation or single step processing [13–15]. They have other advantages to offer as well when compared to thermosets, in particular, superior fatigue performance, excellent fire/smoke/toxicity properties [6] and recyclability [16,17]. The commercially available material suffered a number of problems in the past ranging from uneven geometry to inhomogeneous fiber distribution [18]. As also noted by Gruber et al. approximately 10 years ago, the thermoplastic impregnated tapes that were commercially available at that time were not developed for in situ processing [19]. Since then, material development gained momentum and progress has been made in terms of different quality indices. An example of width spread for tape as received from manufacturer is shown in Fig. 1. However, for aerospace applications the quality in terms of inter-laminar shear strength (ILSS) (70–85 % of autoclave) [14,20], flexural strength (68 % of autoclave), flexural stiffness (88 % of autoclave) [20] and open-hole-compression strength (~80 % of autoclave) [20,21], achieved via in-situ consolidation has not been considered on par with autoclave/post-consolidation up until now. Without post-consolidation the technology could still be

<sup>\*</sup> Corresponding author.

E-mail address: [neha.yadav@unileoben.ac.at](mailto:neha.yadav@unileoben.ac.at) (N. Yadav).

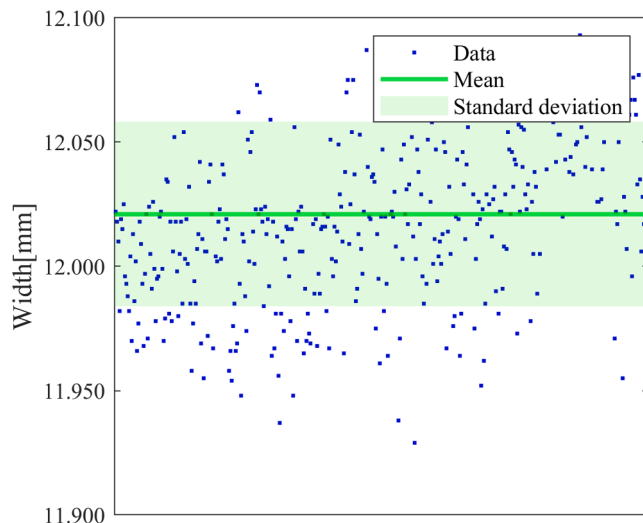


**Fig. 1.** Variation in width for thermoplastic CF-PEEK tape as supplied by manufacturer for a standard width of 12 mm.

used commercially for other sectors. Rapid manufacturing involving complex preforms has been suggested as a commercial outlook for in-situ consolidated samples [14]. According to a fairly recent study [21], improved results have been obtained, where the tensile modulus (22 % higher than autoclave) and shear properties of laminates made by thermoplastic in-situ AFP were found to be better than those of laminates made by autoclave technique. The fracture toughness has also been found to be higher in some cases (30—80 % more than autoclave) [20,22].

The overall yearly improvement rate of ATL, estimated using objective patent-based methodologies, is 13.03 %, and the technology doubles its performance every ~5.3 years. The latest technological advances were centered around productivity, reliability, and geometric flexibility [23]. Among these, the largest industry relevant technological inventions and research focusing on productivity concentrated on inspection and operation control leading to minimal defect layout and in-situ thermoplastic layout [23,24]. Closed loop control of process elements such as tape heating, tape deposition and cutting increases process reliability, which successively increases productivity. Even though the development has been made for over three decades, geometric flexibility is still the main improvement focus of agile compact placement heads [23].

On one hand the scope of the process is increasing in terms of scalability, part size and complexity, materials and applications. On the other hand, the processing time and error margins are decreasing, owing to strict standard of some of the industries. Defect detection is also very important if keeping in line with the primary future development trends in manufacturing, that is implementation of Manufacturing III (atomic and close-to-scale manufacturing (ACSM)) [25]. Flexible methods of automation leading to fast controllable process with minimum defects are needed for further technological advancements. To reach Industry 4.0, especially for aerospace composite manufacturing where the implementation of Industry 4.0 is imminent to meet future demands, end-to-end manufacturing automation throughout the process chain is needed [7].

It has been pointed out by a number of authors that manual visual inspection for defect detection in ATL process is a bottleneck for both productivity and reliability. Inspection and rework for a typical ATL run accounts for 32–63 % of the cycle time [26–30]. Fully automatic inspection can reduce the floor-to-floor cycle times by 20 %, corresponding to a productivity increase of 25 % [26]. As discussed previously, this is an ongoing area of research which is also highly relevant for future process development.

Since the current, most relevant research areas and future research focus is around inline monitoring and control, a detailed structured and chronological review archiving the developments would be beneficial for state-of-the-art awareness, identifying probable research gaps and discovering new trajectories to undertake. An organized knowledge base of the complete process of technological development is pertinent for comprehensive understanding. This encompasses, origin of defects, their effect on structure, different techniques for monitoring, and defect quantification and rectification. This review addresses in-process defect monitoring approaches for ATL and AFP. Evolution of defect detection technologies, best practices according to defect types and most promising approaches are discussed thereof.

### 1.1. Related research

A review of the process, related history and development up until a decade ago is provided by Lukaszewicz [3]. Brasington et al. [24] presented a more recent review, where they enlisted flexible modular solutions, reduced production times and out-of-autoclave methods as the future research focus. Manufacturing defects, process parameter and in-situ monitoring are presented in a rather concise manner. A review from the additive manufacturing perspective for contemporary and modern technologies including ATL and AFP is presented by Frketic [2]. The authors emphasized the need for flexible methods for automation. Campos [23] highlighted the recent patent related technological trajectories for ATL and AFP. The focus is more towards quantitative technology change and innovation study by formalizing broad categories without the specifics about the individual research studies driving the innovation. The current level of automation (LOA) for the technology as a whole and throughout the process chain is reviewed by Jayasekara et al. [7]. Here again as the approach dictates, level of automation is discussed for comprehensive core-process tasks and sub-process tasks, rather than the intricate details of the methods and techniques that form the core of the automation. Technologies for changing the LOA subsequently are summarized, but the suitable applications and methods for adaptability and transferability are left out. A detailed review of thermoplastic ATL and AFP is given by Khaled [31]. The review covers details of the process components, parameters, models, mechanical characterization and process optimization. The review about quality assurance comprising of defects and inspection technologies is however, rather limited. Boon [32] presented a review of the process from the perspective of in-situ consolidation. A summary of optimized processing parameters is also listed.

Online monitoring is briefly discussed by Zhang et al. [5], Parmar et al. [33] and Sun et al. [34]. A detailed overview is however omitted. Oromiehie et al. [35] presented a review about manufacturing induced defects and their impact on the structure, but the review leaned more towards parametric effects and optimization and only two technologies are discussed under inline monitoring.

## 2. Manufacturing defects

This section details the occurrence of different types of defects and the effect of defects on the structural performance of the resulting laminate. Commonly occurring manufacturing defects are shown in Fig. 2 (adapted after [8,36]).

Defects occurring in a laminate could be a result of the following: material imperfections - inhomogeneous fiber volume ratio; non-optimized process parameters - degradation due to very high temperature; process environment - layout restrictions, FOD (foreign object debris/defects) or a combination of previously mentioned factors - voids, residual stress. Defects occurring as a result of process mis-handling, steering restrictions and equipment (ATL head) automation errors are the focus of this research. Defects completely or partially inherent to material properties such as uneven bonding, residual stress, crystallization, voids, uneven bonding and surface roughness variation are not



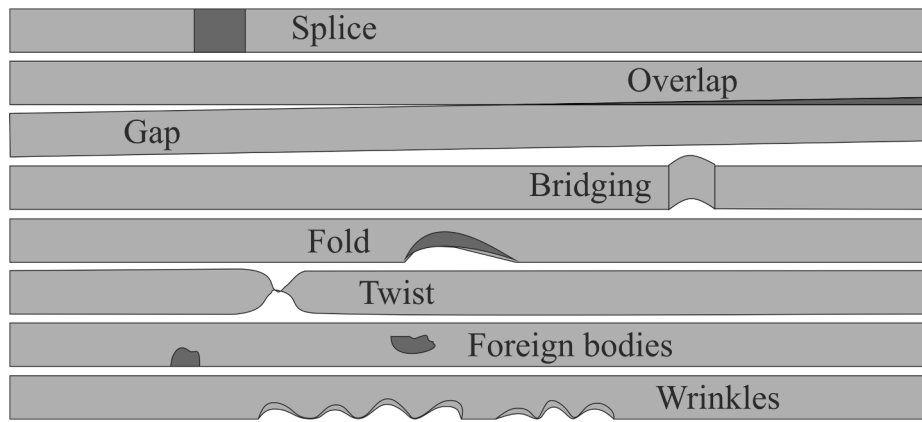


Fig. 2. Common manufacturing defects for ATL process adapted after [8,36].

discussed in detail. There are two reasons for that; first, these defects mostly rely on material quality, which should have strict standards of its own; second, non-destructive inline monitoring for such defects have not been established so far. Likewise, optimization of process parameters is not included as there are extensive reviews that can be found in literature [22,37–46]. Moreover, parametric optimization in most cases are single objective (sometimes 2–3), test-bench and heat-source specific, making it difficult to generalize them.

2.1. Defects

Schmidt et al. [47] listed defects that are crucial for production and quality assurance of composites. They classified common defects that occur during laminate manufacturing according to cause of incidence. These include, positioning defects: gaps, overlaps, missing tows, twisted tows; bonding defects: air pockets, bridging; foreign object defects (FOD): fuzzball and tow defects: splice [47].

Among these, some defects are specific to a particular material type or layup strategy. For instance, waviness and wrinkles are a common incidence for thermoset prepregs and dry fibers. Bakhshi et al. identified five major types of defects for steered prepreg tows namely in-plane fiber waviness, tow pull ups, blisters, sheared fibers, and out-of-plane wrinkles. Formation of these defects is discussed and a finite element model for blisters and wrinkles is presented [48]. To investigate the effects of compaction roller on the quality of layup, an experimental and simulation study was also performed. The effects on manufacturing defects such as tow buckling and blisters were investigated. It was found that under similar processing conditions (compaction force) that results in same level of contact width, solid elastomers are preferred over perforated ones. They provide even pressure distribution and overall better layup quality when compared to the perforated counterparts [49].

Similarly, design and steering restrictions lead to gaps and overlaps in variable angle tow (VAT)/ variable stiffness panels (VSP). When constant width tows are used on curvilinear steering path, gaps and overlaps are created as a result of width distribution within the geometric confines of the rectangular tow. The width perpendicular to the shift direction varies over the course of the curvature due to varying placement angle. The outer edge extends more than the inner edge trying to conform to the steering radius, giving rise to a steering mismatch. If the course width could change continuously, giving rise to perfectly tessellated fibers (varying width fibers), there would no gaps and overlaps [50]. As this is difficult to achieve with constant processing parameters, different strategies for methodical gap and overlap introduction are used in a general case scenario. These strategies are tow dropping and tow overlapping. A ratio called gap coverage parameter (Fig. 3) is used to create either complete gaps and overlaps or a mixture of complete gaps and overlaps[51,52]. For prepreg VAT/VSP laminates having small steering radii (400 mm steering radius for 6.35 mm wide tape [53,54]), the large mismatch in length between the inner and outer radii causes out-of-plane wrinkles. In addition to this, other defects common defects found in steered tows are, in-plane buckling, splitting of tows due to in-plane shear and localized delamination from substrate [55].

According to a study listed by [57], among the various types of defects, adjacent gaps/overlaps are the most commonly occurring defects, accounting to over 57 % of all defects [57]. As can be seen above, positioning defects such as gaps and overlaps cannot be avoided for certain layup configurations unless modified layup methods are developed.

Harik et al. [58] defined defect identity cards for various defect types. The identity cards give information about anticipation (prediction of defect occurrence), existence (describing the detectable aspect of

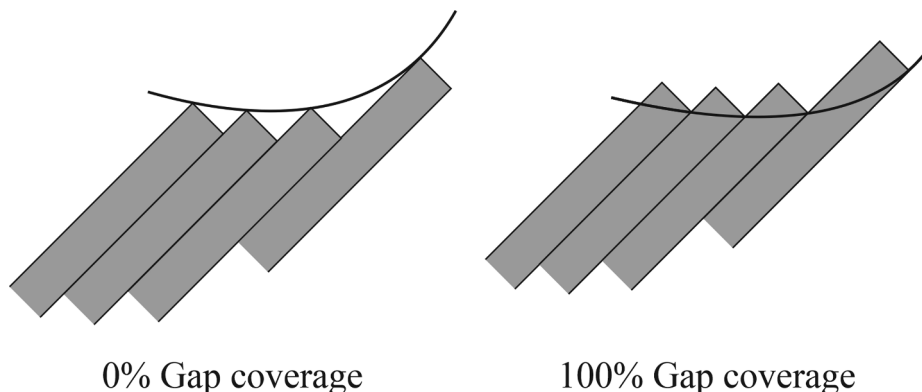


Fig. 3. Gap coverage parameter/ratio, adapted after [51,56].

defects from an inspection point of view), significance (effect of defect on part quality and performance) and progression (defect evolution under service conditions) of defects. Later on, Chevalier [59] extended the list to build upon another category, disposition (defect treatment: repair, rework, remove, replace, reject).

## 2.2. Effect of defects

Most studies pertaining to effect of defects studies have been focused around gaps and overlaps, and limited research has been conducted on experimental and analytical effect of the rest of the defect types on performance of composites. A summary of effect of defects (except gaps and overlaps) is discussed below, and a summary of effect of gaps and overlaps in a chronological order is discussed consecutively. All studies are specific to ATL and AFP, unless stated otherwise.

Hsiao [60] investigated both experimentally and analytically the effect of out-of-plane fiber waviness on strength and stiffness reduction under compressive loading for carbon-epoxy and S-glass-epoxy laminates. Fiber waviness was found to be detrimental for strength and stiffness. Uniform waviness has been found to cause a 42 % reduction in Young's modulus and graded waviness has been found to cause a 6 % reduction in modulus along with a 30 % reduction in compressive strength. The leading failure mechanism for such composites manufactured using tape-winding was found to be interlaminar shear stress [60]. Belnoue et al. [61] studied the effect of out-of-plane wrinkle formation during debulking and autoclave curing of laminates. A multi-scale multi-physics predictive model was also developed to study the evolution of fiber path defects due to embedded gaps and overlaps. The model has been found to be capable of predicting internal geometry and ply configurations for complex arrangements of gaps and overlaps [61]. Wrinkling has been identified as the primary cause for strength reduction for gaps and overlaps specimens. For steered tows, tow wrinkling is observed in all tows at each location where the laminate substrate has defects such as gaps and overlaps. When heat is applied to areas containing wrinkles, it was observed that the loss in stiffness in the prepreg helps the small wrinkles in a small localized area to merge into one big wrinkle [55].

### 2.2.1. Experimental investigation

Sawicki and Minguet [62] studied the effect of gaps and overlaps on compression strength of IM6/3501-6 composite laminates. Significant reductions in strength (8.6–20 %) were observed for defects as wide as 0.03", beyond which there was no considerable reduction for wider defects. The number of defects were found to have insignificant effect on the strength reduction. The predominant factor for strength reduction was out-of-plane fiber waviness. Similar strength reductions were observed for unnotched and open hole specimens [62].

Croft et al. [52] studied the effect of gap, overlap, half gap/overlap and twisted tow on ultimate strength at both lamina (fiber tension, fiber compression and in-plane shear) and laminate level (open hole tension and open hole compression) for carbon-epoxy prepreg. It was discovered that single and isolated defects have minimal effects on mechanical performance at lamina level, ~5 % compared to laminate level ~13 %. Varying angle in plies creates secondary defect called fiber waviness around the existing primary defect. Including the ply angle, this secondary defect is influenced by factors such as defect geometry, position and compaction pressure. These factors, as a result of fiber waviness, can influence the final geometry of the defect, which in effect influences the structural compression properties [52].

Falcó et al. [51] experimentally investigated the effect of fiber angle discontinuities (effectively leading to gaps and overlaps) between different tow courses in a ply on the open-hole and un-notched tensile strength of the variable stiffness laminate. Experiments were conducted on HexPly AS4/8552 pre-impregnated CFRP (carbon-fiber reinforced plastic) laminates. The influence of staggering and percentage coverage was studied and results indicated that a combination of ply staggering

and 0 % gap coverage helps in reducing the influence of defects in such laminates. Staggering led to a tensile strength reduction of 8.6 %, while 0 % gap coverage (all gaps) led to a reduction of 22.1 %. A possible explanation for this is reduced local thickness variation due to superposition of defects through laminate thickness [51].

Lan et al. [63] studied the effect of embedded gap and overlap on shear and compression for carbon-epoxy laminates (8552/AS4/RC34/AW194 from Hexcel). The characterization of the microstructure was performed using Scanning electron microscopy (SEM). In-plane shear and compression tests were conducted and results indicated that gaps are more critical for shear properties, particularly when caul plate was used. A reduction of about 6–20 % in absolute shear strength and slight increase (12 %) to significant reduction (52 %) in compressive strength based on the defect size (0.5–3.175 mm) was observed. The local variation in thickness and fiber content in adjacent plies makes shear properties more susceptible to large gaps (3.175 mm) [63].

Elsherbini [64] investigated the effect of gaps on fatigue behavior of unidirectional carbon/epoxy laminates (CYCOM 977-2-35-12 K HTS-145). For tension-tension fatigue tests, it was found that as the maximum applied stress increases, so does the severity of effect of gaps. This effect diminished at lower stresses. The main damage mechanism as a result of gap was delamination. High interlaminar stresses are generated at the edge of gaps as a consequence of fiber cuts during manufacturing. Delamination is initiated at the interface between the defected layer and the surrounding layers owing to the out-of-plane stresses [64]. They further conducted fatigue tests on unidirectional, four-angle ( $0^\circ/90^\circ/\pm 45^\circ$ ) and cross-ply carbon-epoxy laminates containing gaps. A threshold stress level was discovered in gap specimens. Below this threshold value, a reduced effect of gaps on fatigue is observed. They also discovered a bilinear relation between the applied stress and the rate of the temperature increase from which this threshold stress could be obtained. For fatigue stresses lower than the threshold value, the effect of gaps in specimens becomes equivalent to the effect of heterogeneities in pristine/reference specimen. This eliminates the effect of the gap on the fatigue life [65].

Marouene [66] attempted to predict the effect of gaps and overlaps on open-hole compression strength both experimentally and numerically for carbon/epoxy composites (G40-800/5276-1). Depending on their location defects were found to have slight negative (5–13 %), negligible (0–1 %), or slight positive (3–8 %) effects on the compression strength. Combination of gaps at various locations showed much worse effect on strength than gaps at a single location [66].

Guin [67] examined the effect of systematic gaps on unnotched tension and compression and open hole compression tests for IM7/8552-1 prepreg laminates. For systematic and organized gaps, as is the case with VAT/VSP laminates, substantial amount of fiber waviness is witnessed. The fiber waviness was found to be prevalent throughout the thickness of the specimen. The effect of fiber waviness on strength reduction was found to be independent of load case, the effect on modulus was however, dependent on the ply loading direction. Degree of fiber undulations get exacerbated under compressive loading, causing out-of-plane fiber waviness, affecting elastic properties and reducing compressive modulus. It was also observed that 0.05" gaps (higher degree of fiber waviness) placed in  $90^\circ$  plies would not affect the mechanical properties so long as they are not systematically present in each ply [67].

Woigk et al. [68] studied the effect of gaps, overlaps, combination of gaps and overlaps and staggered gaps on carbon fiber prepreg (IM7/8552 by Hexcel). Their results confirmed that in contrast to systematic gaps, isolated gaps and overlaps do not have a significant impact on strength of the specimen. A combination of both gaps and overlaps however had considerable influence on the laminate strength (7.4 % and 14.7 % for tension and compression respectively). Further adding to the postulate that systematic defects occurring repeatedly at a particular location are more dangerous than random ones. The driving parameter for failure behavior is level of ply-waviness. Interlaminar shear stresses

and out-of-plane normal stresses due to out-of-plane fiber misalignments promote earlier occurrence of failure compared to pristine laminates [68].

Nguyen et al. [69] manufactured carbon fiber T800S/3900 prepreg specimens with varying sizes and distribution of gaps and overlaps. The change in geometry due to defects was also examined. Gaps, especially of larger size (0.5") were shown to have significant knockdown in stiffness and strength compared to overlaps, which had negligible change in compressive strength and slight improvement in tensile properties. Tensile tests showed a maximum of 20 % reduction in stiffness and 55 % reduction in strength for 0.5" gaps; and a 20 % increase in modulus and -15 to +20 % variation in strength for 0.5" overlaps. Compressive tests showed a maximum of 30 % reduction in stiffness and 55 % reduction in strength for 0.25" gaps; and a 10 % increase in modulus and -20 to +15 % variation in strength for 0.25" overlaps. Tensile and compressive stiffness and strength have shown to have a strong correlation with gaps size. Staggering of defects almost always shows a lower knockdown in strength. Staggering of gaps (0.5") led to 20 % reduction in tensile strength and 35 % reduction in compressive strength, whereas staggering of overlaps (0.25") led to an increase of 20 % in both tensile and compressive strength. In case of gaps, fiber misalignment and resin rich pockets are formed post-curing. With an increase in compaction pressure, an increment in the amount of overlap was observed. The increment in overlap length leads to a reduction in thickness and tow misalignment [69].

Zenker [70] investigated the effect of gaps and overlaps on thermoplastic carbon fiber with polyphenylene sulphide (PPS) matrix. Gaps were found to have caused significant to detrimental reduction in both ultimate compressive and tensile strength even after going through autoclave cycle. The reduction in compressive strength could be as high as 25 % (autoclave) - 60 % (variothermal press). The reduction in tensile strength was 20 % (autoclave) - 80 % (variothermal press) [70].

Ghayour [71] experimented with the effect of periodically introduced 2.0 mm gaps (8 % volume) on medium velocity impact loading on thin carbon epoxy laminates (977-2/35-12 K HTS-145). Gaps led to a significant decrease (17 %) in maximum impact force and were found to accelerate delamination initiation and propagation. Gaps can also change the shape of delamination pattern and increase the area of delamination up to 50 %, lowering the delamination threshold compared to pristine/baseline samples. Local thickness reduction and local fiber volume fraction variation due to resin rich areas was also observed. These effects might decrease the bending rigidity (resistance against bending deformation) of the structure (as the bending/flexural rigidity decreases, so does the strength of the beam to resist bending) [71].

Rossi et al. [57] experimentally investigated the effect of half gap/half overlap on tension, compression and fatigue behavior of carbon-epoxy composites (unidirectional Toray T800S/3900-2 and cross ply woven Toray T400/3900-2). Compression (average reduction of about 20 %) was found to be more critical than tension (average reduction of about 5 %), possibly due to increased fiber waviness (greater than 5°). In general strength decreases as the number of defects increases while increasing the defect width does not necessarily decrease the maximum strength [57].

Suemasu [72] used experimental and analytical approach to study the effect of arbitrarily inclined gaps on the stress and strain distribution in Hexcel 8552/AS4 prepreg laminates. Even though both tensile and compressive strength showed significant decrease (~6 % increase in stress), contrary to expectation, tensile strength reduction was worse than compressive strength reduction. Their present analysis could not explain this unexpected result. It is however suggested that two-dimensional analysis is not sufficient to understand the underlying material mechanics. Three-dimensional and damage growth analysis accounting for the stress change in the thickness direction is more appropriate for such investigations. Localized stress increase in the neighboring layers at the gap ends should also be studied in detail [72].

Cartie et al. [73] investigated the effect of gaps/overlaps on crack propagation behavior in carbon-epoxy (AS4/8552 prepreg) laminates. The crack propagation behavior for interlaminar fracture under out-of-plane loading is adversely affected by gaps, worsening as the defect size increases. Under Mode I and Mode II loading conditions gaps were found to promote unstable crack growth by slowing down crack propagation [73].

Böckl et al. [74] studied the effects of gaps and overlaps on tensile, flexural and shear strength of prepreg laminates (HexPly 8552 unidirectional prepreg slit tapes with IM7). Tensile strength showed a significant knockdown for specimens with severe fiber undulations. For the same size of defects, gaps (20 %) had worse effect on tensile strength than overlaps. Owing to higher degree of undulations of load bearing fibers in case of induced gaps. Bending and in-plane shear showed a decrease in strength for gaps and increase for overlaps. Gaps caused a decrease of 11-29 % bending strength and 5 % in-plane shear strength. The knockdown in in-plane shear can be attributed to missing fibers (resin rich areas) in the gap regions. Overlaps led to an increase of 5-7 % bending strength and 6 % in-plane shear strength. A possible reason for the increase in bending strength is increased distance to the neutral axis because of out-of-plane undulations [74].

### 2.2.2. Analytical studies

For VSP laminates, if a constant thickness is desired, tow-drop areas at the course boundary are inevitable. These gaps result in small triangular resin rich areas. Blom et al. [56] numerically investigated the influence of these tow-drop areas on the strength and stiffness of VSP laminates. They concluded that regions with high fiber orientation angles in tow-drop areas serve as damage initiation sites. For wider tows, the tow-drop areas are larger and so is its negative impact on strength. Staggering was found to improve the strength, while no apparent relationship was found with tow thickness and strength [56].

Marrouzé and Abdi [75,76] used finite element approach using multiscale progressive failure analysis (MS-PFA) to study the effect of gaps and delamination on the strength of the laminate. They concluded that fiber waviness induced by the gaps reduces compression strength and the degree of waviness is affected by the height of the gap, or the tape thickness rather than the width or the length. Once the knockdown factor has reached the critical value, no further decrease in strength is observed by increasing the gap size (stress concentration is reduced) [75,76].

Fayazbakhsh and Nik et al. [50,77] used 'defect layer' method, a finite element approach to study the geometry and location of gaps and overlaps. A defect layer is a composite layer with embedded defects (gaps or overlaps), hence having modified properties and thickness. The defect area percentage (gaps or overlaps area per element area) is used to modify the properties of the defect layer. Gaps were found to have a significant effect on both buckling load (~12 %) and in-plane stiffness (~15 %). In contrast to which, overlaps were found to have a positive impact (~10 % increase in stiffness and ~30 % increase in buckling load) on the structural performance. The improvement in performance is however dependent on the loading and boundary conditions. They further investigated how the parameters governing the formation of defects impact the in-plane stiffness and buckling load. It was discovered that increasing the number of tows within a constant width course, that is reducing the width of an individual tow, leads to a reduction in occurrence of defects (gap and overlap area percentages within the laminate). Moreover, using a wider course leads to deviation in fiber angle from the centerline further leading to reduced buckling load. Similarly, using a wider tow significantly increases the number of defects (gap area percentage). Tow width of 12.7 mm creates a gap area of about 11.4 %, leading to a reduction in both buckling load (10-12 %) and in-plane stiffness (10-14 %) depending on the laminate layout. In summary, an increased number of small width tows leads to least gap and overlap defects within the laminate [50,77].

Li et al. [78] created a 3D meshing tool to automatically generate

ply-by-ply gaps and overlap complex models, in which both the ply thickness variations and the out-of-plane waviness are utilized. Reduction of strength as a function of magnitude and type of the defects can be predicted for various sizes and distributions of both isolated and interacting gaps and overlaps [78].

### 2.3. Critical analysis

#### 2.3.1. Defect geometry

Adjacent tows and plies adjust according to the neighboring layers to fill gaps and accommodate overlaps [52,57,66]. A **thickness reduction** is observed as the adjacent layers are pressed towards the gap due to high pressure in autoclave during curing. Similarly, for overlaps, thickness increment is restricted [51]. Similar observations were made by Rossi et al. [57], where after curing, the size of the gap decreased and the size of the overlap increased. The movement of the adjacent plies creates **out-of-plane fiber waviness** (tow misalignment) and resin rich areas [51,52,57,67–69]. Gaps can thus induce large waviness/undulations (up to 7°) [69]. The predominant factor for **strength reduction** (especially compressive strength) is this out-of-plane fiber waviness [52,57,62,67–69,72,74–76]. It is also observed that the severity of the fiber misalignments/undulations has a greater impact on the damage mechanisms than the number of defects in the structure [68].

With **staggering**, superposition of defects is reduced and the thickness variation and undulations are meagre compared to aligned defects [51,69]. Aligned, centered defects have worse effect on strength than staggered defects [51,66,68,78] and staggering of overlaps is especially useful for both tensile and compressive strength [69]. The use of a **caul plate** also reduces thickness variation and local fiber content variation in laminates. It limits buckling tendency and reduces the negative effect of defects on mechanical properties [57,63,78].

#### 2.3.2. Failure modes

The failure mode during tensile testing of specimens remained the same as pristine specimens [51,52,63,66,68]. Compressive failure in the presence of defects is driven by in-plane compression and interlaminar shear stresses [62]. Severe defects could lead to buckling before failure [63,67] and buckling could introduce premature delamination leading to fiber rupture [68]. For open-hole tension test, failure mechanism is initiated via matrix cracking and delamination at the hole edge. Following which, damage propagates across the width of the specimen leading to a complete collapse [51]. The failure mechanism for open-hole compression tests is characterized by fiber micro-buckling, followed by matrix microcracking and shear failure of the fiber–matrix interface [66].

#### 2.3.3. General trends

Gaps in general have worse effect on mechanical properties than overlaps. In general, gaps induce larger undulations than overlaps [69]. Compared to overlaps, gaps have been found to have a larger negative effect on tensile strength [68–70,74], compressive strength [69,70], flexural strength [74], in-plane shear strength [63,74] and buckling load and in-plane stiffness [50,77]. For overlaps, a possible reason for the increase in bending strength is increased distance to the neutral axis because of out-of-plane undulations [74].

Compressive loading for defect specimens is worse than tensile loading. A gap in fiber loading direction causes severe impact on mechanical properties due to missing fibers (resin rich areas) in the gap regions. Similarly, an increase in strength for overlap specimens is due to additional load bearing fibers [57,69,74]. The degree of fiber waviness/undulation in the laminate under tensile load is presumably reduced as fibers are straightened out. Conversely, under compressive loading, the undulations are exacerbated causing increased out-of-plane waviness [67]. Moreover, unnotched compressive loading (average reduction of about 20 %) was found to be more critical than unnotched tensile loading (average reduction of about 5 %), possibly due to increased fiber

waviness (greater than 5°) [57]. An exception to the above discussion is a study by Suemasu [72], where tensile strength reduction was worse than compressive strength reduction. While making strength evaluations, attention should however be paid to the representative area used for open-hole tension/compression test. An increased delamination area near the hole (reduced local stress concentrations) could lead to misleading overestimated strength calculations even though the site will eventually accelerate failure initiation [51,52].

Contradictory observations have been made regarding the effect of **number of defects** [57,62] and **defect size** on strength [69,75,76]. It is probable that a threshold/critical value exists beyond which the effect is stabilized. A generalized statement regarding the effect cannot be made for different studies due to differences in layup configurations, stacking sequence, defect amount and configuration, and sample thickness. For compressive strength, in one study [62] 0.762 mm gaps (26 ply laminate, centered defects) caused 20 % reduction, in another study [67] 1.27 mm gaps in all plies (8 ply laminate) led to a reduction of 27 %, and in yet another study [63] 3.175 mm gaps (11 ply laminate, centered defects) caused 52 % reduction. Similarly, under tensile loading, in one study [67] 1.27 mm gaps in all plies (8 ply laminate) led to a reduction of 35 %, in another study [68] 2 mm gaps (6 gaps in 24 ply laminate, centered defects) caused 1.3 % reduction and in yet another case [74] 3.175 mm gaps (4 gaps in 16 ply laminate, centered defects) caused 20 % reduction.

Variation in fiber volume fraction have been observed (39–67 %) in gap, overlap and defect free areas [57,67]. Strength scatter (15 %) due to quality variation in manufacturing process (process parameters) has also been observed [68]. Strength variation (5 %) between laminates manufactured using hand-layup and AFP manufactured samples are also witnessed [69]. It should be noted that among the work mentioned in this review, Sawicki and Minguet [62] and Woigk et al. [68] used hand-layup for sample manufacturing; Nguyen et al. [69] utilized both hand-layup and AFP; and Ghayour [71] compared hand-layup manufactured samples as baseline to AFP manufactured defect samples. It should also be noted that only Guin [67] normalized strength by cured ply thickness, which should be taken into consideration as thickness variation is significant for defect samples.

Another anomaly is marginally better performance of notched defect samples compared to unnotched samples [51,67]. The reason for this is again attributed to material behavior (stacking sequence, defect configuration) as notched specimen testing is less prone to minor defects [67].

In the past decade, 450–470 articles dealing with ATL/AFP have been published (Web of Science and Scopus). Among these, roughly 120 articles focus on thermoplastic materials. In this past decade, a total of 120 studies overall have dealt with defects (detection, analysis, effect and parametric influence) and only 15 of these relate to thermoplastics. It should be noted that the number of published articles in 2021 alone (ATL/AFP focus) were 110, out of which 30 focused on defects. Defect analysis has been the latest research hotspot, likewise once the number of studies related to thermoplastics come into focus, so will the defect analysis for such materials.

#### 2.3.4. Summary

Based on the literature listed above, it can be concluded that thermoplastics for ATL have received little to no attention for defect testing. In terms of stacking sequence, cross-ply layups and for test mode, fatigue testing has had very few representative studies so far. A summary of the effect of defects studies, highlighting the effect of defects on structural performance is listed in Table 1. The most important highlights are the following:

- Gaps are more critical for mechanical properties than overlaps, especially under tensile loading. Single, isolated and incidental gaps and overlaps have almost no effect on strength. A combination of defects has much worse effect than individual defects. In most cases,

**Table 1**  
Summary of effect of defects, OHC is abbreviated for Open Hole Compression test.

Reference Study	Year	Material	Layup (stacking sequence)	Defect location and occurrence (random, systematic, staggered)	Defect size (mm)	Mechanical tests	Effect on structure	Cause
Sawicki & Minguet [62]	1998	IM6/3501-6	Four-angle	One isolated overlap/gap defect in each of the 90° plies	0.762, 2.54	Unnotched compression and OHC	Negative	Out-of-plane fiber waviness
Croft et al. [52]	2011	Carbon-epoxy prepreg	Quasi-isotropic	Centre plies	One tow width and two tows thick	Tension, Compression, In-plane shear, OHT, OHC	Mixed	Fiber waviness
Falcó et al. [51]	2014	HexPly AS4/8552	Quasi-isotropic	100 % gap coverage, 0 % gap coverage, 0 % gap coverage with staggering	6.35 (width of the tow) × 29.9 (triangle)	Unnotched tensile and Open hole tensile	Mixed	
Lan et al. [63]	2016	Hexcel 8552/AS4/RC34/AW194	Alternating ± 45, cross-ply	Superposed, outer plies for shear, all 90° plies for compression	0.5 and 3.175 (half width of a tow)	In-plane shear and compression	Mixed	
Elsherbini [64,65]	2016	CYCOM977-2-35-12 K HTS-145	Unidirectional, cross-ply, four-angle	One gap in the middle ply	3 × 6.35	Fatigue	Negative	Delamination
Marouene [66]	2017	Cytec G40-800/5276-1	Quasi-isotropic	All the plies 0° and/or the 90° plies	Width of one fiber tow, 12.5 × 3.175 (triangle)	OHC	Mixed	
Guin [67]	2018	IM7/8552-1	Quasi-isotropic	Gaps in each of the 90° plies, gaps in all of the plies	1.27	Unnotched tension, unnotched compression, OHC	Mixed	Fiber waviness
Woigk et al. [68]	2018	Hexcel IM7/8552	Quasi-isotropic	Gaps, overlaps, staggered gaps and combination of gaps and overlaps	2	Tension and compression	Mixed	Ply waviness
Nguyen et al. [69]	2019	Toray T800S/3900	Quasi-isotropic (four angle)	0° and 90° plies	0.79, 1.59	Tension and compression	Mixed	Fiber misalignment
Zenker [70]	2019	Celstran CFR-TP CF60-01	Quasi-isotropic	Distributed and agglomerated	Gaps: 7.35, 2.5 and overlaps: 7.35, 1	Tension and compression	Mixed	
Ghayour [71]	2020	CYCOM 977-2/35-12 K HTS-145	Quasi-isotropic	Periodic gaps in all layers	Gaps: 2	Impact response	Negative	Local thickness reduction and fiber volume variation
Rossi et al. [57]	2021	Toray T800S/3900-2	Quasi-isotropic	Various configurations of defect width, number and orientation	Width: 1.27-2.54, length: 6.35	Tension, compression and fatigue	Negative	Out-of-plane waviness, healing of gaps during curing
Suemasu [72]	2021	AS4/8552	Quasi-isotropic	Arbitrarily inclined gaps and overlaps	3.175 (half width of tow) ± 0.5 (accuracy)	Tension and compression	Negative	Out-of-plane waviness, stress increase at gaps
Cartie et al. [73]	2021	AS4/8552	Cross-ply	Centre plies	Gap: 0.5, 3.175, 6.35 and overlap: 6.35	Short beam shear, Interlaminar fracture toughness	Negative	
Böckl et al. [74]	2022	HexPly IM7/8552	Quasi-isotropic, alternating ± 45	Around 90° center plies, center plies	3.175 (one tape width)	Tension, bending and shear	Negative (gaps)	Fiber undulations

a critical defect size can be recognized. Strength reduction is insensitive to any further increase in defect size beyond this critical value. Usually small defects as wide as 1.27 mm, lead to negligible changes. In essence, a few random defects will not have a detrimental effect, unless their appearance is repetitive and cannot be dispensed with. For VSP laminates and laminates with ply-drops, this problem persists. In this case, even though the defects cannot be eliminated, their position can be controlled. Staggering should help reduce the negative effects for such scenarios. Another strategy would be to use large number of tows with small width to have minimum defect area.

- Gaps and overlaps lead to secondary defects such as fiber waviness, undulations, misaligned fibers, resin rich areas, variation in thickness and fiber volume fraction. These combined effects lead to a knockdown in mechanical properties and might serve as damage initiation sites, especially delamination. Fiber waviness is the most common manifestation of such defects, which is influenced by several factors such as defect height, defect geometry, location within the laminate and fiber and ply orientation angle. Use of a caul plate is recommended for lesser undulations.

### 3. Monitoring techniques

In-process inspection for ATL and AFP until recently mostly relied on labor and time intensive manual visual inspection, where probability of undetected flaws is quite high. Automated in-process inspection solutions help in early detection, localization and disposition of defects. This in-turn increases productivity (reduced inspection times), reliability (quality assurance) and time and cost saving for post consolidation/curing flaw repair and part scrapping. A distinction is made between ply-by-ply, inline/in-situ and online monitoring techniques. Ply-by-ply are static systems that wait until after each layup and the ATL machine is inactive to conduct inspections. Inline/in-situ and online systems are capable of inspecting while the ATL machine is performing the layup. An online system gives instantaneous real-time results with which the process can be controlled effectively during the process run. Inline/in-situ systems monitor the running process but need time for post-processing of results. Inline systems eventually aim to have online capabilities. Commonly used in-process monitoring techniques are shown in Fig. 4.

There is no commercial online monitoring system available for integration in ATL and AFP processes. There are however, mentions of

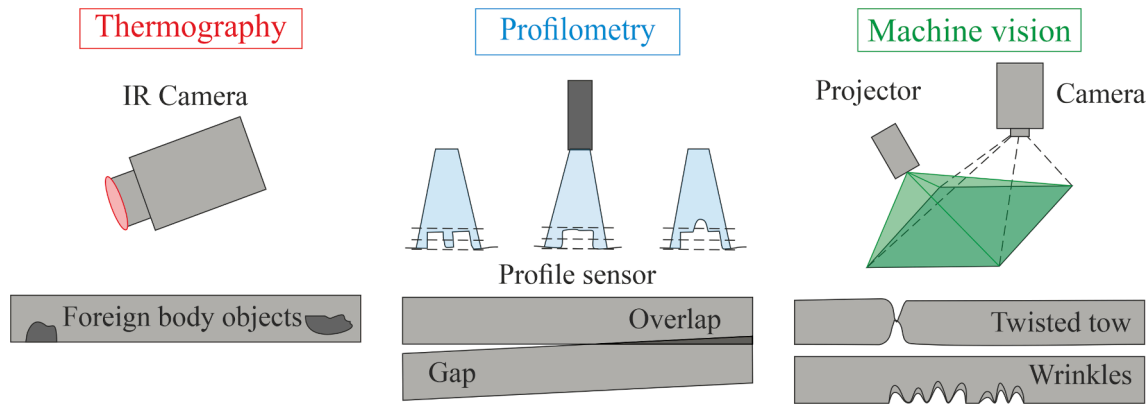


Fig. 4. Detection of FOD using infrared camera (left), gaps and overlaps detection using profilometry (middle) and detection of twisted tows and wrinkles using machine vision (right).

new advances, published studies and prototypes. The sensor-based monitoring tools and their applications and results are discussed next.

### 3.1. Thermography (IR camera)

Denkena and Schmidt et al. [29,47,79–81] proposed an inline monitoring tool utilizing thermal camera. Thermal contrast between the laid-up tow and the substrate is used for identifying defects such as gaps, overlaps, twisted tows, FOD and bridging. A combination of path planning and tow localization helps in online detection of temperature anomalies. The effect of process parameters such as lay-up speed, tooling temperature and compaction pressure on the thermal contrast was also analyzed. Brüning et al. [81] used machine learning approach for the same system for planning, optimization and inspection of the AFP processes. Automated data capturing, storing, modeling and optimizing is accomplished. The authors further used deep learning-based method, convolution neural networks (CNN) for classification of thermographic images [80]. A laser triangulation sensor is used to measure the contour of the tow with respect to the subsurface. Width and thickness of the tow are used to deduce the cross-sectional area. Moreover, using the cross-sectional area and the supposition of a constant dry fiber roving, the fiber–matrix-ratio is deduced. Thermal camera is used to detect thermal contrast for inhomogeneous temperature distribution caused by varying tow geometry and fiber–matrix-ratio. Hence, incorrect geometry, varying fiber–matrix-ratio and temperature difference defects are monitored as a part of the quality assurance concept. Different defects are generated for training the CNNs. The CNNs are trained and tested for different tasks such as classification of prepreg materials, material individual classification of defects and material independent classification of defects. However, possibly due to limited training data set, the transferability of characteristics of each class for reliable monitoring of non-trained prepreg materials is not given so far. The presented concept still needs further investigations to become more reliable and adaptable for different prepreg materials. The high frame rate of the thermal camera, 100 Hz, makes the process suitable for online application, but a concept of the same is not discussed. Furthermore, if a combination of data from both laser triangulation sensor and thermal camera is desired, the data acquisition speeds, processing speeds and analysis speeds of both systems should work in synchronization for optimum online solutions [80].

Similar monitoring approach was adopted by Juarez and Gregory [28,82–84]. They demonstrated in-situ inspection of individual ply layers with a thermal camera using a preheated substrate as a through transmission heat source. Gaps, laps, twists and puckering can be identified as is. With further data processing, areas of reduced adhesion can be identified as well. Two methods of data collection are identified. In-situ method, similar to Denkena and Schmidt [29,47,79–81], where defects are identified along the layup length using the thermal contrast

between the ply being laid and the substrate. Here the substrate should be colder than the ply being laid for sufficient thermal contrast. The second method is referred to as a ‘scan’, where data is collected after the ply is already placed. This top surface is heated using the main heat source mounted on the ATL/AFP head and the temperature anomalies are detected as defects. Based on the method used, the defect will appear either as a hot or a cold spot, for example, delamination would appear as a cold spot in in-situ inspection but as a hot spot in a scan inspection. The scan approach is useful when position data is not easily available and position is inferred based on the part geometry, therefore having a constant speed and tow orientation helps in accuracy. Moreover, scan approach is better in identifying tow peel-up that occurs over time after the course is placed [28,82–84]. This system was then further developed in to ‘In Situ Thermal Inspection System (ISTIS)’, as a fast and reliable real-time inspection system requiring minimal modifications to the manufacturing process [28]. Calibration and performance assessment tests were performed analyzing the capability of ISTIS in detecting artificial manufacturing induced defects (gap, overlap and FOD). Most defects can be identified with an error accuracy of 0.762 mm of the actual size of the defect. Thick FOD defects lead to bridging effects and were difficult to detect. Data reduction methods to account for perspective and lens distortion are also described.

### 3.2. Profilometry (laser triangulation sensor)

There have been a few mentions of use of profilometry for studying compaction behavior of dry fibers, such as, detecting cross-sectional profiles or contour for different compaction forces [85]. The use case for ATL/AFP integrated process started more than a decade ago. Early work using laser light-section sensor system (LLSS), involving carbon fiber textile preforms was done by Schmitt [86–88]. The contour position of each textile layer is determined through edge scanning of the carbon fiber textile preforms. The exposure time for data acquisition has to be adapted to the reflection properties of the surface of the material under inspection. Higher exposure times are necessary for carbon fiber fabrics due to their poor reflection properties. Attention should be paid to the number of detected surface points. The lateral measurement range may get decreased if the detected points are insufficient [86]. The authors further developed a combined machine vision and LLSS based inline inspection system. The inspection system is specific to textile reinforcement layers and serves as a guide for dimensional and placement accuracy. A closed-loop process control is employed to achieve the said objectives. Here laser light-section technology based on the principles of triangulation is utilized for the detection of the fiber alignment and placement of the fabric layers and the machine vision system is used for determining the fiber orientation, detecting flaws in the textile structure and intelligent material and fabric recognition and

classification [87]. Further modifications and experiments were done for prepreg tapes, instead of textile preforms. LLSS is used to conduct an in-process surface scan. Height profiles are used to derive 3D geometrical measurements. The height profiles are further processed to obtain sub-pixel accuracy. Two sensors are used to measure the geometry of the tape and the edge position respectively. Tape width is found to be measured with a combined standard uncertainty of 54  $\mu\text{m}$ . The measurement results obtained during the layup are compared with a CAD/CAM model. This comparison helps in detecting gaps, overlaps and misalignment [88].

Krombholz et al. [89] developed a quality assurance system consisting of two laser light section sensors. The relative position of adjacent material is determined, which can later be used for path correction. The developed strategy works on forerun, a real-time and a follow-up sensor system. The edge position of a laid-up neighbor material is detected by the forerun sensor system. A subsequent path correction is enabled to control material overlaps and gaps. The real-time sensor system controls the contact pressure with the help of a force-torque sensor system and compensates for vibrations using sensors and actuators. The monitoring system is used to detect layup defects, such as gaps, overlaps, and foreign objects. Based on the measurement results, rectification can be implemented. Moreover, the measured edge contour from first sensor can be used as the base for the forerun edge detection of neighbor material courses for the second sensor. Thereby, online path correction and gap control are enabled [89].

Sacco et al. [90–93] developed a ply-by-ply machine learning based vision system inspection using laser profilometry. It was shown through case studies that the automated defect detection method gives very precise information with respect to the size and shape of the defects. The inspection system was also utilized to aid in the repair of composite cylinders, as a part of the case study. This precise characterization of defects serves as a step forward in evaluation of defect effects on structural performance. The data from the inspection process can further be used for prognostic analysis of the effect of defects on the structure. Mapping the inspection data back to the machine processing parameters may allow online instantaneous defect detection. The data can further be mapped to the process planning stage, an area currently under development for ATL/AFP [90–92]. The system was later upgraded to a new network architecture (U-Net topology instead of ResNet structure) and loss function (Jaccard loss). A total of 15 defects can be identified and classified with RGB (Red, Green, Blue) color values [93].

Another algorithm, called cross-sectional line-processing algorithm for processing point clouds for laser profilometers is presented by Tang et al. [94]. The experimental results indicated real-time detection of gap, overlap, FOD, wrinkle, bridging and blister. Most algorithmic approaches try to treat the point cloud as a whole, instead of individual profiles. The algorithm proposed by Tang et al. focuses on individual treatment of laser lines. The processed results are then clustered together. In a first step, feature extraction is carried out, where segmentation is used to find defects and layup features. Feature clustering is performed in a second step, constructing the extracted feature clusters of multiple laser lines. The layup defects can therefore be recognized. Information related to the dimensions of the layup features can also be extracted. The overall defect type recognition accuracy rate is about 78 %. Misclassification of similar defect types, imperfect defect criteria and small sample size are a few shortcomings of the study [94].

They went on to adopt an improved deep learning algorithm with two stage segmentation, called AFP-seg [95]. In a first stage, point clouds are fed into a semantic segmentation network. The point clouds at this stage already contain information related to the sampling position data. After going through the segmentation network a semantic label is attached to each point. To decrease the segmentation difficulty, the fused point clouds are annotated into four typical labels. Profile and point cloud-based datasets are created from these annotated point clouds. In the second stage, post-processing algorithm is used to cluster the point clouds with specified semantic labels obtained from the first

step. Information specific to the defects regarding defect types, sizes, and positions is acquired. About 200 profiles (128,000 points) can be processed within one second.

The experimental results showed that the defect missing detection rate is less than 5 % and the defect classification precision and recall could be above 0.77 and 0.84 [95]. Compared to their previous approach, segmentation and clustering operations can be executed independently and asynchronously. The new method is found to have reduced processing time (33–66 %), lesser sensitivity to the noise and can handle more complex situations. The method is modular enough to be easily adjusted based on the actual engineering inspection specifications, for instance a real-time AFP in-process inspection system [95]. Meister et al. [96,97], reported difficulties in distinguishing gap and overlap defects due to similar geometric properties after point-cloud transformation into gray scale images. The method proposed by Tang et al. [95] was able to accurately classify all gap and overlap defects as they have significant depth differences after segmentation. Unlike [90], who assigned a label to each type, just four types of labels were found to be enough to be fed to the post-processing algorithm, that further refines the inspection results. A few drawbacks of their own method have also been pointed out. Point-wise annotations were found to be expensive (time intensive), and the consistency of data annotation cannot be ensured easily. Furthermore, bigger data set is needed to train a better generation capability network. A few suggestions were also made to improve the performance. Semi-supervised, weakly supervised and machine learning methods can be employed to boost the defect type classification performance. Point cloud object detection framework can be considered to accelerate the inspection efficiency. The AFP process can be further optimized by smart Industry 4.0 solution such as digital twin, taking the help of complete in-process inspection system [95].

A sample illustration of visualization of defect detection using infrared thermography and profilometry is shown in Fig. 5. The figure depicts the machine integrated use of two of the recommended best practices for defect monitoring. Gaps, overlaps and material geometry before and after consolidation are detected and monitored using profilometry. Uneven bonding and FOD (temperature anomalies) are detected and localized after consolidation using infrared thermography.

### 3.3. Machine vision (laser projector and camera system)

A review of real-time structured light profilometry is provided by Jeught [98]. Technical improvements both in terms of hardware and data processing are discussed. The tradeoff between speed and accuracy to produce high quality 3D surface maps is highlighted. The underlying principles that allow these surface mapping systems to operate in real-time applications have been presented. They also made suggestions for further improvements pertaining to the present challenges [98]. A review of state of the art in defect detection based on machine vision is provided by Ren et al. [25]. Machine vision is a type of real-time inline detection, consisting of two components, optical illumination platforms and image acquisition hardware. A suitable combination of both is a prerequisite to produce high-quality images. For defect detection, further image processing and image analysis are needed. In the review, traditional defect detection algorithms are discussed and the importance of deep learning is highlighted followed with a description of defect classification, localization and segmentation. The real-time performance is dependent on the amount and complexity of data. Another challenge is defect detection dependence on the image acquisition environment, which should be reduced to increase the robustness. In general, an intelligent algorithm that can provide real-time solutions with efficiency, speed and accuracy is still an open area of research [25]. Pertaining to ATL and AFP, noteworthy studies are discussed hereafter.

Tao et al. [99] devised an online defect detection system using multi-lighting source illumination system, and a charge-coupled device (CCD) camera. Images are captured and after pre-processing, a region of interest with gaps is identified using computer vision methods. With the

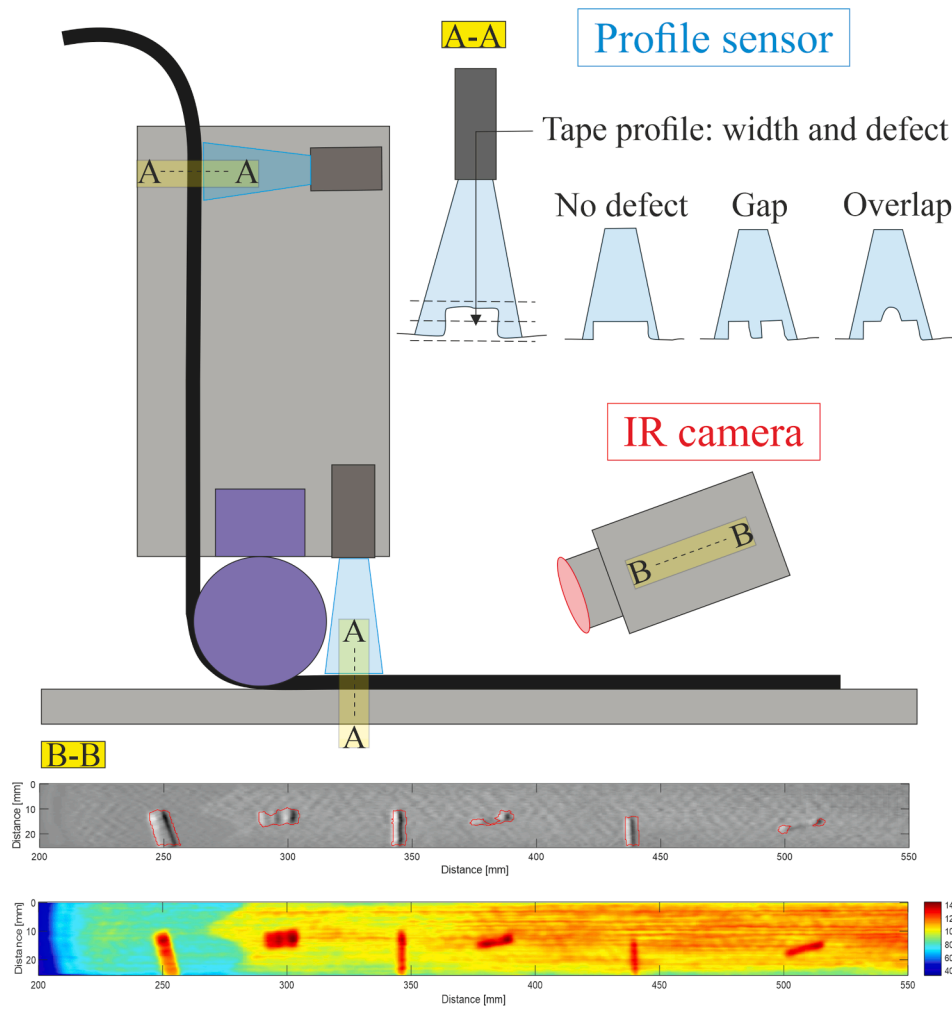


Fig. 5. Sample defect detection using profilometer (laser triangulation sensor) and infrared thermography.

help of edge detection and post-processing methods, gap widths signifying placement accuracy of each fiber tows are acquired. To improve accuracy, an image enhancement method based on histogram stretching is applied. A maximum absolute error of 0.034 mm corresponding to a maximum relative error was 7.17 % was achieved during experimental investigations [99].

Machine vision setup has also been used at National Aeronautics and Space Administration (NASA) for Automated Ply Inspection (API) [26]. The utilized sensor is a commercial-of-the-shelf (COTS) laser line scanner which acquires the two-dimensional profile (typically comprised of 1000– 1500 discrete points) of a laser line projected onto the layup surface. A dense point cloud covering the whole surface is generated by automated scanning. Owing to the very high rate of line scan, a large, high density, very accurate data is generated, capturing the minute details of the layup surface. Using a-priori knowledge of the position of the sensor, the 2D data points are converted into 3D coordinates. The point cloud contains the identity and location of layup features important to part quality such as tape edges, tape ends, overlaps, gaps and splices. These features embedded in the point cloud have to be extracted for further processing and defect recognition and localization. A successful demonstration of initial trials is mentioned, along with the need for improved feature extraction and classification is highlighted [26].

Cemenska [100] developed a ply-by-ply inspection system comprising of laser profilometer, laser projector and camera. Laser profilometers are used to detect gaps and overlaps, while images from camera are used to measure ply boundary locations [100].

Shadmehri et al. [101,102] implemented a laser-vision system to

detect ply location, tow angle deviation and gap defects. They pointed out two concerns for effective implementation of the system: reflection interference with image capture and accuracy loss for highly contoured surfaces [101,102].

Zambal et al. [103,104] formulated AFP defect detection as an image segmentation problem and introduced an end-to-end deep learning defect detection and segmentation approach using artificially generated training data. They used a probabilistic model for the generation of training images and annotations. A deep neural network inspired (U-Net architecture) is implemented. This network infers pixel labels from observed depth maps which are generated using a laser light scanner. They achieved a combined classification accuracy of 99.4 % for gaps, overlaps, missing tows and fuzzball. However, the accuracy of defect detection for real data was approximately 95 %, lower than the accuracy for synthetic data [103,104].

Schuster et al. [105] proposed a flexible concept for inline data acquisition, storage and evaluation. The laser light sheet measurement setup comprises of a line laser with a deflection mirror and a camera. Instead of evaluating the point cloud map, profile depth maps are evaluated. The pixel coordinates signify x and y directions. The pixel value/z-value denotes profile height. Even though lacking exact calibration, this approximation can still be used with computer vision or machine learning algorithms. After processing, the defects can be mapped to a 3D point cloud. For the present system, a 2D evaluation using computer vision is used to detect geometric tolerances and defects. Inline evaluation capability of defects such as gaps, overlaps and missing tows is also discussed. For inline detection, 2D evaluation of profiles is



considered. The evaluation speed will depend on a combination of triggering, acquisition and evaluation speeds. Here the speed requirements are mostly dictated by the maximum layup speed. For a complete inline solution, geometric limitations such as geometric footprint of highly reflective carbon tapes have to be considered as well [105].

Mesiter et al. [96,97,106,107] conducted detailed experiments for imaging sensor data modelling, evaluation, segmentation and classification of defects using laser line scan sensor. The setup consists of a laser line scanner and a camera. The laser line scanner projects a line, which gets reflected back to the camera. The laser-camera system is then adjusted according to the surface being mapped. For each laser line height profile, an image is captured. These images are clustered together to create a surface depth map. First crucial step towards a reliable inspection system is accurate image data acquisition. The image quality is affected both by the material and the sensor system used for data acquisition. A model is presented to characterize this effect of the sensor system, in particular the laser spot. Modelling sensor behavior for various scenarios helps in evaluating signal quality. Using this information, optimization strategies for the sensor parameters and the sensor setup are devised. Moreover, the behavioral variation of defect detection and classification algorithms with signal quality can be evaluated [106].

The authors [96] also presented a review of image segmentation techniques for layup defect detection for AFP. They evaluated 29 statistical, spectral and structural algorithms (not including machine learning) against nine criteria based on literature and process requirements. Out of these 29, seven algorithms were studied experimentally in conjunction with a laser line scanner. The data contained 50 sample images for five defect categories each. Adaptive Thresholding and Cell Wise Standard Deviation Thresholding were found to be most effective in detecting defects. They achieved an accuracy over 97 %. However, it should be noted that individual case specific pre-processing might be required for images prior to effective segmentation processing [96].

The authors [97] further investigated methods for synthetically generating training data sets that can be used for defect classification. Large training data sets can be quite difficult and time consuming to produce in a reliable production process, hence the need for synthetic data. A rather small number of real defect images, 50 in this case, are used to generate large amount of synthetic training dataset. The defect images represent six common manufacturing defects and a Deep Convolutional Generative Adversarial Network (DCGAN) is employed for image generation. These synthetic images are used to train the neural network classifier. The GAN-Train GAN-Test method was applied for the validation of artificially generated image data. It should be noted here that the method inherently links the diversity and realism of the images to another defined comparison data set and should be treated accordingly. It is also important to ensure that the initial training images are diverse and contain many potential defect characteristics. The most critical aspect for such an approach is extracting such striking defect images from a real process. The word 'striking' implies contrasting characteristics, which can be used to differentiate between various defect types. Since the defects occurring during the actual process have very similar characteristics, there is a possibility that the minimum quantity of training images mentioned here might not be enough [97].

An approach for analyzing the classification procedure of fiber layup defects is also presented, where 20 Explainable Artificial Intelligence methods from the literature are evaluated [107]. The Convolutional Neural Network is evaluated for its applicability with unknown and manipulated data. It was found that Smooth Integrated Gradients and Deep Learning Important Features with Shapley Additive Explanations are suitable for such an evaluation [107].

Brysch et al. [30] used SiamMask (Siamese object tracking) network for automatic image processing. The inspection system is camera based. The images are segmented and then classified. Artificial neural network (ANN) is trained to recognize individual carbon fiber tapes and to

subsequently segment them for further analysis. This object segmentation is then post-processed to identify individual tapes. The SiamMask network runs on two networks, one of them acts as a template and the other as a detection-branch. A pre-selected marked image section is fed to the template branch, which serves as a template for processing the remaining images. The template branch provides an abstract representation of the object. The detection branch uses this representation as a search template. The detection branch is fed the rest of the images individually as search images and much in the same way as the template branch, performs abstraction. A probability analysis of area of interest containing the defect is performed. The segmentation contains information about the detection of defects such as existence of gaps, overlaps, and their size. The distance and angle between the CF tapes is also detected. A measurement accuracy of 0.0422 mm is achieved with the present setup. For improved results, a few points should be noted, virtual training should be applied conditionally, accompanied by a manual check to avoid segmentation errors. A larger training data set with realistic parametric adaptations will help with a robust system. Recent developments in Siamese networks might allow direct feature extraction bypassing the need for segmentation. The primary aim of monitoring in this case is machine control with optimized layup quality using automatic real-time machine movements, which can further be used for enabling a digital model [30].

### 3.4. Other approaches

Fiber Bragg grating (FBG) sensors have been used increasingly in ATL and AFP processes for residual strain and temperature monitoring [108–112]. Simultaneous strain and temperature monitoring using a single FBG in real-time is also shown to be feasible. An added advantage of using FBG sensors is that they can later be used for structural health monitoring (SHM). In terms of processing induced defects, FBGs are shown to be able to detect gaps and overlaps [113].

Schmidt et al. [114] used eddy current (EC) testing for NDT (after manufacturing) and online inspection of AFP defects. As an NDT technique, EC can be used to detect FOD and fiber orientation but with limitations in penetration depth and resolution. Tests were also performed for uncured prepreg with the primary aim of detecting fiber misalignment. Due to long measurement time and low resolution, a complete online solution is not feasible [114].

Han et al. [115] investigated the use of strain gauges to determine a relationship between stress wave and manufacturing induced defects. Ultrasonic tests and optical microscope were conducted after curing to formulate a relationship model for voids. Stress wave and ultrasonic tests results before curing are combined with ultrasonic test results post curing to estimate the void content before curing. Better accuracy and model formation are required before the system can be applied online real-time detection of internal defects [115].

Rajan et al. [55] used in-situ StereoDIC (Digital Image Correlation) to study the behavior of prepreg slit tape during AFP. The occurrence of out-of-plane wrinkle and in-plane deformation were investigated. Even though the experiments are conducted in-situ, the extensive post-processing and more importantly invasive behavior of speckle pattern application for each ply makes the technique unfeasible for inline use [55]. Shadmehri [116] used DIC as well to study in-situ shape deformation for thermoplastic composites. A digital projector was used to project the speckle pattern instead of using paint. It was shown that gaps and overlaps as small as 0.4 mm can be detected. The early proof of concept study was also demonstrated for recognizing twisted and damaged tow. The processing time and practical realization on a test bench are however not shown [116].

### 3.5. Critical analysis

Most of the studies and published works represent an initial technological readiness level, currently focusing on feasibility studies and

performance tests. Since a matured and established performance phase has not been achieved yet, a direct comparison regarding absolute values and exact results (defect detection accuracy, resolution and speed) could be misleading. However, general similarities between different monitoring techniques concerning same defect type and comparisons between various defect types using same monitoring technique is useful in establishing best practices.

Considering impact to the structural performance, gaps and overlaps are the defects of concern. Wrinkles and twists are of concern for VAT/VSP laminates and prepreg materials. FOD and bonding defects are frequently encountered defects. Generally, these defects are divided into three geometric categories for the ease of classification and segmentation. FOD; gaps and overlaps; and wrinkles and twists. Gaps and overlaps have very similar geometrical characteristics, flat with almost no topological changes. Wrinkles and twists protrude from the layup surface and lead to prominent height differences. Geometrically, FOD lie somewhere in between these two categories. Gaps and overlaps can be detected using edge detection, however surface detection is required for the rest of the defects.

In one study using thermography, the gap detection rate has been found to be only 0.8–6.5 %. Moreover, with 0.15 mm wide tow gaps, the edge between single tows cannot be detected [29]. In another study using thermography, FOD (as small as 3.175 mm) can be detected with an average size estimation error of 6 %, while gaps and overlaps (1.2–3.5 mm) can be detected with an error of 15 % [28]. It should be noted that bonding defects might not create visually detectable features and thermal analysis might be needed in this situation. Also, small FOD that might go unnoticed in other techniques, might still create thermal contrast that can be visualized as a sub-surface defect using thermography. FOD and bonding defects can thus be detected well using thermography, compared to other techniques.

In one study utilizing profilometry, the classification accuracy for gaps (0.77), overlaps (0.43) and twists (0.75) has been found to be on par with wrinkles (0.01) and FOD (0.0) for Fully Convolutional Network (FCN). Wrinkles (0.49) and FOD (0.31) are the most mis-identified defects in case of no defect. FOD are often mistaken for twists (0.63) [90]. Similarly, in another study employing profilometry, gaps (1.0, 1.0), overlaps (1.0, 0.75) and wrinkles (1.0, 0.81), have shown better classification accuracy and recall than FOD (0.25, 0.5) [95]. Profilometry is better suited for gaps and overlaps detection than any other defect type.

Difficulties have been reported in distinguishing gaps and overlap (similar geometric properties) using machine vision. Defect detection classification rates with machine vision using CNN architecture for wrinkles (100 %), twists (100 %) and FOD (100 %) using different algorithms are slightly better than those obtained for gaps (96.81 %) and

overlaps (98.94 %) [96,97]. Wrinkles and twists can be detected easily using machine vision.

### 3.5.1. Summary

A tabulated summary of monitoring techniques, working principles and best practices by defect type can be found in Table 2. Best practices and most promising approaches for defect detection involve:

- Thermography: FOD
- Profilometry: Gaps and overlaps
- Machine vision: Wrinkles and twists

For practical applications where only one monitoring technique is preferred due to cost restrictions, machine vision would be able to detect most of the defects successfully.

## 4. Defect rectification

As discussed previously, defect identification leads to defect rectification. Since the focus is strictly manufacturing induced flaws, rectification strategies covering such defects are discussed. Commonly known strategies such as repass and autoclave are not mentioned as they have been used mostly for voids and consolidation related quality improvement.

A few strategies have focused on redistribution of defects, such as staggering and layering techniques [56,117]. Staggering is used to offset the defects in different locations through-the-thickness of a laminate. To further restrict the curvilinear ply defects to the interior of the laminate, the two outer plies in a symmetric lay-up are constrained to straight fiber plies [118]. For VAT/VSP laminates, a combination of ply staggering and 0 % gap coverage is used to lessen the influence of defects [51]. These techniques can reduce or reorganize the defects but cannot eliminate them completely. Defect rectification by elimination and rework is rarely discussed in literature.

Kim [119,120] devised a technique called ‘Continuous Tow Shearing (CTS)’ to reduce process induced defects such as fiber wrinkling, fiber discontinuity and resin rich areas for variable angle tows. The device uses in-plane shear deformation characteristic of dry tow to avoid gaps and overlaps for continuously shifting tows. The maximum shear angle however limits the layup of half circle. The laminate also has induced thickness variation and the process in general has limited layup accuracy and speed compared to conventional AFP [119,120]. CTS has been adopted and developed further by iCOMAT Ltd. into rapid tow shearing (RTS), having a higher deposition rate [121].

Rakhshbahar [122] proposed using Additive Layer Manufacturing

**Table 2**  
In-process monitoring techniques, principles and best practices for defect types.

Technique	Approach	Defects	Defect type	Detection type	Best practices	Rectification/control	Requirements/drawbacks
Thermography	Temperature anomaly	Gaps, overlaps, twisted tows, FOD and bridging	Surface	Ply-by-ply, inline and online	FOD	Temperature	Thermal contrast, image processing
Profilometry	Laser triangulation	Gaps, overlaps, twisted tows, folds, wrinkle and FOD	Edge, surface	Inline and online	Gaps and overlaps	Layup, width and force	Reflection, algorithm accuracy, sample size
Machine vision	Laser projector and camera	Gaps, overlaps, twisted tows, wrinkle and FOD	Surface	Inline and online (limited)	Twisted tows and wrinkles		Reflection, accuracy loss for highly contoured surfaces, point cloud computing, algorithm speed
FBG	Strain/stress	Strain, gaps and overlaps	Volume	Inline and online		Strain, SHM	Intrusive, stress concentration
Eddy current	C-scan	FOD, fiber orientation	Surface and volume (limited)	Inline			Penetration depth and resolution, online capability (processing time)
Strain gauges	Strain/stress	Strain, voids	Volume	Inline			Intrusive
DIC	Speckle pattern and camera	Wrinkles, gaps, overlaps and twisted tows	Surface	Inline			Intrusive, speckle pattern projection, processing time

(ALM) to fill gaps produced in thermoplastic AFP laminates. Gaps are detected using profile sensors after placement and then are filled with the aid of a 3D printer with carbon continuous-fiber reinforced plastics. The mechanical properties of laminates with filled gaps were better than laminates with gaps and quite similar to the performance of laminates without gaps. Although this requires integrating the 3D printer head with the AFP head [122].

Clancy et al. [123] developed a spreading system for thermoplastic tapes, which can provide continuously tessellated tapes, to eliminate gaps and overlaps occurring in VAT/VSP laminates. The device works pre-consolidation, where pressure and heat are applied to produce desired width spread. Constant width tapes are shown to be produced with negligible changes in cross-sectional area, void content and fiber volume fraction before and after consolidation. There is however no reference to continuously variable width tows or if the system can be adapted for such a requirement, which is a necessity for VAT/VSP laminates. Besides, the tapes effectively undergo two consolidation cycles and the mechanical characterization to analyze effects of spreading on structural performance remains to be investigated [123].

Sacco et al. [93] conducted experimental investigations to examine the effect of manual rework on the part quality. They produced a doubly-curved part using AFP which was inspected using their custom automated inspection method [90–92], repaired and inspected again. The effect on size distribution of defects before and after repair was analyzed. They discovered a new defect, transverse wrinkling, forming as a result of rework. It was found that gaps and overlaps show limited improvement to worsening effects after manual repair, possibly leading to other defects in the final laminate including wrinkles, length mismatch in fiber direction or migration of defect to a different location. Similarly, only large wrinkles should be reworked, as the rework on small wrinkles causes them to redistribute to other locations. As noted by the authors themselves, the fundamentals of rework as a mechanism to change the laminate quality are poorly characterized. They also pointed out some future avenues for further research, such as rework-time considering ergonomic and human factors, mechanisms to improve rework-time, rework and repair at lamina and laminate level and simulation effort for repair and rework, with a focus on effect of rework on structural performance post-cure. One such scenario would be examining if the rework induced residual stresses in the laminate [93].

#### 4.1. Remarks

Design modifications such as staggering, layering [51,56,117] and adjusting stacking sequence [118], distributes and limits the negative effect of defects, following which defects might still have to be rectified. Going beyond defect removal and reworking [93], preemptive strategies for defect elimination and prevention would be immensely helpful in furthering process reliability. This approach inherently necessitates process and parameter control. To reduce the defects even further, the working principles of the machine have to be customized, such as tow shearing [119–121], tow spreading [123] or combing two different techniques [122]. A complete defect management and monitoring concept requires crucial understanding of defect significance (effect of defect), defect detection, defect treatment and process control.

The results of inline monitoring could be best utilized when the ply-by-ply (single individual layer) inline inspection is used immediately for defect management. The learnings from effect of defects studies should be utilized here to ascertain the severity of defect to the structural performance and if the defect is significant enough for removal and rework. Here, attention should be paid to snowball/cascading effects of added uncertainties on untreated defects over multiple layers. The impact of an incidental single defect gets exacerbated when combined with multiple defects present throughout the laminate. However, as pointed out earlier, reworking each individual defect (especially of smaller size) might not be the best strategy either [93]. Large defects

should be worked upon immediately and small defects should be kept in check unless leading to critical damage to the structure.

From a monitoring perspective, sub-surface defects (large ones unless reworked) might lead to new morphed defects which could be difficult to detect using existing geometrical defect classification criteria. Even if not leading to new defects, the existing sub-surface defects can only be seen partially via thermography. Optical vision-based techniques would not be useful here. A data-base creation and documentation is therefore highly recommended.

## 5. Conclusion

Among the various manufacturing defects, gaps are the most prevalent ones that cause the most damage to the structural performance of the laminate. Their occurrence is predominant in steered tows, as the formation of gaps and overlaps is unavoidable for certain path geometries. For prepreg steered tows, wrinkles are classified as both primary and secondary defects. Gaps and overlaps in such layups lead to in- and out-of-plane wrinkle formations. Most process induced defects, FOD, gaps, overlaps, twisted tows and wrinkles can be detected inline. Infrared thermography, profilometry and machine vision have been the leading technologies for such endeavors. Thermography has proved itself useful as both an inline monitoring and NDT quality assurance tool. However, when focusing on highest probability of defect detection with greatest accuracy, a combination of different techniques should be favored over individual methods. Similar to NDT results, best-practices for defect types are often a result of contrasting criteria and two or more techniques would help to better evaluate, validate and enhance the final results.

In-process defect detection is the first step towards a holistic quality assurance approach for process manufacturing. Using the knowledge base of effect of defects on mechanical properties and progression of defects during service life, strategies for defect treatment could be developed. Defect rectification based on the severity of defect may comprise of removing the defect, reworking the locally impacted area and repairing the overall structure. Certain parts might still have to be rejected or replaced, but the probability of that happening reduces drastically and the anticipation becomes more reliable. In the longer run it saves cost, time, material and effort. More research is required for characterization of defects and the impact they have throughout the service life of the structure. This will include focusing on different material types (thermoplastic), stacking sequences (cross-ply) and testing modes (fatigue). A combination of defect types should be tested at multi-scale level to have robust simulation and prediction models. Defect anticipation when closely linked with process control leads to precise layups having very high tolerances. This impacts both, the level of automation and the scale of manufacturing, bringing the technology closer to the goals of Industry 4.0 and Manufacturing III.

The future research in this area would focus more towards defect reduction and elimination with the help of pre-established tools. Monitoring concept should be used as a part of process parameter and defect control. Based on the defect detection and rectification approaches, a summary of in-process inspection technologies that demonstrate the capability to be used as an active element (closed-loop active feedback control) of in-process control are summarized in Table 2. Thermography can be used for active temperature control. Thermal degradation, and bond inhomogeneity (dis-regarding material variation) can be controlled by having very strict tolerances for temperature variation. In terms of defects, FODs can be detected real-time. Because of the nature of the defect that it occurs post layup, FODs can be reworked/removed based on the severity of their size and effect of structural performance. Profilometry can be used for placement defect control. This can be achieved partly prior to and during the layup itself. Based on path planning, width of the tow/tape and compaction force can be controlled accordingly. This can even be implemented for defect prevention (gaps).

## Declaration of Competing Interest

The authors declare that they have no known competing financial interests or personal relationships that could have appeared to influence the work reported in this paper.

## Data availability

Data will be made available on request.

## Acknowledgement

The authors kindly acknowledge the financial support through project InP4 [project no. 864824] provided by the Austrian Ministry for Climate Action, Environment, Energy, Mobility, Innovation and Technology within the frame of the FTI initiative "Produktion der Zukunft", which is administered by the Austrian Research Promotion Agency (FFG).

## References

- Baran I, Cinar K, Ersoy N, Akkerman R, Hattel JH. A review on the mechanical modeling of composite manufacturing processes. *Arch Computat Methods Eng: State Art Rev* 2017;24(2):365–95. <https://doi.org/10.1007/s11831-016-9167-2>.
- Frketic J, Dickens T, Ramakrishnan S. Automated manufacturing and processing of fiber-reinforced polymer (FRP) composites: An additive review of contemporary and modern techniques for advanced materials manufacturing. *Addit Manuf* 2017;14:69–86. <https://doi.org/10.1016/j.addma.2017.01.003>.
- Lukaszewicz D-H-J, Ward C, Potter KD. The engineering aspects of automated prepreg layup: History, present and future. *Compos B Eng* 2012;43(3):997–1009. <https://doi.org/10.1016/j.compositesb.2011.12.003>.
- Sobhani Aragh B, Borzabadi Farahani E, Xu BX, Ghasemnejad H, Mansur WJ. Manufacturable insight into modelling and design considerations in fibre-steered composite laminates: State of the art and perspective. *Comput Methods Appl Mech Eng* 2021;379:113752. <https://doi.org/10.1016/j.cma.2021.113752>.
- Zhang L, Wang X, Pei J, Zhou Y. Review of automated fibre placement and its prospects for advanced composites. *J Mater Sci* 2020;55(17):7121–55. <https://doi.org/10.1007/s10853-019-04090-7>.
- Oliveri V, et al. Design, manufacture and test of an in-situ consolidated thermoplastic variable-stiffness wingbox. *AIAA J* 2019;57(4):1671–83. <https://doi.org/10.2514/1.J057758>.
- Jayasekara D, Lai NYG, Wong K-H, Pawar K, Zhu Y. Level of automation (LOA) in aerospace composite manufacturing: Present status and future directions towards industry 4.0. *J Manuf Syst* 2022;62:44–61. <https://doi.org/10.1016/j.jmsy.2021.10.015>.
- Heinecke F, Willberg C. Manufacturing-Induced Imperfections in Composite Parts Manufactured via Automated Fiber Placement. *J Compos Sci* 2019;3(2):56. <https://doi.org/10.3390/jcs3020056>.
- Maung P, Prusty BG, White JM, David M, Phillips AW, St John NA. Structural performance of a shape-adaptive composite hydrofoil using automated fibre placement. *Eng Struct* 2019;183:351–65. <https://doi.org/10.1016/j.engstruct.2019.01.014>.
- Kuder IK, Fasel U, Ermanni P, Arrieta AF. Concurrent design of a morphing aerofoil with variable stiffness bi-stable laminates. *Smart Mater Struct* 2016;25(11):115001. <https://doi.org/10.1088/0964-1726/25/11/115001>.
- Rodríguez-García V, Guzman de Villoria R. Automated manufacturing of bio-inspired carbon-fibre reinforced polymers. *Compos B Eng* 2021;215:108795. <https://doi.org/10.1016/j.compositesb.2021.108795>.
- Baley C, et al. Flax/PP manufacture by automated fibre placement (AFP). *Mater Des* 2016;94:207–13. <https://doi.org/10.1016/j.matdes.2016.01.011>.
- Hoang V-T, et al. Postprocessing method-induced mechanical properties of carbon fiber-reinforced thermoplastic composites. *J Thermoplast Compos Mater* 2020;089270572094537. <https://doi.org/10.1177/0892705720945376>.
- Qureshi Z, Swait T, Scaife R, El-Dessouky HM. In situ consolidation of thermoplastic prepreg tape using automated tape placement technology: Potential and possibilities. *Compos B Eng* 2014;66:255–67. <https://doi.org/10.1016/j.compositesb.2014.05.025>.
- Martin I, Del Saenz Castillo D, Fernandez A, Güemes A. Advanced thermoplastic composite manufacturing by in-situ consolidation: A review. *J Compos Sci* 2020;4(4):149. <https://doi.org/10.3390/jcs4040149>.
- Shiino MY, Cipó TCG, Donadon MV, Essipchouk A. Waste size and lay up sequence strategy for reusing/recycling carbon fiber fabric in laminate composite: Mechanical property analysis. *J Compos Mater* 2021;55(28):4221–30. <https://doi.org/10.1177/00219983211037047>.
- Lin TA, Lin J-H, Bao L. A study of reusability assessment and thermal behaviors for thermoplastic composite materials after melting process: Polypropylene/thermoplastic polyurethane blends. *J Clean Prod* 2021;279:123473. <https://doi.org/10.1016/j.jclepro.2020.123473>.
- Schledjewski R. Thermoplastic tape placement process – in situ consolidation is reachable. *Plast, Rubber Compos* 2009;38(9–10):379–86. <https://doi.org/10.1179/146580109X12540995045804>.
- Gruber MB, Lockwood IZ, Dolan TL, Funck SB, Grimsley BW. Thermoplastic in situ placement requires better impregnated tapes and tows. *SAMPE* 2012.
- Ray D, et al. Fracture toughness of carbon fiber/polyether ether ketone composites manufactured by autoclave and laser-assisted automated tape placement. *J of Applied Polymer Sci* 2014;vol. 132(11):n/a-n/a. <https://doi.org/10.1002/app.41643>.
- van Hoa S, Duc Hoang M, Simpson J. Manufacturing procedure to make flat thermoplastic composite laminates by automated fibre placement and their mechanical properties. *J Thermoplast Compos Mater* 2017;30(12):1693–712. <https://doi.org/10.1177/0892705716662516>.
- Comer AJ, et al. Mechanical characterisation of carbon fibre-PEEK manufactured by laser-assisted automated-tape-placement and autoclave. *Compos A Appl Sci Manuf* 2015;69:10–20. <https://doi.org/10.1016/j.compositesa.2014.10.003>.
- Alves de Campos A, Henriques E, Magee CL. Technological improvement rates and recent innovation trajectories in automated advanced composites manufacturing technologies: A patent-based analysis. *Compos B Eng* 2022;238:109888. <https://doi.org/10.1016/j.compositesb.2022.109888>.
- Brasington A, Sacco C, Halbritter J, Wehbe R, Harik R. Automated fiber placement: A review of history, current technologies, and future paths forward. *Composites Part C: Open Access* 2021;6:100182. <https://doi.org/10.1016/j.jcomc.2021.100182>.
- Ren Z, Fang F, Yan N, Wu Y. State of the Art in Defect Detection Based on Machine Vision. *Int J of Precis Eng and Manuf-Green Tech* 2022;9(2):661–91. <https://doi.org/10.1007/s40684-021-00343-6>.
- Maass D. Progress in automated ply inspection of AFP layups. *Reinf Plast* 2015;59(5):242–5. <https://doi.org/10.1016/j.repl.2015.05.002>.
- Denkena B, Schmidt C, Weber P. Automated Fiber Placement Head for Manufacturing of Innovative Aerospace Stiffening Structures. *Procedia Manuf* 2016;6:96–104. <https://doi.org/10.1016/j.promfg.2016.11.013>.
- Juarez PD, Gregory ED. In Situ Thermal Inspection of Automated Fiber Placement for manufacturing induced defects. *Compos B Eng* 2021;220:109002. <https://doi.org/10.1016/j.compositesb.2021.109002>.
- Schmidt C, Denkena B, Völtzer K, Hocke T. Thermal image-based monitoring for the automated fiber placement process. *Procedia CIRP* 2017;62:27–32. <https://doi.org/10.1016/j.procir.2016.06.058>.
- Brysch M, Bahar M, Hohensee HC, Sinapius M. Single system for online monitoring and inspection of automated fiber placement with object segmentation by artificial neural networks. *J Intell Manuf* 2022;33(7):2013–25. <https://doi.org/10.1007/s10845-022-01924-1>.
- Yassin K, Hojjati M. Processing of thermoplastic matrix composites through automated fiber placement and tape laying methods. *J Thermoplast Compos Mater* 2018;31(12):1676–725. <https://doi.org/10.1177/0892705717738305>.
- Di Boon Y, Joshi SC, Bhudolia SK. Review: Filament Winding and Automated Fiber Placement with In Situ Consolidation for Fiber Reinforced Thermoplastic Polymer Composites. *Polymers* 2021;vol. 13(12). <https://doi.org/10.3390/polym13121951>.
- Parmar H, Khan T, Tucci F, Umer R, Carlone P. Advanced robotics and additive manufacturing of composites: towards a new era in Industry 4.0. *Mater Manuf Process* 2022;37(5):483–517. <https://doi.org/10.1080/10426914.2020.1866195>.
- Sun S, Han Z, Fu H, Jin H, Dhupia JS, Wang Y. "Defect characteristics and online detection techniques during manufacturing of FRPs using automated fiber placement a review". *Polymers* 2020;12(6). <https://doi.org/10.3390/polym12061337>.
- Oromiehie E, Prusty BG, Compston P, Rajan G. Automated fibre placement based composite structures: Review on the defects, impacts and inspections techniques. *Compos Struct* 2019;224:110987. <https://doi.org/10.1016/j.compstruct.2019.110987>.
- Veldenz L, Di Francesco M, Giddings P, Kim BC, Potter K. Material selection for automated dry fiber placement using the analytical hierarchy process. *Adv Manuf Polym Compos Sci* 2018;4(4):83–96. <https://doi.org/10.1080/20550340.2018.1545377>.
- Tierney J, Gillespie JW. Modeling of in situ strength development for the thermoplastic composite tow placement process. *J Compos Mater* 2006;40(16):1487–506. <https://doi.org/10.1177/0021998306060162>.
- Sonmez FO, Akbulut M. Process optimization of tape placement for thermoplastic composites. *Compos A Appl Sci Manuf* 2007;38(9):2013–23. <https://doi.org/10.1016/j.compositesa.2007.05.003>.
- Khan MA, Mitschang P, Schledjewski R. Parametric study on processing parameters and resulting part quality through thermoplastic tape placement process. *J Compos Mater* 2013;47(4):485–99. <https://doi.org/10.1177/0021998312441810>.
- Stokes-Griffin CM, Compston P. The effect of processing temperature and placement rate on the short beam strength of carbon fibre-PEEK manufactured using a laser tape placement process. *Compos A Appl Sci Manuf* 2015;78:274–83. <https://doi.org/10.1016/j.compositesa.2015.08.008>.
- Stokes-Griffin CM, Kollmannsberger A, Compston P, Drechsler K. The effect of processing temperature on wedge peel strength of CF/PA 6 laminates manufactured in a laser tape placement process. *Compos A Appl Sci Manuf* 2019;121:84–91. <https://doi.org/10.1016/j.compositesa.2019.02.011>.
- Cheng J, Zhao D, Liu K, Wang Y. Process modeling and parameter optimization based on assumed inherent sensor inversion for composite automated placement.

- J Reinf Plast Compos 2017;36(3):226–38. <https://doi.org/10.1177/0731684416680456>.
- [43] Venkatesan C, Velu R, Vaheed N, Raspall F, Tay T-E, Silva A. Effect of process parameters on polyamide-6 carbon fibre prepreg laminated by IR-assisted automated fibre placement. *Int J Adv Manuf Technol* 2020;108(4):1275–84. <https://doi.org/10.1007/s00170-020-05230-z>.
- [44] Chen J, Fu K, Li Y. Understanding processing parameter effects for carbon fibre reinforced thermoplastic composites manufactured by laser-assisted automated fibre placement (AFP). *Compos A Appl Sci Manuf* 2021;140:106160. <https://doi.org/10.1016/j.compositesa.2020.106160>.
- [45] Schaefer PM, Gierszewski D, Kollmannsberger A, Zaremba S, Drechsler K. Analysis and improved process response prediction of laser-assisted automated tape placement with PA-6/carbon tapes using design of experiments and numerical simulations. *Compos A Appl Sci Manuf* 2017;96:137–46. <https://doi.org/10.1016/j.compositesa.2017.02.008>.
- [46] Zhang C, et al. The effects of processing parameters on the wedge peel strength of CF/PEEK laminates manufactured using a laser tape placement process. *Int J Adv Manuf Technol* 2022;120(11–12):7251–62. <https://doi.org/10.1007/s00170-022-09181-5>.
- [47] Schmidt C, Denkena B, Hocke T, Völtzer K. Influence of AFP process parameters on the temperature distribution used for thermal in-process monitoring. *Procedia CIRP* 2017;66:68–73. <https://doi.org/10.1016/j.procir.2017.03.220>.
- [48] Bakhshi N, Hojjati M. An experimental and simulative study on the defects appeared during tow steering in automated fibre placement. *Compos A Appl Sci Manuf* 2018;113:122–31. <https://doi.org/10.1016/j.compositesa.2018.07.031>.
- [49] Bakhshi N, Hojjati M. Effect of compaction roller on layup quality and defects formation in automated fibre placement. *J Reinf Plast Compos* 2020;39(1–2):3–20. <https://doi.org/10.1177/0731684419868845>.
- [50] Arian Nik M, Fayazbakhsh K, Pasini D, Lessard L. Optimization of variable stiffness composites with embedded defects induced by automated fiber placement. *Compos Struct* 2014;107:160–6. <https://doi.org/10.1016/j.compstruct.2013.07.059>.
- [51] Falcó O, Mayugo JA, Lopes CS, Gascons N, Costa J. Variable-stiffness composite panels: Defect tolerance under in-plane tensile loading. *Compos A Appl Sci Manuf* 2014;63:21–31. <https://doi.org/10.1016/j.compositesa.2014.03.022>.
- [52] Croft K, Lessard L, Pasini D, Hojjati M, Chen J, Yousefpour A. Experimental study of the effect of automated fiber placement induced defects on performance of composite laminates. *Compos A Appl Sci Manuf* 2011;42(5):484–91. <https://doi.org/10.1016/j.compositesa.2011.01.007>.
- [53] Clancy G, Peeters D, Oliveri V, Jones D, O'Higgins RM, Weaver PM. A study of the influence of processing parameters on steering of carbon fibre/PEEK tapes using laser-assisted tape placement. *Compos B Eng* 2019;163:243–51. <https://doi.org/10.1016/j.compositesb.2018.11.033>.
- [54] Rajasekaran A, Shadmehri F. Steering of carbon fiber/PEEK tapes using Hot gas torch-assisted automated fiber placement. *J Thermoplast Compos Mater* 2023;36(4):1651–79. <https://doi.org/10.1177/08927057211067962>.
- [55] Rajan S, et al. Experimental investigation of prepreg slit tape wrinkling during automated fiber placement process using StereoDIC. *Compos B Eng* 2019;160:546–57. <https://doi.org/10.1016/j.compositesb.2018.12.017>.
- [56] Blom AW, Lopes CS, Kromwijk PJ, Gurdal Z, Camanho PP. A theoretical model to study the influence of tow-drop areas on the stiffness and strength of variable-stiffness laminates. *J Compos Mater* 2009;43(5):403–25. <https://doi.org/10.1177/0021998308097675>.
- [57] Del Rossi D, Cadran V, Thakur P, Palardy-Sim M, Lapalme M, Lessard L. Experimental investigation of the effect of half gap/half overlap defects on the strength of composite structures fabricated using automated fibre placement (AFP). *Compos A Appl Sci Manuf* 2021;150:106610. <https://doi.org/10.1016/j.compositesa.2021.106610>.
- [58] Harik R, Saïdy C, Williams SJ, Gurdal Z, Grimsley B. Automated fiber placement defect identity cards: cause, anticipation, existence, significance, and progression. *SAMPE* 2018.
- [59] Chevalier PL, Kassapoglou C, Gurdal Z. Fatigue behavior of composite laminates with automated fiber placement induced defects- a review. *Int J Fatigue* 2020;140:105775. <https://doi.org/10.1016/j.ijfatigue.2020.105775>.
- [60] Hsiao HM, Daniel IM. Effect of fiber waviness on stiffness and strength reduction of unidirectional composites under compressive loading. *Compos Sci Technol* 1996;56(5):581–93. [https://doi.org/10.1016/0266-3538\(96\)00045-0](https://doi.org/10.1016/0266-3538(96)00045-0).
- [61] Belnoue J-P-H, et al. Understanding and predicting defect formation in automated fibre placement pre-preg laminates. *Compos A Appl Sci Manuf* 2017;102:196–206. <https://doi.org/10.1016/j.compositesa.2017.08.008>.
- [62] Sawicki A, and Minguett P. The effect of intraply overlaps and gaps upon the compression strength of composite laminates. In: 39th AIAA/ASME/ASCE/AHS/ASC Structures.
- [63] Lan M, Cartié D, Davies P, Baley C. Influence of embedded gap and overlap fiber placement defects on the microstructure and shear and compression properties of carbon–epoxy laminates. *Compos A Appl Sci Manuf* 2016;82:198–207. <https://doi.org/10.1016/j.compositesa.2015.12.007>.
- [64] Elsherbini YM, Hoa SV. Experimental and numerical investigation of the effect of gaps on fatigue behavior of unidirectional carbon/epoxy automated fiber placement laminates. *J Compos Mater* 2017;51(6):759–72. <https://doi.org/10.1177/0021998316655393>.
- [65] Elsherbini YM, Hoa SV. Fatigue threshold-stress determination in AFP laminates containing gaps using IR thermography. *Compos Sci Technol* 2017;146:49–58. <https://doi.org/10.1016/j.compscitech.2017.04.006>.
- [66] Marouene A, Legay P, Boukhili R. Experimental and numerical investigation on the open-hole compressive strength of AFP composites containing gaps and overlaps. *J Compos Mater* 2017;51(26):3631–46. <https://doi.org/10.1177/0021998317690917>.
- [67] Guin WE, Jackson JR, Bosley CM. Effects of tow-to-tow gaps in composite laminates fabricated via automated fiber placement. *Compos A Appl Sci Manuf* 2018;115:66–75. <https://doi.org/10.1016/j.compositesa.2018.09.014>.
- [68] Woigk W, Hallett SR, Jones MI, Kuhtz M, Hornig A, Gude M. Experimental investigation of the effect of defects in automated fibre placement produced composite laminates. *Compos Struct* 2018;201:1004–17. <https://doi.org/10.1016/j.compstruct.2018.06.078>.
- [69] Nguyen MH, Vijayachandran AA, Davidson P, Call D, Lee D, Waas AM. Effect of automated fiber placement (AFP) manufacturing signature on mechanical performance of composite structures. *Compos Struct* 2019;228:111335. <https://doi.org/10.1016/j.compstruct.2019.111335>.
- [70] Zenker T, Bruckner F, Drechsler K. Effects of defects on laminate quality and mechanical performance in thermoplastic automated fiber placement-based process chains. *Adv Manuf Polym Compos Sci* 2019;5(4):184–205. <https://doi.org/10.1080/20550340.2019.1703334>.
- [71] Ghayour M, Hojjati M, Ganesan R. Effect of tow gaps on impact strength of thin composite laminates made by automated fiber placement: Experimental and semi-analytical approaches. *Compos Struct* 2020;248:112536. <https://doi.org/10.1016/j.compstruct.2020.112536>.
- [72] Suemasu H, Aoki Y, Sugimoto S, Nakamura T. Effect of gap on strengths of automated fiber placement manufactured laminates. *Compos Struct* 2021;263:113677. <https://doi.org/10.1016/j.compstruct.2021.113677>.
- [73] Cartié D, Lan M, Davies P, Baley C. Influence of embedded gap and overlap fiber placement defects on interlaminar properties of high performance composites. *Mater (Basel, Switzerland)* 2021;14(18). <https://doi.org/10.3390/ma14185332>.
- [74] Böckl B, Wedel A, Misik A, Drechsler K. Effects of defects in automated fiber placement laminates and its correlation to automated optical inspection results. *J Reinf Plast Compos* 2022;073168442210932. <https://doi.org/10.1177/07316844221093273>.
- [75] Marrouzé JP, Housner J, and Abdi F, editors. Effect of manufacturing defects and their uncertainties on strength and stability of stiffened panels: Concordia Centre for Composites, 2013.
- [76] Abdi F, Gürdal Z, and Huang D. Certification Modeling of Composites Fuselage, Considering Effect of Defects from Fiber Placement Manufacturing Processes. In: AIAA SciTech Forum: 55th AIAA Aerospace Sciences Meeting, Grapevine, Texas, 2017.
- [77] Fayazbakhsh K, Arian Nik M, Pasini D, Lessard L. Defect layer method to capture effect of gaps and overlaps in variable stiffness laminates made by automated fiber placement. *Compos Struct* 2013;97:245–51. <https://doi.org/10.1016/j.compstruct.2012.10.031>.
- [78] Li X, Hallett SR, Wisnom MR. Modelling the effect of gaps and overlaps in automated fibre placement (AFP)-manufactured laminates. *Sci Eng Compos Mater* 2015;22(2):115–29. <https://doi.org/10.1515/secm-2013-0322>.
- [79] Denkena B, Schmidt C, Völtzer K, Hocke T. Thermographic online monitoring system for automated fiber placement processes. *Compos B Eng* 2016;97:239–43. <https://doi.org/10.1016/j.compositesb.2016.04.076>.
- [80] Schmidt C, Hocke T, Denkena B. Artificial intelligence for non-destructive testing of CFRP prepreg materials. *Prod Eng Res Devel* 2019;13(5):617–26. <https://doi.org/10.1007/s11740-019-00913-3>.
- [81] Brüning J, Denkena B, Dittrich M-A, Hocke T. Machine learning approach for optimization of automated fiber placement processes. *Procedia CIRP* 2017;66:74–8. <https://doi.org/10.1016/j.procir.2017.03.295>.
- [82] Juarez PD, Cramer KE, and Seebo JP. Advances in situ inspection of automated fiber placement systems. In: *Thermosense: Thermal Infrared Applications XXXVIII*, Baltimore, Maryland, United States, 2016, p. 986109.
- [83] Gregory E, Juarez P. In situ thermal nondestructive evaluation for assessing part quality during composite automated fiber placement. *J Nondestruct. Evaluat. Diagnos. Prognos. Eng. Syst.* 2018;1(4). <https://doi.org/10.1115/1.4040764>.
- [84] Gregory ED, and Juarez PD, editors. In-situ thermography of automated fiber placement parts, 1949th ed.: AIP Conference Proceeding; 2017.
- [85] Kastanis D, Steiner H, Fauster E, Schledjewski R. Compaction behavior of continuous carbon fiber tows: an experimental analysis. *Adv Manuf Polym Compos Sci* 2015;1(3):169–74. <https://doi.org/10.1080/20550340.2015.1114794>.
- [86] Schmitt R, Niggemann C, and Mersmann C. Contour scanning of textile preforms using a light-section sensor for the automated manufacturing of fibre-reinforced plastics. In: *Optical Sensors 2008*. Strasbourg, France, 2008, 700311.
- [87] Schmitt R, Niggemann C, and Mersmann C. Laser light-section sensor automating the production of textile-reinforced composites. In: *Optical Sensors 2009*, Prague, Czech Republic, 2009, 73560P.
- [88] Schmitt R, Mersmann C, Damm B. In-process 3D laser measurement to control the fiber tape-laying for composite production. In: *Optics, Photonics, and Digital Technologies for Multimedia Applications*, Brussels Belgium; 2010. 77230R.
- [89] Krombholz C, Perner M, Bock M, and Röstermundt D. Improving the production quality of the advanced Automated Fiber Placement process by means of online path correction. In: 28th International Congress of the Aeronautical Science.
- [90] Sacco C, Baz Radwan A, Anderson A, Harik R, Gregory E. Machine learning in composites manufacturing: A case study of automated fiber placement inspection. *Compos Struct* 2020;250:112514. <https://doi.org/10.1016/j.compstruct.2020.112514>.
- [91] Sacco C, Radwan AB, Harik R, and van Tooren M. Automated fiber placement defects: automated inspection and characterization. In: *SAMPE 2018 Conference and Exhibition NF1676L-29116*, May. 2018. [Online]. Available: <https://ntrs.nasa.gov/citations/20190027133>.

- [92] Sacco C, Radwan AB, Beatty T, Harik R. Machine learning based AFP inspection: A tool for characterization and integration. In: SAMPE 2019.
- [93] Sacco C, et al. On the effect of manual rework in AFP quality control for a doubly-curved part. *Compos B Eng* 2021;227:109432. <https://doi.org/10.1016/j.compositesb.2021.109432>.
- [94] Tang Y, Wang Q, Wang H, Li J, Ke Y. A novel 3D laser scanning defect detection and measurement approach for automated fibre placement. *Meas Sci Technol* 2021;32(7):75201. <https://doi.org/10.1088/1361-6501/abda95>.
- [95] Tang Y, Wang Q, Cheng L, Li J, Ke Y. An in-process inspection method integrating deep learning and classical algorithm for automated fiber placement. *Compos Struct* 2022;300:116051. <https://doi.org/10.1016/j.compstruct.2022.116051>.
- [96] Meister S, Werms MAM, Stüve J, Groves RM. Review of image segmentation techniques for layup defect detection in the automated fiber placement process. *J Intell Manuf* 2021;32(8):2099–119. <https://doi.org/10.1007/s10845-021-01774-3>.
- [97] Meister S, Möller N, Stüve J, Groves RM. Synthetic image data augmentation for fibre layup inspection processes: Techniques to enhance the data set. *J Intell Manuf* 2021;32(6):1767–89. <https://doi.org/10.1007/s10845-021-01738-7>.
- [98] van der Jeught S, Dirckx JJ. Real-time structured light profilometry: a review. *Opt Lasers Eng* 2016;87:18–31. <https://doi.org/10.1016/j.optlaseng.2016.01.011>.
- [99] Tao Y, Jia S, Duan Y, Zhang X. An online detection method for composite fibre tow placement accuracy. *Proc Inst Mech Eng B J Eng Manuf* 2016;230(9):1614–21. <https://doi.org/10.1177/0954405416640189>.
- [100] Cemenska J, Rudberg T, Henscheid M. Automated in-process inspection system for AFP machines. *SAE Int J Aerosp* 2015;8(2):303–9. <https://doi.org/10.4271/2015-01-2608>.
- [101] Shadmehri F. Laser vision inspection system and method. US10408603B2, United States, 2019.
- [102] Shadmehri F, Ioachim O, Pahud O, Brunel J-E, Landry A, Hoa SV, and Hojjati M, editors. *Laser-Vision Inspection System for Automated Fiber Placement (AFP) Process: 20th International Conference on Composite Materials (ICCM20)*, 2015.
- [103] S. Zambal, C. Heindl, C. Eitzinger, and J. Scharinger, Eds., *End-to-end defect detection in automated fiber placement based on artificially generated data*: SPIE, 2019.
- [104] S. Zambal, C. Heindl, and C. Eitzinger, "Machine Learning for CFRP Quality Control," in *SAMPE Europe Conference 2019*.
- [105] Schuster A, Mayer M, Willmeroth M, Brandt L, Kupke M. Inline Quality Control for Thermoplastic Automated Fibre Placement. *Procedia Manuf* 2020;51:505–11. <https://doi.org/10.1016/j.promfg.2020.10.071>.
- [106] Meister S, Grundhöfer L, Stüve J, Groves RM. Imaging sensor data modelling and evaluation based on optical composite characteristics. *Int J Adv Manuf Technol* 2021;116(11–12):3965–90. <https://doi.org/10.1007/s00170-021-07591-5>.
- [107] Meister S, Werms M, Stüve J, Groves RM. Investigations on explainable artificial intelligence methods for the deep learning classification of fibre layup defect in the automated composite manufacturing. *Compos B Eng* 2021;224:109160. <https://doi.org/10.1016/j.compositesb.2021.109160>.
- [108] Oromiehie E, Gain AK, Prusty BG. Processing parameter optimisation for automated fibre placement (AFP) manufactured thermoplastic composites. *Compos Struct* 2021;272:114223. <https://doi.org/10.1016/j.compstruct.2021.114223>.
- [109] Oromiehie E, Gangadhara Prusty B, Compston P, Rajan G. "In-situ simultaneous measurement of strain and temperature in automated fiber placement (AFP) using optical fiber Bragg grating (FBG) sensors". *Adv Manuf Polym Compos Sci* 2017;3(2):52–61. <https://doi.org/10.1080/20550340.2017.1317447>.
- [110] Sorensen L, Gmür T, Botsis J. Residual strain development in an AS4/PPS thermoplastic composite measured using fibre Bragg grating sensors. *Compos A Appl Sci Manuf* 2006;37(2):270–81. <https://doi.org/10.1016/j.compositesa.2005.02.016>.
- [111] Saenz-Castillo D, Martín MI, Calvo S, Güemes A. Real-time monitoring of thermal history of thermoplastic automatic lamination with FBG sensors and process modelling validation. *Smart Mater Struct* 2020;29(11):115004. <https://doi.org/10.1088/1361-665X/abaa97>.
- [112] Zhan Y, Lin F, Song Z, Sun Z, Yu M. Applications and research progress of optical fiber grating sensing in thermoplastic composites molding and structure health monitoring. *Optik* 2021;229:166122. <https://doi.org/10.1016/j.ijleo.2020.166122>.
- [113] Oromiehie E, Prusty BG, Compston P, Rajan G. Characterization of process-induced defects in automated fiber placement manufacturing of composites using fiber Bragg grating sensors. *Struct Health Monit* 2018;17(1):108–17. <https://doi.org/10.1177/1475921716685935>.
- [114] Schmidt C, Schultz C, Weber P, Denkena B. Evaluation of eddy current testing for quality assurance and process monitoring of automated fiber placement. *Compos B Eng* 2014;56:109–16. <https://doi.org/10.1016/j.compositesb.2013.08.061>.
- [115] Han Z, Sun S, Li W, Zhao Y, Shao Z. Experimental study of the effect of internal defects on stress waves during automated fiber placement. *Polymers* 2018;10(4):pp. <https://doi.org/10.3390/polym10040413>.
- [116] Shadmehri F, van Hoa S. Digital image correlation applications in composite automated manufacturing, inspection, and testing. *Appl Sci* 2019;9(13):2719. <https://doi.org/10.3390/app9132719>.
- [117] larve EV, Kim R. Strength prediction and measurement in model multilayered discontinuous tow reinforced composites. *J Compos Mater* 2004;38(1):5–18. <https://doi.org/10.1177/0021998304038215>.
- [118] Tattling BF, Guerdal Z, and Jegley D. Design and Manufacture of Elastically Tailored Tow Placed Plates. NASA/CR-2002-211919, Aug. 2002. [Online]. Available: <https://ntrs.nasa.gov/citations/20020073162>.
- [119] Kim BC, Potter K, Weaver PM. Continuous tow shearing for manufacturing variable angle tow composites. *Compos A Appl Sci Manuf* 2012;43(8):1347–56. <https://doi.org/10.1016/j.compositesa.2012.02.024>.
- [120] Kim BC, Weaver PM, Potter K. Manufacturing characteristics of the continuous tow shearing method for manufacturing of variable angle tow composites. *Compos A Appl Sci Manuf* 2014;61:141–51. <https://doi.org/10.1016/j.compositesa.2014.02.019>.
- [121] R. Lincoln, P. Weaver, A. Pirrera, and R. M. Groh, Manufacture and buckling test of a variable-stiffness, variable-thickness composite cylinder under axial compression, in: AIAA SCITECH 2022 Forum, San Diego, CA & Virtual, 01032022.
- [122] Rakhshbahar M, Sinapius M. A Novel Approach: Combination of Automated Fiber Placement (AFP) and Additive Layer Manufacturing (ALM). *J Compos Sci* 2018;2(3):42. <https://doi.org/10.3390/jcs2030042>.
- [123] Clancy G, Peeters D, O'Higgins RM, Weaver PM. In-line variable spreading of carbon fibre/thermoplastic pre-preg tapes for application in automatic tape placement. *Mater Des* 2020;194:108967. <https://doi.org/10.1016/j.matdes.2020.108967>.

## 2.2 Motivation and Research Questions

Considering the state of the art, a few research gaps have been identified. In general, **thermoplastics** for ATL are not researched enough even though they offer a lot of advantages. **Manufacturing defects**, especially **gaps** should be controlled/reduced if not eliminated for VSP laminates and other structures that make use of curvilinear fibers and varying angle of layup. If thermoplastic tape materials can conform to the layup tool structure with varying width, it would result in perfectly **tessellated geometry** without gaps or overlaps.

The focus here is on defects occurring as a result of layup restrictions and process environment. Defects inherent to material quality should be covered as a part of material development. Similarly, quality assurance as a part of NDT is excluded, as it is more of a testament of repeatability and conformance to certain industry specific standards. The objective is to focus on the process itself, that is, after the material qualification tests and before NDT checks. There are currently no commercial solutions for **inline process monitoring**. Even though often neglected, these defects have proven to be detrimental to the structure to the extent of complete failure as a result of complex damage initiation and progression mechanics within composites.

Different prototypes and set-ups so far have concentrated on individual sensor specific solutions for particular defects. A synergy between different systems for a complete monitoring of the process is rarely witnessed. Trial and error approaches are most often employed for single technology trying to detect all possible defects. The approach is ‘how many defects can be detected with a single technique’, rather than a structured approach of ‘which defects are crucial for detection and what aspects should be monitored for comprehensive modular solutions’. A disconnect between different studies is also witnessed, where one aspect of monitoring concept is not/cannot be applied to another process step. Effect of defect studies are seldom used for defect monitoring, and defect monitoring is rarely used for defect rectification (removal, rework and repair). A **knowledge hierarchy** is missing.

A similar trend is seen for defect and process control. The technologies identified so far represent the first stage of process **monitoring concept** (*Figure 4*). A complete monitoring concept life cycle would consist of identifying the most important defects, their detection and management (rectification, reduction and elimination) via back and forth feedback and analysis of the process behavior. As discussed earlier, an implementation of such a concept would increase productivity, accuracy and reliability of the process. To summarize, the main research question addressed in this dissertation is:

*What are the most promising approaches for a robust and modular inline defect monitoring and control system for ATL process?*

Subsequently the main proposition of this research work is: *Devising a combination of different monitoring techniques resulting in holistic defect detection and treatment within the process cycle*. With respect to the same, the following sub-questions are discussed and answered in this thesis:

1. Which manufacturing defects are crucial for detection and can they be detected inline?  
[Answered in Chapter 2]

2. Which techniques (individual or combined) are best suited for manufacturing defect monitoring concept?  
[Answered in Section 3.4 and Chapter 4]
3. Can these defects be reduced/eliminated during the process? Which aspects of defects and process behavior should be monitored for this?  
[Answered in Chapter 4]
4. Is there any correlation between certain defects and process parameters? Which models are required for process monitoring and control?  
[Answered in Section 4.3]

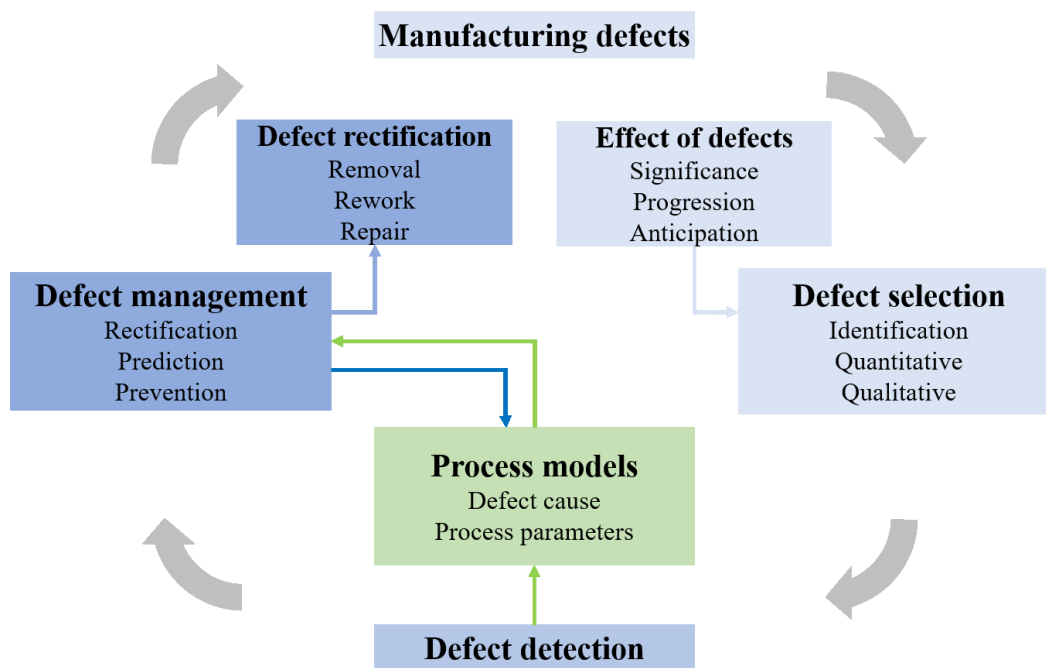


Figure 4 Process monitoring concept and control life cycle

## 2.3 Approach and Scope

**Approach:** The methodology of this thesis involves the evaluation of manufacturing defects requiring analysis of physical properties of the thermoplastic tape material. For this purpose, the thermal behavior of the material, material geometry and morphological changes are measured and examined using infrared thermography, profilometry and force sensor respectively. The thermal behavior is used to recognize FOD and bonding defects, described in Section 4.1. Material geometry recorded using light section sensors helps in detecting positioning defects (gaps and overlaps) and the morphological changes serve as input for the consequent force sensor modelling and control, elaborated in Section 4.2. Subsequently, parametric influence on material behavior and sensor model is described in Section 4.3.



**Scope:** The purpose of this study is to provide an overview of the applicability and performance of various techniques for inline monitoring and detection of manufacturing defects for thermoplastic ATL. The individual defects and sensor technologies are investigated in detail. The thesis provides a complete **engineering solution-based monitoring concept** with easy integration, accuracy and effectiveness for real manufacturing processes. Robotics and automation are an integral part of the described work but are not discussed in detail as they exceed the scope of the dissertation thematically. The main premise of the dissertation is **process development**, therefore topics related to measurement techniques and data handling, including sensor control, data processing programs and data enhancement algorithms are not examined in detail. Consequently, potential process improvements through the integration of an inline inspection system are highlighted but not analyzed in detail. Parametric optimization and in-situ consolidation even though lucrative and useful in parts, are not direct objectives of this research. Therefore, thermal modelling, process simulation, mechanical performance tests and extensive design of experiments (DoE) for process optimization are avoided. Moreover, benchmarking tests for individual sensor technologies and defect types are described in detail for the test-rig prototype without consideration of aviation certification cycle. Certification is a separate area of research far exceeding the scope of this thesis. However, the findings of this research might provide indications for such a certification procedure. Even though the inspection system is custom built for ATL process, it can be easily adapted for other manufacturing processes. Likewise, the monitoring concept and process control can be implemented irrespective of the material and defect detection technology used.

# 3

## Experimental

This chapter describes the materials, test-rig configuration, and technical specifications relevant for the experimental research work presented in this thesis. In addition, a capability analysis involving Fiber Bragg Grating (FBG) sensors as a part of pre-trials is presented (*Article B*).

### 3.1 Materials

This research work uses thermoplastic unidirectional tape based on carbon fiber-reinforced polyamide 6 (PA6), supplied by SGL Carbon. The material data is listed in *Table 1*. CF-PA6 is considered as an engineering grade material due to cost-effectiveness and lower melting point compared to other aerospace grade thermoplastics. Since the focus of this work is defect monitoring and control, the material specific structural performance is irrelevant to a great extent.

CF-PA6 absorbs water at room temperature. Usually the material is dried right before laying. From extensive experiments the water content for the present material in atmosphere is found to be 1.94 %. The characterization is important for structural analysis but has no significant implication for inline monitoring.

*Table 1 Technical data for the CF-PA6 tapes*

Fiber type	SIGRAFIL® C T50-4.4/255-T140
Matrix type	PA6
Melting temperature	200 °C
Glass transition temperature	58 °C
Density	1.42 g/cm <sup>3</sup>
Fiber volume content	42 %
Width	25.4±0.1 mm
Thickness	0.2 mm

### 3.2 Test-bench

Automated tape laying involves continuous material placement resulting in melt bonding with the application of heat and compaction force. The bond formation for thermoplastics is a multi-mechanism process and the quality of the bond is dependent on both material properties and processing conditions. The main process parameters are laying speed (material transport), heat and compaction force. The leading mechanisms are as follows. **Heat transfer**, leading to the formation of a temperature field, influencing other phenomena occurring throughout the process. Application of compaction force leads to an interfacial area contact between substrate and incoming tape, referred to as **intimate contact**. This in turn is followed by **autohesion/healing**. Healing refers to the interdiffusion of molecular chains across the polymer interface between tapes. The next mechanism, **consolidation/squeeze flow** involves the removal of interlaminar voids, followed by **solidification** of the tape. Other phenomena occurring as a consequence of the bond development are void growth, crystallization, polymer degradation and residual stress development [23–26]. A schematic of the test-rig used for this research work is shown in *Figure 5*.

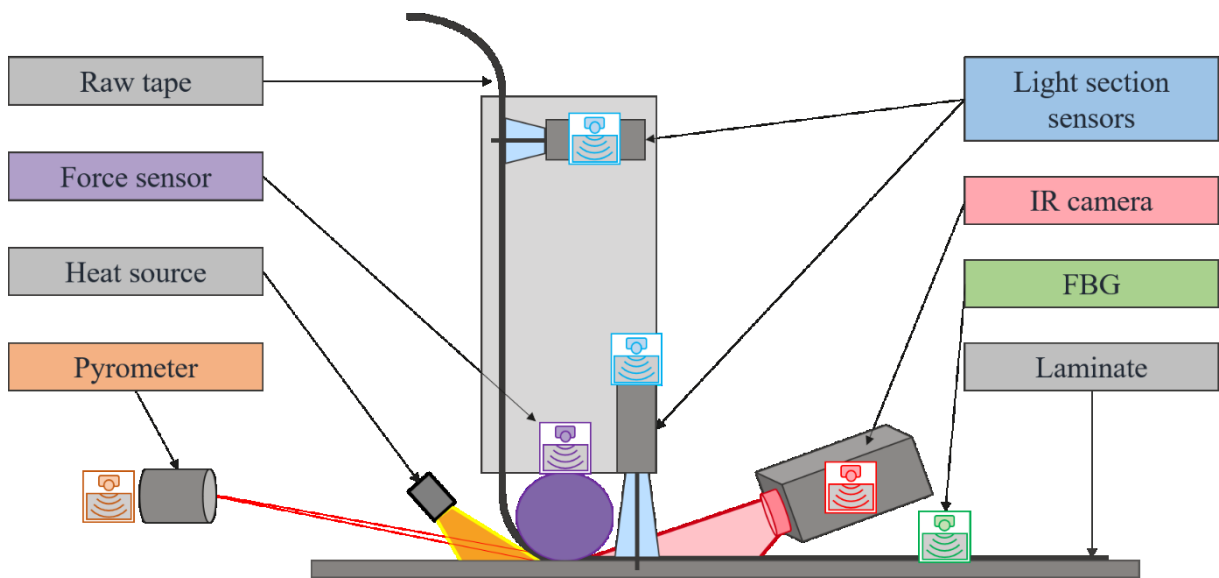


*Figure 5 Schematic of the ATL test-rig with integrated sensor technology*

A holistic approach is adopted for the monitoring concept and defect detection. The integrated sensors are listed in *Table 2*. A detailed description of individual sensor technology is covered in *Section 3.3*.

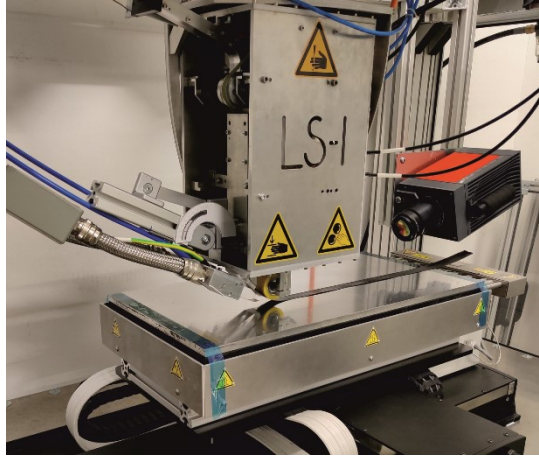





Figure 6 ATL lab-based test-rig with integrated sensor technology

Table 2 Holistic ATL monitoring system

- 
**Before consolidation:** Raw material defect and dimension detection using **light section sensor**
- 
**During consolidation:** Process parameter monitoring; nip-point temperature using **pyrometer** and compaction force using **force sensor**
- 
**After consolidation:** Laminate properties such as surface temperature anomaly and foreign objects debris using **infrared (IR) camera**; placement defects and tape dimensions after consolidation using **light section sensor**; and manufacturing strain using **fiber Bragg grating (FBG)** (also used for structural health monitoring during service life)

### 3.3 Technical Specifications

A soft conformable silicon roller (Maschinenbau-kieler, Germany) is used as the compaction roller. The roller has a width of 30 mm, outer diameter of 50 mm and a hardness level of 70 (DIN ISO 7619-1 Shore A).

For heating, a Xenon flashlamp, humm3® (Heraeus Noblelight, UK) system is used as the main heat source. The working principle is based on pulsed radiation emitted in the range of visible light and near-infrared spectrum. The flashlamp consists of a quartz glass tube, filled with pressurized Xenon gas. The glass tube has a metallic anode and cathode, which when supplied with voltage beyond the lamp's breakdown voltage, transforms the Xenon gas into a plasma [27]. The power output of the heat is dependent on three adjustable parameters: voltage, frequency and pulse duration. The best working parameters for the process for CF-PA6 based on a small DoE are presented in *Table 3*.

Table 3 Process parameters for CF-PA6 using humm3®

Heat	Speed	Force	Tool temperature
Output power: 2.9 kW			
Voltage: 120 V	50 mm/s	200 N	30 °C
Frequency: 60 Hz			
Pulse duration: 2 ms			

All sensors integrated on the test-rig are chosen based on the requirements of inline monitoring. A trade-off between resolution, accuracy, efficiency, cost and ease of integration was made before finalizing the sensor concept. Hardware and software considerations for all sensors are listed below along with individual aims and specifications. Considering defect detection, FOD, gaps and overlaps are given a priority over twisted tows and wrinkles as the latter are a rare occurrence for thermoplastics in general. Residual stress monitoring was considered in a preliminary study only. Pyrometers are used for temperature monitoring and force sensor monitors compaction force. These sensors do not detect manufacturing defects directly. For a complete overview of the test-rig and monitoring concept, all sensors are mentioned irrespective of their actual application for defect detection.

## FBG

Technical specifications for FBG sensors are given in *Table 4*.

Table 4 Technical specifications for FBG

Use	Intermittent and global residual strain monitoring
Integration	Inside the laminate (intrusive)
Specifications	<p>Polyimide coated silica core (Sylex, Slovakia), active length 8 mm, outer diameter 145 <math>\mu\text{m}</math> and peak wavelength 1550 nm</p> <p>Data acquisition using Benchtop BraggSCOPE FS5500 interrogator (FiberSensing, Portugal), sampling rate up to 10 kHz, resolution 0.1 pm and repeatability <math>\pm 10</math> pm, corresponding strain resolution 0.12 <math>\mu\epsilon</math> (0.01 °C) and repeatability 12 <math>\mu\epsilon</math> (1 °C)</p> <p>Reflection spectra collection using an SI-405 interrogator (HBM, Germany), resolution 1 pm, strain measurement resolution 2 <math>\mu\epsilon</math> and temperature resolution 0.1 °C</p>
Considerations	Strain sensitivity to integration angle, structural performance reliance on cross-sectional area of FBG, temperature and strain discrimination uncertainties and non-standardized strain assessment methods

## Pyrometer

Technical specifications of the pyrometer sensors are given in *Table 5*.

*Table 5 Technical specifications for pyrometer*

Use	Nip-point (laminated) temperature monitoring
Integration	Behind the compaction roller and the heat source
Specifications	Infrared pyrometer with laser sighting CTL-SF75-C3 (Micro-epsilon, Germany) Temperature measurement range -50 to 975 °C, acquisition time 120 s, resolution 0.1 °C and reproducibility $\pm 0.5$ °C
Considerations	Limited viewing angle and test-rig space requirement dependent on focal length

## IR camera

Technical specifications of the IR camera are given in *Table 6*.

*Table 6 Technical specifications for infrared camera*

Use	FOD detection and temperature field monitoring
Integration	In front of the compaction roller and the heat source
Specifications	High-speed thermography ImageIR 8390 HP-B/25 mm (InfraTec, Germany) Image resolution 640x512 pixel, temperature resolution 20 mK and frequency up to 300 Hz (full size image)
Considerations	Limited viewing angle owing to material reflection, temperature range limited by integration time and test-rig space requirement dependent on focal length

### Light section sensor

Technical specifications for the light sectioning sensor are given in *Table 7*.

*Table 7 Technical specifications for light section sensor*

Use	Tape width monitoring and detection of gaps and overlaps
Integration	Before and after the compaction roller, directly above the thermoplastic tape
Specifications	Compact laser scanner for high precision scanCONTROL LLT2900-25/BL (Micro-epsilon, Germany) Range 23.4 to 29.1 mm, resolution 2 $\mu\text{m}$ , up to 1280 points per profile and frequency up to 300 Hz
Considerations	Limited spatial range for higher spatial resolution and tedious data processing

### Force sensor

Technical specifications of the force sensor are given in *Table 8*.

*Table 8 Technical specifications for force sensor*

Use	Compaction force detection and variation (tape width control)
Integration	Directly above the compaction roller
Specifications	6-axis force/torque sensor K6D40 500N/20Nm/MP11 (ME-Meßsysteme, Germany) Maximum force in z-direction 2000 N, resolution 0.2 N, accuracy $\sim 4$ N and settling time 1 ms Force application via double-acting compact air cylinder (AND 50-20-I-P-A, Festo), regulated using a proportional pressure control valve regulator (VPPM 6L-L-1-G18, Festo), maximum force 1200 N (10 bar), pressure hysteresis 0.05 bar and linearity error of 1 %
Considerations	Sensitivity to temperature and torque constraints on steep surfaces

## 3.4 Capability Analysis: FBG

*Article B [28]: “In-line residual strain monitoring for thermoplastic automated tape layup using fiber Bragg grating sensors”*

A short overview of the article is provided here. The article is supplemented directly after the overview. Residual stress (strain) is a manufacturing induced defect that is influenced by process

parameters and material properties. In the scope of this thesis, such defects have been discarded from the perspective of inline monitoring and control as they do not occur purely due to process environment or manufacturing restrictions. The complex phenomena and interlinked mechanisms make it difficult to characterize and control such defects. Voids, consolidation quality, surface finish, crystallinity and thermal degradation are such phenomena that occur during the ATL process. Despite the challenges, an exception was made and this feasibility study was conducted to characterize residual stress formation. The main motivation behind this is to study the scope of limiting shape distortion, which is a consequence of residual stress. Shape distortion affects geometrical tolerances that cannot be rectified after processing, affecting assembly and in-service behavior of the structure. The research question addressed in the research article pertains to: *Which techniques are best suited for manufacturing defect monitoring concept? In particular, which techniques are useful for monitoring and controlling residual strain leading to shape distortion?*

The defect type, effect of defect on the structure, factors influencing the defect formation, and factors that can be controlled are listed below.

- **Defect type:** manufacturing induced residual strain occurring at meso and macro scale
- **Effect of defect:** design, assembly and in-service behavior of the structure; leading to secondary defects such as fiber waviness and shape distortion; failure initiation (exceeding allowable limits) via delamination, matrix cracking and fiber buckling; and detrimental effect on mechanical properties such as tensile, flexural and fracture toughness
- **Influencing factors:** temperature gradient, shrinkage and elastic coefficients of composite elements, crystallinity gradients and fiber volume fraction gradients; which are dependent on processing parameters and material properties (matrix morphology, fiber morphology and fiber-matrix interface properties)
- **Controllable factors:** process parameters
- **Determination technique:** FBG integrated inside the structure
- **Application:** localizing parts with stress concentration (prognosis), product optimization and structural health monitoring (SHM)
- **Aim:** feasibility study to analyze the effect of cooling rate on global residual strain leading to shape distortion

Two FBG sensors, placed at a specific angle to each other are embedded in a single thermoplastic tape. Multiple unidirectional tapes are laid on top of these FBGs and the wavelength shift is collected inline. Mechanical and thermal calibration is used for temperature and strain discrimination, which is then validated using thermocouples. Intermittent (inline) residual strain is measured after each layup and is used to determine global residual strain.

Inline monitoring of residual strain helps in understanding the evolution of strain at different levels and therefore helps in recognizing crucial parameters for strain optimization. For unidirectional laminates it is possible to have no shape distortion and nearly zero residual strain for specific processing conditions. Tool temperature affects the cooling rate which in turn affects the residual strain formation. As the cooling rate decreases so does the magnitude of the residual strain.

Strain formation in a single layer can be analyzed using two FBGs. Shape distortion can be characterized to a certain extent using limited sensors, but more data points and detailed



experimental studies are required to establish correlations. It is necessary to use multiple FBGs spread throughout the laminate to form a comprehensive understanding of the mechanisms related to strain build-up and the resulting defects in the structure. To ensure repeatability and statistical relevance, multiple samples must be made, involving enormous amounts of FBGs. Moreover, since the strain values are dependent on process parameters, a detailed parametric study has to be conducted to ensure strain optimization for the overall process. Parametric study would entail multi-objective optimization, involving material and heat source characterization as well. This goes far beyond the scope of strictly manufacturing related defects, especially considering inline monitoring and defect control. Therefore, even though the feasibility study delivered good scientific results, FBGs are not used as a part of the final study.

Considering the research question, it can be concluded that, *FBG sensors can monitor inline residual strain. The resulting shape distortion can be controlled to a certain extent by adjusting the process parameters. However, detailed multi-objective process optimization is required before adjusting process parameters only considering final strain values.*

*Article B [28]: “In-line residual strain monitoring for thermoplastic automated tape layup using fiber Bragg grating sensors”*

## RESEARCH ARTICLE

Polymer  
COMPOSITES

WILEY

# In-line residual strain monitoring for thermoplastic automated tape layup using fiber Bragg grating sensors

Neha Yadav<sup>1</sup> | Karol Wachtarczyk<sup>2</sup> | Paweł Gašior<sup>2</sup> | Ralf Schledjewski<sup>1</sup> | Jerzy Kaleta<sup>2</sup>

<sup>1</sup>Processing of Composites Group,  
Department Polymer Engineering and  
Science, Montanuniversität Leoben,  
Leoben, Austria

<sup>2</sup>Department of Mechanics, Materials and  
Biomedical Engineering, Wrocław  
University Of Science And Technology,  
Wrocław, Poland

## Correspondence

Neha Yadav, Processing of Composites  
Group, Department Polymer Engineering  
and Science, Montanuniversität Leoben,  
Otto-Glöckel-Strasse 2/3, 8700 Leoben,  
Austria.

Email: neha.yadav@unileoben.ac.at

## Funding information

Narodowa Agencja Wymiany  
Akademickiej, Grant/Award Number:  
PPN/BIL/2018/1/00058; OeAD-GmbH,  
Grant/Award Number: PL 05/2019;  
Österreichische  
Forschungsförderungsgesellschaft, Grant/  
Award Number: 864824

## Abstract

Automated tape layup (ATL) has been used extensively for manufacturing composites laminates using unidirectional prepreps for high-performance industries like aerospace. Residual stress is one of the defects that adversely affect the layup quality. These stresses affect geometrical tolerances in the form of distortion of the final product and are found to have a detrimental impact on the mechanical properties. In-line monitoring of such defects will help in productivity increase and achieving a reliable process control. The aim of the present work is to demonstrate the feasibility of fiber Bragg grating sensors for monitoring residual strains. FBGs are embedded inside a thermoplastic UD laminate. Temperature and strain discrimination is performed to recognize intermittent residual strains during the layup. Finally, intermittent residual strain is used to develop an understanding of the global residual strain. Effect of selective process parameter on residual stress formation and the evolution of the same is also analyzed.

## KEYWORDS

fiber Bragg grating, polymer-matrix composites, process monitoring, residual/internal stress, tape placement

## 1 | INTRODUCTION

Automated tape layup mostly relies on manual post manufacturing analysis for defect detection and rectification. As a drawback of manual optical inspection, some flaws go undetected. This leads to higher repair costs and in worst case, rejection of the part causing further material, monetary, and productivity loss.<sup>[1–6]</sup> One such defect is residual stress. In its visible form, it can be seen as shape distortion, which by far is remedied only by trial and error.<sup>[7]</sup> Early in-line detection and quantification of such defects will help in productivity increase and reliable process control.

Understanding and monitoring residual stresses is particularly important for robust design and reliable performance. These stresses have a twofold effect: affecting geometrical tolerances in the form of distortion of the final product and having a detrimental impact on the mechanical properties.<sup>[8–10]</sup> Shape distortion happens in the form of spring-in in curved parts and warpage in flat parts, affecting dimensional accuracy, requiring an expensive and time-consuming trial and error approach to compensate for the geometrical variations. A study done by Hoa<sup>[7]</sup> for flat thermoplastic laminates demonstrates such distortion. Knowledge about the resulting stresses and prediction of distortions will not only improve the productivity but also

This is an open access article under the terms of the Creative Commons Attribution License, which permits use, distribution and reproduction in any medium, provided the original work is properly cited.

© 2022 The Authors. *Polymer Composites* published by Wiley Periodicals LLC on behalf of Society of Plastics Engineers.

help in cost saving and increasing reliability of the process. Furthermore, residual stresses have to be monitored so that the effect on mechanical properties can be analyzed and a mechanical failure of a composite part in service life can be predicted.<sup>[8]</sup>

If exceeding allowable limits, the stresses may cause delamination, matrix cracking, distortion, and fiber buckling or void formation during solidification.<sup>[8,10]</sup> Many studies have been carried out on the negative effect of residual stress on fracture toughness, and tensile and flexural properties. Additionally, residual stresses are found to cause defects, such as fiber waviness, warpage and transverse cracking. Changes in physical and mechanical properties of the matrix such as glass transition temperature and toughness, respectively during service life might also be impaired, affecting environmental resistance adversely.<sup>[11]</sup>

While reduced internal stress will lead to quality enhancement and optimization of the manufacturing process as the structure can withstand higher buckling loads and will have higher fundamental frequency<sup>[3]</sup>; their occurrence is inevitable<sup>[8]</sup> and at best can be minimized and kept within an allowable limit.<sup>[12]</sup> Understanding the effect of residual stress development and operation under non-optimum conditions<sup>[12]</sup> and reduction of the same is among the various research gaps identified to commercialize thermoplastic ATL.<sup>[10]</sup> A knowledge gap related to Structural Health Monitoring (SHM) of through thickness effects of residual stress on mechanical properties of thick laminates was also identified.<sup>[11]</sup>

Another research gap is identified regarding prediction of residual stress via simulation. Simulation studies focusing on prediction of residual stress have been done in the past.<sup>[13–17]</sup> Macroscopic in-plane and instantaneous residual stress are discussed by Chapman<sup>[18]</sup> and Sonmez,<sup>[12,16,19]</sup> respectively. But due to a lack of data for automated tape layup process, press molding results were used for verification in this case.<sup>[19]</sup> In-line monitoring will not only ensure that the residual stresses are within acceptable limits but can also serve as validation for the existing simulation studies.

This research work focuses on feasibility and capability analysis of Fiber Bragg Grating (FBG) sensors to monitor residual stresses in-line. Effect of selective process parameter on residual stress formation and the evolution of the same is also analyzed. The work elaborated here pertains to thermoplastic ATL.

## 1.1 | Formation

The formation of residual stress takes place at micro, macro and global level. On the *micro-mechanical level* or constituent level, the mismatch in coefficient of thermal

expansion between the fibers and the matrix is the governing parameter.<sup>[9,12,20–22]</sup> The residual stresses at this scale are self-equilibrating and do not cause any distortions of the composite laminate. They do however adversely affect the strength of the laminate by matrix cracking.<sup>[8,22]</sup> During cooling/solidification, residual stresses arise due to the difference in volumetric shrinkage, which is much higher for the thermoplastic matrix than the fiber. This results in residual compressive stress in the fiber along the longitudinal axis and radial direction, and a residual tensile stress in the matrix in the longitudinal and radial direction, assuming that fiber–matrix bonding is present during cooling.<sup>[22]</sup>

*Macro-mechanical* or lamination residual stresses are present on a ply-to-ply scale due to lamina anisotropy.<sup>[8,20–22]</sup> The residual stresses arise due to a difference in coefficient of thermal expansion in the transverse and longitudinal ply. For example, for cross-ply composites, because of the difference in thermal shrinkage directions, the 90° fibers and 0° fibers impose a mechanical constraint on each other during cooling. Much like the behavior of a bi-metallic strip, the anisotropic shrinkage may result into deformation of unbalanced and unconstrained laminate.<sup>[22]</sup>

*Global* residual stresses or skin-core stresses are caused by a gradient in cooling rate, temperature or moisture conditions throughout the thickness of the composite laminate and are typically parabolic in distribution with compressive residual stresses in the surface plies and tensile stresses in the center plies.<sup>[18,20–22]</sup> Thermal and mechanical tool-part interaction is one such factor driving these stresses. The difference in the coefficient of thermal expansion (CTE) between the tool and the composite part can result in compressive residual stresses in the surface plies (assuming the tool has higher CTE than the composite) and ultimately into warpage or fiber waviness. This could be exacerbated by interfacial stress transfer induced by forced shrinkage in the surface ply due to the friction between the two surfaces.<sup>[8,22]</sup>

The residual stresses can further be categorized as *thermoelastic* and *non-thermoelastic*. Thermoelastic residual stresses are reversible. They are caused by the difference between in-plane thermal strains and through-thickness thermal strains and any distortion can be eliminated by heating the part to its stress-free temperature (SFT). Non-thermoelastic residual stresses are irreversible.<sup>[8]</sup> In general, the main parameters causing residual stresses are: temperature gradient, shrinkage of composite constituents, elastic coefficients of these constituents, crystallinity gradients and fiber volume fraction gradients.<sup>[8,22]</sup> These are, in turn, largely dictated by processing parameters and material properties like matrix morphology, fiber morphology and fiber-matrix interface properties.<sup>[22]</sup>

## 1.2 | Influencing parameters

This section discusses the process parameters that influence residual stress formation. This information is useful for recognizing the major contributing parameters, and if possible, controlling them and reducing the induced stress.

The major processing parameters that influence the quality of the consolidation bond are heat, layup velocity and compaction pressure.<sup>[23]</sup> Since the pressure levels are relatively low, compaction pressure has limited effects on both bond quality<sup>[24]</sup> and residual stress.<sup>[22]</sup> Heat distribution depends on the test set-up/environment including heat source settings, material and temperature of the layup tool and material and temperature of the compaction roll. The magnitude of the residual stresses is most dependent on the shrinkage behavior of the thermoplastic matrix during processing and the most important processing condition that affects residual stress formation is the cooling rate.<sup>[22]</sup> The effects of remaining processing parameters are also evaluated in terms of heat distribution. A few studies<sup>[16,19]</sup> have been conducted on the same and the results are described below:

Increasing the velocity increases the residual stress. At high speeds due to localized heating, high temperature gradients give rise to increased residual stress. Increasing the heated length ratio (substrate/incoming) reduces the residual stress. Increasing the preheating temperature reduces the temperature difference between the heated zone and the remaining region, slowing down the cooling rate and decreasing the residual. Similarly, a large heated length leads to lower residual stress due to slowing down of the cooling rate. Increasing the roller radius decreases the residual stress, as small rollers induce a highly concentrated stress distribution.<sup>[16,19]</sup> In general, processing parameters resulting in a more localized temperature distribution lead to higher residual stresses.<sup>[12,16]</sup>

The mechanism related to cooling rate is discussed here. For amorphous thermoplastics, the higher the cooling rate in the glass transition region, the higher the residual stresses. For semi-crystalline thermoplastics, two competing mechanisms are involved. For high cooling rates, lower residual stresses occur because of lower stress-buildup temperature and less crystallization shrinkage and higher residual stresses occur due to fast cooling of the amorphous phases.<sup>[22]</sup> Overall, increasing the cooling rate increases the residual stress. At high cooling rate, the viscous to elastic transition temperature increases, increasing the volumetric change associated with crystallization.<sup>[18]</sup> This is further supported by the effect of stress-free temperature on residual stress. The higher the difference between the cool-down (service/tool temperature) from the SFT, the more residual stresses reside in the composite.<sup>[22]</sup> An interesting study

performed for thermoformed PEEK relates the effect of tool temperature to warpage and suggests that the higher the tool temperature, the lower the warpage.<sup>[25]</sup>

A few important observations were made about the accumulation of residual stresses at ply level, which are described here. Residual strains were found to accumulate at different rates for each layup.<sup>[22]</sup> This is further confirmed by Sonmez.<sup>[12]</sup> The research further proposed that the existing residual stresses in substrate are partially destroyed with placement of a new layer due to locally induced high temperatures, but also contribute to the said stresses while cooling down. Given that unbalanced laminates become flat at the stress-free temperature, they advocated that layers experiencing temperatures above stress free temperature during placement of last layer would either have minimum (layers having fiber orientation transverse to rolling direction) or close to zero (layers having fiber orientation parallel to the rolling direction) residual stress. Along the same lines, it can be concluded that layers experiencing temperatures less than stress free temperature during placement of last layer, will have minimum residual stress if the fiber orientation is in the rolling direction. For cross-ply APC-2 laminate this value is about 70 MPa, which is within the range obtained by the standard press molding process.<sup>[12]</sup> It should be noted that non-thermoelastic stresses are not considered here.

After processing, stress relaxation can be carried out via annealing, especially for skin-core stresses.<sup>[22,26]</sup> For semi-crystalline thermoplastics, increasing the annealing time below the glass transition temperature ( $T_g$ ), relaxes and decreases the residual stresses. For amorphous thermoplastics, annealing does not significantly relax the residual stresses.<sup>[22]</sup>

It is important to note that the studies mentioned above highlight parametric impact on residual stress without considering other components of laminate quality. For process optimization, minimizing residual stress is one of the criteria, besides degree of consolidation bond, level of crystallinity, percentage of voids and level of degradation among others.

## 1.3 | Determination

A number of techniques can be used to measure residual stresses. A summary of the techniques employed so far is discussed here.

### 1.3.1 | Destructive techniques

First ply failure method: The transverse tensile strength of symmetric cross-ply ( $0^\circ/90^\circ$ ) laminates is measured to

be lower than the transverse tensile strength of unidirectional ( $0^\circ$ ) laminates. The tensile strength for cross-ply laminate is recorded at the first audible crack and the difference between the transverse tensile stresses between cross-ply and unidirectional laminates provides an estimate for the interlaminar residual stress.<sup>[26–28]</sup>

**Layer removal method:** Progressive mechanical removal of layers from a symmetrical balanced flat laminate results into deformation (warping), which can be monitored, for example using Moire interferometry<sup>[26]</sup> or traveling microscope.<sup>[27]</sup> The strains can be detected by strain gauges. The resulting deformation and strains are then used to calculate residual stresses in the laminate before layer removal,<sup>[28]</sup> often using classical lamination theory (CLT).<sup>[26,27,29]</sup>

**Hole drilling method:** This method involves fixing a strain gauge rosette to the surface of the specimen and then drilling a hole through the specimens in the center of the rosette. The strains produced at the surface are used to deduce the stresses present prior to hole drilling using semi-empirical models.<sup>[26,28,29]</sup> Another variation of this technique is slot drilling, where single or multiple slots/grooves/slits are incrementally cut into a specimen and the resulting strain is measured using strain gauges.<sup>[26]</sup>

**Chemical probe technique:** This is a speculative approach based on establishing reference data (for specific polymer-environment combinations) for the relationship between stress and time to crazing and/or cracking. Specimen with unknown residual stress is exposed for a specific period to an environment and cracking/crazing indicates whether the stress is above or below the reference value. This is repeated for progressively harsher environments to estimate the residual tensile stress.<sup>[29]</sup>

Except first ply failure, the rest of the techniques involve stress relaxation. Removing material causes deformation and releases stress due to additional free surface creation. These monitored stresses are used to measure original residual stresses that existed in the laminate. Stress relaxation techniques can be used to measure global through thickness (skin-core) residual stresses.<sup>[26]</sup>

### 1.3.2 | Non-destructive techniques

There are non-destructive measurement techniques that detect the change in material's intrinsic properties due to thermal residual stresses in one of the components of the composite. These techniques can be employed to measure intra-ply (micro-mechanical) and inter-ply (macro-mechanical) stresses. This includes, laser/micro-Raman

spectroscopy based on change in Raman peak of the crystalline phase,<sup>[9,26]</sup> photo elasticity method based on change in refraction of light,<sup>[26]</sup> bi-refringence measurement detecting change in polarization<sup>[29]</sup> and monitoring changes in electrical conductivity.<sup>[26]</sup>

Other techniques take use of embedding foreign sensors inside the composite material. Given a sufficient mechanical interaction between the composite and the sensor, when exposed to strains, the sensor shows measurable change in properties. Sensors, which have found use in literature so far are: strain gauges,<sup>[26]</sup> along with stress wave propagation<sup>[30,31]</sup>; embedded metallic particles in combination with X-ray diffraction<sup>[26]</sup> and fiber optical sensors (FOS).<sup>[21,26,28,32–34]</sup> Among the listed sensors, only FOS are found to be able to detect strains at all three levels, inter-ply, intra-ply and laminate, the can detect inter-ply and/or intra-ply stresses.

Digital image correlation<sup>[35]</sup> and digital volume correlation in conjunction with in-situ synchrotron radiation computed tomography<sup>[36]</sup> have also been used for inspection and testing. Since the testing involves subjecting the component to external loads post-processing, this can severely damage (intended) the component.

Among the various methods discussed above, FOS have maximum advantages, minimum disruption of the specimen, minimum effort for sample preparation, and high resolution of measured strain at all three levels. What is also important—FOS are widely used for monitoring the structure during its exploitation (SHM), e. g. monitoring of high pressure vessels for hydrogen storage,<sup>[37]</sup> so they can serve as two-stage (manufacturing and exploitation) sensors. There are many types of FOS, fiber Bragg gratings (FBG), being one of them, have found extensive use in literature for strain monitoring and are therefore selected for the present research. Recently, embedded FBG sensors have shown the capability to measure strain developed by hygroscopic aging,<sup>[38]</sup> environmental effects on strain can therefore also be monitored. Regarding SHM, studies found in literature<sup>[39,40]</sup> can be used for validating the results.

Few papers describe the usage of FBG sensors for the in-situ monitoring of the ATL process.<sup>[33,34,41]</sup> In these papers, in-situ strain and temperature measurement was investigated, however usage of FBG sensors for build-up of residual strain after each layup was not addressed.

## 1.4 | Inferences and hypotheses

Distortion is one of the indications of existing residual stresses but residual stresses will be present whether a distortion can be seen or not. For unidirectional (UD) layup, since micro-mechanical or intra-ply stresses

are self-equilibrating,<sup>[8,22]</sup> and inter-ply (macro-mechanical) stresses are absent (as there is no ply-to-ply lamina anisotropy<sup>[8,20–22]</sup>), any distortion observed is a result of global stresses arising from tool part interaction. Moreover, for a constant set of processing parameters, the residual stress should be a constant value near zero (following from Section 1.2).<sup>[12]</sup>

Balanced flat symmetric cross-ply laminates, will also have no distortion in the absence of a tooling constraint.<sup>[8]</sup> However, unbalanced and unconstrained cross-ply laminate may result into warpage.<sup>[22]</sup> For unsymmetrical laminate, the shape of the distortion depends on the width-to-thickness ratio. Thin laminates (compared with in-plane dimensions) will tend to deform into a right circular cylinder. For two and four ply double curvature laminates, one curvature tends to restrain the other, leading to an anticlastic saddle shape.<sup>[13,27]</sup> It was also found that the higher the curvature of a laminate, the higher the residual stresses.<sup>[26]</sup> The magnitude of stress would depend on the fiber orientation of the final layer (following from Section 1.2).<sup>[12]</sup>

Increasing the cooling rate increases the global residual stress.<sup>[18]</sup> The nature of this stress depends on the position of the layer, with compression in surface plies, tension in center plies and overall parabolic distribution.<sup>[18,20–22]</sup> Further, the magnitude of this residual stress gradient is much higher in cross-ply laminates than unidirectional laminates.<sup>[22]</sup>

Hypotheses:

1. Laminates with unidirectional balanced layup should have very less residual strain (at least when compared to cross-ply laminates) and almost no distortion (if neglecting stress due to tooling constraint). In comparison, unbalanced cross-ply laminates should have pronounced stress distribution, increasing with the curvature of the distortion and dependent on stacking sequence and fiber orientation of the final layer.
2. Cooling rate is maximum for lowest tool temperature, and hence, residual stress should be maximum. Residual stress for surface plies should be compressive in nature.

Based on the overview, theoretical knowledge including simulations detailing parametric influence on residual strain and experimental experience about strain measurement using FBG can be found in the literature. However, a direct experimental verification of impact of these process parameters on the residual strain has not been done before. This research work tries to link the two separate knowledge pools and bring about a better understanding and deeper insight regarding the underlying phenomena with the help of sensor technology. This

research work is the first attempt to establish a working model to verify the theory and justify FBG usage and can be expanded for future investigations.

As concluded from above, residual stress depends on the cooling rate, which is affected by the temperature of the tool. In this case, FBG sensors will be used for the determination of residual stresses for varying temperature levels.

## 2 | EXPERIMENT DETAILS

This section describes the materials and methods employed to integrate FBG inside the composite laminate. The preliminary tests and data analysis methods used to measure residual strain for different process parameters are also described.

### 2.1 | Experimental setup

In-house built ATL machine by Montanuniversität Leoben (MUL), is used for the experiments elaborated in this research. The main heat source used is a flash lamp based, *humm3*<sup>®</sup> system (Hereaus Noblelight GmbH, Germany), with heat output of 2.9 kW. The layup tool is made out of aluminum and is temperature controlled. Thermoplastic CF-PA6 tapes from SGL Carbon, having a melting point of 220°C and a glass transition temperature of 58°C are used throughout the experiments, unless stated otherwise. The tapes used are 25.4 mm wide. The compaction force is maintained at 200 N. The layup velocity is kept constant at 50 mm/s, unless stated otherwise. Three unidirectional samples were manufactured and only the tooling temperature was varied for these three samples, all the rest of the parameters were kept same. It is noteworthy to mention that the comparisons done in past with theory also utilized similar/limited data sets. In our case, extreme care has been taken and data checks have been performed at each step starting from procurement of the sensor, pre-calibration, integration check to post manufacturing calibration. We can safely conclude that accuracy of the data (from FBG) is sufficient to compare the theory with the results gained with minor deviations.

A conformable silicon roll having a diameter of 50 mm and 70 shore A hardness is used as compaction roll. It should be noted here that a study done by Sarrazin<sup>[10]</sup> shows that size of the roller between 50–200 mm have little effect on the stresses. A 15-layered UD laminate is manufactured using the set-up. One layer consists of one tape. Here, the terms ply and layer are used interchangeably. The experimental set-up and layup scheme are shown in Figure 1.

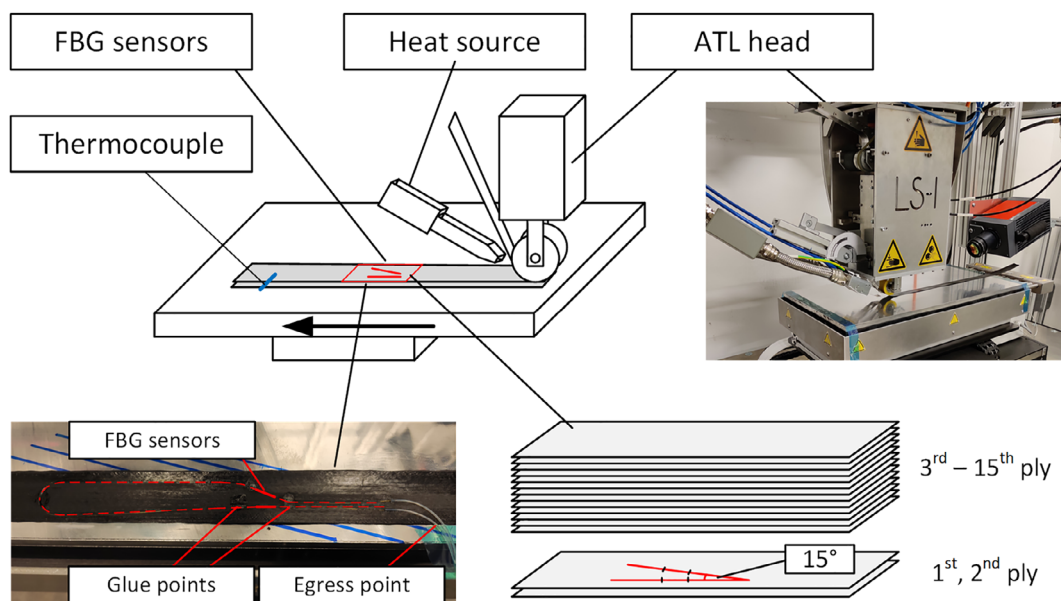


FIGURE 1 Placement of FBG inside the composite. The red lines mark the orientation

## 2.2 | Fiber Bragg grating sensors

For ATL monitoring, polyimide coated silica core fiber with Fiber Bragg Gratings (Sylex, Slovakia) are used. The length of the active FBG is 8 mm and the outer diameter of the fiber is 145  $\mu\text{m}$ . Temperature resistance of the polyimide coating allows operation at a temperature up to 350°C, which is well above the temperature expected during the layup for CF-PA6. This type of coating has also been shown as capable of being used for CF-PEEK (higher melting point than CF-PA6) without compromising their functionality.<sup>[34]</sup>

Peak wavelength is approximately 1550 nm. Data acquisition is done with the Benchtop BraggSCOPE FS5500 interrogator (FiberSensing, Portugal). This interrogator allows to simultaneously measure the wavelength shift of 4 FBG sensors with a sampling rate up to 10 kHz with resolution of 0.1 pm and  $\pm 10$  pm repeatability, which corresponds to resolution of 0.12  $\mu\epsilon$  or 0.01°C and repeatability of 12  $\mu\epsilon$  or 1°C. For the tests, two FBGs with 1 kHz sampling rate are used. Additionally—for comparison reasons, reflection spectra between consecutive layups are collected with an SI-405 interrogator (HBM, Germany). Detection of peaks with the HBM device is performed with resolution of 1 pm, which gives strain measurement resolution of 2  $\mu\epsilon$  and temperature of 0.1°C.

It should be noted here that after the placement all 15 layers, optical spectra of sensors showed no distortion or splitting of peaks, indicating that the strain readings from FBG are reliable.

Integrated optical fibers influence the host material. If not placed parallel to the fibers (30°/45° to the CF),

they can cause discontinuity of the FRPs, by creating resin pockets around the optical fiber.<sup>[42–44]</sup> Such pockets cause stress concentration and compromise the strength of the material. However, this effect is not strictly connected with residual stresses. It is worth mentioning that in our paper FBG sensors are placed parallel or at a low angle to the CF fibers (15 degrees), so the influence of the material around is neglectable.

The second point is that the driving force causing the residual stress in thermoplastics is the mismatch of the CTE between the composing materials. In this case, optical fiber has a very small cross-section area, so even though there is a mismatch in CTE, the effective force would not be enough to significantly differ the overall residual stress. FBG has a cross section of  $\sim 0.012$  mm<sup>2</sup>, while one layer of CF-PA6 has a cross-section of 5.08 mm<sup>2</sup>.

It is also worth mentioning that the HBM interrogator used in this paper requires FBG sensors to measure the strain. For this reason, different methods for the determination of residual stress would be required to compare the influence of FBG itself on the composite. The large number of the residual stress assessment methods provided in the paper shows there is still a challenge to describe residual stresses of materials and their comparison requires separate research. On another note, readings from FBG integration (pre-tension) before the start of the layup are recorded and subtracted from the overall strain. This is done for each sample, ensuring there is no additional strain due to the FBG itself. Moreover, calibration tests ensured that the strain calculated using coefficients is the actual strain experienced by the composite irrespective of the FBG.



## 2.3 | Preliminary tests

To ensure accurate and reliable strain transfer from composite to the FBG, it is important to make sure that the FBG is well integrated (bonded) within the composite. A few different preliminary tests were done to check the quality of integration (placement technique) of FBG inside the composite structure.

Initial trials proved that flash tape was not enough to hold the FBG in place. To maintain pretension and orientation, adhesive glues were tested. The criteria for which were: short bonding time in free-air, non-intrusive or spreadable with no thickness increase, ability to hold the pretension and quality of adhesion. Based on the results, it was decided to use a primer and Loctite 406.

## 2.4 | Simultaneous strain and temperature measurement

The main aim of the experiments was: simultaneous measurement of the strain and temperature and to discriminate the two to measure the influence of tool temperature on residual strain of unidirectional layup.

FBG sensors were glued between on the 2nd layer of the 15 layered unidirectional laminate. A single FBG sensor was placed parallel (straight, 0°) to the fiber direction and another FBG was placed at 15° (angled) to the fiber direction. Placement of the two FBG sensors on the CF tape is shown in the figure below. A K-type thermocouple (TC), having 0.5 mm diameter was also integrated in the same layer, in the vicinity of the FBG. The placement of each layer was then monitored in-line. Thermocouple data at 10 Hz and FBG data at 1000 Hz were recorded for each layup. The temperature data obtained from thermocouple is compared with temperature results from FBG. FBG spectrum data was also collected after each layup, before a new layer is placed.

A total of three samples were manufactured, having same processing conditions except for tool temperature. Sample 1 had tool temperature at 30°C, sample 2 at 60°C and sample 3 at 120°C.

### 2.4.1 | Temperature and strain discrimination

Various methods have been employed in the past to distinguish temperature and strain, including: encapsulated FBG to instill temperature insensitivity,<sup>[33]</sup> twisting one FBG over the other<sup>[32]</sup> and having one FBG at an angle to the other.<sup>[34]</sup> In the latter two cases, the temperature sensitivity of the sensors is assumed to be the same with

respect to the other FBG sensor. The present research work uses an approach similar to,<sup>[34]</sup> but it will be shown later on that calibration tests for temperature sensitivity are indispensable and have an enormous impact on final results.

Wavelength shift caused by temperature and mechanical response is given by the following equation:

$$\Delta\lambda_B = K_\varepsilon \cdot \varepsilon + K_T \cdot \Delta T \quad (1)$$

where,  $\lambda_B$  is the Bragg wavelength,  $K_\varepsilon$  and  $K_T$  are strain and temperature sensitivities respectively.  $\Delta T$  is temperature shift and  $\varepsilon$  is strain.

Usage of straight and angled FBGs at the same time can be used for simultaneous measurement of temperature and strain. Following the above equation, if we assume that  $\Delta T_S = \Delta T_A$  and  $\varepsilon_S = \varepsilon_A$  (because we are investigating only longitudinal direction), equation used for determination of wavelength shift can be written as<sup>[32,34]</sup>:

$$\begin{bmatrix} \Delta\lambda_{B_S} \\ \Delta\lambda_{B_A} \end{bmatrix} = \begin{bmatrix} K_{\varepsilon_S} & K_{T_S} \\ K_{\varepsilon_A} & K_{T_A} \end{bmatrix} \begin{bmatrix} \varepsilon \\ \Delta T \end{bmatrix} \quad (2)$$

$$\begin{bmatrix} \varepsilon \\ \Delta T \end{bmatrix} = \left( \begin{bmatrix} K_{\varepsilon_S} & K_{T_S} \\ K_{\varepsilon_A} & K_{T_A} \end{bmatrix} \right)^{-1} \begin{bmatrix} \Delta\lambda_{B_S} \\ \Delta\lambda_{B_A} \end{bmatrix} \quad (3)$$

As noted by, Saenz-Castello,<sup>[33]</sup> the sensitivity coefficients are different when embedded in a host material compared to free-space (air), since the thermal expansion of the host material is different. To find the true sensitivities, calibration tests are performed.

### 2.4.2 | Calibration tests

The calibration test was done on all individual samples containing 15 layers each. Since the calibration is directly done on the manufactured sample, additional tests for different number of layers is not needed. Intermittent and global residual strain for near surface layers (between 2nd and 3rd layers) can be calculated with the data provided. If a relationship between residual stress in surface layers and layer 2–15 is desired, then such calibration might be of use.

For strain and temperature sensitivity, using Equation (1) and considering constant temperature and zero external mechanical strain respectively, we get:

$$K_\varepsilon = \frac{\Delta\lambda_B}{\varepsilon} \left[ \frac{\text{pm}}{\mu\varepsilon} \right] \text{ and } K_T = \frac{\Delta\lambda_B}{T} \left[ \frac{\text{pm}}{^\circ\text{C}} \right] \quad (4)$$

Tensile test is used to calculate strain sensitivities. Manufactured laminates with integrated sensors were mounted in the MTS 793 testing machine. Strain was measured with MTS extensometer having 50 mm gauge length located on the top of FBGs. Tensile load was applied in the elastic range of the sample. To find the sensitivity coefficients between  $\lambda_B$  and  $\varepsilon$ , linear regression is performed, as shown in Figure 2.

To measure temperature sensitivities, samples with FBG sensors were subjected to thermal cycle inside an oven. Temperature was held at three levels 25°C, 55°C, and 85°C. Average Bragg wavelength collected on each level was used to calculate the temperature sensitivities.

Calculated coefficients of proportion are given in the Table 1:

Only for sample 1 difference in the strain coefficient between straight and angled FBG was significant (19%). On the other hand—differences in the temperature sensitivities for all samples were quite distinct. For samples S01 and S02 temperature sensitivity of the angled sensor was almost two-fold as high as for the straight one. This could be caused by significant thermal expansion coefficient of PA6, which prevailed in the direction perpendicular to the fibers. These coefficients are used for accurate temperature and strain discrimination. Thermocouple data is used to verify the temperature results gained after discrimination, as discussed in Section 3.2. These results are different than the one presented by Oromiehie,<sup>[34]</sup> since the author reproduced strain and temperature readings with an assumption of equal temperature sensitivities.

Variation of calibration coefficients between the samples could be caused by changes in the direction of FBG sensors during its integration. Since high temperature melts the thermoplastic material around the FBG, it could cause some changes in the FBG directions.

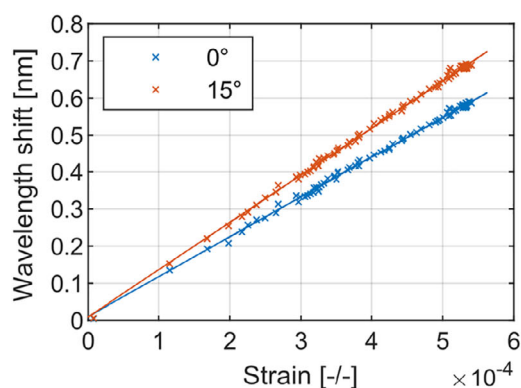


FIGURE 2 Wavelength shift for straight and tilted FBG during the mechanical calibration for Sample 1 (S01) (left), a sample mounted in the testing machine (right)

### 3 | RESULTS AND DISCUSSION

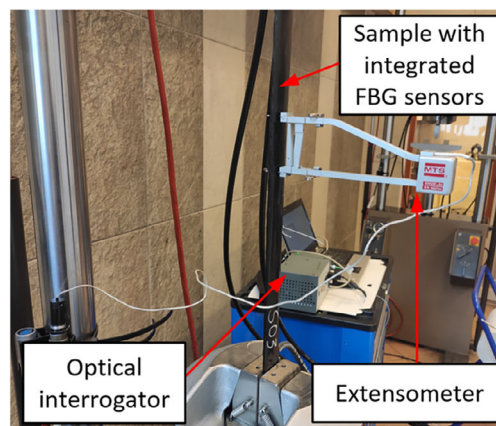
In-line monitoring of the process was used for measuring residual strain of unidirectional composite manufactured with ATL process. During the process, the wavelength shift for both FBG sensors (straight and angled) was collected. Mechanical and thermal calibration were used to discriminate wavelength shifts into strain and temperature during the lay-up process (in-line monitoring). Validation of the evaluation technique was performed by comparing the obtained temperature results (FBG) with temperature reading from thermocouple. Finally, intermittent (in-line) residual strain after each layup was measured and used for global residual strain and stress assessment.

#### 3.1 | In-line monitoring (during layup)

Plots of wavelength shift from the inline monitoring of layup for Sample 2 (S02) using straight FBG are presented below (Figure 3). Layups are synchronized at point when compaction roller presses the tool. The compaction zone is marked with gray color. As a lot of information cannot be obtained from this plot alone, hence the results only from Sample 2 are shown. Individual results from

TABLE 1 Strain and temperature sensitivities for straight and angled FBG embedded inside the UD laminate

Sample	$K_{\varepsilon_S} \left[ \frac{\text{pm}}{\mu\text{E}} \right]$	$K_{\varepsilon_A} \left[ \frac{\text{pm}}{\mu\text{E}} \right]$	$K_{T_S} \left[ \frac{\text{pm}}{^\circ\text{C}} \right]$	$K_{T_A} \left[ \frac{\text{pm}}{^\circ\text{C}} \right]$
Sample 1 (S01)	1074	1273	8650	17,399
Sample 2 (S02)	1102	1169	8890	18,448
Sample 3 (S03)	1166	1163	9116	14,686



all samples are shown whenever required in later sections.

Looking at Figure 3, it can be concluded that, as the thickness of the stack increases (increasing the number of layers), the amplitude of the wavelength shift (deformation + temperature effect) decreases. Moreover, the dynamics of peak wavelength shift changes as the number of layers increase. The longer the time needed to achieve maximum wavelength shift during consolidation, the slower the decrease in wavelength shift after the consolidation. These effects are associated with reduction in cooling rate as the thickness of the layers above FBG increases and are in accordance with literature.<sup>[33,34]</sup> These results are also in alignment with the rest of the samples.

Using the equations and sensitivity coefficients described in Section 2.4, temperature and strain sensitivity were separated from the wavelength shift and the results obtained are discussed next.

### 3.1.1 | Simultaneous measurement of temperature and strain

Assuming constant heat flux, the temperature values recorded by FBG should correspond to those of the thermocouple. It should be noted here that for this purpose, temperature calibration tests are necessary. The sensitivity coefficients have shown to be highly dependent on the orientation of integration. This can be attributed to highly directional properties of the composite material itself. The maximum temperature recorded by thermocouple and FBG for 15-layered UD laminate is shown in Figure 4. TC and FBG data show similar trends with a good correlation. The comparison not only helps in validating the survival and proper integration of FBG inside the composite, it also substantiates the data measurement and analysis techniques. The slight difference in values can arise from differences in the quality of integration, which is also dependent on the diameter of the sensor.

Temperature profile over the course of the layup of 7th layer for sample 2 (S02) is shown (Figure 5, left) as the representative of the temperature curve obtained from the two sensors. Strain and temperature discrimination during the layup of layer 7 for sample 2 (S02) is shown in Figure 5. Temperature reading from FBG sensors is well correlated with data from thermocouples. The TC and FBG reading of temperature for this test show a difference of only 4°C. The sharp temperature drop at the beginning of the compaction zone could be a result of the pressure applied by the roller, which could induce birefringence in the fiber. The evolution of such errors with temperature has been described in detail by Sorensen.<sup>[21]</sup>

Following the strain curve, in the compaction zone when the compaction roll is moving past the FBG, there is a slight compression, followed by prominent tension and immediately followed by compression again. These results are in agreement with Saenz-Castillo.<sup>[33]</sup>

### 3.2 | Intermittent residual strain

The strain monitored after placing each layer is termed here as intermittent/transient residual strain for layer 2 (as the FBG is placed close to the surface of the laminate, between layer 2 and layer 3), for that particular layup. Intermittent strains were obtained in two ways: in-line monitoring during the layup and from the spectrum collected before consecutive layups. Procedure is shown in the figure below (Figure 6):

Strain measured after 30 s of placement of each layer, is depicted here as “in-line” strain after temperature-compensation has been accounted for. Strain values immediately after the layup were found to change/adjust before the next layer is placed as the laminate gets more time to cool and the strain can stabilize. Therefore, strain measured after 30 s of placement was collected as strain values were found to stabilize 30 s after layup considering cooling effects. Data from this dataset were later

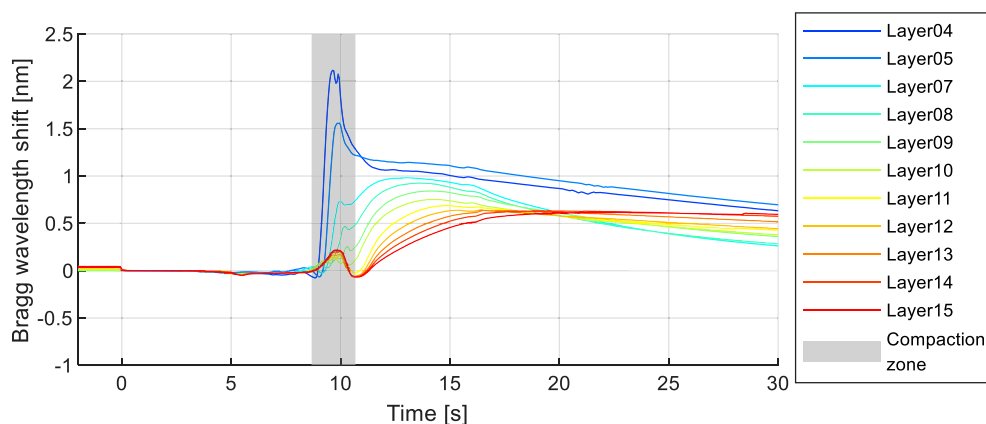
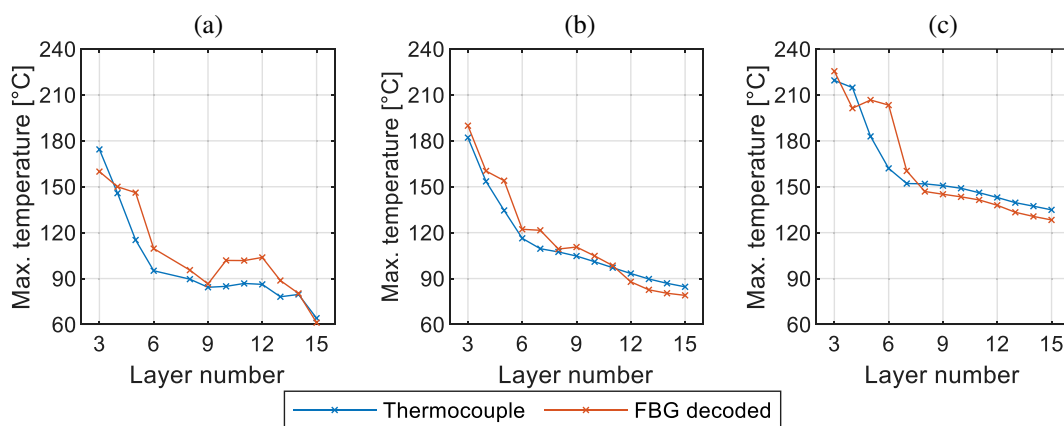
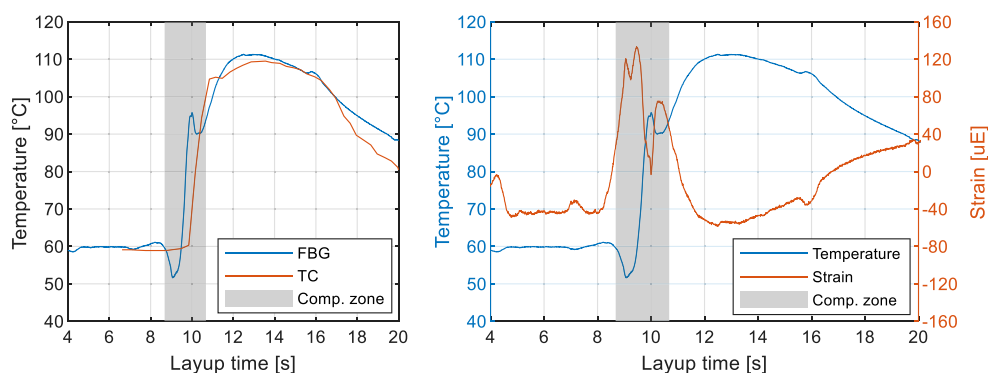


FIGURE 3 Wavelength shift for straight sensor for Sample 2 (S02)



**FIGURE 4** Maximum temperature recorded using thermocouple and FBG for all layers for (A) S01 30°C, (B) S02 60°C, and (C) S03 120°C

**FIGURE 5** Temperature data comparison for FBG and thermocouple for Sample 2 (S02), over the course of 7th layer (left), in-line strain and temperature (right)



discriminated into temperature and strain data. Strain measured with this method gives information about residual strain changes right after the consecutive layup, and to obtain complete information about the current intermittent residual strain, results from all previous layups are presented.

After cooling down of the sample to the tool temperature, and before placement of next layer, full optical spectrum was collected (from straight FBG). Using this spectrum absolute wavelength shift caused by residual strain could be validated. A remark should be made here, angled FBG will provide a combination of longitudinal and transverse strain and the results are therefore omitted.

The sum of strain obtained in-line and before next layup is termed as mean intermittent residual strain for that layup, also shown in the Figure below (Figure 7). For example, mean intermittent residual strain for layer 3 is the sum of in-line residual strain after placing layer 3 and residual strain obtained from spectrum data collected before placing layer 4.

Residual strain build-up is compressive and non-monotonic. This is in agreement with transient stress development results modeled by Sonmez.<sup>[12]</sup> Rapid changes in the intermittent residual strain are visible for

the first layers. After layer number 7–8, the strain reaches almost a constant value and stays the same for the rest of the layers. This is also the point where the rate of temperature decrease (cooling rate) within the laminate slows down (refer to Figure 4). As the number of layers increase, heat dissipation slows down, influencing crystallization shrinkage taking place at the investigated depth. It can be inferred that a slower cooling rate leads to lower strain.

The main point of difference between sample 1–2 and sample 3 is the starting few layers. In this case, the increased crystallization leads to more stresses and outweighs the lower stress due to slow cooling of the amorphous phase. As the layers increase and the heat dissipation decreases, the amorphous phase becomes dominant again. Most importantly, the global residual strain for all the samples corresponds to the literature.

### 3.3 | Final residual stress

Strain value (mean value shown in Figure 7) after the placement of layer 15 is considered as the final global residual strain. Global residual strain for different tool

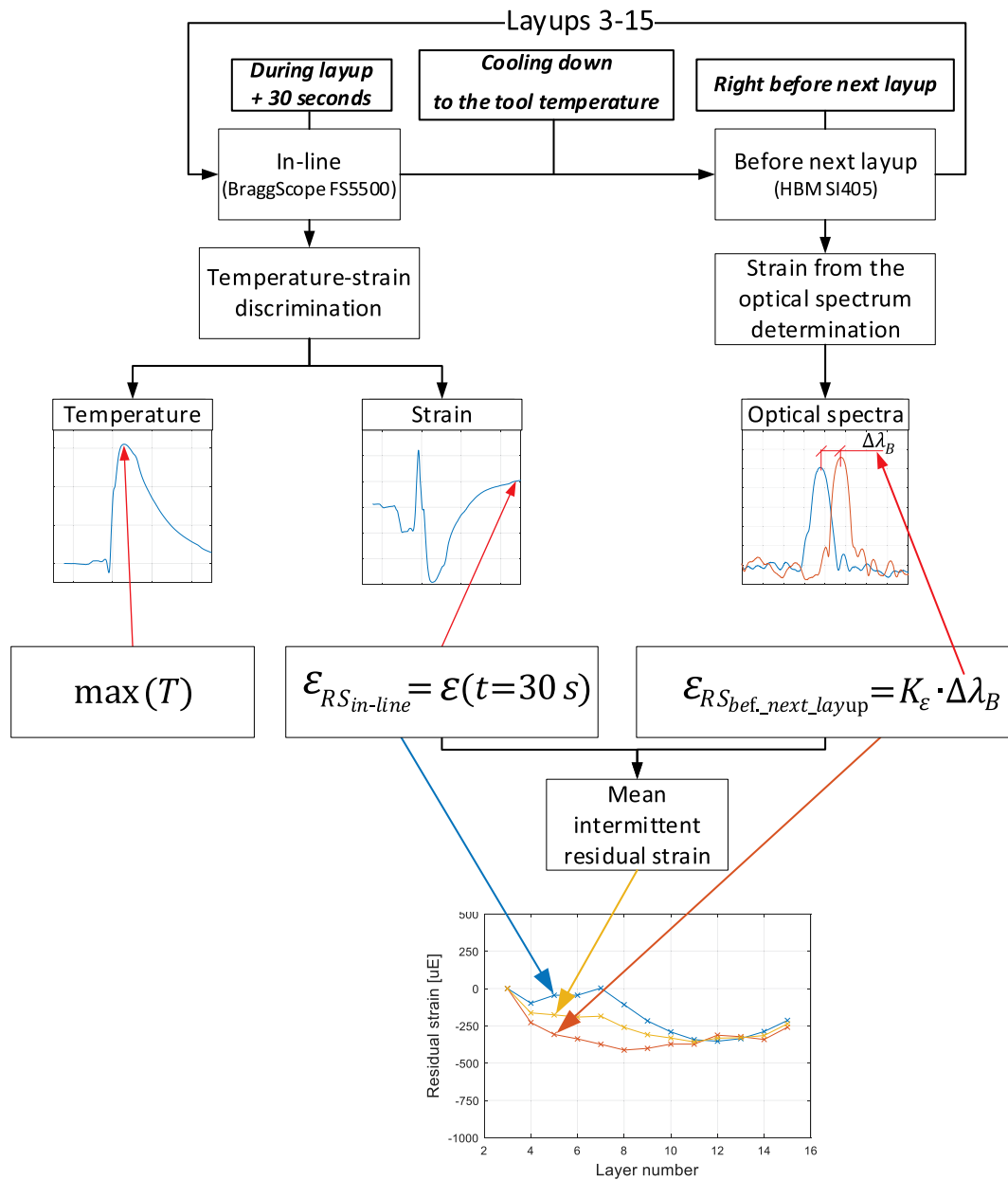


FIGURE 6 Intermittent residual strain data and results determination

temperatures allow us to assess the impact of cooling rate on the mentioned values. Taking use of mechanical calibration tests, modulus of elasticity is calculated and strain to stress conversion is made possible. Final global residual stress for different tool temperatures is shown in the figure below (Figure 8):

Figure 8 exhibits a trend of decreasing global longitudinal residual strain with increasing tool temperature. As the tool temperature increases, cooling rate decreases and so does the residual strain for surface plies. At tool temperature 120°C global residual strain drops almost to 0. These results correspond to strain prediction for APC-2 40 ply UD laminate by Chapman.<sup>[18]</sup> Longitudinal strain

through thickness is parabolic in nature and becomes asymptotically close to zero with a decrease in cooling rate. Irrespective of the cooling rate, as one proceeds from surface plies (most sensitive to cooling rate) to center plies, the compressive strain goes to zero and becomes tensile. In this case, ply number 7/8 show zero stress for a 40-ply laminate.<sup>[18]</sup> As found here as well, the compressive strain of surface plies has shown to be very sensitive to cooling rate, decreasing in magnitude as the cooling rate decreases. A remark should be made here that certain plies will have almost zero stress regardless of the magnitude of the global stress, but for the whole laminate to have low stress, slow cooling rate is recommended.

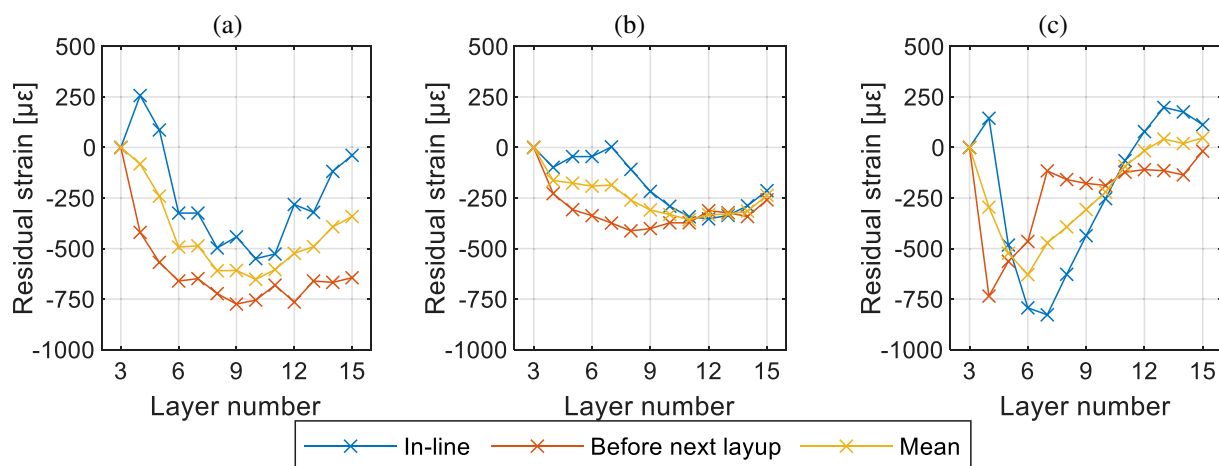


FIGURE 7 Intermittent residual strain over the course of the layup for (A) S01 30°C, (B) S02 60°C, and (C) S03 120°C

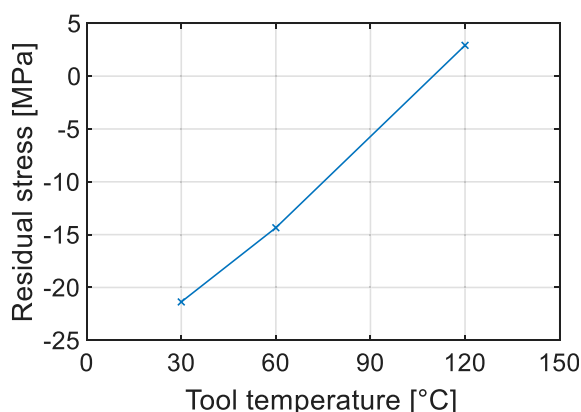


FIGURE 8 Global longitudinal residual stress in surface layer for different tool temperatures

## 4 | CONCLUSION AND OUTLOOK

This research work details effective applicability of FBG for in-line residual strain monitoring. Process parameters influencing residual stress formation are identified and a case study is performed where residual strain is monitored for different layup tool temperatures. Process parameter changes resulting in different strain levels can be successfully identified using FBG sensors and linked to the literature and simulation studies done in the past. The results obtained are in agreement with the inferences and hypotheses based on such literature review. The main findings pertaining to the state of residual strain in surface ply of a UD laminate being:

1. It is possible to have no distortion and near zero residual strain and for specific processing parameters: Justifying hypothesis 1
2. Residual strain build-up in surface ply is compressive and non-monotonic: Justifying hypothesis 2

3. Tool temperature affects laminate cooling rate and in turn residual stress, decreasing in magnitude as the cooling rate decreases: Justifying hypothesis 2

In-line monitoring helps in understanding the evolution of stress (transient to final) throughout the process and in recognizing the crucial parameters for stress reduction. Information about transient stresses is useful in localizing the occurrence of extreme transitory residual strain and assessing their severity during service life. Such prognostic analysis helps in early detection of probable instances of cracks or delamination. While it is important to make sure that the final residual stress is within allowable limit, combined knowledge about different stages of development of stress is required for robust life cycle analysis.

For future work, integration of multiple FBG at different layers is suggested, as it will provide comprehensive look at the global residual stress of the whole laminate. Further, a detailed parametric analysis can be aimed and based on design requirements, process optimization can be performed and different approaches towards stress reduction can be adopted. Moreover, study of cross-ply layup would be crucial from an application point of view. Here, highly birefringent (HiBi) sensors could be employed to map both longitudinal and transverse strain. Furthermore, SHM of such parts is highly recommended to have better insight on the working of residual strain behavior during service life.

## ACKNOWLEDGMENTS

This work has been supported by the OeAD – Austria's Agency for Education and Internationalisation under Project No. PL 05/2019 and the Polish National Agency for Academic Exchange (NAWA) under Grant No. PPN/BIL/2018/1/00058. The authors kindly

acknowledge the financial support through project InP4 (project no. 864824) provided by the Austrian Ministry for Climate Action, Environment, Energy, Mobility, Innovation and Technology within the frame of the FTI initiative “Produktion der Zukunft”, which is administered by the Austrian Research Promotion Agency (FFG).

## DATA AVAILABILITY STATEMENT

The raw/processed data required to reproduce these findings cannot be shared at this time as the data also forms part of an ongoing study.

## ORCID

Neha Yadav  <https://orcid.org/0000-0002-1972-1831>

Ralf Schledjewski  <https://orcid.org/0000-0003-3121-6771>

## REFERENCES

- [1] E. D. Gregory, P. D. Juarez, *AIP Conf. Proc.* **2018**, 1949(1), 60005.
- [2] B. Denkena, C. Schmidt, K. Völtzer, T. Hocke, *Compos. B: Eng.* **2016**, 97, 239.
- [3] E. Oromiehie, B. G. Prusty, P. Compston, G. Rajan, *Compos. Struct.* **2019**, 224(2), 110987. <https://doi.org/10.1016/j.compstruct.2019.110987>
- [4] E. Gregory, P. Juarez, *ASME J. Nondestruct. Eval.* **2018**, 1(4), 41007-1. <https://doi.org/10.1115/1.4040764>
- [5] J. Brüning, B. Denkena, M.-A. Dittrich, T. Hocke, *Procedia CIRP* **2017**, 66, 74.
- [6] C. Schmidt, B. Denkena, K. Völtzer, T. Hocke, *Procedia CIRP* **2017**, 62, 27.
- [7] S. van Hoa, M. Duc Hoang, J. Simpson, *J. Thermoplast. Compos. Mater.* **2017**, 30(12), 1693.
- [8] I. Baran, K. Cinar, N. Ersoy, R. Akkerman, J. H. Hattel, *Arch. Comput. Methods Eng.* **2017**, 24(2), 365.
- [9] C. Filiou, C. Galiotis, D. N. Batchelder, *Composites* **1992**, 23(1), 28.
- [10] K. Yassin, M. Hojjati, *J. Thermoplast. Compos. Mater.* **2018**, 31(12), 1676.
- [11] P. P. Parlevliet, H. E. Bersee, A. Beukers, *Compos. Part A: Appl. Sci. Manuf.* **2007**, 38(6), 1581.
- [12] F. O. Sonmez, M. Akbulut, *Compos. Part A: Appl. Sci. Manuf.* **2007**, 38(9), 2013.
- [13] G. Jeronimidis, A. T. Parkyn, *J. Compos. Mater.* **1988**, 22(5), 401.
- [14] S. C. Mantell, G. S. Springer, *J. Compos. Mater.* **1992**, 26(16), 2348.
- [15] H. Sarrazin, G. S. Springer, *J. Compos. Mater.* **1995**, 29(14), 1908.
- [16] F. O. Sonmez, H. T. Hahn, *J. Thermoplast. Compos. Mater.* **1997**, 10(4), 381.
- [17] C. Dedieu, A. Barasinski, F. Chinesta, J.-M. Dupillier, *Int. J. Mater. Form.* **2017**, 10(4), 633.
- [18] T. J. Chapman, J. W. Gillespie, R. B. Pipes, J.-A. Manson, J. C. Seferis, *J. Compos. Mater.* **1990**, 24(6), 616.
- [19] F. O. Sonmez, H. T. Hahn, M. Akbulut, *J. Thermoplast. Compos. Mater.* **2002**, 15(6), 525.
- [20] J. A. Barnes, G. E. Byerly, *Compos. Sci. Technol.* **1994**, 51(4), 479.
- [21] L. Sorensen, T. Gmür, J. Botsis, *Compos. Part A: Appl. Sci. Manuf.* **2006**, 37(2), 270.
- [22] P. P. Parlevliet, H. E. Bersee, A. Beukers, *Compos. Part A: Appl. Sci. Manuf.* **2006**, 37(11), 1847.
- [23] R. Pitchumani, J. W. Gillespie, M. A. Lamontia, *J. Compos. Mater.* **1997**, 31(3), 244.
- [24] M. A. Khan, P. Mitschang, R. Schledjewski, *J. Compos. Mater.* **2013**, 47(4), 485.
- [25] G. Y. Fortin, G. Fernlund, *Polym. Compos.* **2019**, 40(11), 4376.
- [26] P. P. Parlevliet, H. E. Bersee, A. Beukers, *Compos. Part A: Appl. Sci. Manuf.* **2007**, 38(3), 651.
- [27] K. D. Cowley, P. W. Beaumont, *Compos. Sci. Technol.* **1997**, 57(11), 1445.
- [28] B. Seers, R. Tomlinson, P. Fairclough, *Polym. Compos.* **2021**, 42(4), 1631.
- [29] A. Turnbull, A. S. Maxwell, S. Pillai, *J. Mater. Sci.* **1999**, 34(3), 451.
- [30] Z. Han, S. Sun, W. Li, Y. Zhao, Z. Shao, *Polymers* **2018**, 10(4), 413. <https://doi.org/10.3390/polym10040413>
- [31] H. Y. Fu, W. Q. Li, S. Z. Sun, Z. Y. Han, *IOP Conf. Ser.: Mater. Sci. Eng.* **2017**, 213, 12031.
- [32] O. Frazão, L. A. Ferreira, F. M. Araújo, J. L. Santos, *J. Opt. A: Pure Appl. Opt.* **2005**, 7(8), 427.
- [33] D. Saenz-Castillo, M. I. Martin, S. Calvo, A. Güemes, *Smart Mater. Struct.* **2020**, 29(11), 115004. <https://doi.org/10.1088/1361-665X/abaa97>
- [34] E. Oromiehie, B. Gangadhara Prusty, P. Compston, G. Rajan, *Adv. Manuf.: Polym. Compos. Sci.* **2017**, 3(2), 52.
- [35] F. Shadmehri, S. van Hoa, *Appl. Sci.* **2019**, 9(13), 2719.
- [36] E. Schöberl, C. Breite, A. Melnikov, Y. Swolfs, M. N. Mavrogordato, I. Sinclair, S. M. Spearing, *Compos. Part A: Appl. Sci. Manuf.* **2020**, 137, 105935. <https://doi.org/10.1016/j.compositesa.2020.105935>
- [37] P. Gąsior, M. Malesa, J. Kaleta, M. Kujawińska, K. Malowany, R. Rybczyński, *Compos. Struct.* **2018**, 203, 718.
- [38] S. Mohanta, Y. Padarathi, J. Gupta, S. Neogi, *Polym. Compos.* **2021**, 42(9), 4717.
- [39] T. S. Mesogitis, A. A. Skordos, A. C. Long, *Polym. Compos.* **2017**, 38(12), 2642.
- [40] G. Ban, J. Jia, Y. Liang, *Polym. Compos.* **2020**, 41(6), 2508.
- [41] E. Oromiehie, B. G. Prusty, P. Compston, G. Rajan, *Struct. Health Monit.* **2018**, 17(1), 108.
- [42] E. Udd, M. Winz, S. Kreger, D. Heider, *Proc. SPIE* **2005**, 5758, 409. <https://www.spiedigitallibrary.org/conference-proceedings-of-spie/5758/1/Failure-mechanisms-of-fiber-optic-sensors-placed-in-composite-materials/10.1117/12.603626.short?SSO=1>
- [43] D. Balageas, C.-P. Fritzen, A. Güemes, *Structural health monitoring*, ISTE, London **2006**. <http://worldcatlibraries.org/wcpa/oclc/440668745>
- [44] K. Shivakumar, L. Emmanwori, *J. Compos. Mater.* **2004**, 38(8), 669.

**How to cite this article:** N. Yadav, K. Wachtarczyk, P. Gąsior, R. Schledjewski, J. Kaleta, *Polym. Compos.* **2022**, 43(3), 1590. <https://doi.org/10.1002/pc.26480>

## Defect Monitoring and Control

Following up on *Chapter 2*, FOD, bond defects as well as gaps and overlaps are identified as defects of concern. For a comprehensive and modular monitoring concept, a combination of multiple sensor technologies is used to detect defects throughout the manufacturing process. Information gained from defect detection and process parameter monitoring is used to reduce/eliminate defects and control process quality. Defect management strategies considering industrial applications are devised and implemented.

FOD and bond inhomogeneity detection and benchmarking are discussed in *Section 4.1*. Gaps and overlaps detection and width control is described in *Section 4.2*. Correlation models are subsequently discussed in *Section 4.3*.

### 4.1 FOD and Bond Inhomogeneity: Thermography

*Article C [29]: “Ply-by-ply inline thermography inspection for thermoplastic automated tape layup”*

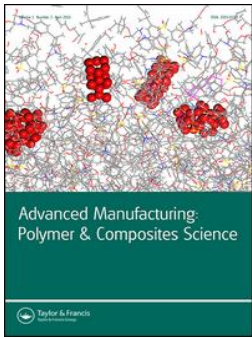
A short overview of the article is provided here. The article is supplemented directly after the overview. The research question addressed in this section as well as the subsequent *Section 4.2* is, *which techniques are best suited for FOD and bond defect detection?*

*Article C* listed below analyses the capability of infrared thermography to detect FODs and bond inhomogeneity. An online monitoring system utilizing IR camera is integrated on an in-house purpose-built ATL test-rig (*Figure 6*). Post-consolidation, ply-by-ply inline inspection is done and surface thermal history is recorded over the course of the layup. Temperature gradient (thermal contrast) is used to recognize foreign bodies and bonding defects. Such defects introduce a temperature anomaly either as a hot or cold spot, which can be detected and localized.

For inline FOD detection, the monitoring system is shown to be capable of detecting defects as small as 2.5 mm, in agreement with active thermography results [29]. Temperature statistics based on processing conditions, enabling online defect localization are discussed. Temperature evolution and temperature gradient through thickness, and in adjacent tapes are used to determine average temperature levels. Temperature anomalies are found by comparison to this average temperature level and are marked as a defect. Based on the camera set-up, bonding defects and therefore, integrity of the embedded sensors, such as FBG can also be checked, according to the findings presented in *Article C* [29].



*Article C [29]: “Ply-by-ply inline thermography inspection for thermoplastic automated tape layup”*



## Ply-by-ply inline thermography inspection for thermoplastic automated tape layup

Neha Yadav, Beate Oswald-Tranta, Ralf Schledjewski & Karol Wachtarczyk

To cite this article: Neha Yadav, Beate Oswald-Tranta, Ralf Schledjewski & Karol Wachtarczyk (2021): Ply-by-ply inline thermography inspection for thermoplastic automated tape layup, *Advanced Manufacturing: Polymer & Composites Science*, DOI: [10.1080/20550340.2021.1976501](https://doi.org/10.1080/20550340.2021.1976501)

To link to this article: <https://doi.org/10.1080/20550340.2021.1976501>



© 2021 The Author(s). Published by Informa UK Limited, trading as Taylor & Francis Group.



Published online: 13 Sep 2021.



Submit your article to this journal [↗](#)



Article views: 129



View related articles [↗](#)



View Crossmark data [↗](#)

## Ply-by-ply inline thermography inspection for thermoplastic automated tape layup

Neha Yadav<sup>a</sup>, Beate Oswald-Tranta<sup>b</sup>, Ralf Schledjewski<sup>a</sup>  and Karol Wacharczyk<sup>c</sup>

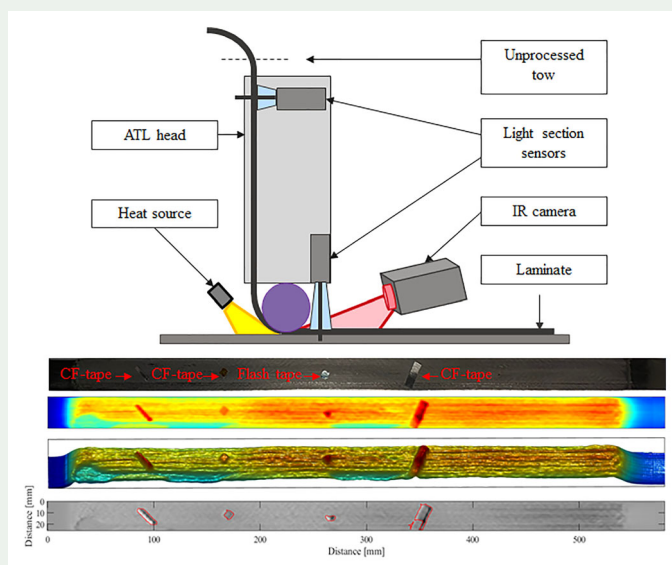
<sup>a</sup>Processing of Composites Group, Department Polymer Engineering and Science, Montanuniversität Leoben, Leoben, Austria;

<sup>b</sup>Chair of Automation, Department Product Engineering, Montanuniversität Leoben, Leoben, Austria; <sup>c</sup>Department of Mechanics, Materials and Biomedical Engineering, Wrocław University of Science and Technology, Wrocław, Poland

### ABSTRACT

Automated tape layup (ATL) largely employs post manufacturing manual visual inspection techniques for defect detection, which severely affects the productivity. Inline monitoring and defect prediction can help in making the process faster and more reliable. The presented work details the use of thermography as an inspection tool for thermoplastic tape material. A new online monitoring system is developed containing Infrared camera integrated on a purpose build ATL test rig. The capability of the tool to identify various defects is analyzed. Moreover, detailed temperature and cooling behavior analysis is done for defect prediction.

### GRAPHICAL ABSTRACT



### KEYWORDS



Inline; thermography; monitoring; automated tape layup; temperature analysis

## 1. Introduction

Growing demand for composite manufacturing requires processes with high productivity. Automated tape layup (ATL) is one such process that promises high level of automation and cost effectiveness. The process has been widely used in high performance industries like aerospace for production of composite laminates from unidirectional prepregs [1–3]. Traditionally used for thermosets, thermoplastics based flat laminates have continuously been researched due to their easy formability,

enhanced mechanical properties and the possibility to have in-situ consolidation, with no requirement for post processing [4].

Even though the process is highly automated, defects are a common occurrence whether due to material inconsistency or manufacturing variability. To maintain constant quality, defects have to be recognized and remedied. State of the art for detection is limited to manual visual inspection, which is labour and time intensive. One study showcased the downtime comprising of material refilling, error correction and cleaning, and can be as high as 50%

**CONTACT** Neha Yadav  neha.yadav@unileoben.ac.at  Department Polymer Engineering and Science, Montanuniversität Leoben Department Kunststofftechnik, Otto-Glöckel-Strasse 2/3, Leoben, Styria, 8700, Austria

© 2021 The Author(s). Published by Informa UK Limited, trading as Taylor & Francis Group.

This is an Open Access article distributed under the terms of the Creative Commons Attribution License (<http://creativecommons.org/licenses/by/4.0/>), which permits unrestricted use, distribution, and reproduction in any medium, provided the original work is properly cited.



**Figure 1.** Summary of defects capable of being detected inline *via* surface or edge detection.

[1]. Another study reported that the downtime for inspection and repair is between 32% and 63% of the overall production time [2]. According to another study [5], of the total machine cycle time required for a fuselage section, only 32% comprises of deposition time, 41% of the overall process duration is needed for manual quality assurance and rework. This is the case when the defects can be detected before curing/consolidation. Of course, not all flaws can be detected visually, undetected flaws lead to higher repair costs and in worst case, rejection of the part causing further material, monetary and productivity loss [2, 3, 6–9].

A monitoring tool, capable of in-situ inspection with early detection, quantification and localization capabilities is needed for process monitoring and quality assurance. Our research group has developed a ply-by-ply online monitoring and inspection tool and the presented work elaborates the effort to check the capability and feasibility of the tool.

### 1.1. Defect types

A multitude of defects can arise during the layup which can be categorized either by cause of occurrence or method of detection. Common defect types classified by cause of incidence and crucial for quality assurance according to DIN29971 [10] are: positioning defects like gaps, overlaps, missing tows, twisted tows; bonding defects such as bridging, air pockets; foreign object defects (FOD) such as fuzz-ball and tow defects such as splice. A summary of defects being capable of detected inline are shown in Figure 1.

A review of defects is also provided by [3, 5, 11]. While [3] talks about selective defects, effects and their identification [5], divides the defects into primary and secondary and summarizes the potential secondary effects that may accompany or result from of manufacturing induced primary imperfections. There are defects that cannot be seen by naked eyes and hence cannot be detected during manual inspection. Some examples being, uneven

bonding/de-bonding, voids, degradation, residual stress and surface roughness variation. Some of them are discussed in [3]. The cause, anticipation, existence and significance entailing the defects are discussed in [11].

Positioning defects, causes and their influence mechanical properties including the tensile, compression, shear, fatigue and vibration properties are discussed in detail in [12]. Experimental and simulative study of tow steering defects is detailed in [13]. A review of the effects of defects on mechanical properties can be found in [3, 11, 12]. While Oromiehie et al. [3] discuss the individual effect of each processing parameter on the quality of the laminate along with the review of experimental and analytical results of such defects, the significance and progression of each defect is described by Harik et al. [11]. Sun et al. [12] present a review of positioning defects in conventional and variable stiffness laminate and various methods to control the defects. The experimental investigation of effects of gaps and overlaps is conducted by Woigk et al. [14], with a distinction between lamina and laminate level by Croft et al. [15]. Zenker et al. [16] conducted statistical analysis with multiple null-hypotheses investigating the effects of consolidation process, defect type, defect size and stacking sequence on the mechanical performance of the thermoplastic laminate. Although the consensus is that defects are detrimental to the mechanical performance, some experimental results point otherwise. In some cases, a defect can improve one property while retarding the other. Therefore, based on the mechanical requirements and ease of controllability, defects can either be selectively placed or avoided altogether.

The quantitative and qualitative characterization of defects caused during processing, their significance and progression analysis, will help in prognosis analysis to enable damage progression models capable of predicting remaining life accurately. For delamination defects, depth analysis is indispensable, as depth is directly related to damage progression [17]. A thorough ply by ply inspection having size

and depth information related to defects must be acquired for such an analysis. Based on the significance and severity of progression of the defect, damage mitigation strategies can then be adopted.

Most of the defects are caused by optimized parameter selection, machine variability and material variability. The defects arising due to machine and material variability itself can be characterized but are hard to control. Parameters on the other hand can be selected based on desired output, degree of consolidation, crystallinity level, degradation limit, residual stress limit, given a good understanding about parameter relation and the output. Process temperature history also influences crystallinity, residual stress, void content and degradation [18, 19]. This is especially important if considering in-situ consolidation for thermoplastics. Temperature history a direct influence on consolidation homogeneity and internal part quality. There are some commercial software solutions that help in selecting optimum parameters. These solutions are however based on static offline programming of process equipment, with no feedback control. Since the control is based on kinematics of the layup head, they are not flexible enough to have a material adaptive temperature control [20, 21]. Temperature history based control will therefore increase both productivity and quality of the laminate [20].

Improved automated inspection enabling the manufacturer in finding flaws and reworking on them if required prior to placing another layer will help in cost, material and time saving [6]. Implementing reliable process window based on advanced temperature prediction will also help in improving part quality [2, 20].

## 1.2. Defect detection

Over the years, many different online defect detection methods have been researched upon, but as discussed earlier, most of the present systems still employ time and cost intensive visual inspection [6]. Based on the defect type defect detection techniques can broadly be divided into two groups, surface defect detection and internal defect detection.

For internal defects, especially residual stress, a number of embedded sensor techniques have been used. Some of them being, embedding metallic particles in combination with X-ray diffraction [22], using strain gauges or stress wave [23, 24]. Optical coherence tomography (OCT) can detect both surface and internal defects [12]. More recently, fibre bragg gratings (FBG) have been demonstrated to be able to detect gaps and overlaps based on temperature and strain detected by the sensor. They can be used for both online monitoring and structural

health monitoring (SHM) but, the embedding difficulties, cross-sensitivity to temperature and, strain and low temperature resistance reduce the ease and range of operation [25].

Surface detection is more common, the simplest utilization of which is a camera system mounted on the ATL head, which continuously takes images and analyses them. The reliability of such a system is dependent on intensive illumination to differentiate between black single tow and already laid up plies, complex image analysis and concentration of the operator. Since the detection quality depends on ambient conditions, the reliability is questionable [2]. A slightly different approach makes use of laser profilometry or laser triangulation sensors. They rely on edge detection and can easily localize the position of the tow, but do not deliver as much information about the layup quality as the camera [2, 6]. A combination of the above two results into a laser-vision inspection system. A laser projector scans and then projects predefined geometrical shapes on the inspection area. This is captured in an image by the vision system. 3D ply location, gaps and the fiber orientation can be detected by such a system. Similar to a camera, the usage is limited by the reflective properties of tapes and precise image projection onto highly contoured parts [26]. Digital image correlation (DIC) is another technique used to inspect surface defects [27, 28]. It was demonstrated that 3D DIC can be used for ply inspection during manufacturing for defects like gaps, laps, twisted tow and damaged tow. However, an optical random pattern projector needs to be developed for this purpose [27].

Most of the above mentioned techniques are either intrusive or require special working environment and tools. Infrared (IR) thermography is however, a non-invasive, non-contact technique and thermal contrast helps in easy identification of inhomogeneity during layup, thus helping in identifying the defects with ease. Large aerospace components made up of aluminum, composites and hybrid fibre metal laminates make use of such IR inspection. The technology has been shown capable of detecting a variety of defects like delamination, porosity, fibre/matrix cracking, thermal stress cracking, interlaminar disbond and impact damage for carbon fibre reinforced composites (CFRP) [29, 30]. Other advantages of this method are, coverage of large surface area and ease of inspection without the need to couple the whole volume [31]. The fast pace and accuracy makes it suitable for ATL process. The most prominent disadvantage is difficulty in identifying deeply embedded defects, which will be deemed unnecessary if using ply-by-ply online inspection.

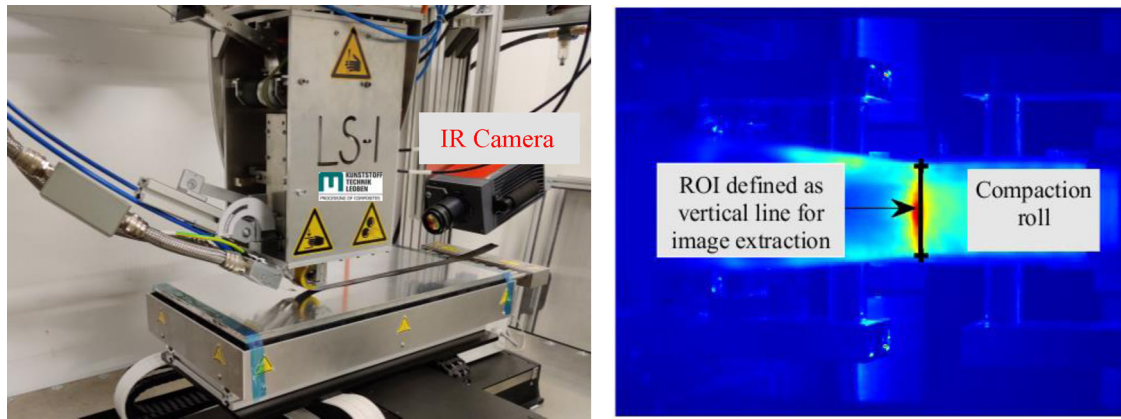


**Figure 2.** IR camera mounted on the ATL test rig behind the compaction roll (left) and sample image used for defining ROI (vertical line) for image extraction (right).

Patents have been filed for online thermographic tool (US patent 7513964 B2 [32], by Boeing), but practical realization has only been achieved at individual research institutes. No industrial use has been reported so far [2, 6]. Research done by Gregory et al. [6, 7], Schmidt and Denkena et al. [2, 9, 10] use similar approach adopted in this paper but lack either holistic data analysis or system behavior identification. This paper tries to fill in that gap that can serve to actively control the process.

## 2. Methodology

### 2.1. Process description

This research work focuses on thermoplastic tape laying. The major control variables that influence the quality of the layup are heat, speed of layup and pressure [33]. ATL requires continuous layup of material with simultaneous application of force and heat. Tapes are brought together and compressed, resulting into intimate contact. With continuous application of heat, healing of the tape in molten state results into intermolecular diffusion. As the tapes cool down, consolidation follows [34]. Based on the material and processing requirements, a variety of heat sources are employed for ATL processes like hot gas torch [25], laser [35] and LED heating [36] among others. The present work utilizes, a radiation based pulsed light energy system, *humm3* as the main heat source.

### 2.2. Monitoring tool

The thermal camera records the radiation of the specified region. The thermal contrast of the surroundings and the lay-up process provides a visual representation of surface temperature of the part. This surface history when collected over time, with a priori knowledge of heating conditions, provides temperature information about the volume [5]. The thermal contrast is affected by compaction force,

lay-up speed, heat input by the heat source, material and temperature of compaction roll and layup tool material and temperature. Other influences include process kinematics and environmental effects [21].

According to method of detection, defect recognition can be categorized as, edge detection and surface detection. Edge detection helps in identifying positioning defects like end of tow, twisted tow, gaps and overlaps using tow geometry details. The research facility at Montanuniversität Leoben (MUL), utilizes a laser triangulation sensor for edge detection. Along with the defects detected by edge detection, surface detection can further be used for recognizing bonding defects, tow defects and foreign bodies [2]. The IR camera takes use of surface detection.

As the compaction roll is cold compared to the substrate/incoming tow, the temperature contrast is highest right behind the compaction roll, rendering it most suitable for tow localization.

If all the process parameters and machine kinematics remain constant, any inhomogeneity in the surface temperature would be the result of a defect. This would influence the heat transfer from the substrate to the tow surface and in turn the bonding. Same applies for foreign bodies. As different objects have different optical and thermal properties, any inclusion of foreign bodies will result in a change of surface temperature [2]. By defining a region of interest (ROI), and a threshold based on average surface temperature, temperature anomalies as hot or cold spots can be detected and localized [37].

A new online monitoring system is developed by MUL containing Infrared camera integrated on a purpose build ATL test rig. Post consolidation, inline ply-by-ply inspection is done. Surface thermal history for the layup course over time is recorded, which is then extracted along the width of the tape (ROI). The end result is a single image containing sequence of the extracted line detailing the temperature data over the length of a single tape.

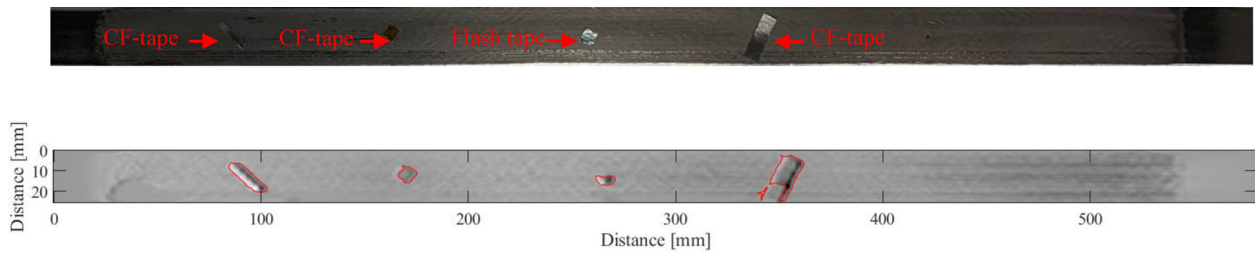


**Figure 3.** Sample with artificial foreign objects placed on top of first layer (top) and thermal image with localized defects after a second layer is laid on them (bottom).

Temperature gradient throughout the layup is then used to recognize positioning, foreign bodies and bonding defects. The presented work details the capability and feasibility of this tool.

The IR camera is mounted behind the compaction roll, having horizontal view as shown in Figure 2 (right). This position was most suitable to avoid excessive reflections. The setup is shown in Figure 2. Inline measurement is done in the online mode by accessing the camera data directly *via* a Software Development Kit (SDK), which was provided with the camera. The recorded infrared images are analyzed by the software developed by MUL, in order to locate defects. The software can be used during the measurement (online) or the recorded infrared sequences can be evaluated later on in offline mode. The details of the evaluation technique and the Graphics User Interface (GUI) in both online and offline mode are explained in detail in [38]. Some of the features used in this work are described below.

1. **Localization:** To automatically locate the defects. Two consecutive images are extracted directly after the consolidation roll and their difference image ( $x$ -gradient) is used for object location/segmentation. The objects are located using edge detection (Canny operator). The accuracy relies on the contrast between the two consecutive images. This is demonstrated in Figure 3, where the objects are automatically located and the shape is outlined with a red boundary.
2. **Rectification:** To analyze the cooling behavior as a function of distance from the compaction roll, the conic field of vision from the camera has to be made rectangular. Rectification is used to remodel the perspective. The extracted images are then shifted accordingly to align at the same  $x$  position (length). The points for such rectification can be chosen interactively, and the user sets the dimensions of the rectangle. It should be noted here that the accuracy of the software is directly related to accurate measurement of the distance of camera from the consolidation roll. An example of this feature can be seen in Figure 4.

3. **Statistics:** Temperature history is recorded in the form of statistics (mean, standard deviation, skewness, kurtosis) and is used to analyze anomaly in temperature. Temperature history is calculated across the  $y$ -position (width) for all  $x$ -positions (length). The temperature history of an ideal layup (free of defects) can also be used for defect prediction.

### 3. Experiment details

#### 3.1. Process specifications

The monitoring unit comprises of an InfraTec camera, with a 25 mm lens. The camera captures images at  $640 \times 512$  pixel and has a typical resolution of 20 mK for temperature (Noise Equivalent Temperature Difference, NETD). For the present work, the spatial resolution is  $\sim 4.8$  pixel/mm based on the position of the camera. The measurements for presented work are recorded at 100 Hz and 200  $\mu$ s integration time.

Thermoplastic unidirectional CF-PA6 tape manufactured by SGL Carbon SE having a width of 25.4 mm and a melting point of 220  $^{\circ}$ C is used. A soft conformable silicon roll having a diameter of 50 mm and 70 shore A hardness is used. The layup speed is kept constant at 50 mm/s. A compaction force of 200 N is applied throughout the process. The heat output of the humm3 system is maintained at 2.9 KW. The layup tool is made out of aluminium and is temperature controlled.

All results shown are with emissivity set to 1. Extensive experiments were done to find the true emissivity value for the carbon fibre tape and the following relationship is found as shown below. Where  $\varepsilon$  denotes emissivity and  $T$  denotes surface temperature recorded with emissivity set to 1, in  $^{\circ}$ C

$$\varepsilon = 1.0026 - 0.0003 * T \quad (1)$$

This emissivity value can be used to find the exact temperature values. Since the aim of this research is to get comparative data, to find temperature anomalies, this conversion is not done. The average emissivity over 30  $^{\circ}$ C to 150  $^{\circ}$ C (temperature range for 200  $\mu$ s integration time) is 0.91.

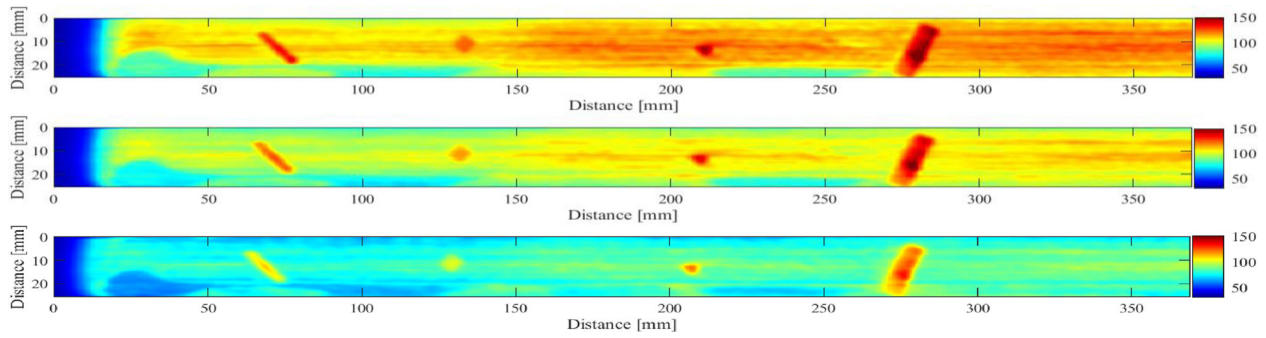


**Figure 4.** Cooling behavior of defects compared to the substrate after 0.01 s (top), 0.12 s (middle) and 0.35 s (bottom).

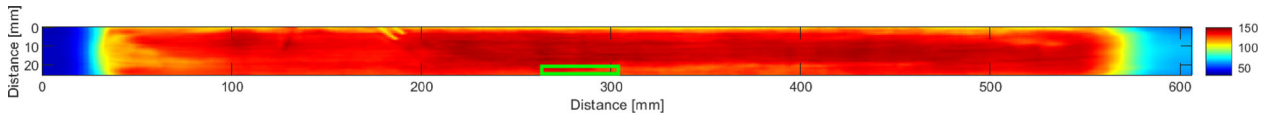


**Figure 5.** Thermogram of direct layup over FBG embedded in substrate with layup tool at 60 °C. Green box marks the position for temperature statistics.



**Figure 6.** Active thermography analysis of laminate with artificial defects, image source: FACC Operations GmbH.

To determine emissivity, a layer of CF- PA6 tape was placed on the layup tool, which was set to a starting temperature of 30 °C. A fine wire K type thermocouple with a diameter of 0.05 mm was soldered into the surface of the tape to ensure the best possible contact with the surface. The temperature of the layup tool was increased in steps of 20 °C (up to 150 °C) and the subsequent temperature readings from thermal camera (with emissivity set to 1) and thermocouple were recorded. A linear regression between temperature values gives the relation for emissivity.

For the present research, a single ply is used to denote a single tape and tow defects for automated fibre placement (AFP) are analogous to tape defects where applicable, and the terms are used interchangeably.

A remark should be made here, that no interference was observed due to the *hum3* system. The CF-tape and consolidation roll blocked direct effect of the pulsed light. Moreover, the spectral range for *hum3* system is between 200 and 1000 nm range which is out of the range of the IR camera, having spectral range between 2000 and 5000 nm.

### 3.2. Artificial defect detection

Artificial defects are introduced in unidirectional ply-on-ply layup. A description of the defects is given below. A comparison is also made between post-consolidation volume active thermography and ply-by-ply inline thermography and to assess their

ability to recognize various defects and validate the tool.

For this research work pulse/flash active thermography is used. Inline thermography does not require any external stimulus as enough thermal contrast is available during the process itself. Active thermography requires an external thermal stimulus to produce thermal contrast to visualize the defects. Short powerful flash with broad frequency range can be used to retrieve information at different depths [7]. The detection technique is sensitive to surface geometry variation and reflectivity from the environment [9]. The camera used for analysis has a resolution of 640 × 512 pixel/ 20–50 mK. Typically, 6 mm × 6 mm defects can be detected. Depending on camera position and sample thickness, detection of smaller defects is also possible.

Threshold of large and small defects according to aerospace standards are 7.35 mm for large defects for both gaps and overlaps, 2.5 mm for small gap and 1 mm for small overlap [16]. The foreign object inclusions for defect introduction are chosen to conform to those standards.

For artificial defect inclusion, a single layer of tape is laid on layup tool maintained at 30 °C. Defects are placed on top and another tape is laid. The defects introduced from left to right are. 2.5 mm wide carbon fibre tape, 6 mm × 6 mm Kapton tape, 6 mm × 6 mm flash tape and 7.35 mm wide carbon fibre tape, as shown in Figure 3. The occurrence of these defects is probable during the running process.



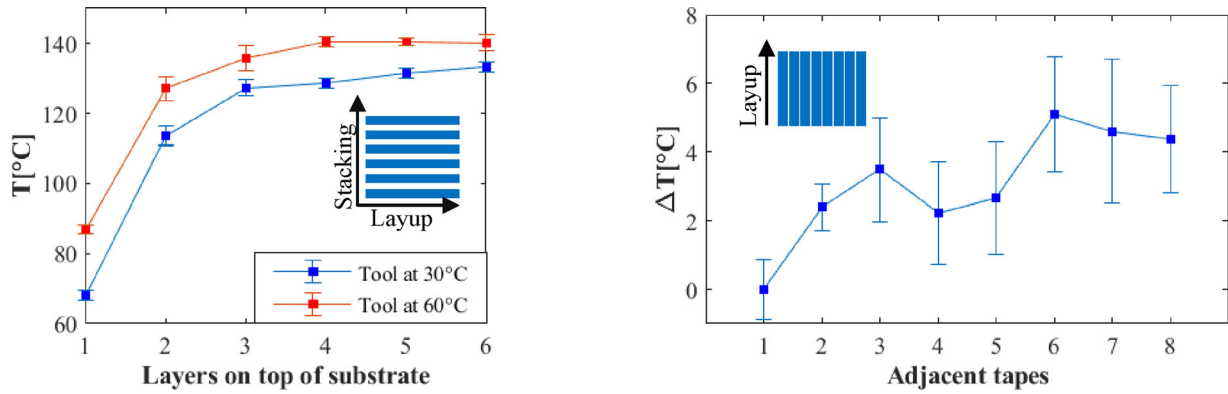


**Figure 7.** Temperature evolution through thickness (left) and temperature gradient in adjacent tapes for tool temperature 30°C (right).

### 3.3. Temperature analysis

Ideally, the temperature over the course of the layup having constant process parameters and machine kinematics should stay constant. Due to the resistance in heat flow through thickness (and ATL head heating up with each layup) of a composite laminate, the substrate temperature depends highly on the previously laid layers. For a laminate with several plies, this effect will be pronounced and can eventually lead to hot spots or degradation in worst case. It is therefore necessary to take thermal prediction or experimental thermal history into account for path planning and homogenous laminate quality [21].

Experiments are conducted to analyse temperature progression through thickness over the course of the layup to be used for temperature prediction and defect control. Cooling behaviour as a function of distance from the compaction roll is also analyzed.

## 4. Results and discussion

### 4.1. Defect detection

#### 4.1.1. Foreign object inclusions

For a constant heat flux, homogenous temperature over the layup is expected unless some flaw is encountered. High thermal conductivity and large surface area of the tool helps it in dissipating heat quite quickly. When substrate is laid on this tool, the composite layer having comparatively lower thermal conductivity will restrict the heat flow. As the laminate thickness builds up, this leads to a non-linear increase in the surface temperature of the subsequent layers. Therefore, when defects like tape slit, missing tape, and gap appear as cold spots as the substrate is colder. Splice and overlap further restrict heat flow to the tool and lead to hot spots. Based on the conductivity, foreign object inclusion can appear as either cold spots or hot spots.

The carbon fibre tape here acts as splice/overlap and the temperature is  $\sim 20^\circ\text{C}$  higher than the surrounding tape, shown in Figure 4. This is analogous to placing a third layer and the temperatures are in accordance with Figure 7 (left image). The Kapton tape and flash tape also show up as hot spots and have temperature  $>10^\circ\text{C}$  than the composite tape. The high temperature of FOD compared to the laid tape, eases localization, shown in Figure 3.

The cooling behavior of defects compared to the composite tape for different time stamps is shown above in Figure 4. The highest contrast is right after detection, 0.01 s (top image). The contrast sharply reduces till 0.4 s (20 mm from the roll) and after 2 s (100 mm from the roll) no demarcation could be made between the defects and the tape. As also seen in Figure 8 (left image), the temperature gradient is steepest until 0.4 s and gradually recedes off to 2 s, where the temperature stabilizes.

Another use of such inline monitoring tool is to verify structural integrity of the laminate after sensor embedment. As discussed above FBG have found extensive use for structural health monitoring (SHM). Absence of hot/cold spot despite foreign object inclusion (FBG sensor in this case), indicates good adhesion to the substrate. The data received from such a sensor is reliable.

In Figure 5, polyimide coated FBG is integrated in the laminate. Except the coating from the tail (190 mm), the sensor itself (200 mm–350 mm) cannot be located. Placement of the tail inside the laminate should be avoided to ensure perfect bonding between the sensor and composite.

#### 4.1.2. Active thermography: validation and comparison

The defects shown in Figure 6, from left to right are as follows: extra tape (twice), Kapton film, washer and flash tape (twice). The defects are introduced on single tape substrate and then another tape is laid on top of the defects, as shown from 50 mm to 250 mm tape length. A stark phase difference can be seen from consolidated region (50 mm–450 mm) to

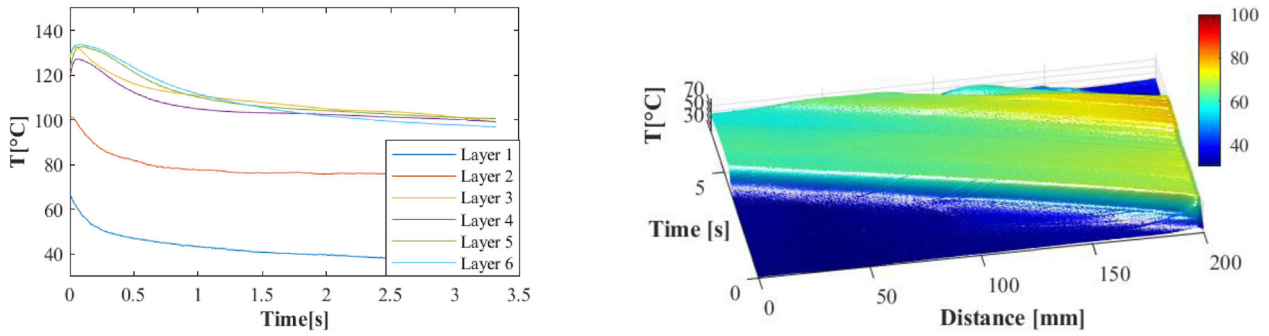


**Figure 8.** Cooling behavior through thickness (left) and temperature as a function of distance from compaction roll (right) most point at 200 mm being closest to the roll) for tool temperature 30 °C (right).

unconsolidated region/lose tape (450 mm–600 mm). A remark should be made here; the defects introduced in this case have different size (bigger) than the ones for inline thermography.

Active thermography results are in agreement with inline thermography results (although both analyze different size of defects). Both inline and active thermography can detect foreign body inclusions to varying degree of clarity. Inline thermography for this particular setup had a better resolution and could detect defects smaller than 2.5 mm. Inhomogeneity in temperature over the length can be seen in inline thermography, while volumetric analysis using active thermography shows quite homogenous quality throughout the layup. The depth of defect cannot be determined if using only active thermography in transmission mode. Since inline thermography relies on continuous monitoring, depth probing is dispensed with. Since post-manufacturing volumetric defects cannot be envisioned with inline thermography, post quality checks can be done with active thermography.

#### 4.2. Temperature analysis for online defect control

As discussed earlier, most simulation tools make use of static modelling without considering material and test rig configuration effects, for example, a setup using a silicon compaction roll. This decreases accuracy of temperature prediction. Therefore, to be able to predict the temperatures for individual layers reliably, following experimental results are deemed necessary. This historical temperature data is used as a threshold for mean temperature for the ROI to detect defects online. With a-priori knowledge of the mean temperature, regions exceeding the threshold (mean temperature  $\pm$  SD) are localized and marked as defects.

The compaction roll completes approximately 3 rotations during one layup for the present setup. As the silicon roll gets heated over the course of layup and affects the temperature distribution, the layup course and temperature profiles are divided into

three regions. The temperature statistics shown below (Figure 7) are averaged out for the green box (10 mm  $\times$  40 mm) shown in Figure 5. It should be noted here, that the box is positioned approximately in the middle of the heated region and is so chosen to ease the software for online control and better accuracy. Changing the position from bottom to middle or top gave similar results. The standard deviation over length (green box, 40 mm) is within 2 °C for the first two layers. This then goes on to be within 2 °C from third layer onwards. The standard deviation over width (green box, 10 mm) is within 2 °C throughout. Using this information, the statistics can be extended for the whole layup length.

As mentioned earlier, cold tool helps in faster heat dissipation for the substrate. The higher the tool temperature, the hotter the substrate. A positive temperature gradient exists through thickness (laying tapes on top of the substrate) affecting all subsequent layers until a steady state is reached. This can also be seen in Figure 7 (left image). The standard deviation is within 2 °C. The gradient is similar for both tool temperatures, indicating that the curve can be shifted (except the first layer) to predict temperatures for tools with higher temperature. Although more experiments at different tool temperatures are required to confirm this.

Temperature difference for adjacent tapes compared to the first laid tape is shown in Figure 7 (right image). For the first tape, there is no surrounding material retarding the heat flow in transverse direction and hence it is colder compared to the rest of the tapes. There is a gradual rise in temperature of the adjacent tape because of difficulty of heat dissipation in transverse direction because of the previously laid tape and the compaction roll (and ATL head) gradually becoming hotter. The standard deviation here as well is within 2 °C. This way thermal analysis of the whole laminate having multiple layers (on top of each other) and each layer having multiple plies/tapes (adjacent to each other) can be mapped.

To have the best definition of ROI, temperature and thereby contrast reduction for different layers is

studied. As expected, the cooling behavior through thickness in [Figure 8](#) (left image) shows results in agreement to the discussion above. The cooling rate is almost same for all the layers. After 2 s of layup, all layers above layer no. 3, cool down to the same temperature. The substrate can be assumed to have stable temperature before subsequent layup. This is confirmed by temperatures shown in [Figure 7](#) (left image) for tool temperature 30 °C. The through thickness temperature is almost same from third layer onwards.

Temperature as a function of distance to the compaction roll is also shown in [Figure 8](#) (right image). Here right most point at 200 mm is closest to the roll, and thereby to the nip-point. If the ROI is chosen far behind the compaction roll, the temperature contrast might not be sufficient to detect temperature anomaly. Also, the temperature would have stabilized by then, as seen in cooling behavior through thickness, [Figure 8](#) (left image). Therefore, to have highest contrast and reliable results, ROI should be chosen near the compaction roll.

## 5. Summary and outlook

The monitoring tool detailed in the research work shows capability to detect surface defects. FOD arising in a single ply can be detected and localized inline with ease. The heat absorption and cooling behavior of defects can be further analyzed. These results are also in agreement with active thermography results. Based on the resolution, bonding defects and therefore, integrity of bonded sensor for SHM can also be checked.

Early detection helps with early rectification, and saving the whole part from possible rejection during post manufacturing checks. Depending on the severity of defect on the laminate properties, the ply can be peeled off or a heat pass can be applied. This also helps in avoiding expensive and extensive post manufacturing efforts for defect removal. Overall productivity increase is ensured. To further improve the process productivity, based on the requirements, a trade-off between inline monitoring and post manufacturing NDT can be made. Here, inline monitoring can significantly reduce the effort for post manufacturing quality checks. Since most of the defects can be detected inline, less time is required for other inspections.

The present work illustrates how temperature of first tape within a layer can be extended to subsequent tapes and layers covering the whole laminate. The tool also serves as a basis for temperature prediction and defect control. Historical temperature statistics from previous experiments are used to predict temperature of the incoming tape, given a set

of processing parameters. Using this a priori knowledge, any anomaly is identified as a defect. Since the temperature analysis is done on the present set up configuration, material and environment variability is already accounted for and the results are accurate having a small standard deviation. Instead of having a constant mean temperature as threshold, using the temperature statistics available, a continuously adaptive mean temperature threshold can be built. Further experiments can be done to have information about parametric influence on temperature variation and use this to expand the scope of prediction and control.

## Acknowledgments

The authors kindly acknowledge the contribution provided by Mr. Antonio Galic, FACC Operations GmbH, for results elaborated in active thermography. The authors also acknowledge the financial support through project InP4 (project no. 864824) provided by the Austrian Ministry for Climate Action, Environment, Energy, Mobility, Innovation and Technology within the frame of the FTI initiative “Produktion der Zukunft,” which is administered by the Austria Research Promotion Agency (FFG). Furthermore, we would like to acknowledge the helpful support of our project partner FACC Operations GmbH.

## Disclosure statement

No potential conflict of interest was reported by the authors.

## ORCID

Ralf Schledjewski  <http://orcid.org/0000-0003-3121-6771>

## References

- [1] Lukaszewicz DH-J, Ward C, Potter KD. The engineering aspects of automated prepreg layup: History, present and future. *Compos Part B: Engin.* 2012;43(3):997–1009.
- [2] Denkena B, Schmidt C, Völtzer K, et al. Thermographic online monitoring system for automated fiber placement processes. *Compos Part B: Eng.* 2016;97:239–243.
- [3] Oromiehie E, Prusty BG, Compston P, et al. Automated fibre placement based composite structures: review on the defects, impacts and inspections techniques. *Compos Struct.* 2019;224:110987.
- [4] Schledjewski R. Thermoplastic tape placement process – in situ consolidation is reachable. *Plast Rubber Compos.* 2009;38(9-10):379–386.
- [5] Heinecke F, Willberg C. Manufacturing-induced imperfections in composite parts manufactured via automated fiber placement. *J Compos Sci.* 2019; 3(2):56.

- [6] Gregory ED, Juarez PD. In-situ thermography of automated fiber placement parts. Provo, Utah, USA, 2018. p. 60005.
- [7] Gregory E, Juarez P. In situ thermal nondestructive evaluation for assessing part quality during composite automated fiber placement. *ASME J Nondestruct Eval.* 2018;1(4).
- [8] Brüning J, Denkena B, Dittrich M-A, et al. Machine learning approach for optimization of automated fiber placement processes. *Proc CIRP.* 2017;66:74–78.
- [9] Schmidt C, Denkena B, Völtzer K, et al. Thermal image-based monitoring for the automated fiber placement process. *Proc CIRP.* 2017;62:27–32.
- [10] Schmidt C, Denkena B, Hocke T, et al. Influence of AFP process parameters on the temperature distribution used for thermal in-process monitoring. *Proc CIRP.* 2017;66:68–73.
- [11] Harik R, Saidu C, Williams SJ, et al. Automated fiber placement defect identity cards: cause, anticipation, existence, significance, and progression. 2018.
- [12] Sun S, Han Z, Fu H, et al. Defect characteristics and online detection techniques during manufacturing of FRPs using automated fiber placement: a review. *Polymers.* 2020;12(6):1337.
- [13] Bakhshi N, Hojjati M. An experimental and simulative study on the defects appeared during tow steering in automated fiber placement. *Compos Part A: Appl Sci Manuf.* 2018;113:122–131.
- [14] Woigk W, Hallett SR, Jones MI, et al. Experimental investigation of the effect of defects in automated fibre placement produced composite laminates. *Compos Struct.* 2018;201:1004–1017.
- [15] Croft K, Lessard L, Pasini D, et al. Experimental study of the effect of automated fiber placement induced defects on performance of composite laminates. *Compos Part A: Appl Sci Manuf.* 2011; 42(5):484–491.
- [16] Zenker T, Bruckner F, Drechsler K. Effects of defects on laminate quality and mechanical performance in thermoplastic automated fiber placement-based process chains. *Adv Manuf Polym Compos Sci.* 2019;5(4):184–205.
- [17] Cramer KE. Current and future needs and research for composite materials NDE. Behavior and Mechanics of Multifunctional Materials and Composites XII, Denver, CO, Mar. 2018, p. 500 [Online]. Available: <https://www.spiedigitallibrary.org/conference-proceedings-of-spie/10596/2291921/Current-and-future-needs-and-research-for-composite-materials-NDE/10.1117/12.2291921.full>.
- [18] Stokes-Griffin CM, Kollmannsberger A, Compston P, et al. The effect of processing temperature on wedge peel strength of CF/PA 6 laminates manufactured in a laser tape placement process. *Compos Part A: Appl Sci Manuf.* 2019;121:84–91.
- [19] Stokes-Griffin CM, Compston P. Investigation of sub-melt temperature bonding of carbon-fibre/PEEK in an automated laser tape placement process. *Compos Part A: Appl Sci Manuf.* 2016;84:17–25.
- [20] Hörmann P, Stelzl D, Lichtinger R, et al. On the numerical prediction of radiative heat transfer for thermoset automated fiber placement. *Compos Part A: Appl Sci Manuf.* 2014;67:282–288.
- [21] Lichtinger R, Hörmann P, Stelzl D, et al. The effects of heat input on adjacent paths during automated fibre placement. *Compos Part A: Appl Sci Manuf.* 2015;68:387–397.
- [22] Parlevliet PP, Bersee HE, Beukers A. Residual stresses in thermoplastic composites—a study of the literature—part II: experimental techniques. *Compos Part A: Appl Sci Manuf.* 2007;38(3): 651–665.
- [23] Fu HY, Li WQ, Sun SZ, et al. Experimental study on relationship between processing parameters and stress wave propagation during automated fiber placement process. *IOP Conf Ser: Mater Sci Eng.* 2017;213:012031.
- [24] Han Z, Sun S, Li W, et al. Experimental study of the effect of internal defects on stress waves during automated fiber placement. *Polymers.* 2018;10(4):413.
- [25] Oromiehie E, Gangadhara Prusty B, Compston P, et al. In-situ simultaneous measurement of strain and temperature in automated fiber placement (AFP) using optical fiber Bragg grating (FBG) sensors. *Adv Manuf Polym Compos Sci.* 2017;3(2): 52–61.
- [26] Shadmehri F, et al. Laser-vision inspection system for automated fiber placement (AFP) process. 20th International Conference on Composite Materials [Online]. Available: <http://www.iccm-central.org/proceedings/iccm20proceedings/papers/paper-4217-2.pdf>.
- [27] Shadmehri F, van Hoa S. Digital image correlation applications in composite automated manufacturing, inspection, and testing. *Appl Sci.* 2019;9(13): 2719.
- [28] Schöberl E, Breite C, Melnikov A, et al. Fibre-direction strain measurement in a composite ply under quasi-static tensile loading using digital volume correlation and in situ synchrotron radiation computed tomography. *Compos Part A: Appl Sci Manuf.* 2020;137(5–6):105935.
- [29] Ciampa F, Mahmoodi P, Pinto F, et al. Recent advances in active infrared thermography for non-destructive testing of aerospace components. *Sensors.* 2018;18(2):609.
- [30] Balageas D, Maldague X, Burleigh D, et al. Thermal (IR) and other NDT techniques for improved material inspection. *J Nondestruct Eval.* 2016;35(1):18.
- [31] Gholizadeh S. A review of non-destructive testing methods of composite materials. *Procedia Struct Integrity.* 2016;1:50–57.
- [32] Ritter JA, Sjogren JF. Real-time infrared thermography inspection and control for automated composite material layup: Patent US 7513964 B2.
- [33] Pitchumani R, Gillespie JW, Lamontia MA. Design and optimization of a thermoplastic tow-placement process with in-situ consolidation. *J Compos Mater.* 1997;31(3):244–275.
- [34] Butler CA, McCullough RL, Pitchumani R, et al. An analysis of mechanisms governing fusion bonding of thermoplastic composites. *J Thermoplast Compos Mater.* 1998;11(4):338–363.
- [35] Maurer D, Mitschang P. Laser-powered tape placement process – simulation and optimization. *Adv Manuf Polym Compos Sci.* 2015;1(3):129–137.
- [36] Orth T, Krahl M, Parlevliet P, et al. Optical thermal model for LED heating in thermoset-automated fiber placement. *Adv Manuf Polym Compos Sci.* 2018;4(3):73–82.

- [37] Tashan J, Al-Mahaidi R. Investigation of the parameters that influence the accuracy of bond defect detection in CFRP bonded specimens using IR thermography. *Compos Struct.* 2012;94(2): 519–531.
- [38] Yadav N, Oswald-Tranta B, Schledjewski R, et al. Online thermography inspection for automated tape layup. *Thermosense: Thermal Infrared Applications XLII, Online Only, United States, Apr. 2020–May. 2020, p. 16 [Online]. Available: <https://www.spiedigitallibrary.org/conference-proceedings-of-spie/11409/2559533/Online-thermography-inspection-for-automated-tape-layup/10.1117/12.2559533.full>.*

*Article D [30]: “In-line and off-line NDT defect monitoring for thermoplastic automated tape layup”*

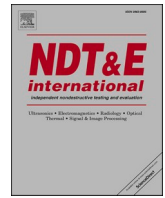
A short overview of the article is provided here. The article is supplemented directly after the overview. Following the feasibility and capability analysis, benchmarking tests are performed to signify industrial application of an infrared thermography-based defect detection tool as presented in *Article D* shown at the end of this section. ATL in-situ consolidated thermoplastic laminates containing artificial defects namely, FODs and bond inhomogeneity are fabricated as test samples. These test samples are inspected using inline thermography and the obtained results are compared with post-manufacturing established NDT methods for composites, specifically active infrared thermography and ultrasonic testing. Quantitative and qualitative analysis of research findings indicate that inline thermography results conform to established industry standards in recognizing FODs. Bond inhomogeneity can be detected inline as a local surface temperature gradient as well. However, volumetric inspection is needed for post-manufacturing defects occurring in the bulk. Inline monitoring tool can therefore be used as a qualified in-process NDT technique for selective manufacturing defect detection.

As per the quality of laminates produced using the ATL test-rig (*Figure 6*), it should be noted that the repeatability and reproducibility of the process is quite high. The ultrasonic attenuation of the in-situ consolidated samples is within 6 dB, which qualifies the threshold for aerospace applications [31]. After post consolidation in an oven, samples previously having attenuation higher than 6 dB show homogeneous internal part quality with attenuation less than 6 dB and no defects.

Material type, size and depth of embedment inside the laminate affect the detection probability and size estimation accuracy of the defects via different techniques. Inline thermography monitors surface temperature, focusing on a small region ply-after-ply. Thermal contrast is an absolute requirement to reliably detect defects for such a technique. Active thermography uses post-manufacturing volumetric inspection based on flash lamp, where external thermal excitation is needed. Depth estimation is limited and defect detection relies heavily on thermal diffusivity. Ultrasonic testing uses post-manufacturing volumetric inspection based on through-thickness transmission of ultrasonic waves. Here a coupling fluid is needed and defect detection and data analysis are time consuming. A combination of various NDT techniques is therefore recommended for best results, in order to ensure a high level of defect detection probability. Using inline inspection, defects can be localized and rectified immediately, significantly reducing the efforts for post-manufacturing quality checks. Similarly, if a combination of automated NDT checks is performed at every process step, the over-reliance on post-manufacturing single NDT can be drastically reduced, increasing efficiency and product trustworthiness.

To answer the research question succinctly, *infrared thermography can be used effectively in detecting FOD and bonding defects inline. As their occurrence cannot be anticipated, the best rectification strategy would be to remove, rework and repair the affected region immediately before next layer is placed.*

*Article D [30]: “In-line and off-line NDT defect monitoring for thermoplastic automated tape layup”*



# In-line and off-line NDT defect monitoring for thermoplastic automated tape layup

Neha Yadav<sup>a,\*</sup>, Beate Oswald-Tranta<sup>b</sup>, Maximilian Gürocak<sup>c</sup>, Antonio Galic<sup>c</sup>, Rene Adam<sup>c</sup>, Ralf Schledjewski<sup>a</sup>

<sup>a</sup> Processing of Composites Group, Department Polymer Engineering and Science, Montanuniversität Leoben, Otto-Glöckel-Strasse 2/3, 8700, Leoben, Austria

<sup>b</sup> Chair of Automation, Department Product Engineering, Montanuniversität Leoben, Peter-Tunner-Straße 25/II, 8700, Leoben, Austria

<sup>c</sup> FACC Operations GmbH, Breitenbach 52, A-4973, St. Martin im Innkreis, Austria

## ARTICLE INFO

### Keywords:

Composite materials  
Defects  
Process monitoring  
Infrared thermography  
Ultrasonic attenuation

## ABSTRACT

Automated tape layup (ATL), is susceptible to a variety of manufacturing defects that affect productivity and mechanical performance of the final part. To increase process efficiency an inline monitoring tool is developed, which detects defects during manufacturing in a ply-by-ply manner. The presented work details the capability analysis of inline non-destructive testing (NDT) by means of thermography compared to industry approved NDT methods, namely, active infrared thermography and ultrasonic testing, which are performed subsequently. Two sets of samples were made, with foreign object and debris (FOD) and without any artificial defects. These in-situ consolidated samples were then checked for FOD and bond inhomogeneity via all three NDT methods. Quantitative and qualitative analysis of research finding was performed. Inline thermography results conform to established industry standards in recognizing FOD defects. These defects can be localized and rectified immediately, increasing process reliability. Inline thermography can be used effectively for inline process control.

## 1. Introduction

Automated tape layup (ATL) is a highly automated composite manufacturing process used in multitudes of industries, including automotive, aerospace and wind energy [1,2]. Commonly used for thermoset composites, the process has been continuously adapted for thermoplastic composites, due to better mechanical properties (high impact resistance), possibility of in situ consolidation [3–5] and recyclability [6,7].

ATL process in general suffers from defect detection-based productivity loss. According to a few studies, manual quality assurance and rework can take up to 50% of the overall production time [1,8,9]. Manual visual inspection risks undetected flaws, higher repair costs and in worst case failure or rejection of the part [2,9–12]. This not only hampers productivity, but existence of flaws also hampers mechanical performance severely [13–15]. To overcome tedious and unreliable manual inspection, robust non-destructive inspection methods with industry approved acceptance criteria should be employed in a holistic way throughout the manufacturing process.

Established non-destructive techniques (NDT) for composites

include ultrasonic testing, infrared thermography, acoustic emission, X ray scanning, shearography and eddy current among a few others [16, 17]. The most commonly applied among these being ultrasonic testing [18] and infrared thermography [19], especially for the aerospace industry [17,20,21].

Manufacturing induced flaws occur in many forms, be it gaps, overlaps, foreign object and debris (FOD), or disbond. A review of manufacturing defects for ATL, along with a review of NDT for inline defect detection is covered in Ref. [22]. Among the various types of defects, FOD can be detected and localized inline, a monitoring tool has been developed for the same, employing infrared thermography [22].

A handbook developed by NASA Langley research center [23], serves as a guidance for selecting appropriate NDT for detecting and characterizing common flaw types in composite structures by providing recommended protocols, best practices, techniques and settings. According to state of practice survey, fabricators listed porosity, foreign material, and fiber waviness, along with delaminations/disbond, at the top of their list of defects they encounter and FOD is listed as a defect of concern [23]. Ultrasonic testing (UT) and thermography are overall recommended practices for delamination, disbond and FOD detection

\* Corresponding author.

E-mail address: [neha.yadav@unileoben.ac.at](mailto:neha.yadav@unileoben.ac.at) (N. Yadav).



[23,24]. Manufacturing defects, namely FOD and disbond can lead to in service defects such as delamination and reduce effective strength, stiffness and service time of composite products [14]. For this reason, present research focuses on these defects, namely FOD and disbond (bond inhomogeneity).

A review of NDT techniques and evaluation of composite structures is covered in Ref. [16]. Review focusing on thermography application for composites is covered in Ref. [17]. A few NDT and comparative studies have been performed in the past. Amenabar et al. has compared UT, shearography, thermography and X-ray Computed Tomography (CT) techniques to analyze delamination defects [25]. Hassen et al. focused on X-ray radiography and ultrasonic testing to detect positioning and FOD defects for glass fibre/PP samples made out of compression moulding [26]. Saenz-Castillo et al. used ultrasonic testing to characterize the effect of processing parameters on void content and mechanical properties [27]. Kersemans et al. evaluated ultrasonic C scans, local defect response and lock in thermography for their effectiveness in detecting damage in composites [21]. These analyses involve post manufacturing NDT and either lack qualitative or quantitative comparison. In one study, the potential of lock-in thermographic NDT method for inline inspection during manufacturing is highlighted but not fully realized. Furthermore, computed tomography is required to verify the thermographic results in the initial phase of the component's qualification [28]. To the best of author's knowledge, a comparison between inline NDT and post manufacturing NDT has not been done before.

Since UT and thermography are established techniques for post manufacturing quality assurance, they can serve as a benchmark for performance assessment of inline monitoring tool developed inhouse. The aim of this research is quantitative and qualitative comparison of defect detection (FOD and bond inhomogeneity) using inline thermography (for more information, refer [22]) and post manufacturing active thermography and UT for out of autoclave/in-situ consolidated thermoplastic composites. Quantitative analysis within the context of this research refers to numerical comparison of methods for FOD detection (size and accuracy), while qualitative analysis is employed for bond inhomogeneity investigations, where the focus is more towards localising the FOD and visualization of consolidation effects. A novel comparison between inline and offline NDT is performed and the inline NDT is benchmarked against industrial NDT techniques. The ATL test-rig, including the inline monitoring tool has been developed inhouse. In-process monitoring is still a field under development for ATL process and this research work aims to qualify a newly developed inline monitoring tool as an established NDT technique for selective defect

detection.

## 2. Material and method

### 2.1. Material

Thermoplastic CF-PA6, SGL carbon SE, having a width of 25.4 mm, thickness of 0.2 mm and melting point of 220 °C is used for the layup process. The layup is done using an in-house custom-built test rig having flash lamp system, humm3® as the heat source. A soft conformable silicon roll having shore A hardness 70 having a diameter of 50 mm is used as the consolidation roll. An Aluminium layup tool is temperature controlled at 30 °C. The compaction force is maintained at 200 N (force applied to compress the material as a pre-step for consolidation), layup speed at 50 mm/s (the speed of layup with which the laminate is built-up and each individual tape is placed), and heat source power at 2.9 kW (the amount of heat radiated to the material to melt it and result into consolidation). The offset between the tapes is selected in a way to result in 1.5 mm overlap. An overview of process parameters along with the sketch of the process is shown in Figs. 1.

### 2.2. Sample manufacturing

Samples are manufactured with embedded artificial defects to be checked for FOD and bond inhomogeneity. The ATL machine is used to manufacture the sample. The machine works on the principles of additive manufacturing, where continuously reinforced thermoplastic tape material is laid down on a placement tool. Heat and pressure are applied to melt and consequently consolidate the material. Tapes are placed adjacent to each other to form a layer and then consecutive tapes on top of the previous layers constitute another layer. The processing parameters are chosen based on an initial processing window based on bond optimization between two tapes, described in detail in Ref. [29]. The heat input is driven by aiming for a maximum degree of bonding on one hand and preventing degradation from too much heat on the other hand. The compaction force is applied in a way to result in an optimum degree of contact and limit the dimensional changes at the same time. Layup speed is limited by the minimum time required for effective use of heat input and compaction force.

For quality inspection, cross-ply [0°/90°]<sub>2s</sub> flat plates are manufactured. Each layer of the laminate consists of 8 tapes and the laminate itself comprises of 8 layers. This is then cut to fit 200 × 200 mm dimension. For bond quality comparison, a reference sample is made by subjecting in-situ consolidated samples to an oven consolidation cycle.

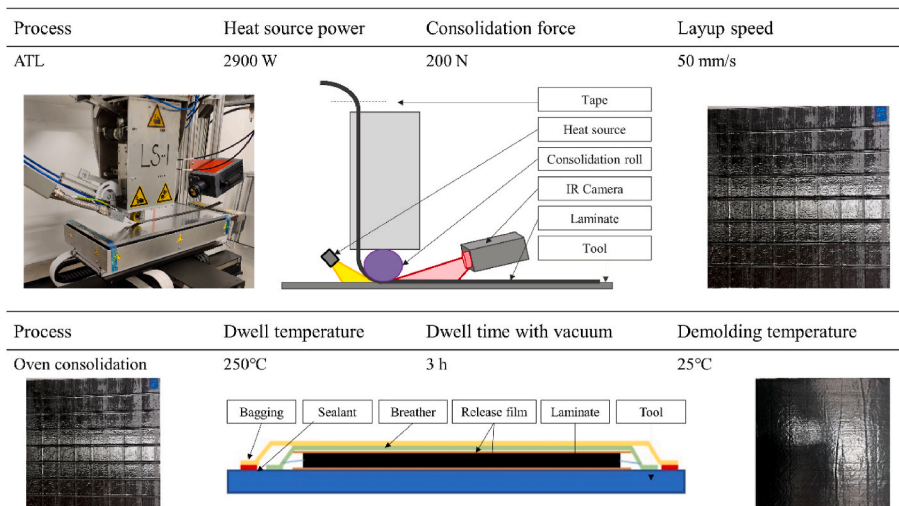


Fig. 1. Overview of process parameters, process chain and final product.

The process is depicted in Figs. 1.

FOD are introduced in the layup in 3 distinct layers as shown in Figs. 2. This way 3 rows of defects exist at 3 levels of depths. The NDT techniques, data acquisition and evaluation methods are discussed subsequently.

### 2.3. Non-destructive evaluation (NDE) methods

The 3 different NDE methods used for quality inspection are described below in detail (see Table 1). Pulse thermography covers a wide range of materials, versatile types of defects and offers fast inspection times [19]. A few other advantages being: non-contact measurement, insensitivity to contour and covers large area. While disadvantages being, FOD is not detectable if the thermal diffusivity is similar to composite, unless it results into poor consolidation due to air gap, and FOD width must be larger the deeper it is in the specimen [23]. Ultrasonic testing also has a high sensitivity to various types of composite defects [30], depending on the acoustic impedance difference inclusions are easy to detect [24], and it is also possible to determine the geometry of the internal damage, its surface area and depth location [31]. A few disadvantages being, requirement of coupling fluid, complex contours require significant effort and automated detection can be time consuming [23].

### 2.4. Inline thermography

A custom-built inline monitoring tool has been developed at Montanuniversitaet Leoben (MUL), consisting of an infrared camera mounted on the ATL rig. The camera is placed behind the compaction roll. The camera captures images over the course the layup of single ply. A region of interest can be selected for image processing, based on which a final image is produced. This final image contains temperature data of this region of interest over the length of the ply (layup over time), using continuous pixel tracing. This way, the whole ply after consolidation can be visualized in a single image, resulting in easy ply-by-ply inspection. More details about the tool can be found in Ref. [22].

Since the environment and tool is much colder compared to the laid tape, surface defects in the form of temperature gradient (hot and cold spots) are easy to localize. This thermal contrast is enough for defect detection and no further thermal excitation is required. The camera used for this research captures images at  $640 \times 512$  pixels and has a typical

temperature resolution of 20 mK. The spatial resolution is 0.208 mm/pixel.

### 2.5. Active thermography

Active thermography is employed for volumetric inspection, post manufacturing. For this research work pulse/flash thermography is used. To visualize the defects in this case, an external thermal stimulus is needed to produce the required thermal contrast. Short powerful flash with a broad frequency range is needed to retrieve information at different depths [21]. Non-uniform heating, surface geometry variation and reflectivity from the environment affect the quality of results [20].

Flash thermography was carried out in two different setups: in transmission and in reflection mode. In transmission mode, or two-sided mode, the flash lamp is placed on one side of the sample and the IR camera on the other side. The energy emitted by the flash lamp is absorbed by the surface of the sample and the heat flows through the sample. The IR camera records the temperature increase on the other side. If there are defects in the sample, they hamper the heat flow, thus becoming visible in the IR images. For this particular setup, a flash lamp of 6 kJ is used, emitting energy every 1 ms. The IR camera used in transmission mode has resolution of  $1280 \times 1024$  pixels and the spatial resolution in this setup is 0.213 mm/pixel. Recording duration is 12 s at 60 Hz framerate. The whole recorded sequence is evaluated by Fourier transformation to a phase image, similar to Ref. [32].

In reflection mode, or one-sided mode, the flash lamp and the IR camera both are positioned on the same side of the sample. If there is a defect in the sample, it disturbs the heat flow and a heat accumulation occurs above the defect, which can be detected in the surface temperature. In this case the IR camera was used in binning mode with  $640 \times 512$  pixels, that means  $2 \times 2$  pixels are recorded together and the spatial resolution is 0.41 mm/pixel. In binning mode, the recording speed is set to 240 Hz. For the evaluation of the recorded sequence the TSR technique was used, similar to Ref. [33], that means after polynomial fitting of the temperature versus time functions for each pixel the 1st and 2nd derivatives are calculated.

The advantage of the transmission mode is that each defect independent of its depth can be well detected, but the depth itself cannot be determined. On the other hand, in the case of reflection mode the deeper the defect, the later the temperature perturbation occurs at the surface, which gives the possibility to estimate the defect depth. But deeper

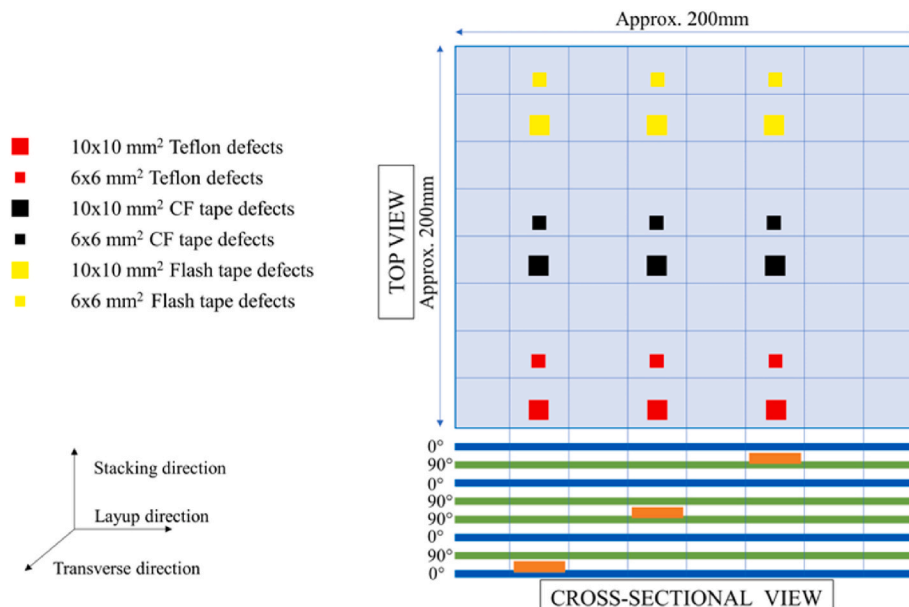


Fig. 2. Cross-sectional and top view of stacking sequence of laminate along with defect introduction.

**Table 1**  
Description of NDT techniques used for the study.

NDT technique	Features	Specifications	Limitations
Inline thermography	Inline surface inspection based on thermal contrast, no need for external thermal excitation	Image: 640 × 512 pixels, temperature: 20 mK, spatial: 0.208 mm/pixel	Thermal contrast
Active thermography	Post-manufacturing volumetric inspection based on flash lamp, external thermal excitation is needed	Transmission - image: 1280 × 1024 pixels, spatial: 0.213 mm/pixel Reflection - image: 640 × 512 pixels, spatial: 0.41 mm/pixel	Defect depth, defect detection reliance thermal diffusivity
Ultrasonic testing	Post-manufacturing volumetric inspection based on through transmission ultrasound	5 MHz probe, 3 dB color scale	Coupling fluid, time consuming

defects have lower signals, and cannot be detected effectively [34].

### 2.6. Ultrasonic testing

Ultrasonic testing (UT) is another volumetric, post manufacturing detection technique, which includes pulse echo (PE), through transmission ultrasound (TTU), pitch catch and guided waves methods. For the present work, TTU C-scan is used. When inspecting composites, typically 1–5 MHz frequencies are used for TTU (C-scan). The frequency of use depends on the thickness of the laminates as depth profiling is directly related to ultrasonic wavelength. Increasing the frequency leads to excessive attenuation of the ultrasonic signal and lowering it reduces the spatial resolution; making thicker laminates easily penetrable but less sensitive to small features [21,24]. 5 MHz frequency has been found to be most suitable for defect detection and is used for the following analysis.

For thin laminates like the ones used in the present research work, an attenuation threshold of 6 dB is extensively used in aerospace applications. Laminates with attenuation levels below 6 dB are considered homogenous and defect free [27]. The C-scan display can either be of transmission or reflection type. Transmission scan shows an integrated view of the part where a feature may be located, while reflection scan provides details about the depth distribution of the feature in the part [21,24]. For the presented work, TTU 5 MHz probe and 3 dB color scale is used.

## 3. Results

For FOD detection, size and depth estimation is chosen as quantitative basis for NDT comparison. To analyze bond defects such as inhomogeneity of consolidation and overall layup quality, inline thermography, active thermography and ultrasonic C-scans are performed. Selective in-situ consolidated samples are oven consolidated. These post-consolidated reference samples are compared to other in-situ consolidated samples for consolidation and surface quality checks.

Extensive comparison between all techniques would include further details such as: effectiveness and accuracy of detection using uncertainty analysis or probability of detection (POD); efficiency of the method in terms of ease of use and ease of rectification of defects; overall time of inspection including time required for operational use, image processing and acquiring final results; cost and ease of industrialization which also depends on installation and maintenance costs and conforming to aerospace/automotive standards. Although important, these specifics are not needed for capability comparison and are therefore beyond the scope of this work.

### 3.1. FOD detection

The laminate consists of 18 pieces of FOD at different depths as illustrated in Figs. 2. The materials for FOD are selected based on probable occurrence during the running process: Teflon inserts, scraps of CF tape, and flash tape.

Inline thermography uses thermal contrast between the substrate and cold layup tool (maintained at 30 °C) to identify and localize

defects. Presence of FOD restricts heat flow to the substrate, appearing as a hot spot. Based on the size and thermal properties, different FOD will have different heating and cooling profiles. Defects introduced after 1st layer are shown in Figs. 3. Individual tapes (8 tapes of 25.4 × 200 mm) are stacked together for a final view of the finished 2nd layer. The thermal contrast between these defects and the substrate is enough for the tool to identify and localize them. Flash tape defects (nearing the end of the layup) have the highest temperature difference followed by extra CF tape and Teflon defects. The cooling curve for all defects look similar and they achieve temperature close to the substrate within 3 s after layup.

The defects are introduced after layer 1 in tape 2, layer 4 in tape 4 and layer 7 in tape 1, 2, 4, 5, 7, 8; and become visible in layer 2, 5 and 8 respectively, as shown in Figs. 2, c. These 8 individual tapes laid over the course of whole layup, with defects are stacked together to get a better overview about detection capabilities. The stacked defects are shown in Figs. 4 (image c). Except Teflon defects in tape 2, tape 7 and tape 8 (counting from top) all other defects can be identified easily.

Transmission type active IR flash thermography delivered better results compared to reflection type active IR. All defects are identifiable using transmission IR. Overall, the thermal contrast for Teflon defects is significantly larger than in CF tape and flash tape defects. The 2nd derivative images of log-log fitted temperature-time functions are shown in Figs. 4 (image e and f). The deeper the defect, the later it become visible.

For reflection mode (Figs. 4, image g and h), thermographic signal reconstruction (TSR) has been used for image processing. Although depth estimation is possible, the last row (deepest) defects are difficult to identify. CF tape and flash tape defects in general show poor visibility but Teflon defects show a good thermal contrast.

TTU C scan (Figs. 4, image d), can recognize defects at different depths with the same clarity. Shape of the defect is preserved. Teflon and flash tape defects are easy to detect, but CF tape defects cannot be detected at all. Near surface defects not easily detectable because of the shadow of overlap (thickness increase) merging with the defect, leading to problems with establishing exact threshold for defect detection.

For size estimation, area detection using inline thermography is done semi-automatically. A region-of-interest (ROI) around the defect has to be selected interactively, following which the program determines a threshold value for separating the background and the defect. The separation (in image processing usually called as segmentation) uses this threshold value to select which pixels belong to background and which ones belong to the object.

The same segmentation method is used for both the inline thermography and for the flash thermography measurements. The difference is that in case of inline thermography, the objects have higher intensity while flash thermography has lower intensity than the background. The accuracy of the method depends on how large is the difference between the object and the background. In terms of heat flow, how strongly an object hampers the heat flow through the layers.

Defects in TTU-C are located by measuring the difference in signal response to a defect free area (ROI) and using a sizing threshold which is predefined (mostly based on results from reference standard inspection). In this case, the threshold was chosen to size the known defect to its theoretical size (36 mm<sup>2</sup> and 100 mm<sup>2</sup>). Accuracy depends on scan

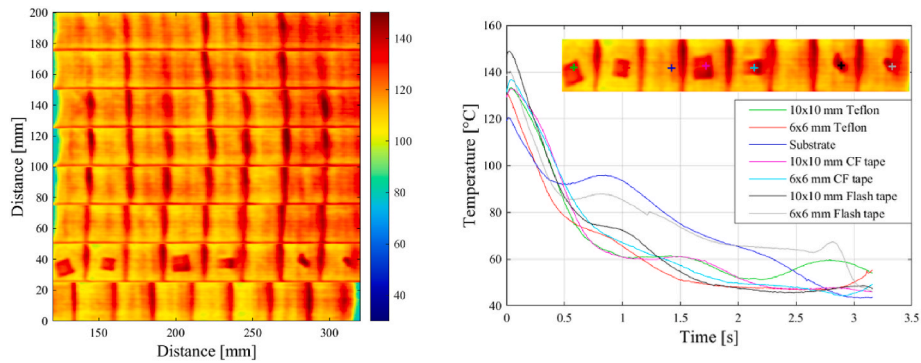


Fig. 3. Defects detected in layer 2 (tape 2) of 8 layered laminate (left), temperature profile of these defects (tape 2) compared to the substrate (right).

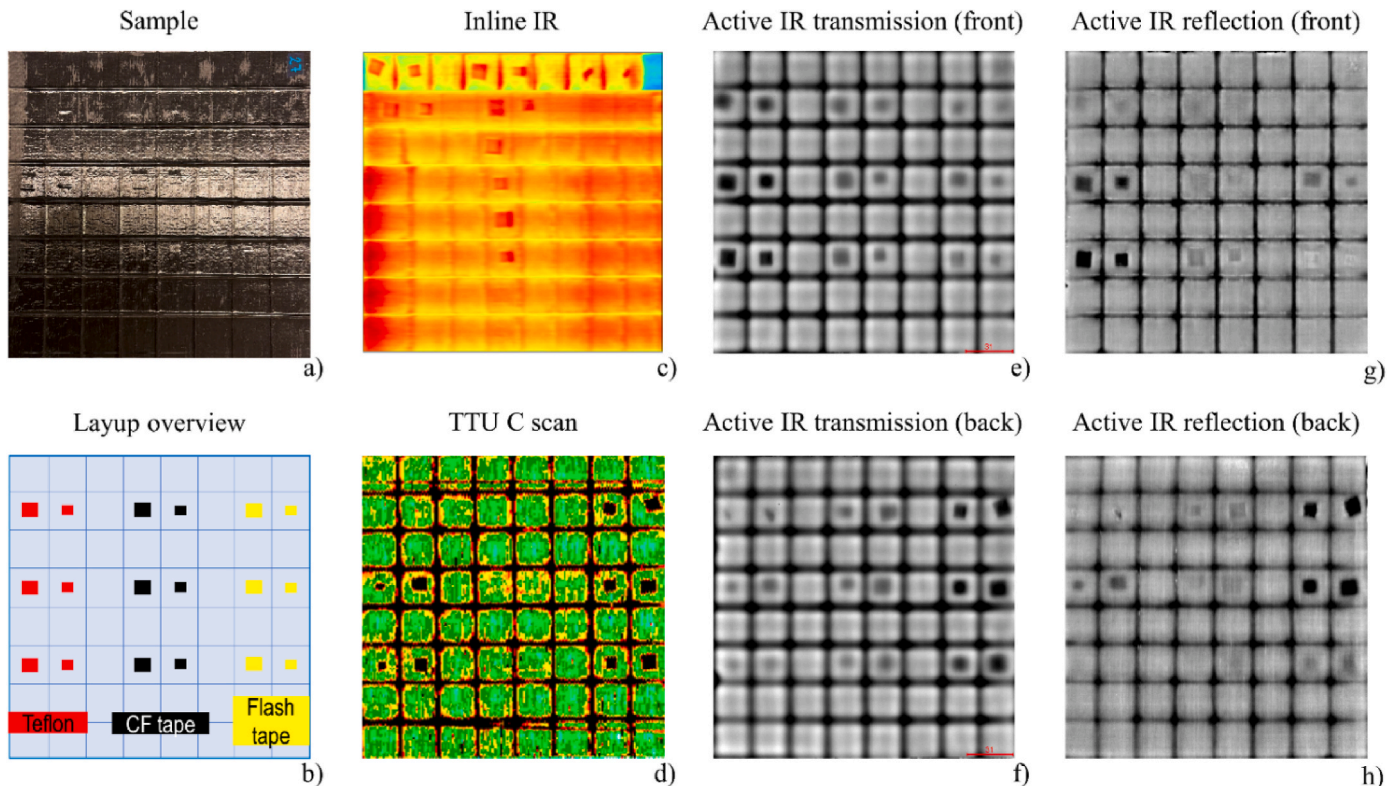


Fig. 4. Defect monitoring using various NDE methods for a) sample, along with b) layup overview. The methods being c) inline thermography, d) TTU C scan, e) active IR transmission (front), f) active IR transmission (back), g) Active IR reflection (front) and h) active IR reflection (back).

resolution, which is given by scan index and repetition rate of measurement. The biggest deviation from the theoretical defect size was  $8 \text{ mm}^2$  with the scan having a resolution of  $1 \times 1 \text{ mm}$ .

The grid pattern seen throughout is a result of overlaps, introduced as baseline artificial defects visible irrespective of the FOD. The quality of these overlaps is therefore overlooked for FOD analysis. The actual ROI (squares surrounded by the overlaps) has homogenous quality enabling FOD detection, conforming to the standards.

Material type, size and depth location affect the size estimation error via different techniques. A comprehensive view of size estimation error with respect to nominal size is shown in Figs. 5. It should be noted that the graph depicts error size for the defect area rather than the edges. The graphs on the left, a), b) and c) illustrate the error in area estimation for different FOD materials at different depths. Y axis here denotes the size and depth of the defect. 10-1 denotes  $10 \times 10 \text{ mm}$  defect in 1st layer and so on. On the right side, d), e) and f) effect of depth on error in area estimation is shown for different NDT techniques. The horizontal line in

the middle of the box denotes median value, the cross 'x' represents the mean, boundaries of the box depict first and third quartile and the whiskers represent the extremities.

Active IR detected most defects (transmission 18, reflection 15), followed by inline IR (14) and then TTU C scan (10). Teflon defects were easiest to locate and all techniques could detect all of these defects (6 out of 6). Flash tape defects were the most difficult in terms of probability of detection by all techniques, active IR reflection (4 out of 6 detected), inline (2 out of 3 detected) and TTU C scan (4 out of 6 detected). This could be because of extremely small thickness of the defect itself (0.02 mm). Although CF tape defects were easily detected by both active and inline IR, TTU C scans could not detect any of these defects (0 out of 6 detected). Noteworthy observation being, absolute error is usually larger for smaller sized defects ( $6 \times 6 \text{ mm}$ ).

TTU C scans provide the most accurate size, with least error, followed by Least error by inline IR and then active IR. Depth of the defect did not have pronounced effect on the size estimation error for inline IR

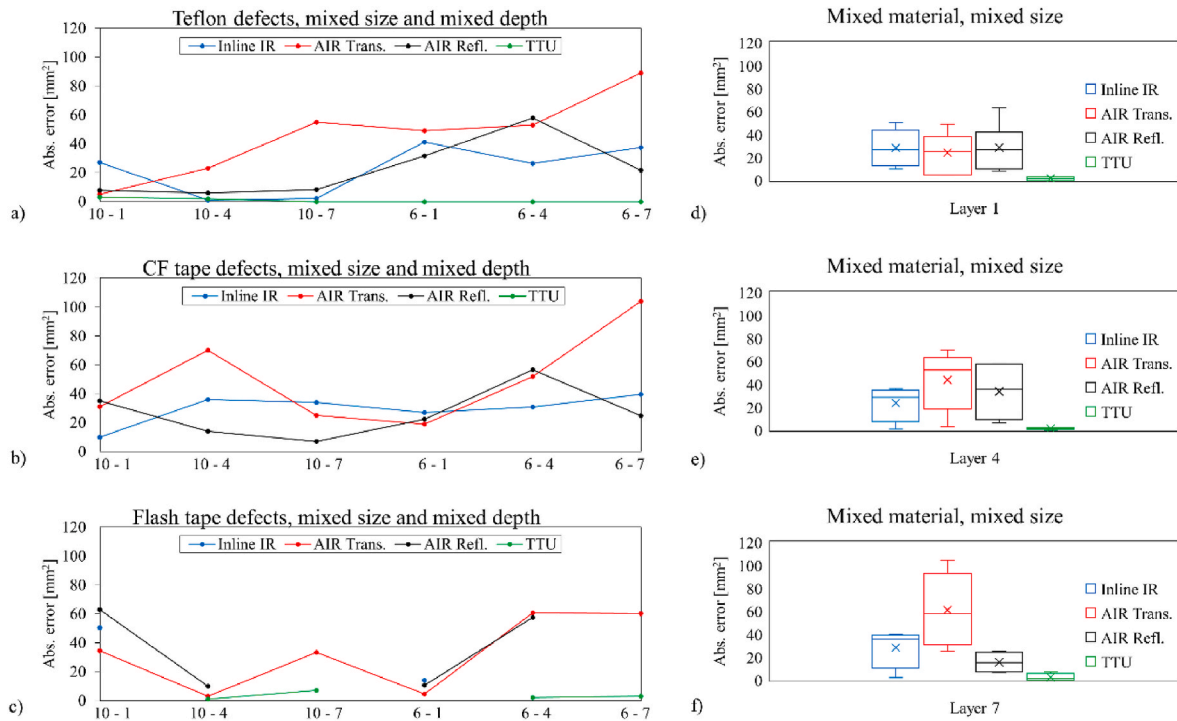


Fig. 5. Size(area) estimation error by defect type, left (a, b and c), and depth, right (d, e and f).

and TTU C scan. However, the error size increases with depth for active IR (transmission). This could be attributed to high attenuation of the thermal diffusion process due to depth limitation. Presence of a defect reduces the diffusion rate, although this helps in locating them in the first place, the thermal front takes time to reach deeper defects [17]. Lateral heat diffusion along with diffusion through the sample gets

added to the error.

The results gained from all three techniques are comparable for lateral defects; depth analysis however is complex and requires further processing. For all NDT solutions, different set of machine parameters and data enhancement techniques can be employed to improve the results [14,31,35,36]. But the purpose of this research is to use most

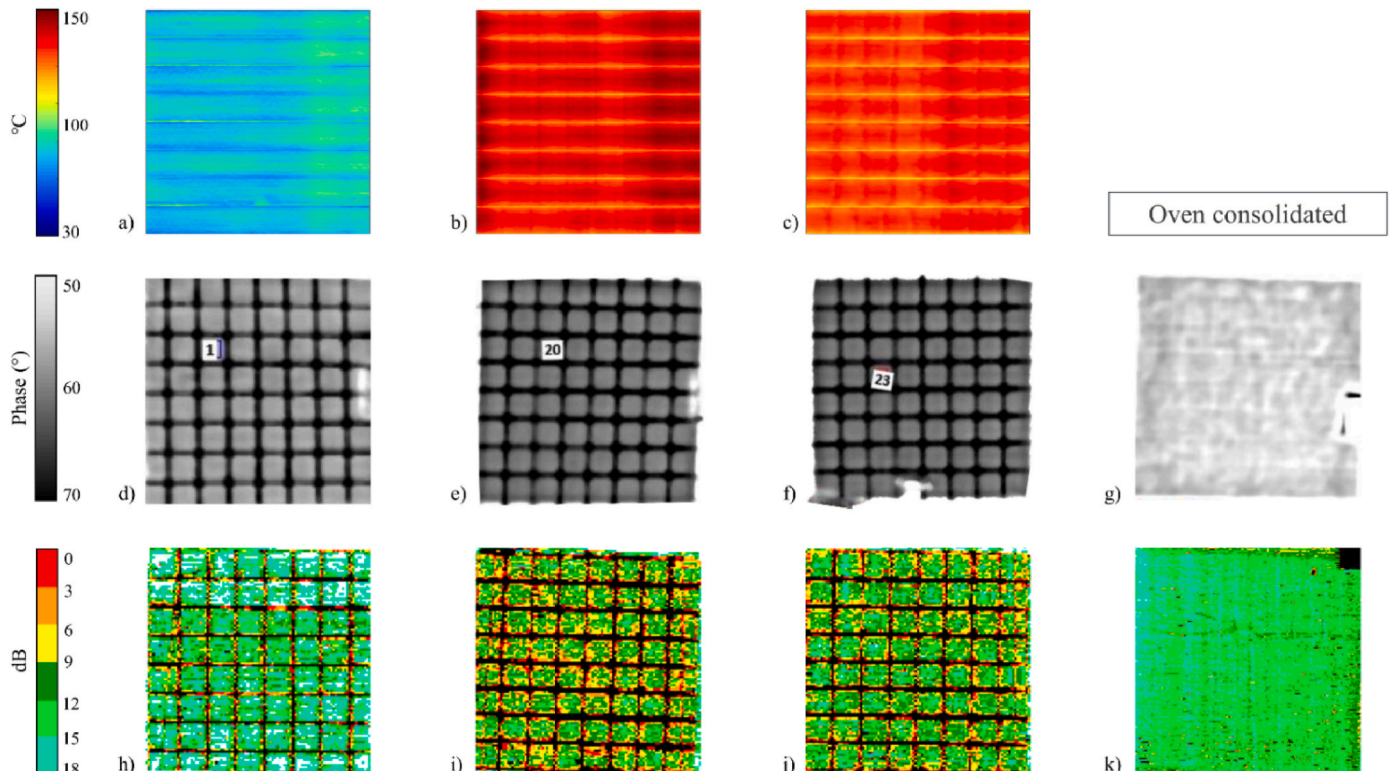


Fig. 6. Bond homogeneity analysis using different NDT techniques.

common NDT methods, with standard settings and compare them with a new NDT method to gain confidence about the capability of the tool. Instead of focusing on one NDT, multiple NDT checks can be employed to reduce over reliability on one single method.

### 3.2. Bond inhomogeneity

Inline thermography provides a good overview of the state of heat flow to the substrate over the course of the layup, as shown in Figs. 6, a) denotes layer 1, b) denotes layer 5 and c) denotes layer 8. Any obstruction whether it be positioning defect, FOD, tow defect or bond defect, appears as a thermal contrast. For ATL, when the layup is done on a cold tool, the temperature of the substrate gradually increases and stabilizes. This is a result of increase in temperature of the consolidation roll and resistance in through thickness heat conductance, which increase with each layup run. Looking through a), b) and c), parts of Figs. 6, three phenomena can be noticed. Temperature increase during the layup of a single tape as a result of heating up of the consolidation roll; temperature increase in adjacent/subsequently placed tapes due to difficulty of heat dissipation in transverse direction and a positive temperature gradient through thickness (through a), b) and c)) until a steady state is reached. Although the bond homogeneity can be checked ply-to-ply, the overall final laminate quality cannot be judged based solely on these results. Final laminate quality is a volumetric property and a volumetric solution is best suited for it. Part quality while processing however can be checked with ease.

Active IR and corresponding ultrasonic TTU C scans for 3 samples (sample 1, sample 20 and sample 23) with same parameters are shown in Figs. 6, d)-f) and h)-j). Except the intentional overlaps, the bond quality is homogenous overall. Thermography inspection shows little to no differences between the three samples. A higher phase angle indicates slower cooling down of the part and therefore suspected inhomogeneity if not caused by part features. Small differences in part homogeneity between samples cannot be detected properly with thermography alone. Unevenly consolidated areas which cause big attenuation in ultrasonic inspection might not create big differences in heat emission and are therefore not clearly visible in thermography inspection. Although attenuation for the three samples is less than 6 dB, the bond quality differences can be better visualized with TTU C scans, here sample 23 has higher attenuation than sample 1, followed by sample 20. Both sample 20 and 23 are with 6 dB attenuation of sample 1. It should be noted that no delamination can be detected whatsoever and the repeatability of the process is fairly high, considering the samples are made with in situ consolidated ATL. Similar results for in situ consolidated samples could be found in Ref. [27]. Overall, thermography inspection confirms C-scan results and a correlation between ultrasonic attenuation and indications on thermography picture can be observed.

Oven consolidated results of the same are shown in g) active IR and k) TTU C scan. It should be noted that post oven consolidation, all samples (even with attenuation greater than 6 dB) show homogeneous internal part quality with attenuation less than 6 dB and no defects whatsoever. For active IR, significant difference in phase angle (greater than 10°) can be observed.

## 4. Summary

A summary of capability analysis based on the characteristics of the defects is shown in Tables 2. The sign 'x' signifies marginal effectivity, 'xx' denotes moderate effectivity, and 'xxx' denotes extreme effectivity. Inline thermography results conform to established industry standards in recognizing FOD defects. These defects can be localized and rectified immediately. This reduces the risk of undetected flaws and therefore helps in increased productivity, process reliability and material saving. Bond homogeneity arising as surface defects (local temperature inhomogeneity) can be detected as well. For in service defects, occurring in the bulk post manufacturing, volumetric inspection is needed. If NDT

## Tables

2 Capability analysis of different NDT techniques for defect detection.

Inspection technique	Defect detection	Lateral sizing	Depth location	Bond homogeneity
Inline IR	Xx	xx	xxx	xx
Active IR	Xxx	xx	x	xx
Ultrasonic TTU	Xx	xxx	x	xxx

checks are performed at every process step, the efforts and dependence on post manufacturing NDT can be drastically reduced, increasing efficiency and product trustworthiness. The research results presented above can serve as a basis for screening based mixed monitoring, where based on inline monitoring (manufacturing defects) results, an optimized monitoring approach for in service defects can be achieved.

## NDTE CRediT author statement

**Neha Yadav:** Conceptualization, Investigation, Validation, Formal analysis, Writing - Original Draft, Visualization. **Beate Oswald-Tranta:** Software, Validation, Writing - Review & Editing. **Maximilian Güröcak:** Software, Validation, Writing - Review & Editing. **Antonio Galic:** Software, Validation, Writing - Review & Editing. **Rene Adam:** Resources, Writing - Review & Editing. **Ralf Schledjewski:** Conceptualization, Resources, Funding acquisition, Writing - Review & Editing.

## Declaration of competing interest

The authors declare that they have no known competing financial interests or personal relationships that could have appeared to influence the work reported in this paper.

## Data availability

Data will be made available on request.

## Acknowledgement

The authors kindly acknowledge the financial support through project InP4 (project no. 864824) provided by the Austrian Ministry for Climate Action, Environment, Energy, Mobility, Innovation and Technology within the frame of the FTI initiative "Produktion der Zukunft", which is administered by the Austrian Research Promotion Agency (FFG).

## References

- [1] Lukaszewicz DH-J, Ward C, Potter KD. The engineering aspects of automated prepreg layup: history, present and future. *Compos B Eng* 2012;43(3):997-1009. <https://doi.org/10.1016/j.compositesb.2011.12.003>.
- [2] Oromiehie E, Prusty BG, Compston P, Rajan G. Automated fibre placement based composite structures: review on the defects, impacts and inspections techniques. *Compos Struct* 2019;224:110987. <https://doi.org/10.1016/j.compstruct.2019.110987>.
- [3] Hoang V-T, et al. Postprocessing method-induced mechanical properties of carbon fiber-reinforced thermoplastic composites. *J Thermoplast Compos Mater* 2020; 089270572094537. <https://doi.org/10.1177/0892705720945376>.
- [4] Martin I, Del Saenz Castillo D, Fernandez A, Güemes A. Advanced thermoplastic composite manufacturing by in-situ consolidation: a review. *Journal of Composites Science* 2020;4(4):149. <https://doi.org/10.3390/jcs4040149>.
- [5] Qureshi Z, Swait T, Scaife R, El-Dessouky HM. In situ consolidation of thermoplastic prepreg tape using automated tape placement technology: potential and possibilities. *Compos B Eng* 2014;66:255-67. <https://doi.org/10.1016/j.compositesb.2014.05.025>.
- [6] Shiino MY, Cipó TCG, Donadon MV, Essiptchouk A. Waste size and lay up sequence strategy for reusing/recycling carbon fiber fabric in laminate composite: mechanical property analysis. *J Compos Mater* 2021;55(28):4221-30. <https://doi.org/10.1177/00219983211037047>.
- [7] an Lin T, Lin J-H, Bao L. A study of reusability assessment and thermal behaviors for thermoplastic composite materials after melting process: polypropylene/thermoplastic polyurethane blends. *J Clean Prod* 2021;279:123473. <https://doi.org/10.1016/j.jclepro.2020.123473>.

- [8] Heinecke F, Willberg C. Manufacturing-induced imperfections in composite parts manufactured via automated fiber placement. *Journal of Composites Science* 2019; 3(2):56. <https://doi.org/10.3390/jcs3020056>.
- [9] Denkena B, Schmidt C, Völtzer K, Hocke T. Thermographic online monitoring system for Automated Fiber Placement processes. *Compos B Eng* 2016;97:239–43. <https://doi.org/10.1016/j.compositesb.2016.04.076>.
- [10] Gregory E, Juarez P. In situ thermal nondestructive evaluation for assessing Part Quality during composite automated fiber placement. *ASME J. Nondestruct. Eval.* 2018;1(4). <https://doi.org/10.1115/1.4040764>.
- [11] Brünig J, Denkena B, Dittrich M-A, Hocke T. Machine learning approach for optimization of automated fiber placement processes. *Proc. CIRP* 2017;66:74–8. <https://doi.org/10.1016/j.procir.2017.03.295>.
- [12] Schmidt C, Denkena B, Völtzer K, Hocke T. Thermal image-based monitoring for the automated fiber placement process. *Proc. CIRP* 2017;62:27–32. <https://doi.org/10.1016/j.procir.2016.06.058>.
- [13] Nguyen MH, Vijayachandran AA, Davidson P, Call D, Lee D, Waas AM. Effect of automated fiber placement (AFP) manufacturing signature on mechanical performance of composite structures. *Compos Struct* 2019;228:111335. <https://doi.org/10.1016/j.compstruct.2019.111335>.
- [14] Juarez PD, Gregory ED. In situ thermal inspection of automated fiber placement for manufacturing induced defects. *Compos B Eng* 2021;220:109002. <https://doi.org/10.1016/j.compositesb.2021.109002>.
- [15] Woigk W, Hallett SR, Jones MI, Kuhtz M, Hornig A, Gude M. Experimental investigation of the effect of defects in Automated Fibre Placement produced composite laminates. *Compos Struct* 2018;201:1004–17. <https://doi.org/10.1016/j.compstruct.2018.06.078>.
- [16] Wang B, Zhong S, Lee T-L, Fancey KS, Mi J. Non-destructive testing and evaluation of composite materials/structures: a state-of-the-art review. *Adv Mech Eng* 2020; 12(4). <https://doi.org/10.1177/1687814020913761>. 1687814020913761.
- [17] Yang R, He Y. Optically and non-optically excited thermography for composites: a review. *Infrared Phys Technol* 2016;75:26–50. <https://doi.org/10.1016/j.infrared.2015.12.026>.
- [18] Hsu DK. 15 - non-destructive evaluation (NDE) of aerospace composites: ultrasonic techniques. In: Karbhari VM, editor. *Woodhead Publishing series in composites science and engineering*, number 43, *Non-destructive evaluation (NDE) of polymer matrix composites: Techniques and applications*. Cambridge UK: Philadelphia PA: Woodhead Pub; 2013. p. 397–422 [Online]. Available: <https://www.sciencedirect.com/science/article/pii/B9780857093448500154>.
- [19] Lahiri BB, Bagavathiappan S, Reshmi PR, Philip J, Jayakumar T, Raj B. Quantification of defects in composites and rubber materials using active thermography. *Infrared Phys Technol* 2012;55(2–3):191–9. <https://doi.org/10.1016/j.infrared.2012.01.001>.
- [20] Deane S, et al. Application of NDT thermographic imaging of aerospace structures. *Infrared Phys Technol* 2019;97(3):456–66. <https://doi.org/10.1016/j.infrared.2019.02.002>.
- [21] Kersemans M, Verboven E, Segers J, Hedayatrasa S, van Paeppegem W. Non-destructive testing of composites by ultrasound, local defect resonance and thermography. *Proceedings* 2018;2(8):554. <https://doi.org/10.3390/ICEM18-05464>.
- [22] Yadav N, Oswald-Tranta B, Schledjewski R, Wachtarczyk K. Ply-by-ply inline thermography inspection for thermoplastic automated tape layup. *Adv Manuf Polym Compos Sci* 2021:1–11. <https://doi.org/10.1080/20550340.2021.1976501>.
- [23] P. A. Howell, "Nondestructive Evaluation (NDE) Methods and Capabilities Handbook," L-21112, Feb. 2020. [Online]. Available: <https://ntrs.nasa.gov/citations/20200002023>.
- [24] Bossi RH, Giurgiutiu V. *Nondestructive testing of damage in aerospace composites. In: Polymer composites in the aerospace industry*. Elsevier; 2015. p. 413–48.
- [25] Amenabar I, Mendikute A, López-Arraiza A, Lizaranzu MI, Aurrekoetxea J. Comparison and analysis of non-destructive testing techniques suitable for delamination inspection in wind turbine blades. *Compos B Eng* 2011;42(5): 1298–305. <https://doi.org/10.1016/j.compositesb.2011.01.025>.
- [26] Hassen AA, Taheri H, Vaidya UK. Non-destructive investigation of thermoplastic reinforced composites. *Compos B Eng* 2016;97:244–54. <https://doi.org/10.1016/j.compositesb.2016.05.006>.
- [27] Saenz-Castillo D, Martín MI, Calvo S, Rodríguez-Lence F, Güemes A. Effect of processing parameters and void content on mechanical properties and NDI of thermoplastic composites. *Compos Appl Sci Manuf* 2019;121:308–20. <https://doi.org/10.1016/j.compositesa.2019.03.035>.
- [28] Huber A, Dutta S, Schuster A, Kupke M, Drechsler K. Automated NDT inspection based on high precision 3-D Thermo-Tomography model combined with engineering and manufacturing data. *Proc. CIRP* 2019;85:321–8. <https://doi.org/10.1016/j.procir.2019.10.002>.
- [29] Yadav N, Schledjewski R. Parameter selection for peel strength optimization of thermoplastic CF-PA6 for Humm3™. *KEM* 2019;809:297–302. <https://doi.org/10.4028/www.scientific.net/KEM.809.297>.
- [30] Rawlings RD. *Materials science and engineering, umc III*. EOLSS Publications; 2009.
- [31] Wronkowicz A, Dragan K, Lis K. Assessment of uncertainty in damage evaluation by ultrasonic testing of composite structures. *Compos Struct* 2018;203(5):71–84. <https://doi.org/10.1016/j.compstruct.2018.06.109>.
- [32] Maldague X, Marinetti S. Pulse phase infrared thermography. undefined; 1996 [Online]. Available: <https://www.semanticscholar.org/paper/Pulse-phase-infrared-thermography-Maldague-Marinetti/3eeaaafd74d5b00b8e535158476fde6008a74a8f>.
- [33] Shepard SM. Automated processing of thermographic derivatives for quality assurance. *OE* 2007;46(5):51008. <https://doi.org/10.1117/1.2741274>.
- [34] Oswald-Tranta B, Maier A, Schledjewski R. Defect depth determination in a CFRP structure using TSR technique. In: *Proceedings of the 2014 international conference. Quantitative InfraRed Thermography*; 2014.
- [35] Wei Y, Zhang S, Luo Y, Ding L, Zhang D. Accurate depth determination of defects in composite materials using pulsed thermography. *Compos Struct* 2021;267:113846. <https://doi.org/10.1016/j.compstruct.2021.113846>.
- [36] Shrestha R, Kim W. Non-destructive testing and evaluation of materials using active thermography and enhancement of signal to noise ratio through data fusion. *Infrared Phys Technol* 2018;94:78–84. <https://doi.org/10.1016/j.infrared.2018.08.027>.

## 4.2 Gaps and Overlaps: Profilometry and Force Control

*Article E [32]: “Inline tape width control for thermoplastic automated tape layup”*

A short overview of the article is provided here. The article is supplemented directly after the overview. Two research questions are discussed in this section. *Which techniques are best suited for gap and overlap detection? Can these defects be reduced/eliminated during the process? If so, which aspects of defects and process behavior should be monitored for this?*

*Article E* listed below investigates the use of light section sensors to detect gaps and overlaps as well as a force sensor to control compaction force. An inline width control (IWC) concept has been devised as an approach towards gap management and control. Inline force control is used to obtain continuous width variation/tessellation during consolidation to adapt the thermoplastic tapes to the desired width spread according to the path geometry. The approach is particularly valuable for complex shaped laminates as well as variable angle tow (VAT) laminates or variable stiffness panel (VSP) laminates.

Material deformation during consolidation is used as the basis of IWC. A combination of pressure and heat leads to morphological changes in the thermoplastic tape. The resulting bond strength is dependent on contact mechanics and parametric effects. Compaction force, even though having a direct impact on the tapes' final geometry, has limiting effect on the bond strength [33]. The correlation between compaction force and tape width can therefore be used for process control. Controlling tape width will lead to the desired final shape of the tape; easily conformable to the mold and easy to steer for varying fiber angle; eliminating steering defects. A minimally intrusive functional design for the ATL head shown in *Figure 6* is presented which is capable of achieving width tessellation as well as gap prevention and elimination. Three practical cases for gap and overlap management are identified: (i) defined width increment for gap and overlap anticipation based on a-priori knowledge of path planning (pre-programmed force); (ii) raw tape (pre-consolidation) width variation detection and gap prediction based real-time/online force variation; and (iii) post consolidation gaps and overlaps monitoring and rectification using heat and pressure repass. In simpler terms this would translate to, **gap prediction** for VAT/VSP and complex geometry surfaces; online **gap prevention** accounting for material variability; and **gap rectification** using post quality checks. The material used in this study has very strict tolerances and for a first model, such deviations are ignored. The focus of this study is limited to pre-programmed inline force variation for known surfaces. It should be noted here that the word 'gap' is used to signify both 'gap and overlap' defects and managing one defect inherently implies managing the other when strictly dealing with width spread.

Successful performance assessment and benchmarking tests for force sensor were performed. An online force variation of 50 N – 1000 N can be obtained with a standard deviation of 10 N. Feasibility study for minimum and maximum attainable width spread for CF-PA6 for the present test-rig configuration demonstrates 5 % to 50 % width increase compared to initial width. The lower and upper bounds for incidental gaps occurring in the course of ordinary ATL operations are 0.762 mm and 1.27 mm respectively. These can be very well covered with the present concept. Moreover, VAT/VSP laminates require a maximum of 41.4 % width spread to eliminate gaps in extreme cases, this can also be achieved with the present IWC concept.

An example of continuous inline width tessellation, in this case a trapezoidal shape, is presented. Force variation influences the resulting shape of the tape, unraveling the possibility of shape



conformity to the tool and complex layup geometry. This gives rise to perfectly laid tapes with no gaps or overlaps. The present concept helps in improving process reliability and productivity by monitoring and controlling process parameters and manufacturing defects. Moreover, gap reduction/elimination leads to improvement in mechanical properties and dimensional accuracy of the resulting laminate. The design flexibility offered by shape conformity opens up possibilities that were made possible only by 3D printing up to now.

Considering the research questions, it can be concluded that, *light section sensors are well apt for inline detection of gaps and overlaps. Gaps and overlaps are formed as a result of material deformation, which can be regulated by controlling process parameters. Having the least impact on bond quality, compaction force is chosen as the suitable process parameter. Tape dimensions and compaction force are monitored and adjusted continuously for gap management comprising of prediction, prevention and rectification.*

*Article E [32]: “Inline tape width control for thermoplastic automated tape layup”*



# Inline tape width control for thermoplastic automated tape layup

Neha Yadav<sup>\*</sup>, Ralf Schledjewski

Processing of Composites Group, Department Polymer Engineering and Science, Montanuniversität Leoben, Otto-Glöckel-Strasse 2/3, 8700 Leoben, Austria

## ARTICLE INFO

### Keywords:

Polymer-matrix composites (PMCs)  
Tape placement  
Defects  
Process monitoring

## ABSTRACT

Automated tape layup, is predisposed to positioning defects like gaps and overlaps which are detrimental to the structural integrity of the part. This work investigates the details of the design of inline width control concept, a technique for inline control of consolidated tape width to eliminate gaps. Continuous inline width variation is achieved by online control of the compaction force, during the layup process. Successful calibration and benchmarking tests using standard pressure measurement sensors are presented. Performance assessment tests are performed which demonstrate online variation of force from 50 N to 1000 N, having a standard deviation of 10 N. Correlation models for width control are obtained and it is shown that a width increase of 5–50 % of initial width is achievable using the prototype. An example of linearly varying force resulting in a trapezium shaped consolidated tape is also shown as a part of the feasibility study.

## 1. Introduction

Composite manufacturing for the aerospace and automotive sectors has found continuous interest in out-of-autoclave manufacturing methods, in particular, automated tape layup (ATL) for the time and cost efficiency it provides. Thermoplastics manufacturing in particular has increasingly attracted attention because they offer the possibility of in-situ consolidation and recyclability [1–4].

Most commonly used for constant stiffness laminates having straight fiber paths, the process finds advanced use in laminates with spatially varying mechanical properties. There are two methods to do this, by varying the thickness by dropping plies, or by varying the fiber angle by steering the fibers [5]. Dropping plies has been found to have negative effects on the structural integrity of tapered composites, affecting static, fatigue and damage tolerance. Existing design and manufacturing based mitigation approaches to reduce the negative effect of ply terminations on tapered composites have been met with limited success so far [6]. The second method, commonly known as VAT (variable angle tow) or VSP (variable stiffness panel) consists of orienting the fibers in a tailored curvilinear fiber path. This approach relies on the in-plane bending deformation of the fibers. Such laminates are found to have higher structural performance and/or lower weight [7–10]. In particular, improved buckling, in-plane stiffness and stress distribution along the desired load path with decreased stress concentration around the cut-outs [11–14]. A study performed by Clancy et al. [15] demonstrates the feasibility of using thermoplastics for VAT/VSP manufacturing. Due

to the manufacturing features inherent to the ATL process, laminates are subjected to positioning defects especially, a VAT/VSP [14,16–18] and complex shaped laminates like doubly curved structures [19].

Ideally the VAT/VSP process should result in perfectly tessellated tapes (tapes with varying width), where all tapes within the tow follow an identical curve, shifted along the assigned shifting direction, without any gaps or overlaps. In practice, however, mismatch of steering radius between the inner and the outer edge of the steered tapes causes gaps or overlaps, as the tapes have constant width throughout the steering path. If the course width could change continuously, there would not be any defects in the laminate [16]. To control the location and the type of defect occurrence, tow overlapping and tow dropping methods are used during path generation. Depending on the strategy or gap coverage parameter, individual tows/tapes are cut to create full gaps, full overlaps or a ratio of full gaps and full overlaps [13,18].

These gaps and overlaps are found to be detrimental to the mechanical strength at both lamina and laminate level [18]. They are also found to have an influence on the impact resistance and delamination, with delamination initiation likely occurring in the gap area [19,20]. For a VAT/VSP, gaps deteriorate both in-plane stiffness and buckling load, whereas overlaps improve the structural performance [14]. According to one study, in-plane shear test results indicated that gaps were more critical than overlaps for shear properties, particularly when the caul plate was used [21]. Another study confirms significant stiffness and strength reduction due to gaps, worsening as the gap sizes increase [22]. It should be noted here, that the mechanical properties are mostly

<sup>\*</sup> Corresponding author.

E-mail address: [neha.yadav@unileoben.ac.at](mailto:neha.yadav@unileoben.ac.at) (N. Yadav).

influenced by systematic tow-to-tow gaps, while the presence of incidental gapping is largely inconsequential [23,24]. To further add to this, the effects of defects to some degree depend on, specific defect and laminate configurations, defect distributions/interactions, and test configurations [23].

Several researchers have established methods to reduce the effects of these defects on a composite structure. Manual rework has been found to worsen the occurrence of gaps [25]. Staggering and layering techniques are used to prevent a nucleation of defects [26,27]. Staggering offsets the defects in different locations through-the-thickness of a laminate in plies of same steering configuration. This is most often followed by constraining the two outer plies in a symmetric lay-up to straight fiber plies forcing curvilinear ply defects to be restricted to the interior of the laminate [28]. Ply staggering and 0 % gap coverage is an effective combination to lessen the influence of defects in VAT/VSP [13]. However, even with these techniques, the defects, even though organized, are still present [18]. A very few rectification techniques have tried to eliminate these defects. Among these, Continuous tow shearing (CTS) uses shear deformation characteristic of dry tow to minimize process induced defects for variable angle tow laminates. The limitation of the CTS technique is the maximum shear angle, which means that the tow path cannot be a perfect half circle [12,29]. Clancy et al. [11] developed a spreading system to be used before consolidation for VAT/VSP to provide tessellated tapes, which can help eliminate gaps and overlaps. The spreading mechanism has been shown to produce constant width tows, with no reference to continuously variable width tows, or any consideration to how long the system might take to adapt the pressure to produce continuously variable width tows. These tows are processed before consolidation with heat and pressure, and undergoing another consolidation cycle during layup affects the geometrical and thermal properties, as also noted by the authors themselves.

Numerous inline monitoring techniques based on visual, optical, acoustic and infrared thermography approaches exist to detect these defects [30,31], but to the best of author's knowledge a technique for inline monitoring and control of process parameter to eliminate gaps does not exist so far. The main aim here is to achieve continuous inline width variation/tessellation by controlling the compaction force to eliminate and/or rectify gaps. The research presented in this article builds upon the concept of Wang and Gutowski [32] that gaps can be rectified through processing by transverse flow during consolidation. They had demonstrated the concept for compression molding, which is not representative of ATL itself. The present research is a practical application of above concept for in-situ consolidated thermoplastic ATL.

A novel approach for defect control is utilized, where inline/online force control is used to obtain desired width increment during consolidation to adapt the tapes to the desired path geometry. As gaps have been found to have worse effect than overlaps, the focus of the present study is gaps rectification. A realistic use case of such a system would be for complex shaped tools and variable stiffness composites where gaps are a common occurrence due to either steering restrictions for curvilinear tapes or material non-conformance to complex surfaces. This would help in establishing enhanced process reliability, dimensional accuracy and mechanical performance. Henceforth, throughout this article, this technique will be referred to as inline width control (IWC).

## 2. Methodology: Inline width tessellation concept

This section describes the scope and the criticalities pertaining to the width variation control mechanism based on theoretical and experimental literature studies. Considerations and assumptions leading to the final prototype and a description of the prototype itself are also discussed.

### 2.1. Theory

The fundamentals of the concept rely on the compaction force's

effect on material deformation under processing conditions. Contact mechanics and parametric effect of the compaction force on bonding are described subsequently. Detailed analysis and discussion of the individual aspect of the overall process is beyond the scope of the presented work. An overview with insights into the most important mechanisms is provided here.

**Contact mechanics:** Force application via a compaction roller results in a contact formation between the compaction roller and the subsequent layer/tape and a contact ensues between the layers themselves. This force application leads to a pressure field formation below the roller which leads to morphological changes of the prepreg material. These changes are dependent on the material rheology and the processing parameters. It is therefore important to study both the contact characteristics and the material morphology. The material morphology physics here is defined by an intimate contact model, geometrically analyzing the contact behavior. For an intimate contact between the layers and eventually healing and consolidation to follow, coalescing of the microscopic asperities is a prerequisite. The geometrical representation of these asperities has evolved from rectangular blocks [33,34] to a fractal cantor set 2D [35] and then, to a 3D representation [36]. The contact of the compaction roller can be divided into a static and a dynamic contact. The static model is consistent with Hertz's contact theory based on elastic solids. The dynamic contact model of the compaction roller is affected by the morphological change of the prepreg [37]. Contact area and pressure distribution under the roller are usually determined using pressure mapping systems.

**Morphological changes** of the prepreg related to the resin flow under the compaction roller has been studied by various researchers. Ranganathan et al. [38] defines the deformation of the prepreg as squeeze flow continuum that is treated as creeping motion for thermoplastics. The rheological properties are dependent on the temperature, fiber volume fraction, and void content. The material is treated as Newtonian compressible continuum where, due to high viscosity and a disproportionate transverse and longitudinal geometry, inertial effects and longitudinal matrix flow in fiber direction maybe ignored. Based on the same, Pitchumani et al. [39] proposed a macroscopic governing equation to determine the pressure distribution. Mathematical models built up on the same principles are used for simulation studies till date [37,40]. It should be noted that, transverse squeeze flow is affected by the orientation of the fibers. Transverse flow perpendicular to the fibers is unrestricted when two 0° plies are placed adjacent to each other. However, squeeze flow is restricted in both plies when a 0° ply is placed on top of a 90° ply as fibers are perpendicular to each other confining the viscous resin [41]. It was also found that squeeze flow phenomenon is mostly restricted to resin rich regions [42] and, through-thickness and in-plane percolation flow is required to impregnate the regions with compressed dry fibers [42,43].

**Parametric study:** For a thermoplastic prepreg, increasing compaction force helps to reduce void content, facilitate intimate contact and improve the mechanical properties of the final laminates [3,44–47]. Heat input and processing velocity have a higher impact on the bond strength compared to compaction force and the results of the parametric studies are most often guided by the heat source used. Even though dedicated parametric study for humm3® (supplied by Heraeus) flash lamp system, the heat source used in this study, is missing; the general trend for bond strength variation with compaction force shows proportionality with limiting effects at higher forces. It should however be noted, that compaction force has a strong dependence on processing velocity. Having a low velocity affects material heating, resulting in a higher temperature of the material and consequently in a lower viscosity of the melt which allows to build up a high degree of intimate contact, and providing sufficient time for polymer healing. At high velocity, even if force is continuously increased, increase in the degree of bonding is not remarkable because of less time available for polymer healing [45]. During a single layup, heat and velocity are usually kept constant to have minimal impact on bonding. Since increment in force is minimally

intrusive towards the degree of bond, it can be varied inline.

## 2.2. Prototype

The prototype is built keeping the above concepts in mind (section 2.1). The sensors and the control systems are integrated based on the following key points: monitoring and analysis of the tape width and the compaction force; formulating a correlation model for the tape width and the compaction force; and inline (in best case online) control of the compaction force which in turn will control the width.

Laser sensors have proven to provide fast inline detection of gaps, overlaps and missing tows using 2D profile evaluation [48]. The projection of a laser light on the composite produces a 2D profile, using which width data is extracted. Two such laser profile scanners, namely scanCONTROL from Micro-epsilon having a resolution of 2  $\mu\text{m}$ , 1280pixels/profile and measuring speed up to 300 Hz are integrated in the in-house built ATL head. The first sensor monitors the geometry of the thermoplastic tape before consolidation. This information is used to predict the formation of gaps and overlaps due to material variability. The second sensor serves two purposes, monitoring the geometry of the tape after consolidation and identifying gaps and overlaps occurring due to process variability and steering restrictions.

The compaction force is applied via a pneumatic pressure system comprising of a double-acting compact air cylinder and a proportional pressure control valve regulator. The regulator helps with pressure stabilization and control. A maximum of 1.2kN force can be applied. In terms of pressure, it relates to 10 bar. The maximum pressure hysteresis is 0.05 bar, with a linearity error of 1 % of the full-scale pressure. A 6-axis force/torque sensor, from ME-Meßsysteme GmbH, placed directly above the compaction roller measures the force applied on the laminate using the pneumatic pressure system during the running process. A linear correlation between pneumatic pressure actuation and applied compaction force is obtained. The force is regulated through a dynamic set-point with the possibility of online variation. The flexibility of both on the fly and static programming are enabled. The inputs and outputs are managed via a GUI (Graphical user interface) designed using LabVIEW software, which then passes this information to a PLC (Programmable logic controller) program. The resolution of the force/torque sensor is 0.2 N, with an accuracy of about 4 N and the settling time is typically 1 ms. There have been mentions of force sensor in the previous two studies [49,50] but, as discussed in section 1, an online force control has not been realized so far.

For obtaining correlation models, a small parametric study is

performed varying the force, while the heat input and the layup velocity are kept constant. The effect of the force on the consolidated tape's width is then characterized. With combined information from the laser profile scanner and the force/torque sensor, an empirical model utilizing applied force and width change is obtained for different process parameters. Using these relations, the force can be varied in accordance to the width spread requirements. Here, three cases for gap prevention and rectification can be defined: defined width increment for gap anticipation based on a priori knowledge of path planning (pre-programmed force); pre-consolidation material width variation detection and gap prediction based real-time/online force variation; and post consolidation gaps and overlaps check and rectification using heat and pressure repress. In simpler terms this would translate to, gap prevention for VAT/VSP and complex geometry surfaces; online gap prevention accounting for material variability; and gap rework and rectification using post quality checks. The material used in this study has very strict tolerances (Fig. 1-2) and for a first model, such deviations are ignored. Rework and rectification techniques require separate parametric study which is out of the scope of this work. The focus of this study is limited to pre-programmed inline force variation for known surfaces.

A schematic of the ATL head with the sensor integration is presented in Fig. 1-1. An integral single roller with soft conformable silicon outer cover is the most commonly used set-up and is used for the present study [37,51,52]. Its large deformation has an important effect on gaps, bridging, and steering and is utilized to fit the curved surface and ease force transmission [52–54].

A schematic of the width control concept is shown in Fig. 1-2. Material variability at the tape manufacturing level and steering restrictions lead to positioning defects. The material variability is quantified in terms of the tape's width, which can be detected using a laser profile sensor. When adjacent tapes are placed, the resulting positioning defects can also be detected using the same sensor. Based on the discontinuity in the width profile, defects can be categorized as gaps or overlaps. A perfect fit is obtained in the case of no defect, i.e., when two tapes lie next to each other with no gaps or overlaps. The gaps arising due to steering restrictions are the defect of interest in this case. The steering plan provides us with required tape width and position information resulting in a laminate having no defects. Using this information, and the force and width correlation, force is varied inline to attain the required width. This way perfectly tessellated tapes are laid continuously to result into a defect free laminate.

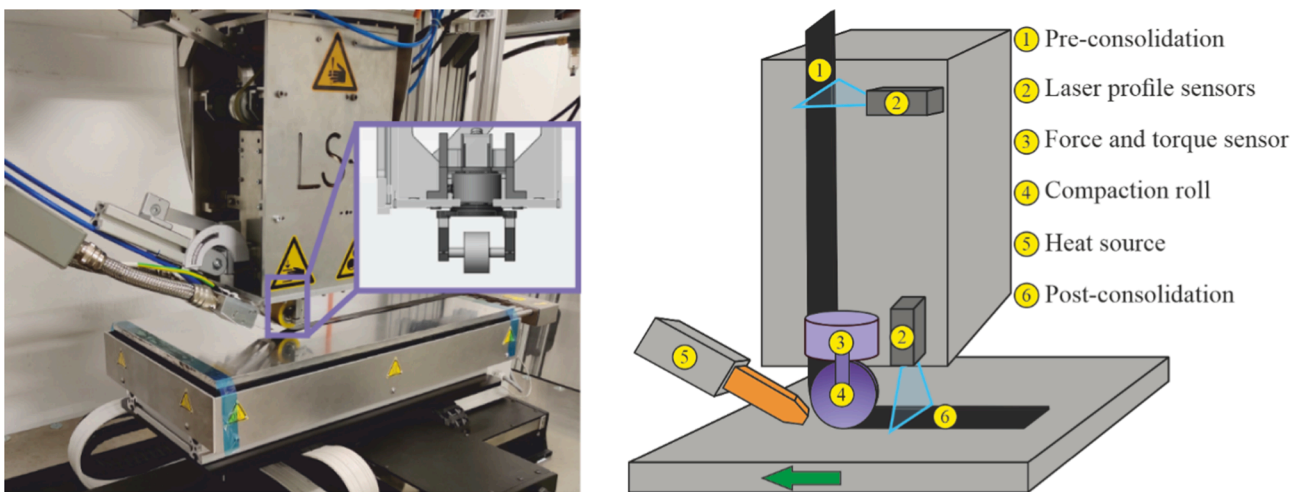
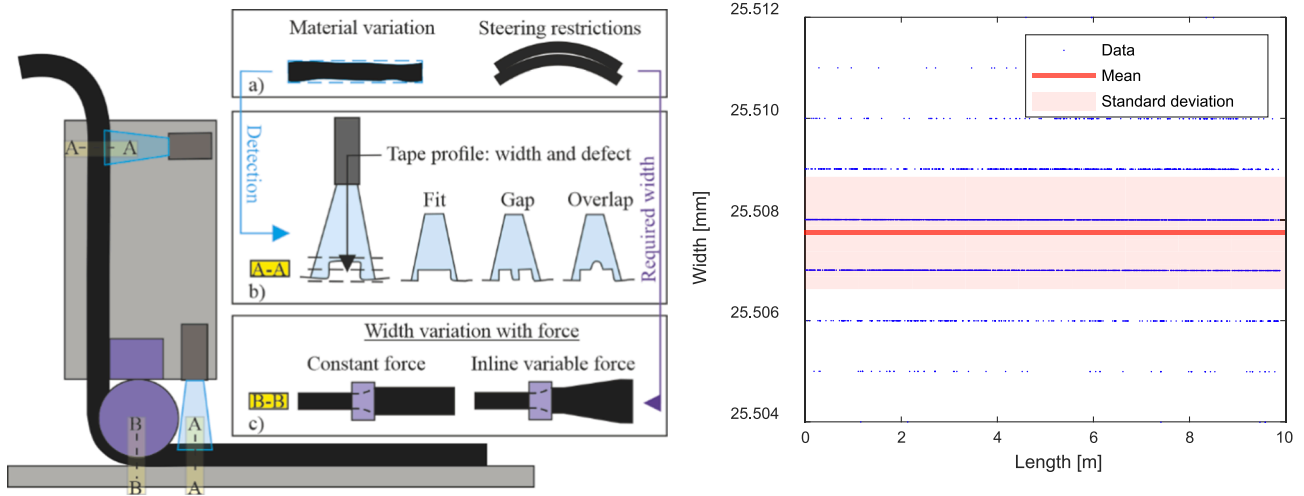


Fig. 1-1. An image of the prototype with a focus on the force/torque sensor, placed directly above the compaction roller (left) and a schematic of the ATL head with relevant sensors (right). The green arrow indicates the layup direction. (For interpretation of the references to colour in this figure legend, the reader is referred to the web version of this article.)



**Fig. 1–2.** Schematics of the width control (left) with a) reasons for positioning defects, b) profile width and defect detection using laser profile sensors and c) force variation according to required width and pre-consolidation tape width variability (right). (For interpretation of the references to colour in this figure legend, the reader is referred to the web version of this article.)

### 3. Experiments

The material used for this study is thermoplastic CF-PA6 tape (supplied by SGL Carbon), having a fiber volume content of 42 %, a width of  $25.4 \pm 0.1$  mm and a thickness of 0.2 mm, as specified by the manufacturer. The melting point is  $220$  °C. Layup tool can be temperature controlled and was maintained at  $30$  °C throughout.

A 30 mm wide, silicon conformable roller with 70 shore A hardness is used as the compaction roller. The ATL head is capable of exerting a force of up to 1.2 kN, but for most of the following experiments a maximum of 500 N is applied, as is commonly used by researchers and industries alike for medium width tapes. Width extraction from 2D profile data is done using scanCONTROL software.

#### 3.1. System characterization

Pre-consolidation tape width characterization study was performed to quantify the effect of material variability at manufacture level on the occurrence of gaps and overlaps, as shown in Fig. 1-2. Profile data was recorded at 50 Hz, which at a layup velocity of 50 mm/s, translates to a profile per mm. The data was recorded for 10 m continuously. The tape width has been found to be highly stable having a mean of 25.5 mm and a standard deviation of  $\sim 0.0011$  mm. Since the tape width was found to be nearly constant, the occurrence of incidental gapping due to material width variation is highly improbable. This is why the effect of material variability on gaps is disregarded.

Initial calibration for the force/torque sensor is done using calibration matrix provided by the manufacturer. An initial verification of successful mounting and commissioning is done by using standard weights.

Static and dynamic validation tests for force measurement were performed using pressure sensitive foils (Prescale, Fujifilm) and pressure mapping sensor (I-scan system, Tekscan). Tests were performed both with and without the CF-tape (carbon fiber). For experiments using pressure sensitive foils, LLW type of foil was selected according to the expected pressure range. These foils have a precision of  $\pm 10$  %. For static tests, a constant force is applied for 2 min and for dynamic tests for 5 s. The imprint of the force is then scanned. Standard continuous pressure chart and standard momentary pressure chart provided by Fujifilm are used to evaluate the imprint area and pixel intensity values using custom built MATLAB code. An average pressure value is calculated which is then converted to a force value using area of imprint. Only static tests were performed using the pressure mapping sensor. Pressure

mapping sensor 5051 was selected in the same way, and calibration and equilibration tests were performed using standard air pressure. The sensor has a resolution of 62senses/cm<sup>2</sup> and provides both pressure distribution and total force. Test with pressure foils were performed for a range of 50–500 N force, with step-size of 50 N. For measurements with pressure mapping sensor, an initial force level of 80 N is applied, after which the force is increased in steps of 50 N, starting from 100 N to 300 N.

As discussed earlier, machine variability might lead to non-uniform force application. System behavior identification tests were performed to characterize this variability.

#### 3.2. Force and width control

The effect of compaction force on the width of the consolidated tape is characterized using force/torque sensor and laser profile sensor, and a correlation between the applied force and the resultant width of tape is obtained. The thermoplastic tape is 25.4 mm (1-inch) wide and is laid up over the course of 500 mm (layup length). The compaction force is varied between 50 N and 350 N in steps of 50 N. A total of 3 layups are performed for each force setting. Profile data is first averaged over the whole layup length of 500 mm, and then over the 3 layups. The layup velocity for these experiments was chosen to be 50 mm/s, as the velocity resulted in optimum bonding. The power output of flash lamp system was set at 2.9 kW, providing enough heat to melt the material without any thermal degradation.

Further experiments are conducted with pre-programmed linear force increase and decrease to assess the width variation possibilities. These tests are performed to verify width conformability for complex shapes.

## 4. Results and discussion

#### 4.1. Performance assessment

Force is applied via compaction roller and is measured by the force/torque sensor placed above the roller, while pressure foils and pressure mapping sensor measure the force under the roller. For sensors placed under the roller, the attributes of the compaction roller and the material between the roller and the sensor play an important role in the force distribution.

Static tests using pressure foils deliver information about the homogeneity of the pressure application and the area of application as the

silicone deforms. The area of application increases with an increase in force, leading to non-linear relation between applied force and resulting pressure under the roller. Higher contact area is favorable for intimate contact development but limits the achievable pressure [42]. Dynamic tests are used as an indicator of precision of force application over time.

The results obtained from the pressure foil measurements are summarized in Fig. 4-1. The static and the dynamic scans without the CF-tape (a and c) show a homogenous pressure distribution. The tests with the CF-tape (b and d) show gradients, with darker pixels indicating the fibers and lighter pixels, the matrix. As can be concluded, fibers are the main load bearing element in the CF-tape. Since the tape is slightly smaller in width than the roller, a separate region of lesser force application on the sides can also be identified. In static tests (a and b), the contact zone of a cylindrical body is also evident. The top and bottom are in the form of an oval shape and the left and right side mark the length of roller contact with sharp pressure concentration, as also noted by [54]. The 2D and 3D representation of pressure distribution is used for calculating average pressure. High values of pressure are restricted to a small region, almost elliptical region.

The forces measured by the force/torque sensor are in good agreement with measurements from the pressure sensitive films and the pressure mapping sensor, as shown in Fig. 4-2. Forces measured by the force sensor and the pressure mapping sensor without the CF-tape are closely related. For measurements with the CF-tape, the noted small discrepancy could arise from force distribution on tape's width. The difference between the width of the roller and the tape leads to a difference in pressure distribution below the roller. Pressure foils show indications of force application outside the width of the tape (Fig. 4-1 b and d), and this whole area is used for force calculation. These values are much closer to the ones measured by the force/torque sensor. For pressure mapping system, only the area under the tape is considered, which leads to an underestimation of calculated force. For future experiments, attention must be paid to the difference between roller and tape width. For model development and simulation studies pressure applied under the roller might be more useful, but for controlling the process, force is a better alternative.

System behavior accounting for machine variability is also analyzed. Detailed analysis of system behavior is crucial for minimum expected width spread. A relation between the target force and the measured force for 50 mm/s layup speed is shown in Fig. 4-3. Data is recorded for 5 layups and the mean and standard deviation are noted. The observed standard deviation for force is  $\sim 10$  N, giving us a step size of 25 N. A stabilization time of 0.3 s is required for online force variation, for a variation of 100 N. The response time could be lowered (less than 0.1 s) if direct PLC programming is used instead of a separate LabVIEW

interface employed currently. It was also observed that, as force increases, the deviation in velocity decreases. A maximum standard deviation of 1.5 mm/s for 100 N is noted. After the detailed tests, it has been established that the compaction force can be controlled online, having a high precision and accuracy compared to the target force.

#### 4.2. Inline width tessellation

As the amount of applied force increases, so does the width of the consolidated tape increases, the increase is however non-linear. Width increase for a force of 50 N-350 N for 1-inch wide tape is shown in Fig. 4-4. A quadratic curve best defines the relationship between the applied force and the resulting width increase. For a wider data set and for comparison purposes, further experiments were performed with same settings except for the heat input. For a 10 % higher heat input, an almost identical quadratic curve is obtained. The width spread differences for respective force settings are also negligible. A possible explanation for this is insignificant change in the melt viscosity of the material for the probed differences in the heat input. If the flow behavior does not show significant changes, the width after consolidation does not change either.

It is observed that an amount of force as small as 50 N is enough to deform the material by more than 1 mm. This accounts for approximately 5 % of the width spread compared to initial width. Although morphological changes can be observed, it is important to establish whether intimate contact development can happen at such low amount of force or not. As noted earlier, the degree of intimate contact generally increases with an increase in force, and 50 N is sufficient to have an intermediate level of degree of bond as noted by [45]. According to Schaefer et al., intimate contact development for thermoplastic CF-PA6 is quite fast, occurring at low to moderate processing temperatures, 10-20 °C above melting point and very low pressures of 1-4 kPa [55]. During static and dynamic tests performed using pressure foils, the average pressure application for 50 N was found to be about 0.6 MPa, which is extremely high compared to the 1-4 kPa listed in literature. It is safe to assume that a force application of 50 N is high enough to ensure intimate contact development. It must also be noted here that even though the degree of intimate contact is solely a function of applied pressure, the degree of bond is also dependent upon the degree of healing, which itself is temperature dependent. If the temperature is high enough to melt the material and the layup velocity allows sufficient time, bond development will take place. This does not mean that high melt temperature can compensate for insufficient amount of force and provide good bonding. A very high melt temperature might lead to polymer degradation and a combination of high temperature and force

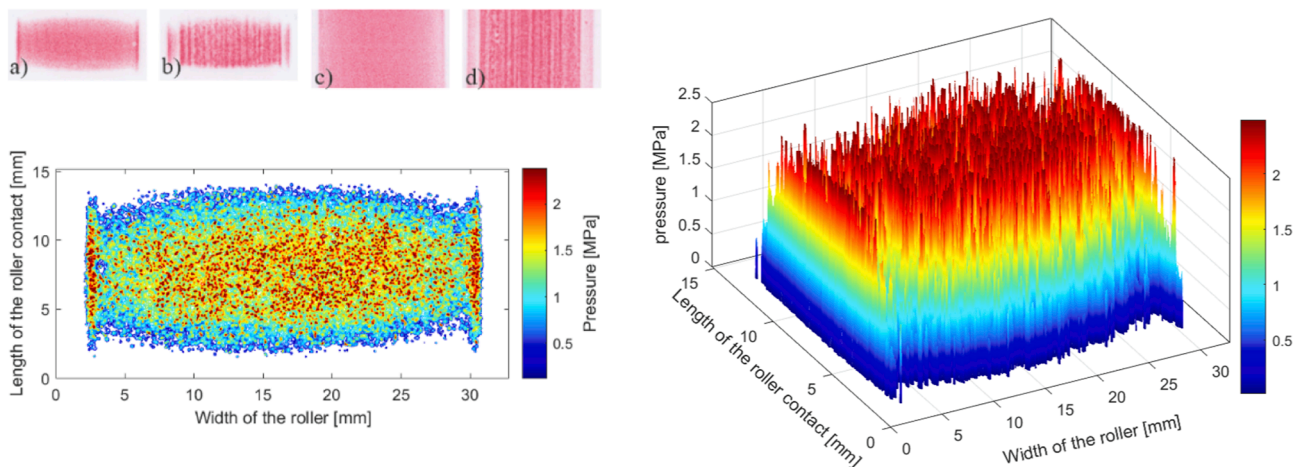


Fig. 4-1. Static and dynamic pressure foil scans for 500 N force (a, b, c and d), a 2D (left, bottom) and a 3D (right) representation of pressure for static tests a) and b) respectively. (For interpretation of the references to colour in this figure legend, the reader is referred to the web version of this article.)

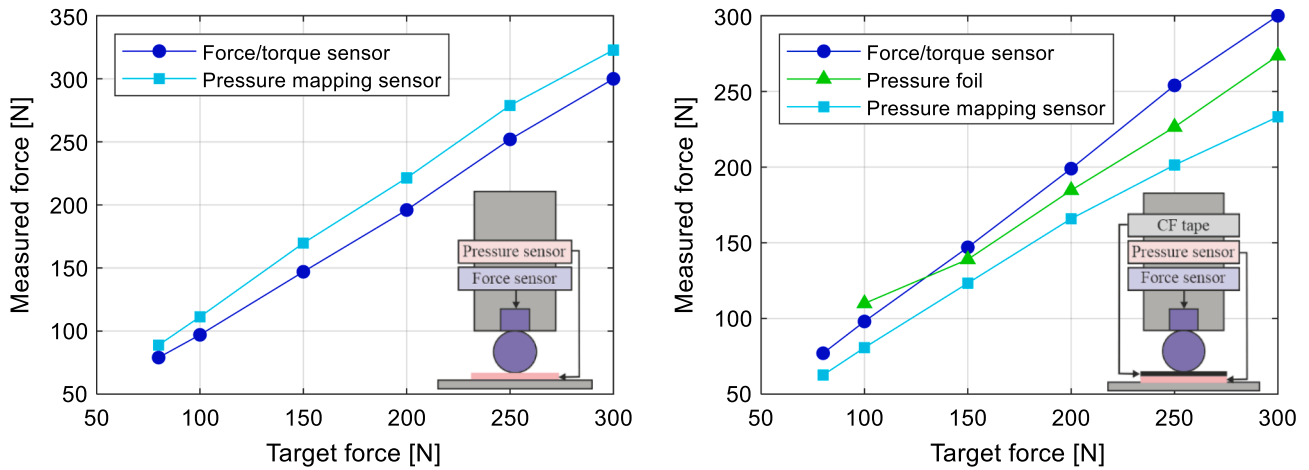


Fig. 4-2. Static force comparison for different sensors without (left) and with (right) CF-tape. (For interpretation of the references to colour in this figure legend, the reader is referred to the web version of this article.)

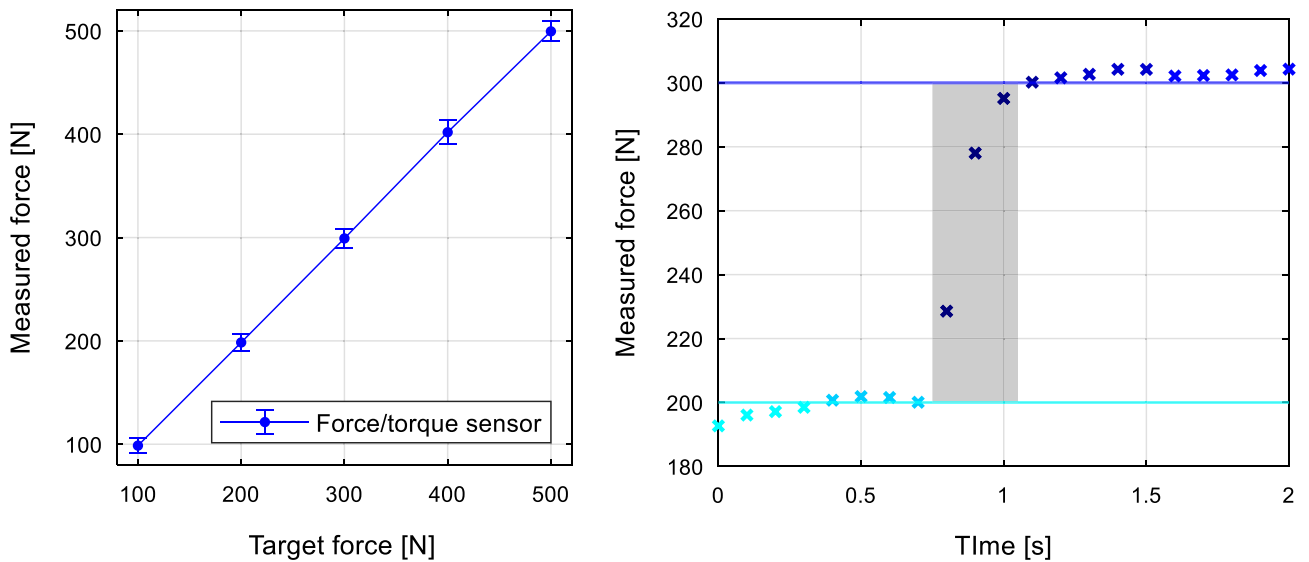


Fig. 4-3. Deviation of measured force from target force (left) and stabilization time for online force variation (right). (For interpretation of the references to colour in this figure legend, the reader is referred to the web version of this article.)

enables matrix flow/squeeze out. For low melt viscosity matrices like PA6 the dominant mechanism for mechanical property loss and thermal degradation is matrix flow/squeeze out rather than polymer degradation [56]. Upper and lower bounds for controlling the process parameters should therefore be established after analyzing their effect on the whole process rather than just one element of it.

For a maximum force of 350 N, a maximum spread of 8.8 % of the initial width or 27.75 mm is observed. The average width spread between each force setting is approximately 0.2 mm. In case of incidental gaps that periodically occur in the course of ordinary ATL operations, a gap width of 0.05" or 1.27 mm represents a conservative upper bound [23] and a gap width of 0.03" or 0.762 mm represents the lower bound [22,23]. With the force control concept demonstrated above it is possible to eliminate these defects. A width spread of 0.2–2.25 mm can be achieved using the present concept which is sufficient according to the aerospace industry standards. For VAT/VSP laminates, a maximum width spread of 41.4 % of the initial width is required to eliminate gaps [11]. To prove the capability of the IWC system in being able to achieve such drastic dimensional changes, higher amount of force should be applied and corresponding width data should be evaluated. Due to hardware restrictions of the present set-up, the laser profile sensor

cannot detect tape width beyond 28 mm. Since the amount of tape spread depends on processing parameters and material properties such as fiber volume fraction, viscosity and the initial width of the tape, a more feasible solution is to use tapes having smaller initial width.

Further experiments are conducted at 500 N and 750 N for tape having an initial width of 6.3 mm and 12 mm. For an initial width of 6.3 mm, a final width of 8.5 mm (34.9 % increase) and 9.5 mm (50.7 % increase) is obtained at a force of 500 N and 750 N respectively. For an initial width of 12 mm, a final width of 14.8 mm (23.3 % increase) and 15.5 mm (29.16 % increase) is obtained at 500 N and 750 N respectively. A further increase in width can be expected for slower layup speeds and higher heat inputs.

A demonstration for inline width tessellation for 12 mm initial width is presented in Fig. 4-5. A linearly varying force ranging from 100 N to 780 N is applied and the corresponding width increase is monitored. Here, a linear or quadratic relation cannot be established easily due to a smaller number of data points and high oscillation in width measurement at both extremities, i.e., very low and very high compaction forces. It must be noted here that the 1-inch wide tape was cut in-house to fit 12 mm dimension and the discrepancy is most probably a result of the cutting method and machine used. Another reason for the discrepancy



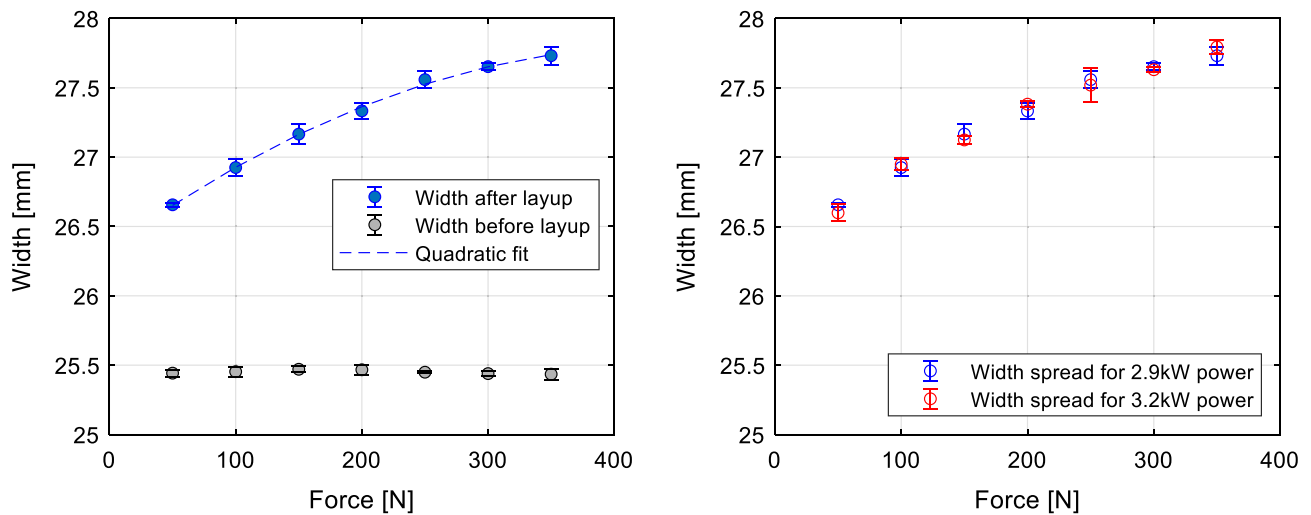


Fig. 4-4. Width and force correlation (left) and width spread for two different power settings of the heat source (right). (For interpretation of the references to colour in this figure legend, the reader is referred to the web version of this article.)

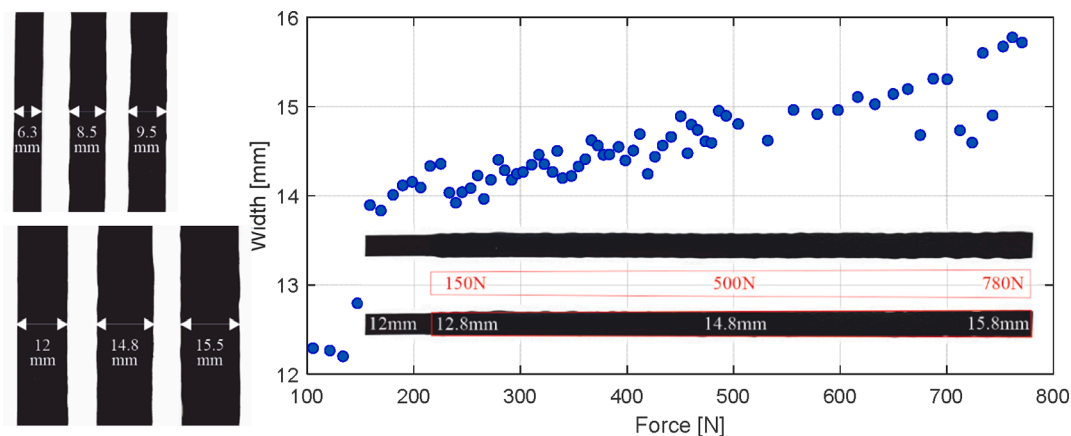


Fig. 4-5. Width spread for initial width of 6.3 mm and 12 mm (left) and inline width tessellation for linearly increasing force (right). (For interpretation of the references to colour in this figure legend, the reader is referred to the web version of this article.)

could be due to pneumatic control hysteresis/residual ripple to continuously achieve varying target force. The width spread however, fits the shape of a trapezium. The trapezoidal shape is a result of linearly increasing force application. In essence, force application behavior has a strong influence on the resulting shape of the laminate and conformance to complex shapes could be achieved based on appropriate force variation. This is especially useful for doubly curved concave/convex shapes and layup tools.

5. Conclusions

The primary objective of this research was to achieve continuous inline width variation/tessellation or inline width control. This has been accomplished via compaction force control and inline/online variation of the same. A prototype for thermoplastic ATL head having minimally intrusive functional design for width tessellation and thereby gaps prevention and elimination is presented. Three practical cases for gap prevention and rectification for the prototype are identified and performance assessment for one of the cases has been presented in detail. For the present system, both force and thereby width control are realized.

System characterization tests comprising of calibration and verification studies have been performed. After initial calibration tests for force/torque sensor using calibration standards provided by the

manufacturer, post commissioning verification tests were performed using standard weights. Static and dynamic tests to assess the homogeneity and validate the readings from force application were carried out using pressure sensitive foils and pressure mapping system. A good agreement between the force/torque sensor and the benchmarks has been obtained. Further tests were performed to characterize the effect machine variability on force stabilization. The prototype is found to be able to vary the force between 50 N and 1000 N in steps of 25 N, having a tolerance of  $\pm 10$  N. A stabilization time of 0.3 s is required for online force variation, for a variation of 100 N.

Force and width correlation models were obtained for standard tape width (1-inch) for inline width tessellation concept implementation. Here a quadratic fit for standard force (50 N-350 N) application is established. Feasibility studies for maximum attainable width spread are also performed. For the layup speed and heat input used in the study, width increase of 5–50 % compared to initial width can be obtained. While physically possible, such drastic increase in the tape width will result in extreme thickness reduction, rendering the material structure and mechanics closer to ‘thin ply composite’. The prominent change can lead to potential drawbacks affecting structural integrity due to dimensional inaccuracy and higher residual stress [57] due to increase in crystallinity [11]. An example of inline width tessellation, in this case a trapezoidal shape is presented. Force variation influences the resulting shape of the tape, unraveling the possibility of shape conformity to the

tool and layup geometry. This gives rise to perfect layup with no gaps or overlaps.

The present concept helps in attaining process reliability and productivity by monitoring and controlling process parameters and resulting defects. Moreover, gaps elimination is followed by improvement in mechanical properties and dimensional accuracy of the resulting laminate. The design flexibility offered by the shape conformity brings the process very close to the possibilities that were made possible only by 3D printing up to now.

Future work would focus on further benchmarking tests and parametric studies to determine the limitations of the IWC concept, particularly with regards to sensitivity to changes in layup parameters or equipment and repeatability of results. The correlation models should be extended to include width changes when adjacent and top plies are laid. Machine learning methods could be employed to establish defined width spread for optimized processing having maximum layup speed. This model can then be employed for rework and rectification studies. Mechanical and material characterization tests should be carried out to assess the structural performance at both lamina and laminate levels.

#### CRedit authorship contribution statement

**Neha Yadav:** Conceptualization, Methodology, Software, Validation, Formal analysis, Investigation, Data curation, Writing – original draft, Writing – review & editing, Visualization. **Ralf Schledjewski:** Conceptualization, Resources, Writing – review & editing, Supervision, Project administration, Funding acquisition.

#### Declaration of Competing Interest

The authors declare that they have no known competing financial interests or personal relationships that could have appeared to influence the work reported in this paper.

#### Data availability

Data will be made available on request.

#### Acknowledgement

The authors kindly acknowledge the financial support through project InP4 (project no. 864824) provided by the Austrian Ministry for Climate Action, Environment, Energy, Mobility, Innovation and Technology within the frame of the FTI initiative “Produktion der Zukunft”, which is administered by the Austrian Research Promotion Agency (FFG).

#### References

- [1] Hoang V-T, et al. Postprocessing method-induced mechanical properties of carbon fiber-reinforced thermoplastic composites. 089270572094537 J Therm Compos Mater 2020. <https://doi.org/10.1177/0892705720945376>.
- [2] Martin I, Del Saenz Castillo D, Fernandez A, Güemes A. Advanced Thermoplastic Composite Manufacturing by In-Situ Consolidation: A Review. J Compos Sci 2020; 4(4):149. <https://doi.org/10.3390/jcs4040149>.
- [3] Qureshi Z, Swait T, Scaife R, El-Dessouky HM. In situ consolidation of thermoplastic prepreg tape using automated tape placement technology: Potential and possibilities. Compos Part B: Eng 2014;66:255–67. <https://doi.org/10.1016/j.compositesb.2014.05.025>.
- [4] Lin TA, Lin J-H, Bao L. A study of reusability assessment and thermal behaviors for thermoplastic composite materials after melting process: Polypropylene/thermoplastic polyurethane blends. J Cleaner Prod 2021;279:123473.
- [5] Peeters D, Deane M, O'Higgins R, Weaver PM. Morphology of ply drops in thermoplastic composite materials manufactured using laser-assisted tape placement. Compos Struct 2020;251:112638. <https://doi.org/10.1016/j.compstruct.2020.112638>.
- [6] Gordon T, Xu X, Wisnom MR, Kim BC. Novel tape termination method for automated fibre placement: Cutting characteristics and delamination suppression. Compos Part A: Appl Sci Manuf 2020;137:106023. <https://doi.org/10.1016/j.compositesa.2020.106023>.
- [7] Blom AW, Stickler PB, Gürdal Z. Optimization of a composite cylinder under bending by tailoring stiffness properties in circumferential direction. Compos Part B: Eng 2010;41(2):157–65. <https://doi.org/10.1016/j.compositesb.2009.10.004>.
- [8] Setoodeh S, Abdalla MM, IJsselmuideen ST, Gürdal Z. Design of variable-stiffness composite panels for maximum buckling load. Compos Struct 2009;87(1):109–17. <https://doi.org/10.1016/j.compstruct.2008.01.008>.
- [9] Rouhi M, Ghayoor H, Fortin-Simpson J, Zacchia TT, Hoa SV, Hojjati M. Design, manufacturing, and testing of a variable stiffness composite cylinder. Compos Struct 2018;184:146–52. <https://doi.org/10.1016/j.compstruct.2017.09.090>.
- [10] Zucco G et al. Static Test of a Thermoplastic Composite Wingbox Under Shear and Bending Moment. In: 2018 AIAA/ASCE/AHS/ASC Structures Structural Dynamics and Materials Conference Kissimmee Florida. January 08-12 2018, Kissimmee, Florida; 2018.
- [11] Clancy G, Peeters D, O'Higgins RM, Weaver PM. In-line variable spreading of carbon fibre/thermoplastic pre-preg tapes for application in automatic tape placement. Mater Des 2020;194:108967. <https://doi.org/10.1016/j.matdes.2020.108967>.
- [12] Kim BC, Potter K, Weaver PM. Continuous tow shearing for manufacturing variable angle tow composites. Compos Part A: Appl Sci Manuf 2012;43(8):1347–56. <https://doi.org/10.1016/j.compositesa.2012.02.024>.
- [13] Falcó O, Mayugo JA, Lopes CS, Gascons N, Costa J. Variable-stiffness composite panels: Defect tolerance under in-plane tensile loading. Compos Part A: Appl Sci Manuf 2014;63:21–31. <https://doi.org/10.1016/j.compositesa.2014.03.022>.
- [14] Fayazbakhsh K, Arian Nik M, Pasini D, Lessard L. Defect layer method to capture effect of gaps and overlaps in variable stiffness laminates made by Automated Fiber Placement. Compos Struct 2013;97:245–51. <https://doi.org/10.1016/j.compstruct.2012.10.031>.
- [15] Clancy G, Peeters D, Oliveri V, Jones D, O'Higgins RM, Weaver PM. A study of the influence of processing parameters on steering of carbon Fibre/PEEK tapes using laser-assisted tape placement. Compos Part B: Eng 2019;163:243–51. <https://doi.org/10.1016/j.compositesb.2018.11.033>.
- [16] Arian Nik M, Fayazbakhsh K, Pasini D, Lessard L. Optimization of variable stiffness composites with embedded defects induced by Automated Fiber Placement. Compos Struct 2014;107:160–6. <https://doi.org/10.1016/j.compstruct.2013.07.059>.
- [17] Chevalier PL, Kassapoglou C, Gürdal Z. Fatigue behavior of composite laminates with automated fiber placement induced defects- a review. Int J Fatigue 2020;140:105775. <https://doi.org/10.1016/j.ijfatigue.2020.105775>.
- [18] Croft K, Lessard L, Pasini D, Hojjati M, Chen J, Yousefpour A. Experimental study of the effect of automated fiber placement induced defects on performance of composite laminates. Compos Part A: Appl Sci Manuf 2011;42(5):484–91. <https://doi.org/10.1016/j.compositesa.2011.01.007>.
- [19] Ghayour M, Hojjati M, Ganesan R. Effect of tow gaps on impact strength of thin composite laminates made by Automated Fiber Placement: Experimental and semi-analytical approaches. Compos Struct 2020;248:112536. <https://doi.org/10.1016/j.compstruct.2020.112536>.
- [20] Falcó O, Lopes CS, Naya F, Sket F, Maimí P, Mayugo JA. Modelling and simulation of tow-drop effects arising from the manufacturing of steered-fibre composites. Compos Part A: Appl Sci Manuf 2017;93:59–71. <https://doi.org/10.1016/j.compositesa.2016.11.015>.
- [21] Lan M, Cartié D, Davies P, Baley C. Influence of embedded gap and overlap fiber placement defects on the microstructure and shear and compression properties of carbon–epoxy laminates. Compos Part A: Appl Sci Manuf 2016;82:198–207. <https://doi.org/10.1016/j.compositesa.2015.12.007>.
- [22] Nguyen MH, Vijayachandran AA, Davidson P, Call D, Lee D, Waas AM. Effect of automated fiber placement (AFP) manufacturing signature on mechanical performance of composite structures. Compos Struct 2019;228:111335. <https://doi.org/10.1016/j.compstruct.2019.111335>.
- [23] Guin WE, Jackson JR, Bosley CM. Effects of tow-to-tow gaps in composite laminates fabricated via automated fiber placement. Compos Part A: Appl Sci Manuf 2018;115:66–75. <https://doi.org/10.1016/j.compositesa.2018.09.014>.
- [24] Woigk W, Hallett SR, Jones MI, Kuitz M, Hornig A, Gude M. Experimental investigation of the effect of defects in Automated Fibre Placement produced composite laminates. Compos Struct 2018;201:1004–17. <https://doi.org/10.1016/j.compstruct.2018.06.078>.
- [25] Sacco C, Brasington A, Saïdy C, Kirkpatrick M, Halbritter J, Wehbe R, et al. On the effect of manual rework in AFP quality control for a doubly-curved part. Compos Part B: Eng 2021;227:109432. <https://doi.org/10.1016/j.compositesb.2021.109432>.
- [26] Blom AW, Lopes CS, Kromwijk PJ, Gürdal Z, Camanho PP. A Theoretical Model to Study the Influence of Tow-drop Areas on the Stiffness and Strength of Variable-stiffness Laminates. J Compos Mater 2009;43(5):403–25. <https://doi.org/10.1177/0021998308097675>.
- [27] Iarve EV, Kim R. Strength Prediction and Measurement in Model Multilayered Discontinuous Tow Reinforced Composites. J Compos Mater 2004;38(1):5–18. <https://doi.org/10.1177/0021998304038215>.
- [28] Tatting BF, Gürdal Z, Jegley D. Design and Manufacture of Elastically Tailored Tow Placed Plates. NASA/CR-2002-211919; Aug. 2002. [Online]. Available: <http://ntrs.nasa.gov/citations/20020073162>.
- [29] Kim BC, Weaver PM, Potter K. Manufacturing characteristics of the continuous tow shearing method for manufacturing of variable angle tow composites. Compos A Appl Sci Manuf 2014;61:141–51. <https://doi.org/10.1016/j.compositesa.2014.02.019>.
- [30] Oromiehie E, Prusty BG, Compston P, Rajan G. Automated fibre placement based composite structures: Review on the defects, impacts and inspections techniques. Compos Struct 2019;224:110987. <https://doi.org/10.1016/j.compstruct.2019.110987>.

- [31] Sun S, Han Z, Fu H, Jin H, Dhupia JS, Wang Y. "Defect Characteristics and Online Detection Techniques During Manufacturing of FRPs Using Automated Fiber Placement: A Review. *Polymers* 2020;12(6):pp. <https://doi.org/10.3390/polym12061337>.
- [32] Wang EL, Gutowski TG. Laps and gaps in thermoplastic composites processing. *Compos Manuf* 1991;2(2):69–78. [https://doi.org/10.1016/0956-7143\(91\)90182-G](https://doi.org/10.1016/0956-7143(91)90182-G).
- [33] Dara PH, Loos AC. Thermoplastic matrix composite processing model, NAS 1.26: 176639; Sep. 1985. [Online]. Available: <https://ntrs.nasa.gov/citations/19860012148>.
- [34] Mantell SC, Springer GS. "Manufacturing Process Models for Thermoplastic Composites", (in English (US)). *J Compos Mater* 1992;26(16):2348–77. <https://doi.org/10.1177/002199839202601602>.
- [35] Yang F, Pitchumani R. "A fractal Cantor set based description of interlaminar contact evolution during thermoplastic composites processing", (in En;en). *J Mater Sci* 2001;36(19):4661–71. <https://doi.org/10.1023/A:1017950215945>.
- [36] Yang F, Pitchumani R. Interlaminar contact development during thermoplastic fusion bonding. *Polym Eng Sci* 2002;42(2):424–38. <https://doi.org/10.1002/pen.10960>.
- [37] Cheng J, Zhao D, Liu K, Wang Y, Chen H. Modeling and impact analysis on contact characteristic of the compaction roller for composite automated placement. *J Reinf Plast Compos* 2018;37(23):1418–32. <https://doi.org/10.1177/0731684418798151>.
- [38] Ranganathan S, Advani SG, Lamontia MA. A Non-Isothermal Process Model for Consolidation and Void Reduction during In-Situ Tow Placement of Thermoplastic Composites. *Journal of Composite Materials* 1995;29(8):1040–62. <https://doi.org/10.1177/002199839502900803>.
- [39] Pitchumani R, Gillespie JW, Lamontia MA. Design and Optimization of a Thermoplastic Tow-Placement Process with In-Situ Consolidation. *J Compos Mater* 1997;31(3):244–75. <https://doi.org/10.1177/002199839703100302>.
- [40] Tierney J, Gillespie JW. Modeling of In Situ Strength Development for the Thermoplastic Composite Tow Placement Process. *J Compos Mater* 2006;40(16):1487–506. <https://doi.org/10.1177/0021998306060162>.
- [41] Shuler S, Advani S. Transverse squeeze flow of concentrated aligned fibers in viscous fluids. *J Nonnewton Fluid Mech* 1996;65(1):47–74. [https://doi.org/10.1016/0377-0257\(96\)01440-1](https://doi.org/10.1016/0377-0257(96)01440-1).
- [42] Çelik O, Peeters D, Dransfeld C, Teuwen J. Intimate contact development during laser assisted fiber placement: Microstructure and effect of process parameters. *Compos A Appl Sci Manuf* 2020;134:105888. <https://doi.org/10.1016/j.compositesa.2020.105888>.
- [43] Barnes JA, Cogswell FN. Transverse flow processes in continuous fibre-reinforced thermoplastic composites. *Composites* 1989;20(1):38–42. [https://doi.org/10.1016/0010-4361\(89\)90680-0](https://doi.org/10.1016/0010-4361(89)90680-0).
- [44] Aized T, Shirinzadeh B. Robotic fiber placement process analysis and optimization using response surface method. *Int J Adv Manuf Technol* 2011;55(1–4):393–404. <https://doi.org/10.1007/s00170-010-3028-1>.
- [45] Khan MA, Mitschang P, Schledjewski R. Parametric study on processing parameters and resulting part quality through thermoplastic tape placement process. *J Compos Mater* 2013;47(4):485–99. <https://doi.org/10.1177/0021998312441810>.
- [46] Schaefer PM, Gierszewski D, Kollmannsberger A, Zaremba S, Drechsler K. Analysis and improved process response prediction of laser-assisted automated tape placement with PA-6/carbon tapes using Design of Experiments and numerical simulations. *Compos Part A: Appl Sci Manuf* 2017;96:137–46. <https://doi.org/10.1016/j.compositesa.2017.02.008>.
- [47] Pitchumani R, Ranganathan S, Don RC, Gillespie JW, Lamontia MA. Analysis of transport phenomena governing interfacial bonding and void dynamics during thermoplastic tow-placement. *Int J Heat Mass Transf* 1996;39(9):1883–97. [https://doi.org/10.1016/0017-9310\(95\)00271-5](https://doi.org/10.1016/0017-9310(95)00271-5).
- [48] Schuster A, Mayer M, Willmeroth M, Brandt L, Kupke M. Inline Quality Control for Thermoplastic Automated Fibre Placement. *Procedia Manuf* 2020;51:505–11. <https://doi.org/10.1016/j.promfg.2020.10.071>.
- [49] Denkena B, Schmidt C, Weber P. Automated Fiber Placement Head for Manufacturing of Innovative Aerospace Stiffening Structures. *Proc Manuf* 2016;6:96–104. <https://doi.org/10.1016/j.promfg.2016.11.013>.
- [50] Bendemra H, Vincent M, Compston P. *8th Australasian Congress on Applied Mechanics: ACAM 8*. [Place of publication not identified]: Engineers Australia; 2014. [Online]. Available: <https://openresearch-repository.anu.edu.au/handle/1885/23067>.
- [51] Yassin K, Hojjati M. Processing of thermoplastic matrix composites through automated fiber placement and tape laying methods. *J Thermoplast Compos Mater* 2018;31(12):1676–725. <https://doi.org/10.1177/0892705717738305>.
- [52] Jiang J, He Y, Ke Y. Pressure distribution for automated fiber placement and design optimization of compaction rollers. *J Reinf Plast Compos* 2019;38(18):860–70. <https://doi.org/10.1177/0731684419850896>.
- [53] Chu Q, Li Y, Xiao J, Huan D, Zhang X. Placeability restricted by in-complete contact between laying roller and mould in an automated fiber placement process. *J Reinf Plast Compos* 2018;37(7):475–89. <https://doi.org/10.1177/0731684417752871>.
- [54] Jiang J, He Y, Wang H, Ke Y. Modeling and experimental validation of compaction pressure distribution for automated fiber placement. *Compos Struct* 2021;256:113101. <https://doi.org/10.1016/j.compstruct.2020.113101>.
- [55] Schaefer PM, Guglhoer T, Sause MG, Drechsler K. Development of intimate contact during processing of carbon fiber reinforced Polyamide-6 tapes. *J Reinf Plast Compos* 2017;36(8):593–607. <https://doi.org/10.1177/0731684416687041>.
- [56] Stokes-Griffin CM, Kollmannsberger A, Compston P, Drechsler K. The effect of processing temperature on wedge peel strength of CF/PA 6 laminates manufactured in a laser tape placement process. *Compos A Appl Sci Manuf* 2019;121:84–91. <https://doi.org/10.1016/j.compositesa.2019.02.011>.
- [57] Parlevliet PP, Bersee HE, Beukers A. Residual stresses in thermoplastic composites—A study of the literature—Part I: Formation of residual stresses. *Compos A Appl Sci Manuf* 2006;37(11):1847–57. <https://doi.org/10.1016/j.compositesa.2005.12.025>.

### 4.3 Correlation Models

For effective gap management, a base model consisting of width spread values for different parametric sets is deemed necessary. Based on the size of the gap, width spread and corresponding process parameters can be selected and used for the process run. This raises the requirement of a parametric study to obtain correlation models. The final research question being addressed here is, *is there any correlation between certain defects and process parameters? Which models are required for process monitoring and control?*

The parametric effect of heat, speed and compaction force on tape width is shown in *Figure 7*. Looking at the top three graphs, it is quite evident that maximum width spread (maximum change in tape width) and maximum range of width spread (minimum and maximum width spread values) are achieved at maximum heat, in this case at 3500 W. The maximum possible width spread is at low speed and high force (3500 W, 50 mm/s and 300 N). A bigger difference in width spread is achieved between 50 mm/s and 100 mm/s than the difference between 100 mm/s and 150 mm/s. For a set speed, the slope of the curves is very similar at different heat inputs. The slope gradually reduces from 50 mm/s to 150 mm/s. The direct implication is that even though the width increases as the heat increases, the increment is not considerable for higher speeds. This can be attributed to time available for polymer healing.

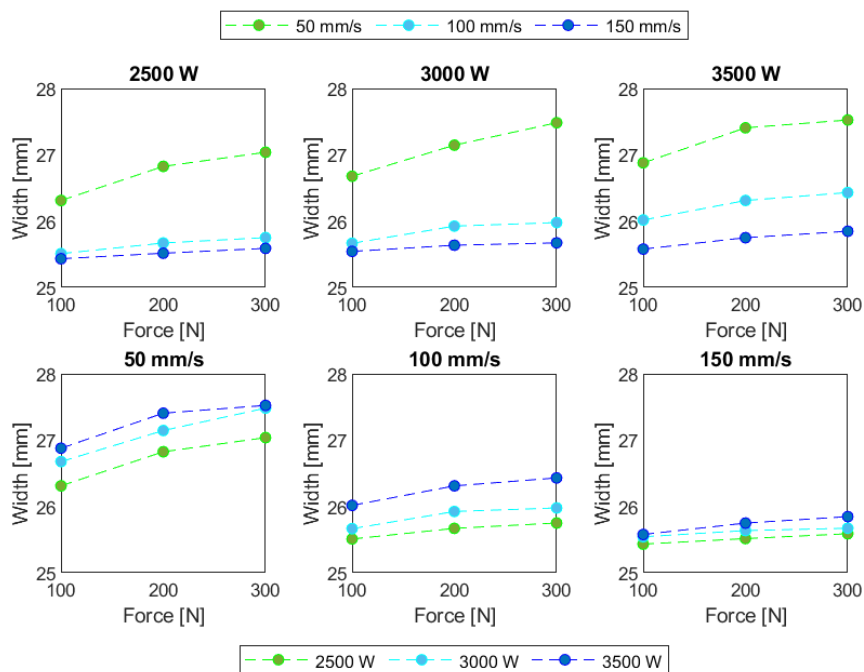


Figure 7 Parametric influence on width spread [34]

As can be seen from the bottom three graphs, speed has a strong influence on the material behavior. For maximum speed, in this case 150 mm/s, the width spread is negligible even when maximum heat and force are applied (150 mm/s, 3500 W and 300 N). At higher speeds the range of width spread becomes smaller and all width values are close to each other. The time available

for polymer healing is decided by the laying speed. Lower speed leads to a higher temperature, resulting in a lower melt viscosity and a higher degree of intimate contact. Compaction force also has a strong dependence on the process speed. At higher speeds, even if compaction force is increased continuously, there will be an inconsiderable change in the degree of bond [35]. A good data point for comparison is minimum and maximum speed. At 50 mm/s, the width spread for least heat and force (50 mm/s, 2500 W and 100 N) is still greater than that for highest speed level at maximum heat and force (150 mm/s, 3500 W and 300 N).

The smallest width increase is achieved at the parametric set (150 mm/s, 2500 W and 100 N) while the maximum is found at (50 mm/s, 3500 W and 300 N). Reducing the speed at the lowest parametric set gives a higher width spread than increasing the heat or force. Conversely, if speed is increased for the highest parametric set, the width spread values drop significantly.

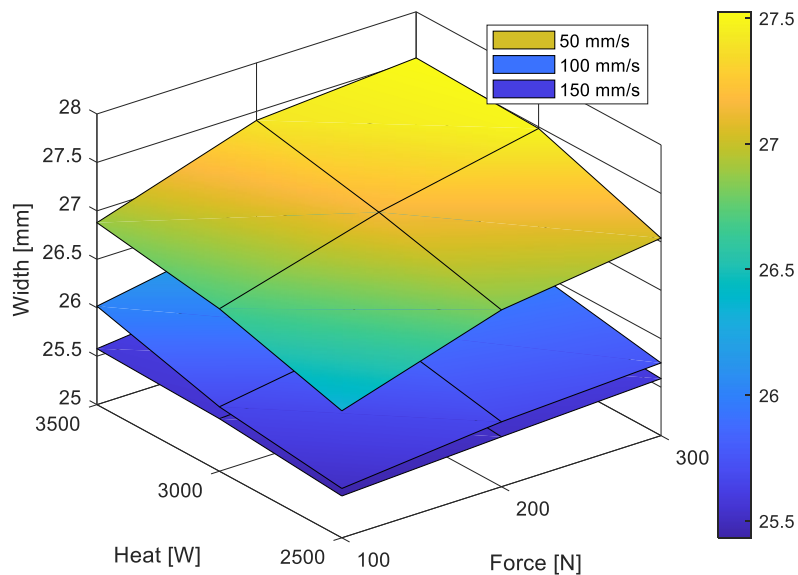


Figure 8 Surface map of parametric influence on width spread [34]

A 3D surface map of laying speed, heat input and compaction force correlation with width spread is shown in *Figure 8*. Process speed can be evidently recognized as the major influencing factor affecting the width spread. It should be noted here that the surface model depicts data points guided by the boundaries of the process window for the present ATL test-rig configuration. The limits for the heat input in the width spread model are decided based on the onset of melting (lower limit) and degradation (upper limit). The position of the heat source, shape of the quartz lamp, parameters affecting heating power and process speed play a crucial role in the final heating behavior of the heat source. For a process run with a set speed and heat, a range of force and corresponding width values can be found from the width spread model. Using force control, desired width changes can be acquired as per the requirements.

The parametric study highlights the influence of process speed on morphological changes in the thermoplastic material. Force and width correlation model in the form of a surface map can be used for gap elimination and path planning. It should be noted that the upper limit for force (hence

larger width increase) can be extended without influencing the heating behavior or bond strength. The wider the range of the width spread, the better the gap elimination possibilities. Along with the process parameters, tape width changes are sensitive to the test-rig configuration. The initial width of the tape, type of heat source and hardware restrictions define the scope of the model and ultimately the process window for robust control. Based on the system characterization, a vast range of possibilities for width variation can be derived.

The answer to the final research question is, *a correlation between positioning defects, namely gaps and overlaps and process parameters exists and is elucidated in the presented thesis. An empirical model illustrating parametric influence on width spread can be used for defect management and process control.*

This chapter provides an overview of the key results of this thesis, which are then subsequently linked to future prospects for the industry in general. Limitations and potential added values of this research for manufacturing composites by means of ATL is further discussed.

## 5.1 Conclusion

The main outcome of this research work is an industry ready engineering solution for a holistic inline defect **monitoring concept** (*Figure 9*). The key findings and learnings of the research work are related to manufacturing defects and sensorics. Most manufacturing defects can be detected inline efficiently. The defects are monitored at each processing step for maximum coverage and accuracy. FBG sensors are shown to be capable of detecting residual strain at both lamina and laminate level. The effect of process parameters on residual strain can be established and investigated. Infrared thermography has been demonstrated as an adept tool for detecting FOD defects as small as 2.5 mm. Local bonding defects and thermal anomaly can be detected as well. Positioning defects such as gaps and overlaps having a size of 0.2 mm and above can be well detected using light section sensors. Sensor specific best practices are highlighted and utilized. A single sensor system even though used for a specific defect type, in practice can cover a wider range of individual defects. These can then be verified by simultaneous detection using other sensor systems, increasing the probability and reliability of detection.

The novelty of the monitoring concept (identification, detection and management) lies in **defect management** (rectification, prediction and prevention) techniques. A complete life cycle consisting of crucial defect identification, detection, treatment and control based on analysis of the process behavior is demonstrated. Going beyond remedial **rectification** (removal, rework and repair), preemptive strategies are discussed and selectively implemented. Defect **prediction** and **prevention** require process and parameter control. For robust process monitoring and control, crucial defects are identified, detected and managed in a cyclic manner (*Figure 4*). For the given set-up, residual strain, substrate temperature and compaction force can be controlled to alleviate shape distortion, bond inhomogeneity as well as gaps and overlaps respectively. Process parameter control ultimately leads to process optimization and time, cost and weight savings.

The process design and development has been made with highest regards to modularity and flexibility. Modification to the present sensor set-up and integration of new sensors can be done with ease. Even though the present system has been designed for thermoplastic CF-PA6, the model can be extended easily with little effort for other materials based on the defect types. Modular systems are also easier to adapt with future technological changes and lead to substantial cost savings in the longer run. From a process control view-point, the inline control mechanisms

have the potential to be used in real-time. The elements required for online control in individual sub-systems are either functional and in dormant use or can be built-up based on the provided proof of concept discussions. A comprehensive, synchronized and synergetic control of all sub-systems as a singular system would be beneficial for overall process optimization. Advanced process simulation can help to reduce the time and effort needed for trial and error approaches in process window formulation. Further speed and accuracy improvements can be made by employing machine learning and artificial intelligence algorithms for defect classification.

The industrial implications of such a holistic process monitoring concept are immense. The toolkit fits the needs of high-performance industries, particularly aviation and aerospace industry, where the exacting nature of productivity and quality standards makes functional technological innovation very challenging. For a successful industrial product, research and innovation are first steps towards technology adoption. It has been discovered that there are existing automation technologies that can improve the level of automation and technology readiness level but suffer from a lack of widespread use [6]. With this dissertation, efforts are made to bridge this existing gap. Here, the test-bench having best practices for inline monitoring implementation with established prototype and benchmarked results will come in handy. The gap and overlap management techniques are especially useful for VAT/VSP and complex shaped laminates. Compared to conventional aircraft wing design, steered tow (VAT/VSP) leads to a performance increase in terms of fuel burn and weight savings [36, 37]. However, the layup rates for such laminates tend to be conservatively very low, due to layup restrictions, defect rectification and quality checks. Inline gap management and width control will single-handedly overcome all these shortcomings. Less overlaps and overall defects will lead to efficient lightweight construction. Shape conformity will help in generating advanced, more complex structures. Defect management on the fly will improve manufacturing rates, bringing the process speed closer to traditionally manufactured components.

Among the technologies used for advanced composite manufacturing, additive manufacturing (3D printing) is the fastest improving domain followed by ATL and AFP. The possible cause for different improvement rates bears witness to main technological trajectories. On demand production with a higher degree of design freedom makes additive manufacturing (AM) lucrative for industries looking at reducing inventory stocks and reshaping supply chains. This sub-domain of AM is improving at a rate comparable to high-grade metal-based AM technologies. It should be noted that the study did not differentiate between technological trajectories for thermoplastic and thermoset composites [20]. The design flexibility offered by width control and shape conformity for thermoplastics will fit right in and better the yearly improvement rate for ATL and AFP. The yearly improvement rates for ATL and AFP however are on par with milling technology, that has been in use for decades in the aerospace industry. Milling technology is an automated subtractive manufacturing technique used for manufacturing metal components. It has been discovered that the advanced manufacturing technologies (ATL and AFP) have the potential to keep substituting high-grade metal-based milling technology for certain components as their relative advantage will increase over time [20]. A fast and accurate quality control system, as described in this thesis, will again help bring about this change faster, making the components lighter and durable. The objective is to combine the best traits traditional manufacturing and 3D printing technologies have to offer. Taking strength characteristics from traditional manufacturing and design freedom and weight savings from 3D printing. Effort is made to expand the design domain and niche for ATL and AFP manufactured components. With the described monitoring concept, the process should be able to accommodate components having a vast range of size and design complexity.



It is worth noting that even though establishing high consolidation quality was not a direct aim, a working set of process parameters resulting in homogenous in-situ consolidation have been recognized. The overall process has been found to be repeatable and for the right set of parameters, the consolidation quality is within limits specified by the aerospace industry. In summary, a monitoring concept is presented that leads to greater design freedom, quality and reliability enhancement, weight and cost savings and productivity rise. These aspects align well with the goals of the European Green Deal, a European Union (EU) initiative to enable sustainable and future oriented fiber composite production [38].

Finally, the technological advancement for ATL and AFP over the decades can be put into perspective when compared to a mature technology such as CNC, which has been in use since the early 1950s (for over 70 years now). Automated coordinate measuring machines (CMM) were introduced roughly over 40 years ago, in the late 1970s, to replace manual inspection for CNC and it took nearly 20 years of development to bring the system to match the productivity and accuracy levels of CNC machines [14]. Considering that ATL and AFP systems were introduced 30 years ago (late 1980s) and automated inline inspection has only gained recognition as an important element in the past couple of years, the improvement trends seem optimistic and forward-looking.

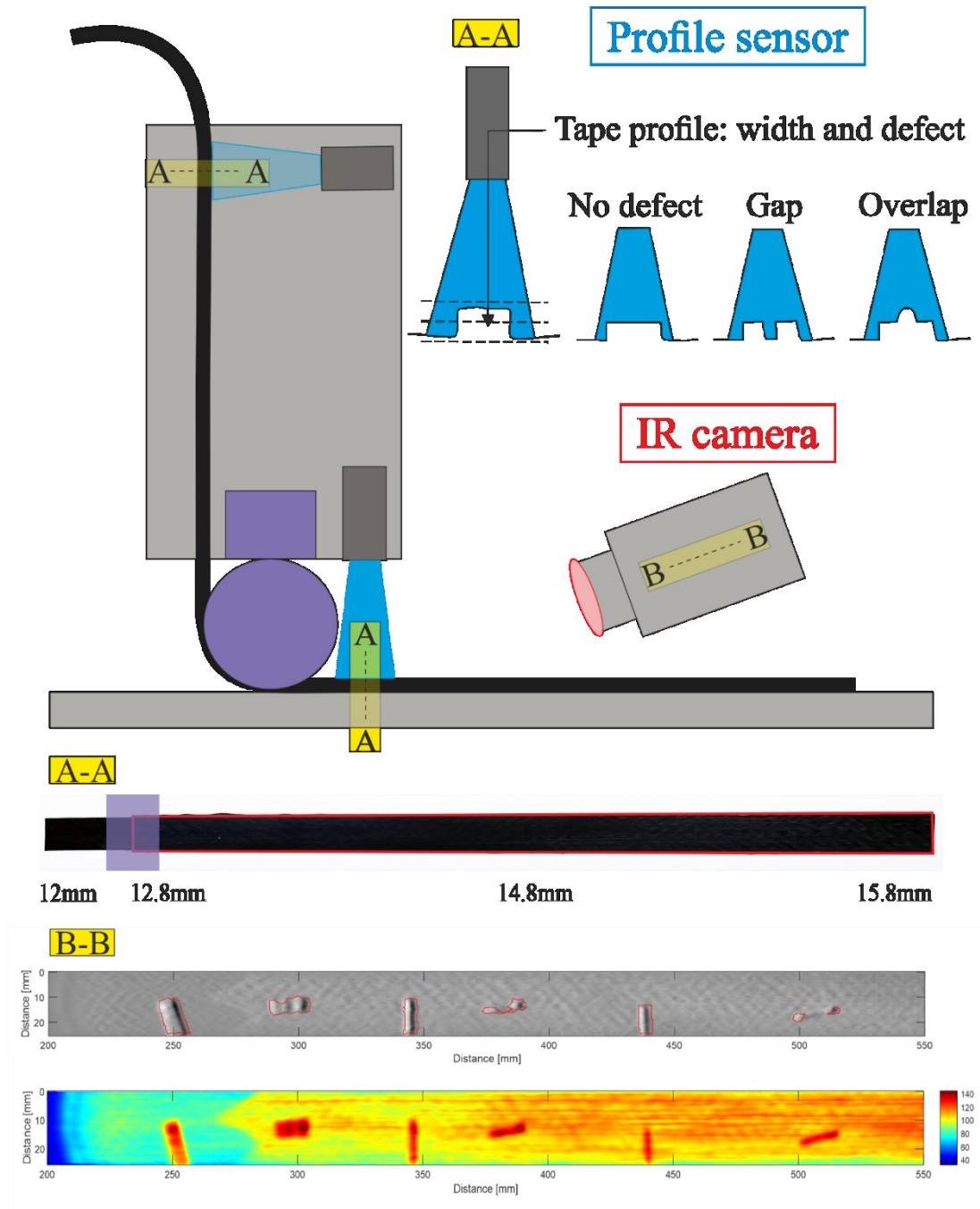


Figure 9 Overview of test-rig having an integrated monitoring concept and process control, adapted from [22, 32]

## 5.2 Outlook

Developing upon the results, criticalities and research gaps described in the course of this dissertation, suggestions for future work with an industrial outlook are presented. Valuable information for transfer and dissemination of findings and further improvement of technology are described. Sensor and test-rig specific developments are the building blocks for overall process

advancement. Both are discussed chronologically. The topics are chosen based on relevance, feasibility, significance and novelty. The suggestions listed below might stimulate curiosity but also lead to meaningful contributions in the research field.

Concerning FBG usage, especially for SHM, the interaction between the embedded sensor and the host material should be studied in detail. Once a reliable and working solution is found, strain handling for bi-stable cross-ply laminates can be investigated. Over time, bi-stable morphing structures have found increasing use in engineering applications [39–41], including aerospace [42] but lack in-depth research.

The infrared thermography-based monitoring tool can be enhanced for better functionality by incorporating speed and heat source control for substrate temperature adjustments. A temperature control mechanism would tremendously benefit composite welding, another application area under research for humm3® systems.

Pertaining to IWC, the model for force and width correlation should be extended to adjacent and top plies for different orientations of plies. The sensitivity and repeatability of the results with regards to initial tape width, extreme width spread and changes in layup parameters and equipment should be well defined. Moreover, the limitation of the characterization method for different material systems and control elements such as hardness of compaction roll should be explored. Mechanical and optical tests to analyze both, the effect of thickness reduction on material properties (fiber volume fraction and crystallinity) and the effect of gap elimination on structural performance at both lamina and laminate level should be performed. An online feedback control accounting for both material variability and parametric influence would lead to efficient gap prevention. An advanced version of the IWC concept can then be implemented for angular tow spreading for drastic curvatures. Another probable use that requires detailed research is IWC for thermosets.

The control mechanisms for individual sensors and parameters when interlinked will create a balanced approach towards process optimization. A multi-objective optimization involving multiple variables and phenomena at various scales when established will transform the way manufacturing works presently. A robust process control necessitates establishing a coherence between empirical, analytical and physical models. For online defect analysis, be it using infrared thermography or light section sensors, a database creation would be helpful for information overview and cross-linking. A cyber-physical system designed on cloud computing would ease the flow of operations. Here, involving a digital twin might be the best solution forward.

Furthering the defect monitoring concept, techniques and strategies for defect rectification as well as - if possible - elimination and in best case prevention would be the emergent field witnessing a surge, especially when thermoplastics certify for single-shot processing. Generative design approaches for biomimetic structures utilizing shape adaptive features would result in disruptive transformation of how products are designed and manufactured.

## References

- [1] D. H.-J. Lukaszewicz, C. Ward, and K. D. Potter, “The engineering aspects of automated prepreg layup: History, present and future,” *Composites Part B: Engineering*, vol. 43, no. 3, pp. 997–1009, 2012, doi: 10.1016/j.compositesb.2011.12.003.
- [2] J. Frketic, T. Dickens, and S. Ramakrishnan, “Automated manufacturing and processing of fiber-reinforced polymer (FRP) composites: An additive review of contemporary and modern techniques for advanced materials manufacturing,” *Additive Manufacturing*, vol. 14, pp. 69–86, 2017, doi: 10.1016/j.addma.2017.01.003.
- [3] B. Sobhani Aragh, E. Borzabadi Farahani, B. X. Xu, H. Ghasemnejad, and W. J. Mansur, “Manufacturable insight into modelling and design considerations in fibre-steered composite laminates: State of the art and perspective,” *Computer Methods in Applied Mechanics and Engineering*, vol. 379, p. 113752, 2021, doi: 10.1016/j.cma.2021.113752.
- [4] L. Zhang, X. Wang, J. Pei, and Y. Zhou, “Review of automated fibre placement and its prospects for advanced composites,” *J Mater Sci*, vol. 55, no. 17, pp. 7121–7155, 2020, doi: 10.1007/s10853-019-04090-7.
- [5] V. Oliveri *et al.*, “Design, Manufacture and Test of an In-Situ Consolidated Thermoplastic Variable-Stiffness Wingbox,” *AIAA Journal*, vol. 57, no. 4, pp. 1671–1683, 2019, doi: 10.2514/1.J057758.
- [6] D. Jayasekara, N. Y. G. Lai, K.-H. Wong, K. Pawar, and Y. Zhu, “Level of automation (LOA) in aerospace composite manufacturing: Present status and future directions towards industry 4.0,” *Journal of Manufacturing Systems*, vol. 62, pp. 44–61, 2022, doi: 10.1016/j.jmsy.2021.10.015.
- [7] F. Heinecke and C. Willberg, “Manufacturing-Induced Imperfections in Composite Parts Manufactured via Automated Fiber Placement,” *J. Compos. Sci.*, vol. 3, no. 2, p. 56, 2019, doi: 10.3390/jcs3020056.
- [8] Y. Zhan, F. Lin, Z. Song, Z. Sun, and M. Yu, “Applications and research progress of optical fiber grating sensing in thermoplastic composites molding and structure health monitoring,” *Optik*, vol. 229, p. 166122, 2021, doi: 10.1016/j.ijleo.2020.166122.
- [9] V.-T. Hoang *et al.*, “Postprocessing method-induced mechanical properties of carbon fiber-reinforced thermoplastic composites,” *Journal of Thermoplastic Composite Materials*, 089270572094537, 2020, doi: 10.1177/0892705720945376.
- [10] Z. Qureshi, T. Swait, R. Scaife, and H. M. El-Dessouky, “In situ consolidation of thermoplastic prepreg tape using automated tape placement technology: Potential and possibilities,” *Composites Part B: Engineering*, vol. 66, pp. 255–267, 2014, doi: 10.1016/j.compositesb.2014.05.025.
- [11] I. Martin, D. Del Saenz Castillo, A. Fernandez, and A. Güemes, “Advanced Thermoplastic Composite Manufacturing by In-Situ Consolidation: A Review,” *Journal of Composites Science*, vol. 4, no. 4, p. 149, 2020, doi: 10.3390/jcs4040149.
- [12] M. Y. Shiino, T. C. G. Cipó, M. V. Donadon, and A. Essiptchouk, “Waste size and lay up sequence strategy for reusing/recycling carbon fiber fabric in laminate composite: Mechanical property analysis,” *Journal of Composite Materials*, vol. 55, no. 28, pp. 4221–4230, 2021, doi: 10.1177/00219983211037047.
- [13] T. A. Lin, J.-H. Lin, and L. Bao, “A study of reusability assessment and thermal behaviors for thermoplastic composite materials after melting process: Polypropylene/ thermoplastic polyurethane blends,” *Journal of Cleaner Production*, vol. 279, p. 123473, 2021, doi: 10.1016/j.jclepro.2020.123473.

- [14] D. Maass, “Progress in automated ply inspection of AFP layups,” *Reinforced Plastics*, vol. 59, no. 5, pp. 242–245, 2015, doi: 10.1016/j.repl.2015.05.002.
- [15] B. Denkena, C. Schmidt, and P. Weber, “Automated Fiber Placement Head for Manufacturing of Innovative Aerospace Stiffening Structures,” *Procedia Manufacturing*, vol. 6, pp. 96–104, 2016, doi: 10.1016/j.promfg.2016.11.013.
- [16] P. D. Juarez and E. D. Gregory, “In Situ Thermal Inspection of Automated Fiber Placement for manufacturing induced defects,” *Composites Part B: Engineering*, vol. 220, p. 109002, 2021, doi: 10.1016/j.compositesb.2021.109002.
- [17] C. Schmidt, B. Denkena, K. Völtzer, and T. Hocke, “Thermal Image-based Monitoring for the Automated Fiber Placement Process,” *Procedia CIRP*, vol. 62, pp. 27–32, 2017, doi: 10.1016/j.procir.2016.06.058.
- [18] M. Brysch, M. Bahar, H. C. Hohensee, and M. Sinapius, “Single system for online monitoring and inspection of automated fiber placement with object segmentation by artificial neural networks,” *J Intell Manuf*, vol. 33, no. 7, pp. 2013–2025, 2022, doi: 10.1007/s10845-022-01924-1.
- [19] A. Brasington, C. Sacco, J. Halbritter, R. Wehbe, and R. Harik, “Automated fiber placement: A review of history, current technologies, and future paths forward,” *Composites Part C: Open Access*, vol. 6, p. 100182, 2021, doi: 10.1016/j.jcomc.2021.100182.
- [20] A. Alves de Campos, E. Henriques, and C. L. Magee, “Technological improvement rates and recent innovation trajectories in automated advanced composites manufacturing technologies: A patent-based analysis,” *Composites Part B: Engineering*, vol. 238, p. 109888, 2022, doi: 10.1016/j.compositesb.2022.109888.
- [21] Z. Ren, F. Fang, N. Yan, and Y. Wu, “State of the Art in Defect Detection Based on Machine Vision,” *Int. J. of Precis. Eng. and Manuf.-Green Tech.*, vol. 9, no. 2, pp. 661–691, 2022, doi: 10.1007/s40684-021-00343-6.
- [22] N. Yadav and R. Schledjewski, “Review of in-process defect monitoring for automated tape laying,” *Composites Part A: Applied Science and Manufacturing*, p. 107654, 2023, doi: 10.1016/j.compositesa.2023.107654.
- [23] R. Pitchumani, S. Ranganathan, R. C. Don, J. W. Gillespie, and M. A. Lamontia, “Analysis of transport phenomena governing interfacial bonding and void dynamics during thermoplastic tow-placement,” *International Journal of Heat and Mass Transfer*, vol. 39, no. 9, pp. 1883–1897, 1996, doi: 10.1016/0017-9310(95)00271-5.
- [24] C. A. Butler, R. L. Mccullough, R. Pitchumani, and J. W. Gillespie, “An Analysis of Mechanisms Governing Fusion Bonding of Thermoplastic Composites,” *Journal of Thermoplastic Composite Materials*, vol. 11, no. 4, pp. 338–363, 1998, doi: 10.1177/089270579801100404.
- [25] R. Pitchumani, J. W. Gillespie, and M. A. Lamontia, “Design and Optimization of a Thermoplastic Tow-Placement Process with In-Situ Consolidation,” *Journal of Composite Materials*, vol. 31, no. 3, pp. 244–275, 1997, doi: 10.1177/002199839703100302.
- [26] M. J. Donough, Shafaq, N. A. St John, A. W. Philips, and B. Gangadhara Prusty, “Process modelling of In-situ consolidated thermoplastic composite by automated fibre placement – A review,” *Composites Part A: Applied Science and Manufacturing*, vol. 163, p. 107179, 2022, doi: 10.1016/j.compositesa.2022.107179.
- [27] humm3®: *Our journey to industrialisation*. [Online]. Available: [https://www.heraeus.com/en/hng/uv\\_ir\\_flash\\_academy/webinars/humm3\\_our\\_journey\\_to\\_industrialisation.html](https://www.heraeus.com/en/hng/uv_ir_flash_academy/webinars/humm3_our_journey_to_industrialisation.html) (accessed: Mar. 28 2023).
- [28] N. Yadav, K. Wachtarczyk, P. Gąsior, R. Schledjewski, and J. Kaleta, “In-line residual strain monitoring for thermoplastic automated tape layup using fiber Bragg grating sensors,” *Polym. Compos.*, vol. 43, no. 3, pp. 1590–1602, 2022, doi: 10.1002/pc.26480.

- [29] N. Yadav, B. Oswald-Tranta, R. Schledjewski, and K. Wachtarczyk, "Ply-by-ply inline thermography inspection for thermoplastic automated tape layup," *Advanced Manufacturing: Polymer & Composites Science*, vol. 7, 3-4, pp. 49–59, 2021, doi: 10.1080/20550340.2021.1976501.
- [30] N. Yadav, B. Oswald-Tranta, M. Gürocak, A. Galic, R. Adam, and R. Schledjewski, "In-line and off-line NDT defect monitoring for thermoplastic automated tape layup," *NDT & E International*, vol. 137, p. 102839, 2023, doi: 10.1016/j.ndteint.2023.102839.
- [31] D. Saenz-Castillo, M. I. Martín, S. Calvo, F. Rodriguez-Lence, and A. Güemes, "Effect of processing parameters and void content on mechanical properties and NDI of thermoplastic composites," *Composites Part A: Applied Science and Manufacturing*, vol. 121, pp. 308–320, 2019, doi: 10.1016/j.compositesa.2019.03.035.
- [32] N. Yadav and R. Schledjewski, "Inline tape width control for thermoplastic automated tape layup," *Composites Part A: Applied Science and Manufacturing*, vol. 163, p. 107267, 2022, doi: 10.1016/j.compositesa.2022.107267.
- [33] M. A. Khan, P. Mitschang, and R. Schledjewski, "Parametric study on processing parameters and resulting part quality through thermoplastic tape placement process," *Journal of Composite Materials*, vol. 47, no. 4, pp. 485–499, 2013, doi: 10.1177/0021998312441810.
- [34] N. Yadav and R. Schledjewski, Eds., *Parametric effect on inline width control for thermoplastic automated tape layup*: ICCM23, 2023.
- [35] M. A. Khan, P. Mitschang, and R. Schledjewski, "Identification of some optimal parameters to achieve higher laminate quality through tape placement process," *Adv. Polym. Technol.*, vol. 29, no. 2, pp. 98–111, 2010, doi: 10.1002/adv.20177.
- [36] T. R. Brooks, J. R. R. A. Martins, and G. J. Kennedy, "Aerostructural Tradeoffs for Tow-Steered Composite Wings," *Journal of Aircraft*, vol. 57, no. 5, pp. 787–799, 2020, doi: 10.2514/1.C035699.
- [37] B. Smith *et al.*, "Passive Aeroelastic Tailoring," NF1676L-34873, Feb. 2020. [Online]. Available: <https://ntrs.nasa.gov/citations/20200001139>
- [38] European Commission, *A European Green Deal*. [Online]. Available: [https://commission.europa.eu/strategy-and-policy/priorities-2019-2024/european-green-deal\\_en](https://commission.europa.eu/strategy-and-policy/priorities-2019-2024/european-green-deal_en) (accessed: Apr. 27 2023).
- [39] S.-W. Kim, J.-S. Koh, J.-G. Lee, J. Ryu, M. Cho, and K.-J. Cho, "Flytrap-inspired robot using structurally integrated actuation based on bistability and a developable surface," *Bioinspir. Biomim.*, vol. 9, no. 3, p. 36004, 2014, doi: 10.1088/1748-3182/9/3/036004.
- [40] S. Daynes, P. Weaver, and J. Trevarthen, "A Morphing Composite Air Inlet with Multiple Stable Shapes," *undefined*, 2011. [Online]. Available: <https://www.semanticscholar.org/paper/A-Morphing-Composite-Air-Inlet-with-Multiple-Stable-Daynes-Weaver/906be7666fbf753e8ae7154ed750e76240ddd79b>
- [41] Z. Zhang *et al.*, "Magnetic actuation bionic robotic gripper with bistable morphing structure," *Composite Structures*, vol. 229, p. 111422, 2019, doi: 10.1016/j.compstruct.2019.111422.
- [42] H. Li, F. Dai, and S. Du, "Numerical and experimental study on morphing bi-stable composite laminates actuated by a heating method," *Composites Science and Technology*, vol. 72, no. 14, pp. 1767–1773, 2012, doi: 10.1016/j.compscitech.2012.07.015.

# Publications

## Journal articles

1. N. Yadav and R. Schledjewski, "Review of in-process defect monitoring for automated tape laying," *Composites Part A: Applied Science and Manufacturing*, p. 107654, 2023, doi: 10.1016/j.compositesa.2023.107654.
2. N. Yadav, B. Oswald-Tranta, M. Gürocak, A. Galic, R. Adam, and R. Schledjewski, "In-line and off-line NDT defect monitoring for thermoplastic automated tape layup," *NDT & E International*, vol. 137, p. 102839, 2023, doi: 10.1016/j.ndteint.2023.102839.
3. N. Yadav and R. Schledjewski, "Inline tape width control for thermoplastic automated tape layup," *Composites Part A: Applied Science and Manufacturing*, vol. 163, p. 107267, 2022, doi: 10.1016/j.compositesa.2022.107267.
4. N. Yadav, K. Wachtarczyk, P. Gąsior, R. Schledjewski, and J. Kaleta, "In-line residual strain monitoring for thermoplastic automated tape layup using fiber Bragg grating sensors," *Polym. Compos.*, vol. 43, no. 3, pp. 1590–1602, 2022, doi: 10.1002/pc.26480.
5. N. Yadav, B. Oswald-Tranta, R. Schledjewski, and K. Wachtarczyk, "Ply-by-ply inline thermography inspection for thermoplastic automated tape layup," *Advanced Manufacturing: Polymer & Composites Science*, vol. 7, 3-4, pp. 49–59, 2021, doi: 10.1080/20550340.2021.1976501.

## Conference contributions

6. N. Yadav and R. Schledjewski, "Parametric effect on inline width control for thermoplastic automated tape layup," in *Proceedings of the 23rd International Conference on Composite Materials, International Committee on Composite Materials: ICCM23, Belfast, Ireland, 2023*.
7. N. Yadav and R. Schledjewski, "Improved layup quality during automated thermoplastic tape layup – inline detection of consolidation force and tape geometry," *Book of abstracts of the fifth International Symposium on Automated Composites Manufacturing: ACM5, Bristol, UK, 2021*.
8. N. Yadav, B. Oswald-Tranta, M. Gürocak, A. Galic, R. Adam, and R. Schledjewski, "In – and off – line NDT in automated in-situ consolidation tape layup," *Proceedings of the SAMPE Europe Conference 2021 Baden/Zurich: Baden/Zurich, Switzerland and online, Society for the Advancement of Material and Process Engineering, Innovating towards perfection, 29-30 September 2021. Red Hook, NY: Curran Associates Inc, 2021*.
9. N. Yadav, B. Oswald-Tranta, R. Schledjewski, and M. Habicher, "Online thermography inspection for automated tape layup," in 2020, pp. 122–130. [Online]. Available: <https://www.spiedigitallibrary.org/conference-proceedings-of-spie/11409/2559533/Online-thermography-inspection-for-automated-tape-layup/10.1117/12.2559533.short>
10. N. Yadav and R. Schledjewski, "Parameter Selection for Peel Strength Optimization of Thermoplastic CF-PA6 for Humm3TM," *Proceedings of the 22nd Symposiums für Verbundwerkstoffe und Werkstoffverbunde - Kaiserslautern, Germany. KEM*, vol. 809, pp. 297–302, 2019, doi: 10.4028/www.scientific.net/KEM.809.297.
11. N. Yadav and R. Schledjewski, "Selective Comparison of Heating Sources for Thermoplastic Automated Tape Placement," *Proceedings of the fourth International Symposium on Automated Composites Manufacturing: ACM4. Lancaster, Pennsylvania: DEStech Publications, Inc, 2019*.